



UNIVERSITÉ DE FRIBOURG  
UNIVERSITÄT FREIBURG

Department of Biology  
University of Fribourg (CH)

# Identification of new TORC1 regulators: from genetic to high-throughput strategies

THESIS

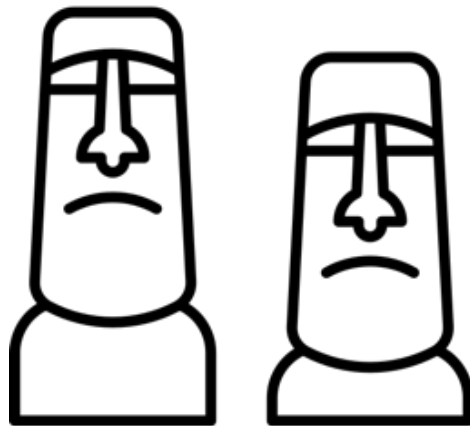
presented to the Faculty of Science and Medicine of the University of Fribourg (Switzerland) in  
consideration for the award of the academic grade of  
*Doctor of Philosophy in Biochemistry*

by

**Guillermo Miguel García Osuna**

from

**Granada, Spain**



Thesis N°:  
UNIPRINT  
2021

**Accepted by the Faculty of Science and Medicine of the University of Fribourg (Switzerland) upon the recommendation of:**

**Prof. Jörn Dengjel, University of Fribourg, Fribourg, Switzerland**

**Prof. Sophie Martin, University of Lausanne, Lausanne, Switzerland**

**Prof. Urs Albrecht (President of the jury), University of Fribourg, Fribourg, Switzerland**

**Fribourg, XX. XX. 2021**

**Thesis supervisor:**

.....

**Prof. Claudio De Virgilio:**

**Dean:**

.....

**Prof. Gregor Rainer:**

*Vincit qui patitur*



# TABLE OF CONTENTS

<b>ABBREVIATIONS.....</b>	<b>7</b>
<b>SUMMARY .....</b>	<b>10</b>
<b>RÉSUMÉ.....</b>	<b>12</b>
<b>GENERAL INTRODUCTION .....</b>	<b>14</b>
<b>CHAPTER 1: APPLICATION OF GENETIC SCREENS FOR THE IDENTIFICATION OF TORC1 REGULATORS .....</b>	<b>17</b>
<b>1.1: INTRODUCTION .....</b>	<b>18</b>
1.1.1: Rag GTPases .....	18
1.1.2: Regulators of the Rag GTPases .....	20
1.1.3: Other TORC1/mTORC1 regulators .....	22
<b>1.2: AIM OF THE CHAPTER .....</b>	<b>24</b>
<b>1.3: RESULTS .....</b>	<b>24</b>
1.3.1: Introduction to the classical genetic suppressor screen .....	24
1.3.2: Pilot screen .....	25
1.3.3: Characterization of the suppressors identified during the pilot classical genetic screen.....	27
1.3.4: EGO, but not TORC1, reaches the vacuolar surface via the AP-3 pathway .....	28
1.3.5: Large classical genetic screen: the seed for new projects .....	30
1.3.6: Characterization of OPY1 as a putative TORC1 regulator .....	31
1.3.7: Introduction to the SATAY project.....	32
1.3.8: Analysis of well-known and putative TORC1 regulators using SATAY .....	35
1.3.9: Gene Ontology (GO) enrichment analysis of the SATAY .....	37
<b>1.4: DISCUSSION AND CONCLUSIONS .....</b>	<b>44</b>
<b>1.5: BIBLIOGRAPHY .....</b>	<b>48</b>
<b>CHAPTER 2: STUDY OF THE CROSSTALK BETWEEN TORC1 AND THE GAAC SIGNALING PATHWAYS .....</b>	<b>55</b>
<b>2.1: INTRODUCTION .....</b>	<b>56</b>
2.1.1: General introduction to the ISR/GAAC pathway .....	56
2.1.2: The Gcn1-Gcn20 Gcn2 regulatory complex .....	57
2.1.3: Activation of Gcn2 by tRNAs .....	57
2.1.4: Activation of Gcn2 by the P-stalk.....	58
2.1.5: Regulation of the protein translation initiation.....	58
2.1.6: Crosstalk between the ISR/GAAC and the mTORC1/TORC1 pathways.....	59
2.1.7: The Gcn2 kinase in disease .....	60
<b>2.2: AIM OF THE CHAPTER .....</b>	<b>61</b>
<b>2.3: RESULTS .....</b>	<b>61</b>
2.3.1: The Gcn2 expression is necessary for inhibiting TORC1 in leucine- or histidine-, but not nitrogen-starved cells .....	61
2.3.2: The transcription factor Gcn4 also mediates TORC1 inhibition in leucine-starved cells .....	62
2.3.3: Discovery of new Gcn2 targets in <i>S. cerevisiae</i> .....	63
<b>2.4: DISCUSSION AND CONCLUSIONS .....</b>	<b>67</b>
<b>2.5: BIBLIOGRAPHY .....</b>	<b>69</b>
<b>CHAPTER 3: RIBOSOMAL PROTEIN DEFECTS UNRAVEL A FUNCTION OF THE ARF1 GTPASE IN CONTROLLING TORC1 ACTIVITY.....</b>	<b>72</b>

<b>3.1: INTRODUCTION .....</b>	<b>73</b>
3.1.1: Transcriptional regulation of the ribosomal components .....	73
3.1.2: 35S pre-rRNA processing .....	74
3.1.3: Pre-ribosomal particles nucleocytoplasmic export.....	76
3.1.4: RP and RiBi regulons .....	76
3.1.5: Transcriptional regulation of the RP genes.....	76
3.1.6: Transcriptional regulation of the RiBi genes.....	77
3.1.7: The crosstalk between rRNA and RPs expression.....	78
3.1.8: Turnover of pre-ribosomal particles and ribosomes .....	78
<b>3.2: AIM OF THE CHAPTER .....</b>	<b>80</b>
<b>3.3: RESULTS .....</b>	<b>80</b>
3.3.1: Bioinformatic analysis of Müllleder's dataset.....	80
3.3.2: Characterization of <i>YGL188C-A</i> and its effects on the downstream gene <i>RPS26A</i> .....	84
3.3.3: Introduction to <i>RPS26A</i> and characterization of its null mutant .....	86
3.3.4: Genetic interaction analysis between <i>RPS26A</i> and well-known regulators within the TORC1 pathway in yeast.....	89
3.3.5: Genetic interaction analysis between <i>RPS26A</i> and potential regulators within the TORC1 pathway in yeast.....	96
3.3.6: Specificity of the <i>RPS26A</i> deletion mutant phenotype.....	101
3.3.7: Proteome analysis of the <i>rps26aΔ</i> strain .....	103
<b>3.4: DISCUSSION AND CONCLUSIONS .....</b>	<b>114</b>
<b>3.5: BIBLIOGRAPHY .....</b>	<b>120</b>
<b>OUTLOOK.....</b>	<b>128</b>
<b>MATERIAL AND METHODS .....</b>	<b>131</b>
Yeast strains, plasmids, and growth conditions .....	132
Saturated transposon analysis in yeast (SATAY) .....	132
Preparation of genomic DNA from yeast .....	134
GO enrichment analyses.....	135
<i>In vivo</i> TORC1 kinase assay .....	136
Tables .....	136
Bibliography .....	140
<b>ACKNOWLEDGEMENTS .....</b>	<b>142</b>
<b>CV.....</b>	<b>143</b>

## ABBREVIATIONS

AAH1: Adenine AminoHydrolase  
ADP: Adenosine DiPhosphate  
AP-3: Adaptor Protein 3  
ARF: ADP-ribosylation factor  
ATP: Adenosine TriPhosphate  
CAD: C-terminal TORC1-Activating Domain  
CORVET: class C cORe Vacuole/Endosome Tethering  
CTD: C-Terminal Domain  
CUTs: Cryptic Unstable Transcripts  
DBA: Diamond-Blackfan-Anemia  
DML: DiMethyl Labeling  
eADA: erythrocyte Adenosine DeAminase  
EDTA: EthyleneDiamine Tetraacetic Acid  
EGOC: Exit from G0 Complex  
EGO-TC: EGO Ternary Complex  
ER: Endoplasmic Reticulum  
FBPase: Fructose-1,6-BiPhosphatase  
FKBP12: FK506 Binding Protein 12  
FLCN: Folliculin  
FYVE: Fab1-YotB-Vac1p-EEA  
GAAC: General Amino Acid Control  
GAPs: GTPase Activating Proteins  
GATOR: GAP Activity TOWard RAGs  
GDIs: GDP Dissociation Inhibitors  
GDP: Guanosine DiPhosphate  
GEFs: Guanine nucleotide Exchange Factors  
GID: Glucose Induced degradation Deficient  
GO: Gene Ontology  
GRFs: General Regulatory Factors  
GTP: Guanosine TriPhosphate  
GTPase: Guanosine TriPhosphatase

HDR: Homology-Directed Repair  
HMG: High Mobility Group  
HOPS: HOMotypic fusion and Protein Sorting  
HRI: Heme-Regulated eIF2 $\alpha$  kinase  
ISR: Integrated Stress Response  
Kog1: Kontroller of growth 1  
LC-MS: Liquid Chromatography-Mass Spectrometry  
LeuRS: Leucyl t-RNA Synthetase  
Met-tRNA<sup>i</sup>: Methionyl-charged tRNA  
MICOS: Mitochondrial contact site and Cristae Organizing System  
mTORC1: mammalian TORC1  
NCR: Nitrogen Catabolite Repression  
NGD: No-Go Decay  
NGS: Next-Generation-Sequencing  
NID: N-terminal TORC1-Inhibiting Domain  
NRD: Non-functional rRNA Decay  
ORF: Open Reading Frame  
PAC: RNA Polymerase A and C promoters  
PERK: PKR-like ER Kinase  
PH: Pleckstrin Homology  
PIC: PreInitiation Complex  
PI3P: Phosphatidylinositol-3-Phosphate  
PI4P: Phosphatidylinositol-4-Phosphate  
PI(4,5)P<sub>2</sub>: Phosphatidylinositol-4,5-bisPhosphate  
PK: Protein Kinase  
PKA: Protein Kinase A  
PKR: double-stranded RNA-dependent Protein Kinase  
PP: Protein Phosphatase  
PP2A: type 2A Protein Phosphatase  
Rag: Ras-related GTP binding protein  
REDD1: REgulated in Development and DNA damage responses 1  
RiBi: Ribosome Biogenesis  
RNA: RiboNucleic Acid  
RNAPI: RNA Polymerase I



RNC: Raptor-like N-terminal–Conserved  
ROS: Reactive Oxygen Species  
RPG: Reads Per Gene  
RPs: Ribosomal Proteins  
RRPE: Ribosomal RNA-Processing Element  
SATAY: SATurated Transposon Analysis in Yeast  
SC: Synthetic Complete  
SD: Synthetic Dextrose  
SDS: Sodium Dodecyl Sulfate  
SEAC: SEh1-Associated protein Complex  
SEACAT: SEAC subcomplex Activating TORC1 signaling  
SEACIT: SEAC subcomplex Inhibiting TORC1 signaling  
SICHH: Swiss Integrative Center for Human Health SA  
SNVs: Single Nucleotide Variants  
SILAC: Stable Isotope Labeling by Amino acids in Cell culture  
SPS: Ssy1-Ptr3-Ssy5  
SSU: Small SubUnit  
TC: Ternary Complex  
TGN: Trans-Golgi Network  
TMDs: TransMembrane Domains  
TOR: Target Of Rapamycin  
TORC1: Target Of Rapamycin Complex 1  
TORC2: Target Of Rapamycin Complex 2  
TPG: Transposons Per Gene  
TSC: Tuberous Sclerosis Complex  
5'UTR: 5'-UnTranslated Region  
v-ATPase: vacuolar ATPase  
VCF: Variant Call Format  
YPD: Yeast extract Peptone Dextrose

## SUMMARY

In eukaryotes, the well-conserved Target Of Rapamycin Complex 1 (TORC1) pathway modulates cellular anabolism and catabolism by regulating processes such as general translation initiation, ribosome biogenesis, and autophagy, primarily in response to nitrogen (*e.g.* amino acids) availability. Due to its pivotal role in cell growth and proliferation, evolution has built around the TORC1 protein kinase a complex regulatory system of which much remains to be discovered. In the budding yeast *S. cerevisiae*, the endosomal/vacuolar EGOC (Exit from rapamycin-induced G0 Complex), which is composed of Ego1, Ego2, Ego3, and the small Rag GTPases Gtr1 and Gtr2, is a well-studied regulator of TORC1 that mediates the presence of amino acids. During my PhD studies, and in collaboration with team members and external members, I developed several strategies to identify new actors and mechanisms involved in the regulation of the EGOC-TORC1 pathway.

In the **first chapter**, we used the Gtr1<sup>S20L</sup> variant, which when overexpressed inhibits TORC1 and hence cell growth, to perform two genetic selections: (i) a classical genetic suppressor selection, and (ii) a transposon-based genetic selection. With the classical genetic selection, we identified suppressor mutants in genes coding for HOPS and AP-3 components, which mediate vacuolar protein sorting. Analysis of these mutants showed that the AP-3 pathway is important for the EGOC (but not TORC1) targeting to the vacuolar surface. We also identified several interesting mutants, among which Opy1<sup>N250K</sup>, as potential TORC1 regulators. Even though the exact mechanism by which Opy1 affects TORC1 remains elusive, its overexpression suppressed the growth inhibition caused by Gtr1<sup>S20L</sup> overexpression. Furthermore, the transposon-based genetic selection led us to identify the GID and Set3 complexes as putative positive and negative regulators of TORC1 activity, respectively. While the GID complex, which has a ubiquitin-ligase function, plays a role in carbon metabolism, the Set3 complex is a histone deacetylase that regulates gene transcription.

In yeast, the GAAC pathway is a conserved pro-survival pathway, which senses the availability of intracellular amino acids in parallel to the TORC1 pathway. Notably, several studies have demonstrated that the GAAC and the TORC1 pathways also regulate one another. In the **second chapter**, we tried to address how the GAAC pathway members affect the TORC1 pathway. Based on phosphoproteomic experiments, we identified Hos4 and Snd1 as possible Gcn2 targets with a potential

role in the TORC1 pathway regulation. We also found a hitherto unknown Gcn4-dependent branch of TORC1 regulation that, in analogy with the mammalian transcription factor and Gcn4 homolog ATF4, may induce the expression of proteins that negatively regulate TORC1 upon amino acid deprivation.

TORC1 regulates, among others, the ribosome biogenesis pathway. However, how ribosome biogenesis may in turn control the TORC1 pathway remains unknown. Previous studies reported that the *YGL188C-A* null mutant, which causes reduced levels of Rps26a expression, accumulates intracellular asparagine and glutamine similarly to a subset of TORC1 pathway mutants. In the **third chapter**, we studied how the loss of Rps26a, which severely impairs ribosome biogenesis, impacts the TORC1 pathway functionality. Our results suggest that the previously described accumulation of intracellular asparagine and glutamine may impact the TORC1 pathway activity in an Arf1 GTPase-dependent manner. Further characterization of the Arf1 mutant is currently needed to confirm our hypothesis and unveil the molecular mechanism by which Arf1 affects the TORC1 pathway.

## RÉSUMÉ

Chez les eucaryotes, la voie de signalisation conservée Target Of Rapamycin Complex 1 (TORC1) module l'anabolisme et le catabolisme cellulaires en régulant divers processus tels que l'initiation générale de la traduction, la biogenèse des ribosomes et l'autophagie, principalement en réponse à la disponibilité de l'azote (par ex., les acides aminés). En raison de son rôle central dans la croissance et la prolifération cellulaires, le complexe protéine kinase TORC1 se trouve lui-même soumis à une régulation hautement élaborée impliquant de multiples acteurs. Notre connaissance des éléments de ce système de régulation est à ce jour encore parcellaire. Chez la levure *S. cerevisiae*, parmi ces éléments, le complexe endosomal/vacuolaire EGO (Exit from rapamycin-induced G0 Complex), composé d'Ego1, Ego2, Ego3 et des petites GTPases Gtr1 et Gtr2, appartient à une branche amont bien étudiée qui informe TORC1 de la présence d'acides aminés. Au cours de mes études doctorales, en collaboration avec les membres de l'équipe et des membres externes, j'ai développé plusieurs stratégies dans le but d'identifier de nouveaux facteurs et mécanismes impliqués dans la régulation de la voie TORC1.

Dans le **premier chapitre**, nous avons utilisé le variant Gtr1<sup>S20L</sup> qui, lorsqu'il est surexprimé, inhibe TORC1 et donc la croissance cellulaire, pour effectuer deux cribles génétiques : (i) un crible génétique classique de supresseurs spontanés, et (ii) un crible génétique impliquant des événements d'intégration aléatoire d'un mini transposon. Avec le crible génétique classique, nous avons identifié des mutations dans les gènes codant des composants des complexes HOPS et AP-3 qui assurent le tri de protéines vers la vacuole. L'analyse de ces mutants a montré que la voie AP-3 est importante pour le ciblage d'EGOC (mais pas de TORC1) à la surface vacuolaire. Nous avons également identifié plusieurs mutants, dont Opy1<sup>N250K</sup>, comme régulateurs potentiels de TORC1. Même si le mécanisme exact par lequel Opy1 affecte TORC1 reste à ce jour imprécis, sa surexpression supprime l'inhibition de la croissance occasionnée par la surexpression de Gtr1<sup>S20L</sup>. En outre, la sélection génétique basée sur des événements de transposition nous a permis d'identifier les complexes GID et Set3 comme de possibles régulateurs, respectivement positifs et négatifs, de l'activité de TORC1. Alors que le complexe GID, qui a une fonction ubiquitine-ligase, joue un

rôle dans le métabolisme du carbone, le complexe Set3 est une histone désacétylase qui régule la transcription de gènes.

Chez la levure, la voie GAAC est une voie de survie conservée qui détecte la disponibilité des acides aminés intracellulaires parallèlement à la voie TORC1. Plusieurs études ont démontré que les voies GAAC et TORC1 se régulent mutuellement. Dans le **deuxième chapitre**, nous avons tenté de déterminer comment les membres de la voie GAAC affectent la voie TORC1. À partir d'expériences de phosphoprotéomique, nous avons identifié Hos4 et Snd1 comme des cibles possibles de la protéine kinase Gcn2 qui pourraient être impliquées dans la régulation de la voie TORC1. Nous avons également découvert une nouvelle branche de la régulation de TORC1 dépendante du facteur de transcription Gcn4. Par analogie avec son homologue chez les mammifères, ATF4, Gcn4 pourrait stimuler l'expression de régulateurs négatifs de TORC1 lors d'une privation d'acides aminés.

TORC1 régule, entre autres, la voie de la biogenèse des ribosomes. Cependant, la manière dont la biogenèse des ribosomes pourrait à son tour contrôler la voie TORC1 demeure inconnue. Des études précédentes ont rapporté que le mutant nul *YGL188C-a*, qui entraîne des niveaux réduits d'expression de Rps26a, accumule l'asparagine et la glutamine intracellulaires de manière similaire à un sous-ensemble de mutants de la voie TORC1. Dans le **troisième chapitre**, nous avons étudié l'impact de la perte de Rps26a, qui nuit gravement à la biogenèse des ribosomes, sur la fonctionnalité de la voie TORC1. Nos résultats suggèrent que l'accumulation précédemment décrite d'asparagine et de glutamine intracellulaires peut avoir un impact sur l'activité de la voie TORC1 d'une manière dépendante de la GTPase Arf1. Une caractérisation plus poussée du mutant *arf1* s'avère nécessaire pour confirmer notre hypothèse et dévoiler le mécanisme moléculaire par lequel Arf1 affecte la voie TORC1.

**GENERAL INTRODUCTION**

Living organisms need to import nutrients and micronutrients from their environment to grow and survive. These provide energy and building blocks for protein, lipid, carbohydrate, and nucleotide biosynthesis. Efficient growth and survival, therefore, rely on appropriate control of processes involved in nutrient uptake, transport, and metabolism. Notably, carbon and nitrogen metabolism are critical for the anabolism of cellular components and energy production. During evolution, eukaryotes have elaborated a series of mechanisms that allow them to control their metabolism in response to nutrient availability, hormones, and growth factors (Laplante et al., 2012; Wullschleger et al., 2006; Zaman et al., 2008).

The budding yeast *Saccharomyces cerevisiae*, the model organism used here, carries out a set of different processes involved in nitrogen metabolism regulation. From sensing to transport and from transport to metabolism, these interconnected processes regulate one another, allowing the cell to fine-tune transcription, translation, and activity of proteins (Magasanik & Kaiser, 2002; Zhang et al., 2018). Among the processes controlling nitrogen metabolism in yeast, the most important ones are the Ssy1-Ptr3-Ssy5 signaling sensor system (SPS sensor system) (Forsberg & Ljungdahl, 2001), Nitrogen Catabolite Repression (NCR) (Hofman-Bang, 1999), the General Amino Acid Control (GAAC) pathway (Hinnebusch, 2005; Masson, 2019; Natarajan et al., 2001), and the Target Of Rapamycin (TOR) regulatory pathway (Conrad et al., 2014).

In 1991, the yeast *TOR1* and *TOR2* gene products were identified as targets of the macrolide rapamycin. Mutations in the corresponding genes conferred resistance to rapamycin-induced growth inhibition (Cafferkey et al., 1993; Heitman et al., 1991; Helliwell et al., 1994; Kunz et al., 1993). Subsequent investigations revealed that the Tor proteins are present and well conserved in all eukaryotes; while mammalian cells possess one *TOR* gene (*mTOR*), the *S. cerevisiae* genome harbors two *TOR* genes called *TOR1* and *TOR2* (Brown et al., 1994; Chiu et al., 1994; Sabatini et al., 1994; Sabers et al., 1995). Tor proteins are serine/threonine protein kinases and members of the phosphatidylinositol protein kinase family (also called phosphatidyl-inositol 3'kinase-related kinases PIKKs) (Cafferkey et al., 1993; Helliwell et al., 1994; Kunz et al., 1993) that are present in two structurally and functionally different complexes (*i.e.*, the TOR complex 1 (TORC1) and the TOR complex 2 (TORC2)) (Eltschinger & Loewith, 2016; Wedaman et al., 2003; Wullschleger et al., 2006), which are highly conserved between *S. cerevisiae* and mammals (Table 1). Notably, TORC2 is insensitive to rapamycin due

to the specific subunit Tsc11/Avo3 that prevents binding of the inhibitory FKBP12/Fpr1-  
rapamycin complex (Gaubitz et al., 2016; Loewith et al., 2002).

Complex	<i>S. cerevisiae</i>	Mammalian cells
<b>TORC1/mTORC1</b>	Tor1 or Tor2	mTOR
	Kog1	Raptor
	Lts8	mLst8
	Tco89	-
	-	PRAS40
	-	DEPTOR
<b>TORC2/mTORC2</b>	Tor2	mTOR
	Avo1	mSin1
	Lst8	mLst8
	Tsc11/Avo3	Rictor
	Bit61 or Bit2	Protor1 or Protor2
	Avo2	-
	-	DEPTOR

**Table 1: Orthologous subunits of the TORC1/mTORC1 and TORC2/mTORC2 complexes in *Saccharomyces cerevisiae* and mammals, respectively.**

The TORC1 and TORC2 complexes control different cellular processes. On one side, TORC1 is involved in a wide range of cellular processes related to nutrient sensing, transport and metabolism, general translation initiation, ribosome biogenesis, mitochondrial functions, and autophagy. On the other side, TORC2 mainly mediates yeast bud growth by regulating cell wall synthesis and the actin cytoskeleton (Cornu et al., 2013; Eltschinger & Loewith, 2016; Sarbassov et al., 2005; Saxton & Sabatini, 2017).

TORC1 constitutes the central hub in the eukaryotic cell growth controlling pathway, balancing anabolic and catabolic processes in response to environmental cues. Hence, it is not surprising that dysregulation of the TORC1 pathway frequently associates with several human diseases, including cancer, type 2 diabetes, and neurodegeneration (Liu & Sabatini, 2020, and references therein). The overarching goal of this thesis is to identify hitherto unknown regulatory mechanisms that impinge on TORC1. To this end, we used, in chapter I, different genetic approaches that are based on the isolation and enrichment of mutants capable of growing under conditions where TORC1, and thus cell growth, is inhibited. In parallel, chapters II and III are devoted to the question of whether and how TORC1, which regulates the GAAC and ribosomal biogenesis pathways in response to nutrient availability, can also be regulated by these pathways and thus contribute to cellular proteostasis.



# **CHAPTER 1: APPLICATION OF GENETIC SCREENS FOR THE IDENTIFICATION OF TORC1 REGULATORS**

## 1.1: INTRODUCTION

### 1.1.1: Rag GTPases

In *S. cerevisiae*, stimulation of TORC1 activity by nitrogen has been shown to involve different regulators. In starved cells, the addition to the culture medium of virtually any amino acid triggers a transient (in the range of minutes) wave of TORC1 stimulation that is Rag GTPase-dependent, while the more robust Rag-GTPase-independent long-term TORC1 stimulation requires preferred nitrogen sources like glutamine (Stracka et al., 2014; Tanigawa et al., 2017). The Rag GTPase-dependent branch of TORC1 regulation is highly conserved between yeast and mammals and has been extensively studied in the past few years. The Rag GTPases represent the catalytic center of multimeric complexes named EGO (Exit from G0 Complex) in *S.cerevisiae* and Ragulator-Rag in mammalian cells (Table 2) (Nicastro et al., 2017, and references therein).

EGOC ( <i>S. cerevisiae</i> )	Ragulator-Rag (mammalian cells)
Gtr1	RagA or RagB
Gtr2	RagC or RagD
Ego1	LAMTOR1/p18
Ego2	LAMTOR5/HBXIP
Ego3	LAMTOR2/p14
-	LAMTOR3/MP1
-	LAMTOR4/C7orf59

**Table 2: Orthologous subunits of the EGO and the Ragulator-Rag complexes in *Saccharomyces cerevisiae* and mammals, respectively.**

Gtr1-Gtr2 in *S. cerevisiae* and RagA/B-C/D in mammalian cells are part of the Rag family of Ras-related GTP-binding proteins (Gong et al., 2011; Nakashima et al., 1999; Schurmann et al., 1995; Sekiguchi et al., 2001). A peculiar characteristic of the Rag GTPases is their extended C-termini, which dimerize, thus forming heterodimeric modules, e.g., Gtr1 with Gtr2 and RagA or RagB with RagC or RagD (Gong et al., 2011; Sekiguchi et al., 2001). The Rag GTPases are recruited to the vacuole and perivacuolar foci (which we recently identified as endosomes) by the EGO-TC (EGO ternary complex composed of Ego1, Ego2, and Ego3) in yeast (Powis et al., 2015; Zhang et al., 2019) and to the lysosomal membrane by Ragulator (LAMTOR1/p18, LAMTOR5/HBXIP, LAMTOR2/p14, LAMTOR3/MP1, LAMTOR4/C7orf59) in mammals (Kim & Kim, 2016).

In particular, the EGO and the Ragulator-Rag are associated with these membranes via the N-terminal myristoylation and palmitoylation of Ego1/Meh1

(Nadolski & Linder, 2009; Roth et al., 2006) and LAMPTOR1/p18 (Nada et al., 2009). The activity of the Rag GTPases is determined by their nucleotide-binding status, which is directly affected by the intracellular amino acid levels in a manner that is still not entirely understood (Nicastro et al., 2017, and references therein). The binding of GTP by Gtr1 or RagA/B and GDP by Gtr2 or RagC/D is promoted under rich amino acid conditions and causes the stimulation of the TORC1 or mTORC1 activity, respectively; in contrast, the opposite nucleotide-binding status is promoted under poor amino acid conditions, thereby promoting the inhibition of TORC1 or mTORC1 (Binda et al., 2009; Demetriades et al., 2014; Gao & Kaiser, 2006; Kim et al., 2008; Kira et al., 2014; Sancak et al., 2008).

In *S. cerevisiae*, the relative distribution of TORC1 between endosomes and vacuoles seems to be affected by the Gtr1-Gtr2 guanine nucleotide loading status (Binda et al., 2009; Kira et al., 2014; Sturgill et al., 2008) and appears to be mediated by the TORC1 components Kog1 and Tco89 (Binda et al., 2009; Bonfils et al., 2012). The control of the relative subcellular distribution of TORC1 is particularly significant as endosomal and vacuolar pools of TORC1 phosphorylate distinct targets, which are involved in different biological processes (Hatakeyama et al., 2019).

In mammalian cells growing in rich conditions, the RagA/B-RagC/D heterodimer is essential for recruiting mTORC1 to the lysosomal membrane where it can be activated by GTP-loaded Rheb (GTP-Rheb) (Fawal et al., 2015; Kim et al., 2008; Sancak et al., 2008; Sancak et al., 2010). In contrast, in poor conditions, the RagA/B-RagC/D heterodimer recruits the Tuberous Sclerosis Complex (TSC) that functions as a GTPase activating protein for GTP-Rheb, thus promoting the hydrolysis of GTP and the subsequent release of mTORC1 from the lysosomal membrane (Averous et al., 2014; Demetriades et al., 2014). Therefore, regulating the Gtr1/2 or RagA/B-C/D nucleotide-loading status is crucial for tuning both TORC1/mTORC1 functionality and localization in *S. cerevisiae* and mammalian cells. For that reason, there exist several regulators that impinge on the Rag GTPases in response to the intracellular availability of amino acids (Figure 1).

### 1.1.2: Regulators of the Rag GTPases

In both *S. cerevisiae* and mammals, the nucleotide-binding status of the Rag GTPase module is influenced by the intracellular amino acid status. In particular, the Rag GTPase nucleotide-binding status and activity is regulated by GTPase activating proteins (GAPs), Guanine Nucleotide Exchange Factors (GEFs), GDP Dissociation Inhibitors (GDIs), and other amino acid sensors (Figure 1) (Hatakeyama & Virgilio, 2016; Nicastro et al., 2017; Tafur et al., 2020). In mammalian cells, Ragulator, apart from serving as a docking platform for the Rag GTPase module, has been proposed to function as a GEF for RagA/B downstream of the vacuolar H<sup>+</sup>-ATPase (v-ATPase) (Bar-Peled et al., 2012). In contrast, more recent studies claim that Ragulator triggers the GTP release from RagC and that the sodium-coupled amino acid transporter SLC38A9 is the GEF for RagA (Shen & Sabatini, 2018). Notably, there is no conserved ortholog for SLC38A9 in yeast; however, Vam6/Vps39 has been shown to promote the GTP binding to Gtr1 (Binda et al., 2009; Valbuena et al., 2012).

In mammalian cells, the GATOR (GAP Activity TOward RAGs) holocomplex, which is made of GATOR1 and GATOR2 subcomplexes (Table 3), regulates the RagA/B guanine nucleotide status in response to amino acids (Bar-Peled et al., 2013). In poor nitrogen conditions, GATOR1 acts as a negative regulator of the mTORC1 signaling pathway by promoting GTPase activity of RagA/B, while GATOR2 has been proposed to act as a positive mTORC1 regulator by keeping GATOR1 inactive in rich nitrogen conditions (Bar-Peled et al., 2013). The GATOR holocomplex localizes to the lysosomal membrane in an amino acid-independent manner through the interaction of GATOR1 with KICSTOR, a protein complex made of KPTN ITFG2, C12orf66, and SZT2 subunits (Peng et al., 2017; Wolfson et al., 2017). In yeast, the equivalent to the GATOR holocomplex is the SEh1-Associated protein Complex (SEAC) (Dokudovskaya & Rout, 2015). Like GATOR, the SEAC is also divided into two functionally and structurally different subcomplexes named SEACIT and SEACAT (Table 3). In poor nitrogen conditions, SEACIT inhibits the TORC1 signaling pathway by promoting the GTPase activity of Gtr1 (Algret et al., 2014; Dokudovskaya et al., 2011; Dokudovskaya & Rout, 2015; Panchaud et al., 2013a, 2013b), while SEACAT acts as a positive TORC1 regulator by keeping SEACIT inactive in rich nitrogen conditions (Panchaud et al., 2013a, 2013b). As of today, the mechanism by which GATOR2 and SEACAT antagonize the GATOR1 and SEACIT activities remains elusive.

Complex	<i>S. cerevisiae</i>	Mammalian cells
<b>SEACIT/GATOR1</b>	Iml1	DEPDC5
	Npr2	NPRL2
	Npr3	NPRL3
<b>SEACAT/GATOR2</b>	Seh1	SEH1L
	Sea2	WDR24
	Sea3	WDR59
	Sea4	MIOS
	Sec13	SEC13
<b>Lst4-Lst7/FLCN-FNIP2</b>	Lst4	FNIP1/2
	Lst7	FLCN

**Table 3: Orthologous subunits of the Rag GTPases regulators in *S.cerevisiae* and mammalian cells, respectively.**

In mammalian cells, the FNIP1/2-FLCN complex is tethered to the lysosomal membrane and strongly binds to RagA/B in starved cells (Petit et al., 2013). After refeeding with amino acids, this complex functions as a GAP towards RagC/D, favoring the hydrolysis of GTP to GDP (Tsun et al., 2013), thereby promoting the activation of the Rag GTPase module, which then recruits TORC1 to the lysosomal membrane through its interaction with Raptor. Recently, it has been proposed that upon amino acid refeeding, the cytoplasmic tail of SLC38A9 is involved in promoting the GAP activity of the FNIP1/2-FLCN complex towards RagC/D (Fromm et al., 2020). In yeast, the equivalent to the FNIP1/2-FLCN complex is the Lst4-Lst7 complex (Péli-Gulli et al., 2015). The Lst4-Lst7 complex localizes to the vacuolar periphery in starved cells. It associates with the Gtr1-Gtr2 heterodimer upon amino acid refeeding and functions as a GAP towards Gtr2, promoting TORC1 activation and subsequent release of Lst4-Lst7 from the vacuole (in a very elegant negative feedback control loop that allows fine-tuning of TORC1 activity) (Péli-Gulli et al., 2017).

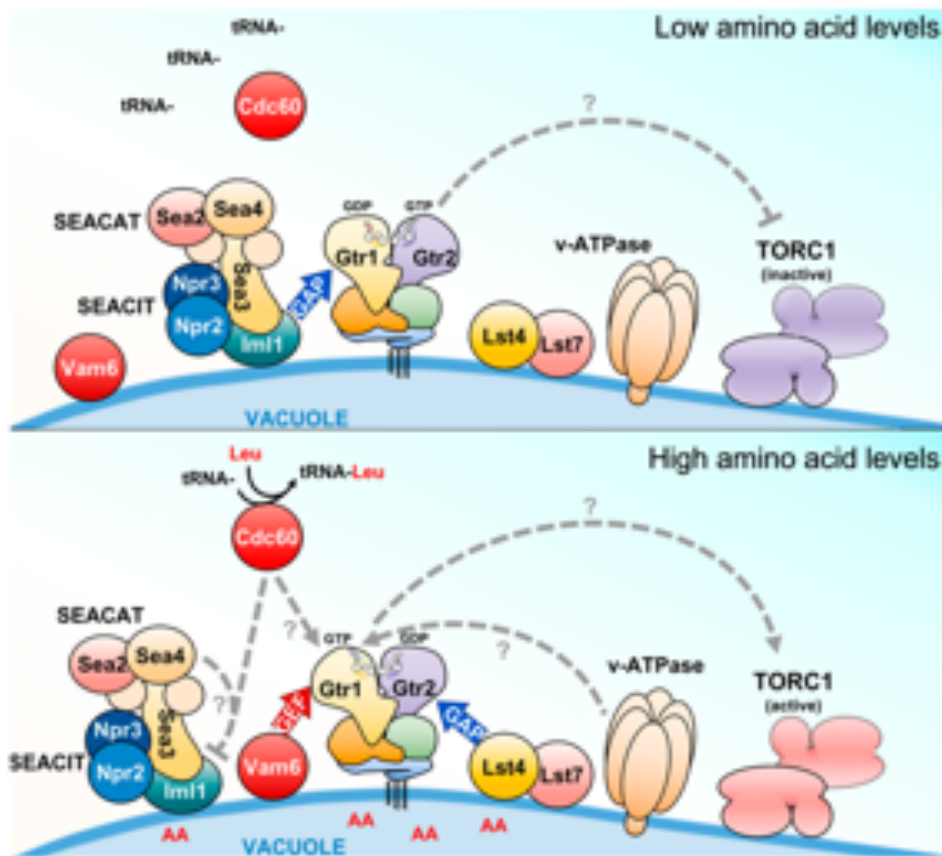
In addition to the complexes described above, eukaryotes express more proteins that function as sensors of specific amino acids to modulate the Rag GTPase guanine nucleotide status (Kim & Guan, 2019 and references therein). For example, Cdc60 in yeast and LeuRS in mammals have been proposed to sense intracellular leucine levels promoting the Gtr1-GTP, and the RagD-GDP-loading status, respectively (Bonfils et al., 2012; Han et al., 2012). Another example in mammalian cells is featured by the respective leucine and arginine sensors Sestrin2 and CASTOR1 (Saxton et al., 2016; Wolfson et al., 2016). In the absence of leucine and arginine, Sestrin2 and CASTOR1 function as negative mTORC1 regulators by binding and inhibiting GATOR2 (Saxton et al., 2016; Wolfson et al., 2016). The binding of leucine by Sestrin2 and arginine by CASTOR1 triggers the release of GATOR2, which inhibits GATOR1 hence promoting

the TORC1 activation. (Saxton et al., 2016; Wolfson et al., 2016). Finally, also in mammals, the S-adenosylmethionine sensor named SAMTOR inhibits TORC1 by associating to GATOR1 and promoting its activity under low S-adenosylmethionine concentrations (Gu et al., 2017; Kim & Guan, 2019). Notably, the yeast equivalents for Sestrin2, CASTOR1, and SAMTOR have not been identified yet. The regulation of TORC1/mTORC1 activity by the EGO/Regulator-Rag modules is complex and involves many proteins. Even if several research groups have contributed to widening our knowledge about this branch of TORC1/mTORC1 regulation, additional amino acid sensors, interactors, and regulators remain to be identified and characterized.

### **1.1.3: Other TORC1/mTORC1 regulators**

In yeast, Pib2 has been proposed to signal to TORC1 in response to the availability of amino acids, particularly in response to glutamine availability (Kim & Cunningham, 2015; Michel et al., 2017; Ukai et al., 2018; Varlakhanova et al., 2017). Pib2-dependent TORC1 regulation requires the targeting of Pib2 to the vacuolar or endosomal membranes, which occurs through the interaction of the FYVE (Fab1-YotB-Vac1p-EEA) domain of Pib2 with phosphatidylinositol-3-phosphate (PI3P) present at endosomal and vacuolar membranes (Burd & Emr, 1998; Hatakeyama et al., 2019; Hayakawa et al., 2004; Kim & Cunningham, 2015). Besides, Pib2 has been shown to harbor a C-terminal TORC1-Activating Domain (CAD) and an N-terminal TORC1-Inhibiting domain (NID) (Michel et al., 2017). Notably, simultaneous loss of Gtr1 and Pib2 leads to a synthetic growth defect (Kim & Cunningham, 2015). However, whether Pib2 regulates TORC1 independently (Michel et al., 2017; Ukai et al., 2018) or in cooperation with the EGO is unclear (Varlakhanova et al., 2017). Even though no ortholog has been found for Pib2 in mammals, the Arf1 protein has been proposed to activate, in parallel to the Rag GTPases, lysosomal mTOR in response to increased glutamine and asparagine intracellular levels (Jewell et al., 2015; Meng et al., 2020). Although Arf1 is well-conserved between mammalian and yeast cells, no Arf1-dependent branch of TORC1 regulation has been yet described in yeast.

**A**



**B**

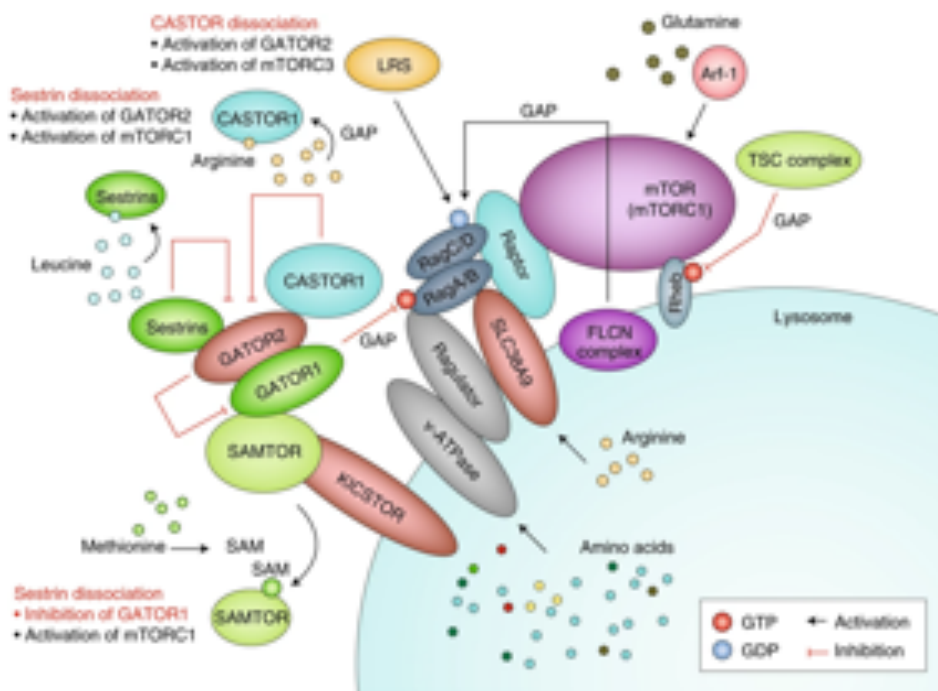


**Figure 1: Amino acid-dependent TORC1 and mTORC1 activation.** (A) TORC1 regulation in response to amino acid availability in *S. cerevisiae*. Taken from Nicastro et al., 2017. (B) mTORC1 regulation in response to amino acid availability in mammalian cells. Taken from Kim & Guan, 2019.

## 1.2: AIM OF THE CHAPTER

The EGOc relays the amino acid signal to TORC1. In rich conditions, when Gtr1 is GTP-loaded and Gtr2 is GDP-loaded, the EGOc positively signals to the TORC1 kinase. In contrast, when Gtr1 is GDP-loaded and Gtr2 is GTP-loaded, the EGOc negatively signals to the TORC1 kinase. However, the exact molecular mechanisms by which EGOc senses amino acids and translates this signal to the TORC1 kinase remain thus far unknown. Many proteins regulate the guanine nucleotide status of the Gtr1-Gtr2 heterodimer according to the cellular nutritional status; however, many regulators may still be missing. In this chapter, apart from new Gtr1-Gtr2 regulators, we aim to discover key players that could mediate the signal from the EGOc to the TORC1 kinase and new regulators of the TORC1 pathway that could work in parallel to the EGOc.

## 1.3: RESULTS

### 1.3.1: Introduction to the classical genetic suppressor screen

Based on a similar mutation in Ras proteins (Farnsworth & Feig, 1991; John et al., 1993; Nassar et al., 2010), the variant Gtr1<sup>S20L</sup> has been proposed to be a nucleotide-free form of Gtr1 (Nassar et al., 2010), likely phenocopying GDP-loaded Gtr1 (Binda et al., 2009; Nakashima et al., 1999). The Gtr1<sup>S20L</sup> allele behaves semi-dominantly (Binda et al., 2009), thus masking its full inhibitory potential when expressed along with wild-type Gtr1. In contrast, in *gtr1*Δ cells, Gtr1<sup>S20L</sup> expression inhibits the TORC1 activity (Binda et al., 2009), and even inhibits cell growth when overexpressed (Binda et al., 2009; Hatakeyama et al., 2019). This, therefore, represents the context of choice for a classical genetic screen. The project described hereafter was carried out in collaboration with the Swiss Integrative Center for Human Health SA (SICHH) and Prof. Dr. Laurent Falquet (Figure 2).

*gtr1*Δ cells expressing galactose inducible Gtr1<sup>S20L</sup> from a plasmid were first grown in glucose-containing rich nitrogen medium and then plated on galactose-containing rich nitrogen plates. On average, after 3-4 days, around 5 colonies (spontaneous suppressors) grew out of 1.5 x 10<sup>6</sup> plated cells. From genomic DNA of isolated suppressor mutants (Figures 2A-B), people at the SICHH were then responsible for preparing the DNA library and sequencing the reads by high-throughput Next-



Generation-Sequencing (NGS) using the instrument NEXTSEQ 500 (Illumina) (Figures 2C-D). Professor Falquet processed the raw reads as previously described (Thoms et al., 2018) to produce an annotated and cured Variant Call Format (VCF) file (Figures 2E-H). Finally, for each suppressor, Professor Falquet identified several SNVs (Single Nucleotide Variants); therefore, to shorten the list of suppressors, we designed a list of chosen candidates by prioritizing those predicted to be HIGH or MODERATE by SnpEff (which predicts the effects of mutations on genes and proteins) and those reported to interact physically or genetically with TORC1 pathway members (Figure 2I).

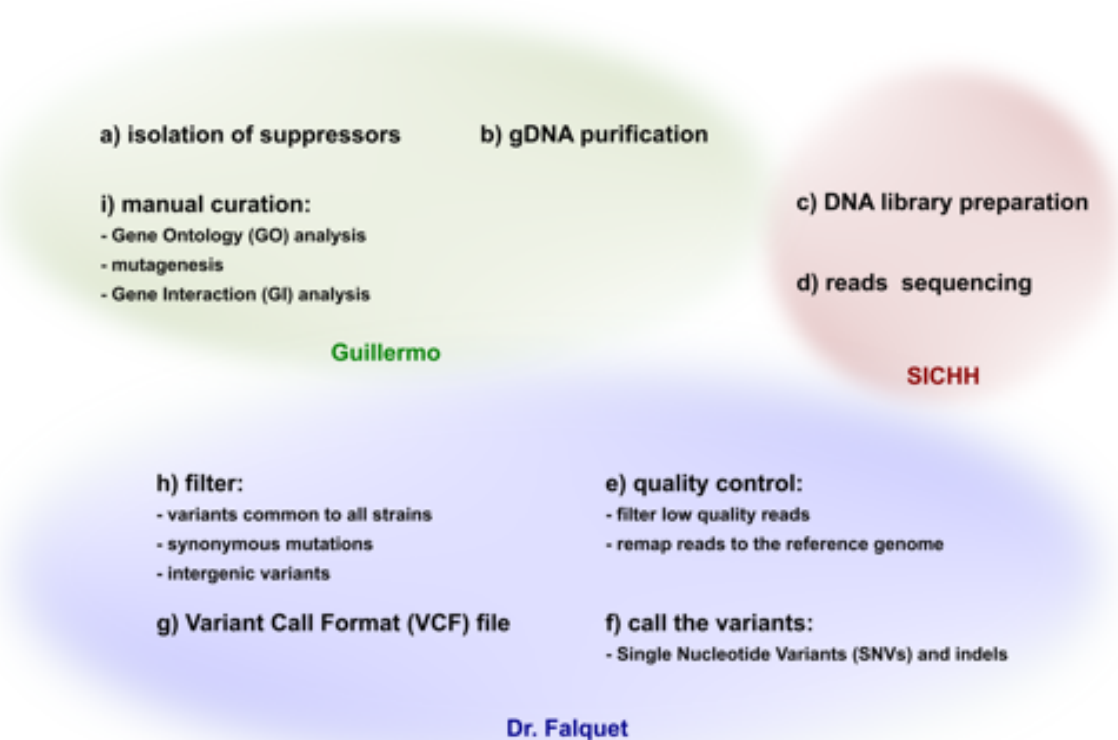


**Figure 2: Pipeline for the classical genetic screen.**

### 1.3.2: Pilot screen

To test the system, we carried out a pilot screen that yielded a total of 17 suppressor candidates (Table 4) (Hatakeyama et al., 2019). As expected, many suppressors harbored mutations in the genes coding for the EGOC components, which most probably are loss of function mutants causing the mislocalization or malfunction of Gtr1<sup>S20L</sup>, thereby relieving TORC1 from the Gtr1<sup>S20L</sup>-mediated growth inhibition. Consistent with a role of Tco89 in targeting TORC1 to the vacuoles and mediating Gtr1<sup>S20L</sup>-dependent TORC1 inhibition (Binda et al., 2009; Hatakeyama et al., 2019;

Varlakhanova et al., 2017), we also identified a loss of function Tco89 mutant (Table 4). Interestingly, we also identified a Tor1 mutant that was able to suppress the Gtr1<sup>S20L</sup>-dependent growth inhibition (Table 4).

Surprisingly, we also identified several mutants within the HOMOtypic fusion and Protein Sorting (HOPS)-tethering complex and the Adaptor Protein 3 (AP-3) complex (Table 4). In yeast, the AP-3 complex (*i.e.*, Apl5, Apl6, Apm3, and Aps3) mediates the cargo-selective trafficking from the trans-Golgi network (TGN) to the vacuole (Cowles et al., 1997) while the HOPS complex (*i.e.*, Vps11, Vps16, Vps18, Vps33, Vam6, and Vps41) mediates the fusion of AP-3-coated vesicles with the vacuole (Bowers & Stevens, 2005; Kuhlee et al., 2015). Finally, we identified a mutant allele for Akr1 (Table 4). Importantly, the Golgi-resident Akr1 enzyme has been shown to palmitoylate, among others, the N-terminus of Ego1, thereby enabling its docking to membranes (Babu et al., 2004; Nadolski & Linder, 2009).

This pilot screen led us to identify, on the one hand, mutations hitting genes coding for well-known TORC1 pathway components (*i.e.*, Ego1, Ego3, Gtr2, Tor1, Tco89, and Vam6) and, on the other hand, genes coding for proteins involved in the Golgi to vacuole transport and protein targeting processes (*i.e.*, Vam6, Vps41, Vps33, Vps11, Apl6, Apm3, and Akr1). Notably, Vam6 has been proposed to exert a dual role both in the formation of the HOPS complex (Caplan et al., 2001; Ostrowicz et al., 2008), and in the EGOc regulation (Binda et al., 2009). The results and conclusions derived from the pilot screen were published in 2019 (Hatakeyama et al., 2019).

Protein/Protein Complex	Mutant Allele
EGOC	Ego1 <sup>N175fs</sup> , Ego1 <sup>R9*</sup> Ego3 <sup>A49P</sup> Gtr2 <sup>E42*</sup> , Gtr2 <sup>E185*</sup> , Gtr2 <sup>C231W</sup> , Gtr2 <sup>L283fs</sup>
TORC1	Tor1 <sup>A1928D</sup> Tco89 <sup>Q140fs</sup>
HOPS	Vam6 <sup>Q391*</sup> Vps41 <sup>N465fs</sup> Vps33 <sup>L18P</sup> Vps11 <sup>Q76*</sup>
AP-3	Apl6 <sup>M1V</sup> , Apl6 <sup>M613R</sup> Apm3 <sup>W31*</sup>
Palmitoyl-transferase	Akr1 <sup>W725*</sup>

**Table 4: List of mutant alleles suppressing the Gtr1<sup>S20L</sup>-mediated growth defect identified during the pilot genetic screen.** Stop codons are marked with an asterisk, and frameshift mutations are denoted with fs. Table published in Hatakeyama et al., 2019.

### 1.3.3: Characterization of the suppressors identified during the pilot classical genetic screen

To prove that the mutations listed in Table 4 (and not other co-occurring mutations) were responsible for the suppression of the Gtr1<sup>S20L</sup>-dependent growth inhibition, we tried to restore the original growth inhibition by expressing, in each case, the wild-type version of these genes. The suppressor mutants (also deleted for *GTR1* and expressing galactose-inducible Gtr1<sup>S20L</sup> from a plasmid) were transformed with either an empty vector (+ C) or a vector coding for a wild-type version of the originally mutated gene (+ *GENE*). The wild-type (WT) and *gtr1*Δ strains were also transformed with the galactose-inducible Gtr1<sup>S20L</sup> and empty vectors, thus serving, respectively, as positive and negative controls for cell growth. When the wild-type versions of the mutant alleles listed in Table 4 were expressed, the Gtr1<sup>S20L</sup>-dependent growth inhibition was restored in the vast majority of the original *gtr1*Δ suppressor mutants (Figure 3A) (Hatakeyama et al., 2019).

Interestingly, the *gtr1*Δ *tor1*<sup>A1928D</sup> suppressor mutant expressing a wild-type version of Tor1 was still partially resistant to the Gtr1<sup>S20L</sup>-mediated growth inhibition (Figure 3A) (Hatakeyama et al., 2019). To independently confirm our results, we decided to delete in the *gtr1*Δ background the respective genes listed in Table 4. The double mutants, the wild-type and the *gtr1*Δ strains were transformed with the galactose-inducible Gtr1<sup>S20L</sup> plasmid and spotted on glucose and galactose-containing plates. In this case, most double mutants, except for the *gtr1*Δ *tor1*Δ and *gtr1*Δ *vam6*Δ strains, suppressed the Gtr1<sup>S20L</sup>-mediated growth inhibition (Figure 3B) (Hatakeyama et al., 2019). Therefore, aside from Tor1<sup>A1928D</sup> and Vam6<sup>Q391\*</sup> variants, most mutant alleles listed in Table 4 can be classified as loss of function mutants.

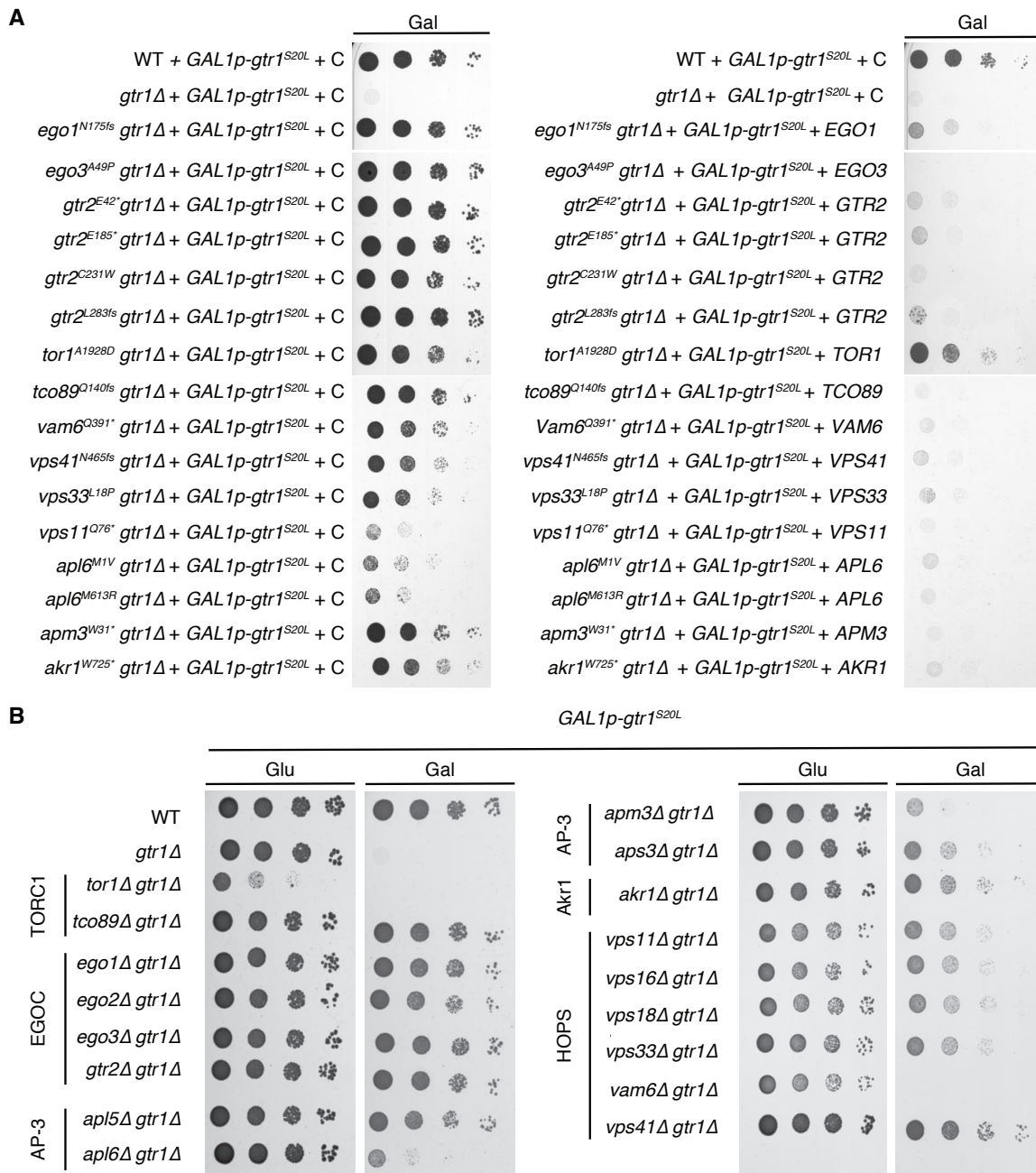


**Figure 3: Characterization of the suppressors listed in Table 4.** (A) Complementation analysis of the mutations (see Table 4) that suppressed the Gtr1<sup>S20L</sup>-mediated growth inhibition. The *gtr1*Δ suppressors were transformed with a plasmid containing the galactose-inducible *gtr1*<sup>S20L</sup> gene, and either an empty vector (+ C) or a vector coding for a wild-type version of the originally mutated gene (+ GENE). The wild-type (WT) and *gtr1*Δ strains were also transformed with the plasmid containing the galactose-inducible *gtr1*<sup>S20L</sup> gene and empty vectors, thus serving, respectively, as positive and negative controls for cell growth. Cells were spotted (10-fold serial dilutions) and grown for 3 days at 30°C on galactose containing plates (Gal). (B) Genes listed in Table 4 were deleted in the *gtr1*Δ background. Strains were analyzed as in (A). Figure published in Hatakeyama et al., 2019.

### 1.3.4: EGOC, but not TORC1, reaches the vacuolar surface via the AP-3 pathway

The fact that we got several mutants within the HOPS and AP-3 complex - which selectively channels cargo from the TGN to the vacuole - led us to entertain a hypothesis by which the EGOC would be palmitoylated (Ego1 particularly) at the TGN

and delivered to the vacuole via the AP-3/HOPS pathway (Hatakeyama et al., 2019). To test this, Dr. Hatakeyama examined the subcellular distribution of Ego1-GFP, GFP-Gtr1, and GFP-Tor1 in a subset of AP-3 and HOPS null mutants (*i.e.*, *apl5* $\Delta$ , *apl6* $\Delta$  and *vam6* $\Delta$ , *vps41* $\Delta$ , respectively) (Figure 4). In wild-type cells (WT), genomically-tagged Ego1-GFP, GFP-Gtr1, and GFP-Tor1 were localized on vacuolar membranes and perivacuolar foci (white arrows).

Surprisingly, loss of Apl5 or Apl6 (AP-3 components) partially diverted Ego1-GFP and GFP-Gtr1, but not GFP-Tor1, to the plasma membrane, although, Ego1-GFP was still detected at perivacuolar foci (Figure 4) (Hatakeyama et al., 2019). More dramatically, loss of Vam6 or Vps41 not only partially diverted Ego1-GFP and GFP-Gtr1 to the plasma membrane but also dispersed them from the fragmented vacuoles (Figures 4A and 4B) (Hatakeyama et al., 2019). Based on these results, we can conclude that EGO1, but not TORC1, travels from the TGN to the vacuoles principally through the AP-3 pathway (Hatakeyama et al., 2019).

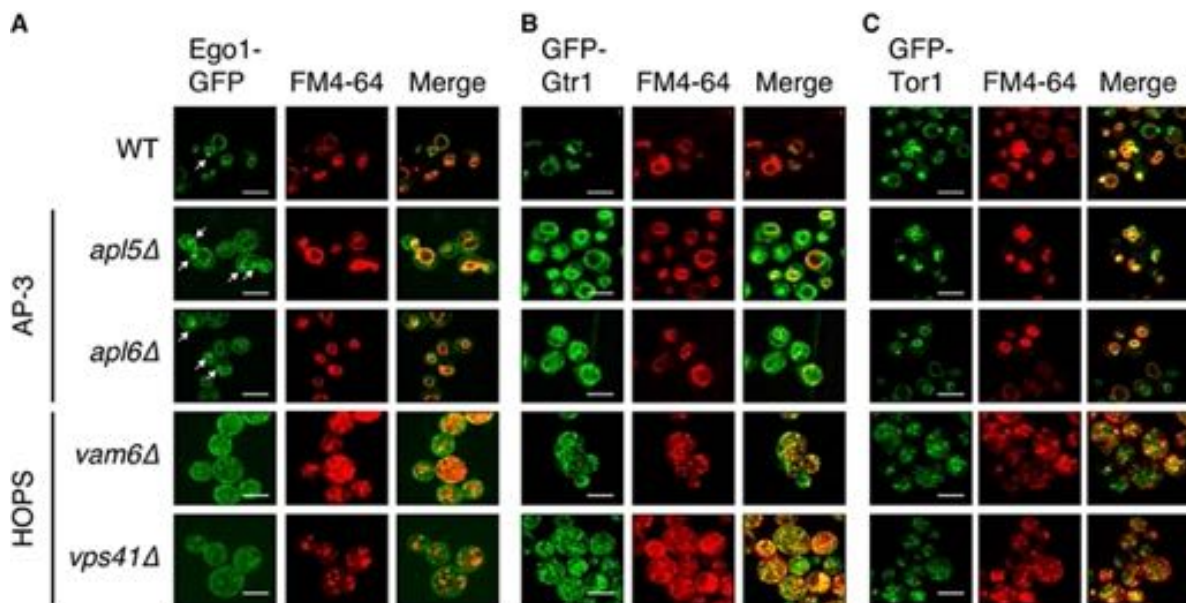


**Figure 4: EGO1, but not TORC1, reaches the vacuolar surface via the AP-3 pathway.** (A and B) Genomically tagged Ego1-GFP (A) and GFP-Gtr1 (B) are localized on vacuolar membranes and perivacuolar foci (white arrows) in wild-type (WT) cells but are partially diverted to the plasma membrane and dispersed from the vacuolar membrane, respectively, in AP-3 pathway (*i.e.*, *apl5* $\Delta$  and *apl6* $\Delta$ ) and HOPS complex (*i.e.*, *vam6* $\Delta$  and *vps41* $\Delta$ ) mutants. Perivacuolar localization of Ego1-GFP was still detectable in AP-3 pathway mutants (A). Moreover, the loss of HOPS complex subunits resulted in the fragmentation of vacuoles. (C) AP-3 and HOPS complex function is not required for vacuolar membrane tethering of genomically tagged GFP-Tor1. All strains were grown to exponential phase in synthetic dextrose (SD) medium, stained with the lipophilic styryl dye FM4-64 to visualize vacuolar membranes, and analyzed by fluorescence microscopy. Scale bars, 5 mm (white). Figure published in Hatakeyama et al., 2019.

### 1.3.5: Large classical genetic screen: the seed for new projects

Given that the pilot screen successfully helped us to understand, hitherto, hidden aspects of the TORC1 signaling pathway, we decided to upscale the screen to identify more mutants following the same pipeline as before (Figure 2). This new screen yielded a total of 101 suppressors (Table 5). As expected, more than 50% of the mutant alleles concentrated on the genes already identified in Table 4 (members of the EGO, TORC1, HOPS, AP-3, as well as the palmitoyl transferase Akr1) (Table 5). Interestingly, we identified more mutations within the *TOR1* sequence. Studying these mutants could unveil different aspects of Tor1 regulation or TORC1 assembly; even though this matter was not explored during our investigations, it could be of particular interest for a new study. Due to time constraints, except for Opy1, we did not have the opportunity to *in vivo* characterize the mutant alleles listed in Table 5.

Proteins	Hits	Mutant Allele
EGOC	20	Ego1 <sup>N175fs</sup> Ego2 <sup>A69D</sup> Ego3 <sup>A49P</sup> , Ego3 <sup>Y139*</sup> Gtr1 <sup>Q65*</sup> , Gtr1 <sup>H126Y</sup> , Gtr1 <sup>Q190fs</sup> , Gtr1 <sup>S230fs</sup> , Gtr1 <sup>R242*</sup> , Gtr1 <sup>S256fs</sup> , Gtr1 <sup>S279*</sup> Gtr2 <sup>E42*</sup> , Gtr1 <sup>G65R</sup> , Gtr2 <sup>A85fs</sup> , Gtr2 <sup>D132Y</sup> , Gtr2 <sup>S176T</sup> , Gtr2 <sup>E185*</sup> , Gtr2 <sup>K22I</sup> , Gtr2 <sup>R251*</sup> , Gtr2 <sup>L283fs</sup>
TORC1	12	Tor1 <sup>T491M</sup> , Tor1 <sup>N1369I</sup> , Tor1 <sup>A1928D</sup> , Tor1 <sup>W2038L</sup> , Tor1 <sup>F2358S</sup> , Tor2 <sup>E2360K</sup> Tco89 <sup>F579V</sup> , Tco89 <sup>Q140fs</sup> , Tco89 <sup>S33*</sup> , Tco89 <sup>G219*</sup> , Tco89 <sup>I315fs</sup> , Tco89 <sup>Q598*</sup>
HOPS/CORVET	14	Vps41 <sup>A130fs</sup> , Vps41 <sup>A169D</sup> , Vps41 <sup>Q190fs</sup> , Vps41 <sup>S204*</sup> , Vps41 <sup>T245fs</sup> , Vps41 <sup>N465fs</sup> Vam6 <sup>Y967*</sup> , Vam6 <sup>I287fs</sup> , Vam6 <sup>L596fs</sup> , Vam6 <sup>W357*</sup> Vps11 <sup>S632*</sup> , Vps11 <sup>K943fs</sup> , VPS11 <sup>E988*</sup> Vps8 <sup>E1219*</sup>
AP-3	5	Apl5 <sup>N229fs</sup> , Apl5 <sup>L74*</sup> , Apl5 <sup>Q567*</sup> Apm3 <sup>W31*</sup> , Apm3 <sup>V428fs</sup>
Akr1	3	Akr1 <sup>K96*</sup> , Akr1 <sup>Q416*</sup> , Akr1 <sup>W725*</sup>
Cyc8	3	Cyc8 <sup>Q262*</sup> , Cyc8 <sup>A540P</sup> , Cyc8 <sup>Q547H</sup>
Nsp1	3	Nsp1 <sup>L355F</sup> , Nsp1 <sup>F380I</sup> , Nsp1 <sup>F450L</sup>
Bbc1	2	Bbc1 <sup>V715E</sup> , Bbc1 <sup>S737P</sup>
Fit3	2	Fit3 <sup>G47A</sup> , Fit3 <sup>G47S</sup>
Kex2	2	Kex2 <sup>D105A</sup> , Kex2 <sup>S708*</sup>
Num1	2	Num1 <sup>E823D</sup> , Num1 <sup>E1364A</sup>
Pir3	2	Pir3 <sup>V113D</sup> , Pir3 <sup>V131G</sup>
Yhr214c-e	2	Yhr214c-e <sup>L21I</sup> , Yhr214c-e <sup>F26C</sup>
Others	30	Aga1 <sup>L237*</sup> , Akl1 <sup>N983H</sup> , Atg33 <sup>T143K</sup> , Bni4 <sup>N406T</sup> , Cin8 <sup>T548K</sup> , Cts1 <sup>G477D</sup> , Fab1 <sup>N590del</sup> , Hek2 <sup>T30P</sup> , Imp2 <sup>D111A</sup> , Isr1 <sup>S360L</sup> , Mit1 <sup>N362del</sup> , Nfi1 <sup>N16del</sup> , Opy1 <sup>N250K</sup> , Pho86 <sup>G289V</sup> , Prm8 <sup>N193T</sup> , Put1 <sup>L140V</sup> , Rrp17 <sup>F213I</sup> , Sgf73 <sup>D146N</sup> , Tao3 <sup>V714M</sup> , Ycr101c <sup>K179T</sup> , Ydl034w <sup>V110G</sup> , Yfr016c <sup>G883E</sup> , Yft2 <sup>F199L</sup> , Ygl177w <sup>E28K</sup> , Yki083w <sup>M13fs</sup> , Ylr412c-a <sup>Q53fs</sup> , Ynl190w <sup>K99Q</sup> , Ypt10 <sup>S193R</sup> , Ysw1 <sup>E451*</sup>

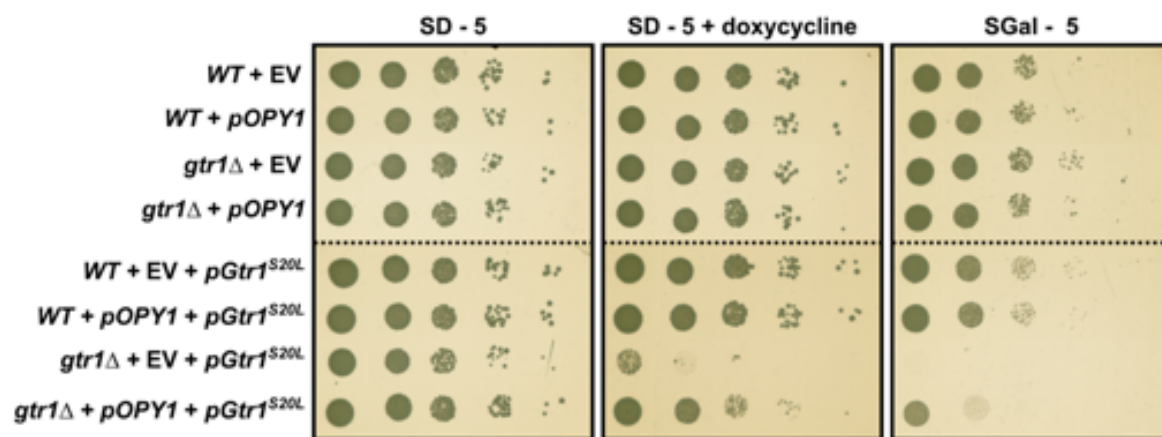
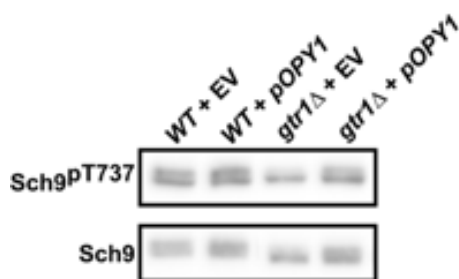
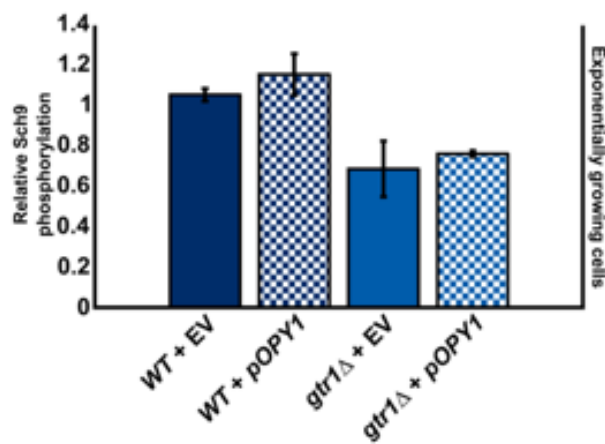
**Table 5: Complete set of mutant alleles that suppressed the Gtr1<sup>S20L</sup>-mediated growth defect.** Stop codons are marked with an asterisk, and frameshift mutations are denoted with fs.

### 1.3.6: Characterization of OPY1 as a putative TORC1 regulator

During the classical suppressor screen, we identified, among others, the *opy1*<sup>N250K</sup> mutation. Hitherto, Opy1 has been proposed to be involved in the metabolism of Phosphatidylinositol-4,5-bisphosphate (PI(4,5)P<sub>2</sub>), a phospholipid present in cell membranes and particularly enriched in the inner leaflet of the plasma membrane. Interestingly, Phosphatidylinositol-4-phosphate (PI4P) and PI(4,5)P<sub>2</sub> have been shown to regulate different steps of the vacuole fusion cycle (Starr & Fratti, 2019 and references therein). Opy1 inhibits Mss4 - the Phosphatidylinositol-4-phosphate 5-kinase - in response to high levels of PI(4,5)P<sub>2</sub> at the plasma membrane (Ling et al., 2012). In detail, Opy1 has two Pleckstrin Homology (PH) domains which are important for recruiting proteins to cellular membranes. The PH1 domain seems to mediate the inhibition of Mss4, while the PH2 domain of Opy1 has been proposed to bind PI(4,5)P<sub>2</sub> (Ling et al., 2012). Interestingly, the mutation identified during the classic screening lies within the PH2 domain (Opy1<sup>N250K</sup>), which may affect the affinity of Opy1 towards PI(4,5)P<sub>2</sub>, thereby affecting its metabolism.

First, we tried to test the effects of *OPY1* deletion. Unfortunately, the *OPY1* sequence lies within the *ATG14* promoter sequence, thus, deleting *OPY1* may affect the expression of *ATG14* (data not shown). For this reason, we decided to test instead the effects associated with its overexpression. As shown before in the text, induced overexpression of Gtr1<sup>S20L</sup> (*pGtr1*<sup>S20L</sup>) in the *gtr1*Δ background leads to cell growth inhibition. For this experiment, we used two different centromeric plasmids coding for Gtr1<sup>S20L</sup> (*pGtr1*<sup>S20L</sup>) under the control of either a doxycycline-inducible promoter or a galactose-inducible promoter. Surprisingly, expressing an extra copy of Opy1 from an integrative plasmid (*pOPY1*) was sufficient to suppress the Gtr1<sup>S20L</sup>-dependent growth inhibition (Figure 5A) in both doxycycline and galactose containing plates. Notably, the expression of an extra copy of Opy1 did not affect the levels of TORC1 activity in exponentially growing cells (Figures 5B and 5C). These findings suggest that Opy1 can influence the TORC1 pathway.



**A****B****C**

**Figure 5: Opy1 overexpression is sufficient to suppress the Gtr1<sup>S20L</sup>-mediated growth arrest.** (A) Opy1 overexpression allows *gtr1*Δ overexpressing Gtr1<sup>S20L</sup> cells to grow. Wild-type (WT) and *gtr1*Δ cells were transformed with two different centromeric plasmids coding for Gtr1<sup>S20L</sup> (*pGtr1<sup>S20L</sup>*) under the control of either a doxycycline-inducible promoter or a galactose-inducible promoter. The specified strains were also transformed either with an empty integrative plasmid (EV) or an integrative plasmid encoding Opy1 (*pOPY1*). Prototrophic cells with the indicated genotypes were grown exponentially in the SD-5 medium (SD; 0.17% yeast nitrogen base, 0.5% ammonium sulfate [AS], 0.2% dropout mix [USBiological, D9540-05], and 2% glucose). Serial 10 fold dilutions were spotted on plates containing SGal-5 (like SD-5 but substituting 2% Glucose with 2% Galactose) medium or SD-5 medium plus either ethanol as vehicle or 10 μg/ml doxycycline. (B) Opy1 overexpression does not affect the levels of TORC1 activity in exponentially growing cells. Wild-type (WT) and *gtr1*Δ cells were transformed either with an empty integrative plasmid (EV) or an integrative plasmid encoding Opy1 (*pOPY1*). Prototrophic cells with the indicated genotypes were grown exponentially in SD-5 medium and then shifted to SC medium (SC; 0.17% yeast nitrogen base, 0.5% ammonium sulfate [AS], 0.2% dropout mix [USBiological, D9515], and 2% glucose). Protein extracts were analyzed by SDS-PAGE and probed with anti-Sch9-<sup>P</sup>Thr737 and anti-Sch9 antibodies. Relative TORC1 activities were determined as the ratio of Sch9-<sup>P</sup>Thr737/Sch9 normalized to that of WT cells. Data represent means ± SEM across subjects (N=3).

### 1.3.7: Introduction to the SATAY project

The classical suppressor screen turned out to be a powerful method to identify new players within the TORC1 signaling pathway. An alternative powerful screen is the SATurated Transposon Analysis in Yeast (SATAY), which couples saturated transposon mutagenesis to high-throughput sequencing (Michel et al., 2017). SATAY is extremely



useful in analyzing genetic interactions and identifying drug targets, conditionally essential genes, and protein domains (Michel et al., 2017, 2019). In this system, we use cells in which the *ADE2* gene is interrupted by a miniDs transposon (Michel et al., 2017, 2019). Besides, we use a 2 $\mu$  plasmid coding for a galactose-inducible Ac transposase and a 600 bp repair template for homology-directed repair (HDR), which, upon galactose induction, helps repair the excision of the miniDs transposon from the *ADE2* locus (Michel et al., 2019). Therefore, upon galactose induction, the transposon inserts elsewhere in the genome, and the *ADE2* gene is reconstituted by HDR, rendering cells prototrophic for adenine (Michel et al., 2019). We can generate libraries of millions of transposon mutants with this system and subject them to different selective pressures.

This screen was conducted in collaboration with Prof. Dr. Kornmann and Dr. Michel (Kornmann's laboratory at the University of Oxford). On our side, we were responsible for the generation (approximately 5600000 transposon mutants) and amplification of the library of *gtr1* $\Delta$  transposon mutants. Subsequently, we performed 2 consecutive rounds of selection (via the overexpression of *Gtr1*<sup>S20L</sup>) by diluting cells down to 0.1 and letting them grow during 5 generations (10 generations in total) while overexpressing of *Gtr1*<sup>S20L</sup>. Cell pellets were collected during the 1st and 2nd rounds of selection and subjected to genomic DNA extraction (Figure 6).

On the other side, Kornmann's lab was responsible for sequencing, aligning - to a reference yeast genome - and quantifying the reads as previously described (Michel et al., 2017). As output, they provided us with the number of transposons per gene (TPG), the number of reads per gene (RPG), and the link to the genome browser where we can revise the genomic transposon distribution sequenced for the *Gtr1*<sup>S20L</sup> overexpressing population and for the already reported wild-type library (No Compound library) (Michel et al., 2019) (DoxA and DoxB correspond to the *Gtr1*<sup>S20L</sup> overexpressing population while 20181122.A-NC\_R1.fastq\_trimmed corresponds to the wild-type population:

[http://genome-euro.ucsc.edu/s/AgnesHM/Guillermo\\_Gtr1S20L\\_Wig\\_25Feb2020](http://genome-euro.ucsc.edu/s/AgnesHM/Guillermo_Gtr1S20L_Wig_25Feb2020)). The number of transposons per gene (TPG) indicates the number of different positions in which transposons were found within a gene (variability), while the number of reads per gene (RPG) accounts for the total number of transposons, regardless of the position, interrupting a gene. In our experiment, we compared the number of TPG and RPG between the wild-type and *Gtr1*<sup>S20L</sup> overexpressing populations for each gene. As a cut-off, we decided to consider only the genes that were interrupted at least in 5 different

sites (5 TPG) and at least a total of 25 times (25 RPG) in either the wild-type or the  $Gtr1^{S20L}$  overexpressing population.

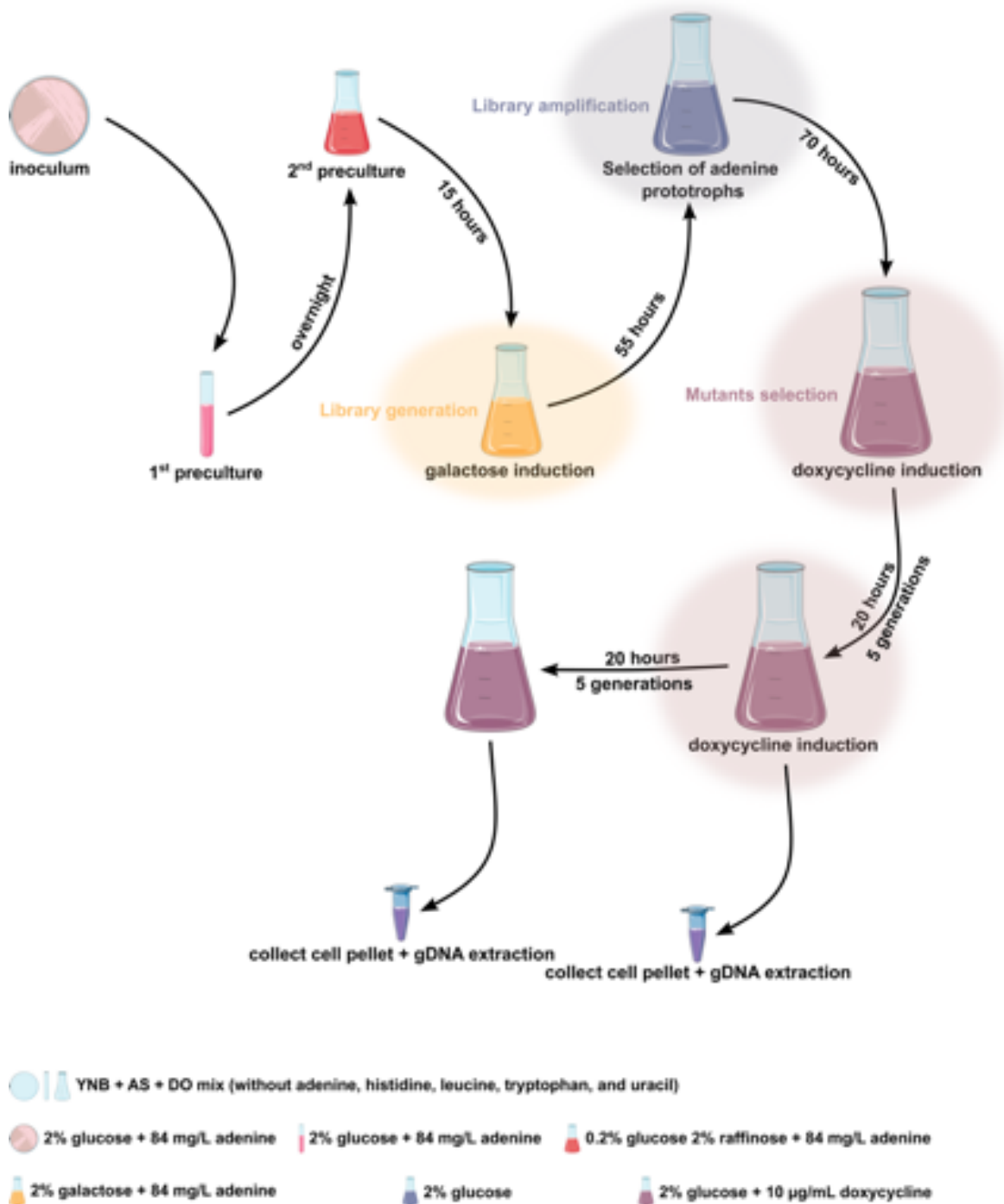


**Figure 6: Pipeline for the SATAY screen.** The icons used here were taken and adapted from Smart. Servier Medical Art. (2020, September 2 ; <https://smart.servier.com/>).

If in the  $Gtr1^{S20L}$  overexpressing population we quantified more TPG and RPG for a particular gene, we hypothesized that the loss of the protein encoded in that gene helps cells suppress the  $Gtr1^{S20L}$ -mediated growth inhibition. In contrast, if in the  $Gtr1^{S20L}$

overexpressing population we quantified fewer TPG and RPG for a particular gene, we considered that the loss of the corresponding protein prevents cells from suppressing the Gtr1<sup>S20L</sup>-mediated growth inhibition. Following this logic and to assess whether our experiment was correctly performed, we analyzed the number of TPG and RPG in a subset of genes coding for well-known TORC1 pathway components (Table 4).

### 1.3.8: Analysis of well-known and putative TORC1 regulators using SATAY

As expected, in the Gtr1<sup>S20L</sup> overexpressing population, genes coding for the EGO components showed higher variability (TPG) and total number of transposon mutants (RPG) - except for *EGO2*, which did not pass the cut-off (Table 6). Most probably, these transposon mutants impair the proper assembly of Gtr1<sup>S20L</sup> in a functional EGO. In contrast, fewer transposition events (both TPG and RPG) interrupting *TOR1* and *TCO89* were found in the Gtr1<sup>S20L</sup> overexpressing population (Table 6).

Gene	TPG	RPG
	log <sub>2</sub> (Fold change)	log <sub>2</sub> (Fold change)
<i>EGO1</i>	2.43	4.77
<i>EGO3</i>	0.23	0.92
<i>GTR1</i>	3.43	5.17
<i>GTR2</i>	1.82	3.68
<i>TOR1</i>	-1.90	-6.69
<i>TCO89</i>	-0.38	-1.48
<i>VPS41</i>	1.40	0.71
<i>VAM6</i>	1.69	3.75
<i>VPS11</i>	0.71	1.55
<i>VPS8</i>	0.86	2.31
<i>APL5</i>	0.88	0.74
<i>APM3</i>	0.22	0.80
<i>AKR1</i>	0.30	-3.36

**Table 6: Number of Transposons Per Gene (TPGs) and Reads Per Gene (RPGs) in a subset of genes that code for TORC1 pathway components.** Only those loci with at least 5 TPGs and 25 RPGs were considered (cut-off).

Besides, we performed a similar analysis for a subset of genes coding for HOPS/CORVET (*i.e.*, *Vps41*, *Vam6*, *Vps11*, and *Vps8*) and AP-3 (*i.e.*, *Apl5*, *Apm3*) components and, as expected, more transposon mutants interrupting these genes (Higher TPG and RPG values) were found in the Gtr1<sup>S20L</sup> overexpressing population (Table 6). These transposon mutants probably relieve TORC1 from the Gtr1<sup>S20L</sup>-mediated growth inhibition by diverting or displacing the EGO from the vacuolar membrane. Finally, we also focused on the *AKR1* locus. Surprisingly, In the Gtr1<sup>S20L</sup> overexpressing population, there was a higher variability (high TPG) but fewer transposon mutants (RPG) interrupting the *AKR1* locus (Table 6). Notably, we identified,



with this, during the classical screen, we identified three *CYC8* mutations from which two of them occurred very close to the codon for the alanine 554 of *Cyc8* (*i.e.*, *Cyc8*<sup>A540P</sup> and *Cyc8*<sup>Q547H</sup>), which lie within the *Cyc8* prion domain. The identification of several mutants within the *Cyc8* prion domain in two independent screens lead us to believe that loss of this domain may be sufficient to suppress the *Gtr1*<sup>S20L</sup>-dependent growth inhibition.

*Cts1* is an endochitinase required for cell separation after mitosis, and recently, it has been shown to play an important role in cellular lifespan (Molon et al., 2018). Analysis of the transposition pattern within the *CTS1* locus in the *Gtr1*<sup>S20L</sup> overexpressing population revealed enrichment of transposon mutants in the codon for asparagine 552, which lies within the chitin-binding domain of this protein. Besides, we identified a point mutation close by the chitin-binding domain of *Cts1* (*Cts1*<sup>G477D</sup>) during the classical suppressor screen.

On the contrary, transposon mutants in the *YNL190W*, *KEX2*, and *OPY1* loci were significantly reduced (low TPG and RPG values) in the *Gtr1*<sup>S20L</sup> overexpressing population. This leads us to suspect that the mutations identified for these genes and listed in Table 5 are, most probably, gain of function mutants. Particularly interesting are *Kex2* and *Opy1* alleles. *Kex2* is a subtilisin-like serine proteinase involved in the processing of alpha-pheromone precursors, killer toxin precursors, and aspartic proteinase propeptides (Bader et al., 2008). In the case of *Opy1*, its overexpression has been shown, in a previous paragraph, to suppress the *Gtr1*<sup>S20L</sup>-dependent growth inhibition. Considering all these results, we can conclude that, based on the analysis of well-known TORC1 components, the results obtained from SATAY appear reliable. It would therefore be worth studying the exact role of *Cyc8*, *Cts1*, *Kex2*, and *Opy1* within the TORC1 signaling pathway.

### 1.3.9: Gene Ontology (GO) enrichment analysis of the SATAY

We sought to understand in which biological processes the genes accumulating more and fewer transposons in the *Gtr1*<sup>S20L</sup> overexpressing population were involved. For that, we selected the genes that, in the *Gtr1*<sup>S20L</sup> overexpressing population, accumulated at least 2.5 times more transposons or at least 3 times fewer transposons with respect to the wild-type population. Figure 8, Table 7, and Table 8 summarize the

genes and the GO terms associated with the transposon-enriched and the transposon-impooverished genes sequenced in the Gtr1<sup>S20L</sup> overexpressing population.

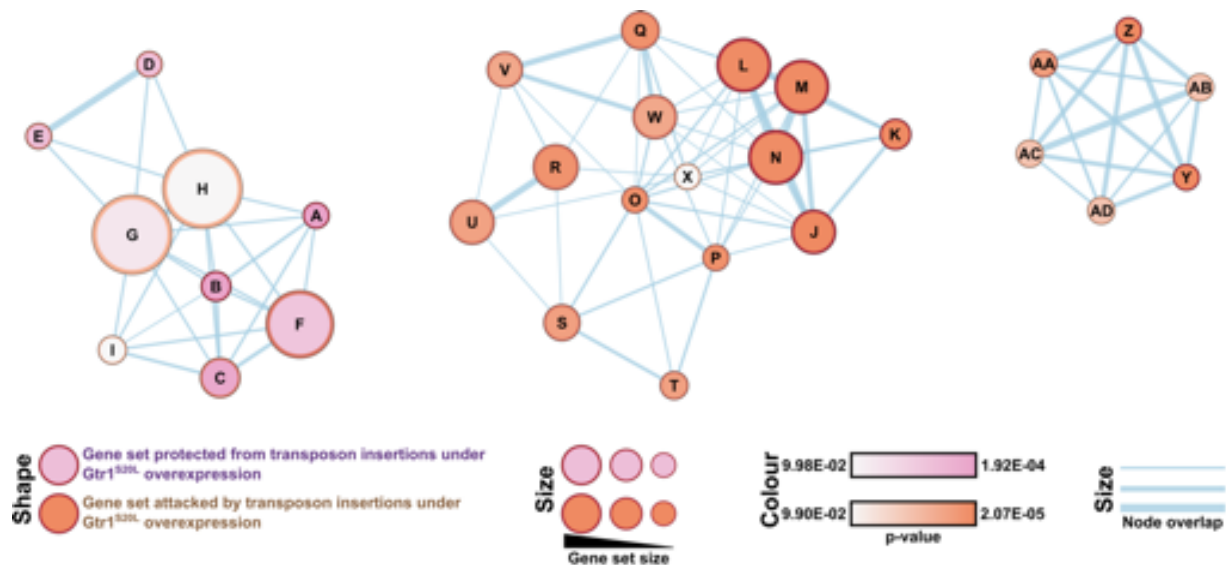


**Figure 8: GO terms associated with the transposon-enriched and the transposon-impooverished genes sequenced in the Gtr1<sup>S20L</sup> overexpressing population.** A functional enrichment analysis was performed using gprofiler applying a p-value < 0.025. Publication-ready enrichment map was generated using Cytoscape. Node cut-off FDR Q value < 0.05 and edge cut-off < 0.5.

Node	GO term	Description	p-value
A	GO:0034967	Set3 complex	1.92E-04
B	GO:0000118	histone deacetylase complex	9.76E-04
C	GO:0000785	chromatin	6.90E-03
D	GO:0045254	pyruvate dehydrogenase complex	3.37E-02
E	GO:0005967	mitochondrial pyruvate dehydrogenase complex	3.37E-02
F	GO:0005694	chromosome	4.07E-02
G	GO:0043231	intracellular membrane-bounded organelle	7.92E-02
H	GO:0043227	membrane-bounded organelle	9.80E-02
I	GO:0097346	INO80-type complex	9.98E-02
J	GO:0034657	GID complex	6.89E-04
K	GO:0045721	negative regulation of gluconeogenesis	8.23E-04
L	GO:0062014	negative regulation of small molecule metabolic process	1.81E-02
M	GO:0010677	negative regulation of cellular carbohydrate metabolic process	5.28E-02
N	GO:0045912	negative regulation of carbohydrate metabolic process	5.28E-02
O	GO:0006111	regulation of gluconeogenesis	5.28E-02
P	GO:0005768	endosome	2.07E-05
Q	GO:0005770	late endosome	1.07E-03
R	GO:0097708	intracellular vesicle	2.15E-03
S	GO:0031410	cytoplasmic vesicle	2.15E-03
T	GO:0031982	vesicle	2.91E-03
U	GO:0033263	CORVET complex	6.96E-03
V	GO:0030897	HOPS complex	6.96E-03
W	GO:0072665	protein localization to vacuole	7.11E-03
X	GO:0061919	process utilizing autophagic mechanism	8.11E-03
Y	GO:0007033	vacuole organization	2.04E-02
Z	GO:0044088	regulation of vacuole organization	2.12E-02
AA	GO:0006914	autophagy	2.19E-02
AB	GO:0006623	protein targeting to vacuole	2.74E-02
AC	GO:0007034	vacuolar transport	2.74E-02
AD	GO:1903778	protein localization to vacuolar membrane	9.90E-02

**Table 7: List of GO terms depicted in Figure 8.** Gene set coding for transposon-enriched genes and Gene set coding for transposon-impoverished genes in the Gtr1<sup>S20L</sup> overexpressing population.

As expected, a higher number of transposon mutants of genes coding for the HOPS (Table 7: GO:0030897) and CORVET (class C core vacuole/endosome tethering) (Table 7: GO:0033263) complexes as well as those involved in the endosome and vacuolar organization (Table 7: GO:0005768, GO:0007033) were enriched in the Gtr1<sup>S20L</sup> overexpressing population. Most probably, these transposon mutants suppress the Gtr1<sup>S20L</sup>-mediated growth inhibition because they abolish the delivery of the EGOc to the vacuolar membrane by interrupting genes coding for proteins involved in the proper delivery of the EGOc to the vacuolar membrane or for proteins involved in the proper formation of the vacuolar membrane *per se*.

Interestingly, transposon mutants interrupting genes involved in the negative regulation of gluconeogenesis were enriched in the Gtr1<sup>S20L</sup> overexpressing population (Table 7: GO:0034657, GO:0045721, GO:0062014, GO:0010677, GO:0045912, GO:0006111). Indeed, the enrichment of transposon mutants interrupting the genes coding for the GID (Glucose Induced degradation Deficient) complex components (Table 7: GO:0034657) is particularly interesting. The GID complex (*e.g.*, Vid30, Rmd5, Vid24, Vid28, Gid7, Gid8, and Fyv10), which has ubiquitin-ligase activity, is involved in the regulation of the carbon metabolism by marking gluconeogenic enzymes such as FBpase (Fructose-1,6-biphosphatase) and Mdh2 (Malate dehydrogenase) for degradation in cells growing in the presence of glucose (Hung et al., 2004; Nakatsukasa et al., 2015; Santt et al., 2008). In contrast, transposon mutants interrupting genes coding for the mitochondrial pyruvate dehydrogenase complex (Pda1, Pdb1, Pdx1 Lat1, and Lpd1) (Table 7: GO:0045254) were reduced in the Gtr1<sup>S20L</sup> overexpressing population. Impairment of the mitochondrial pyruvate dehydrogenase complex formation leads to a disruption of the TCA-cycle flux which has been already shown to affect, negatively, the TORC1 activity by a decrease in the biosynthesis of glutamine from  $\alpha$ -ketoglutarate and by the activation of AMPK (Snf1) by a high ADP: ATP ratio (Kingsbury et al., 2015).

Interestingly, transposon mutants hitting genes coding for subunits of specific chromatin remodelers, such as histone deacetylase complexes, were reduced in the Gtr1<sup>S20L</sup> overexpressing population (Table 7: GO:0034967, GO:0000118, GO:0097346). For instance, the INO80 type-complex (Table 7: GO:0097346), which includes the Srw1 and the INO80 complexes, has already been shown to work



downstream the TORC1 signaling pathway promoting the transcription of TORC1-responsive genes (Beckwith et al., 2018). As another example, transposon mutants interrupting the genes coding for members of the histone deacetylase Set3 complex (Lenstra et al., 2011) were reduced in the Gtr1<sup>S20L</sup> overexpressing population (Table 7: GO:0034967). In sum, the GO enrichment analysis not only confirmed the importance of the HOPS complex integrity (as transposition-induced HOPS mutants may suppress the Gtr1<sup>S20L</sup>-induced growth inhibition by altering the subcellular localization of the EGO) but also unveiled the GID and Set3 complexes as putative new players within the TORC1 signaling pathway.

Gene	Description	Fold Change
TOR1	PIK-related protein kinase and rapamycin target	-103.25
MDM31	Mitochondrial protein that may have a role in phospholipid metabolism	-93.70
PDA1	E1 alpha subunit of the pyruvate dehydrogenase (PDH) complex	-70.03
GEF1	Voltage-gated chloride channel; localized to the golgi, the endosomal system, and plasma membrane; involved in cation homeostasis	-64.89
CAF40	Component of the CCR4-NOT transcriptional complex; evolutionarily conserved; involved in controlling mRNA initiation, elongation, and degradation	-64.89
AGE2	ADP-ribosylation factor (ARF) GTPase activating protein (GAP) effector; involved in Trans-Golgi-Network (TGN) transport	-62.68
LEU4	Alpha-isopropylmalate synthase (2-isopropylmalate synthase); the main isozyme responsible for the first step in the leucine biosynthesis pathway	-56.10
MVP1	Protein required for sorting proteins to the vacuole; Mvp1p and Vps1p act in concert to promote membrane traffic to the vacuole	-51.63
ADH3	Mitochondrial alcohol dehydrogenase isozyme III; involved in the shuttling of mitochondrial NADH to the cytosol under anaerobic conditions and ethanol production	-51.27
PDX1	E3-binding protein of the mitochondrial pyruvate dehydrogenase complex	-48.17
BSD2	Heavy metal ion homeostasis protein; facilitates trafficking of Smf1p and Smf2p metal transporters to vacuole where they are degraded	-40.79
APM1	Mu1-like medium subunit of the AP-1 complex	-40.50
SLT2	Serine/threonine MAP kinase; coordinates expression of all 19S regulatory particle assembly-chaperones (RACs) to control proteasome abundance	-38.85
MRN1	RNA-binding protein that may be involved in translational regulation; binds specific categories of mRNAs, including those that contain upstream open reading frames (uORFs) and internal ribosome entry sites (IRES)	-38.05
SRB8	Subunit of the RNA polymerase II mediator complex	-34.06
PRP4	Splicing factor; component of the U4/U6-U5 snRNP complex	-32.22
TDA7	Cell cycle-regulated gene of unknown function; promoter bound by Fkh2p	-30.91
LGE1	Protein of unknown function; null mutant forms abnormally large cells, and homozygous diploid null mutant displays delayed premeiotic DNA synthesis and reduced efficiency of meiotic nuclear division	-30.70
DIF1	Protein that regulates nuclear localization of Rnr2p and Rnr4p; phosphorylated by Dun1p in response to DNA damage and degraded	-29.86



COX12	Subunit VIb of cytochrome c oxidase; cytochrome c oxidase is also known as respiratory Complex IV and is the terminal member of the mitochondrial inner membrane electron transport chain	-29.04
EAF1	Component of the NuA4 histone acetyltransferase complex	-29.04
CEM1	Mitochondrial beta-keto-acyl synthase; possible role in fatty acid synthesis; required for mitochondrial respiration	-28.44
ORM2	Protein that mediates sphingolipid homeostasis	-28.44
TRS65	Component of transport protein particle (TRAPP) complex II; TRAPP II is a multimeric guanine nucleotide-exchange factor for the GTPase Ypt1p, regulating intra-Golgi and endosome-Golgi traffic	-28.25
ADH4	Alcohol dehydrogenase isoenzyme type IV	-27.28
VTH1	Putative membrane glycoprotein; has strong similarity to Vth2p and Pep1p/Vps10p; may be involved in vacuolar protein sorting	-25.81
MGM101	Protein with a role in mitochondrial DNA recombinational repair; also involved in interstrand cross-link repair; binds to and catalyzes the annealing of single-stranded mtDNA	-25.28
AEP1	Protein required for expression of the mitochondrial OLI1 gene; mitochondrial OLI1 gene encodes subunit 9 of F1-F0 ATP synthase	-25.11
YGR283C	Putative methyltransferase	-24.76
VPS71	Nucleosome-binding component of the SWR1 complex; SWR1 exchanges histone variant H2AZ (Htz1p) for chromatin-bound histone H2A; required for vacuolar protein sorting	-24.42
ECM31	Ketopantoate hydroxymethyltransferase; required for pantothenic acid biosynthesis	-24.25
CGI121	Component of the EKC/KEOPS complex; EKC/KEOPS complex is required for t6A tRNA modification and telomeric TG1-3 recombination	-24.08
GUP1	Plasma membrane protein involved in remodeling GPI anchors; member of the MBOAT family of putative membrane-bound O-acyltransferases; role in misfolded protein quality control	-23.92
RTT105	Protein with a role in regulation of Ty1 transposition	-23.43
YCK2	Palmitoylated plasma membrane-bound casein kinase I (CK1) isoform	-23.26
MED4	Subunit of the RNA polymerase II mediator complex	-23.10
FSF1	Putative protein; predicted to be an alpha-isopropylmalate carrier; belongs to the sideroblastic-associated protein family; non-tagged protein is detected in purified mitochondria; likely to play a role in iron homeostasis	-23.10
AVO1	Component of a membrane-bound complex containing the Tor2p kinase; contains Tor2p kinase and other proteins; may have a role in regulation of cell growth	-22.94
PIB1	RING-type ubiquitin ligase of the endosomal and vacuolar membranes; binds phosphatidylinositol(3)-phosphate; contains a FYVE finger domain	-22.94
SEC12	Guanine nucleotide exchange factor (GEF); activates Sar1p by catalyzing the exchange of GDP for GTP; required for the initiation of COPII vesicle formation in ER to Golgi transport	-22.94
GDA1	Guanosine diphosphatase located in the Golgi; involved in the transport of GDP-mannose into the Golgi lumen	-22.78
MTM1	Mitochondrial protein of the mitochondrial carrier family; high affinity pyridoxal 5'-phosphate (PLP) transporter, important for delivery of PLP cofactor to mitochondrial enzymes	-22.47
YKU80	Subunit of telomeric Ku complex (Yku70p-Yku80p); involved in telomere length maintenance, structure and telomere position effect	-22.47
SNX41	Sorting nexin; involved in the retrieval of late-Golgi SNAREs from the post-Golgi endosome to the trans-Golgi network; interacts with Snx4p	-22.47
HST1	NAD(+)-dependent histone deacetylase	-22.01
KEX2	Kexin, a subtilisin-like protease (proprotein convertase); a calcium-dependent serine protease involved in the activation of proproteins of the secretory pathway	-22.01
YKU70	Subunit of the telomeric Ku complex (Yku70p-Yku80p); involved in telomere length maintenance	-21.86

MRF1	Mitochondrial translation release factor; involved in stop codon recognition and hydrolysis of the peptidyl-tRNA bond during mitochondrial translation	-21.56
SWF1	Palmitoyltransferase that acts on transmembrane proteins; including the SNAREs Snc1p, Syn8p, Tlg1p and likely all SNAREs	-21.56
DEG1	tRNA:pseudouridine synthase; introduces pseudouridines at position 38 or 39 in tRNA	-21.26
OAC1	Mitochondrial inner membrane transporter; transports oxaloacetate, sulfate, thiosulfate, and isopropylmalate; member of the mitochondrial carrier family	-21.26
SLD2	Single-stranded DNA origin-binding and annealing protein; required for initiation of DNA replication	-20.25
CNN1	Kinetochore protein; associated with the essential kinetochore proteins Nnf1p and Spc24p	-19.56
MPC1	Highly conserved subunit of mitochondrial pyruvate carrier (MPC)	-19.16
ROG1	Lipase with specificity for monoacylglycerol; preferred substrate is 1-oleoylglycerol	-18.90
APS1	Small subunit of the clathrin-associated adaptor complex AP-1	-18.64
CSE2	Subunit of the RNA polymerase II mediator complex	-18.51
SPT21	Protein with a role in transcriptional silencing	-18.51
CUP9	Homeodomain-containing transcriptional repressor; regulates expression of PTR2	-18.38
OST6	Subunit of the oligosaccharyltransferase complex of the ER lumen; complex catalyzes asparagine-linked glycosylation of newly synthesized proteins	-18.38
MDM32	Mitochondrial inner membrane protein with similarity to Mdm31p	-18.00
PSY3	Component of Shu complex (aka PCSS complex); Shu complex also includes Shu1, Csm2, Shu2, and promotes error-free DNA repair	-18.00
CYC7	Cytochrome c isoform 2, expressed under hypoxic conditions	-17.88
AIM41	Protein of unknown function; the authentic protein is detected in highly purified mitochondria in high-throughput studies	-17.88
TIM23	Essential component of the TIM23 complex; involved in protein import into mitochondrial matrix and inner membrane	-17.88
FPR4	Peptidyl-prolyl cis-trans isomerase (PPIase); nuclear proline isomerase	-17.88
RSA3	Protein with a likely role in ribosomal maturation; required for accumulation of wild-type levels of large (60S) ribosomal subunits	-17.63
CSM4	Protein required for accurate chromosome segregation during meiosis	-17.39
PDB1	E1 beta subunit of the pyruvate dehydrogenase (PDH) complex	-17.39
WSC3	Sensor-transducer of the stress-activated PKC1-MPK1 signaling pathway	2.60
COG2	Essential component of the conserved oligomeric Golgi complex	2.60
YPT52	Endosomal Rab family GTPase; required for vacuolar protein sorting, endocytosis and multivesicular body (MVB) biogenesis and sorting	2.62
COG6	Component of the conserved oligomeric Golgi complex	2.64
APM2	Protein of unknown function; homologous to the medium chain of mammalian clathrin-associated protein complex; involved in vesicular transport	2.64
UTH1	Mitochondrial inner membrane protein	2.68
VAB2	Subunit of the BLOC-1 complex involved in endosomal maturation	2.71
UBP3	Ubiquitin-specific protease involved in transport and osmotic response; negatively regulates Ras/PKA signaling	2.77
ATG19	Receptor protein for the cytoplasm-to-vacuole targeting (Cvt) pathway	2.85
ATX2	Golgi membrane protein involved in manganese homeostasis	2.87
SWH1	Protein similar to mammalian oxysterol-binding protein	2.89
PEP5	Histone E3 ligase, component of CORVET membrane tethering complex	2.91

YIP3	Protein localized to COPII vesicles; proposed to be involved in ER to Golgi transport	2.99
SEC21	Gamma subunit of coatomer; coatomer is a heptameric protein complex that together with Arf1p forms the COPI coat; involved in ER to Golgi transport of selective cargo	3.01
CCZ1	Subunit of a heterodimeric guanine nucleotide exchange factor (GEF); subunit of the Mon1-Ccz1 GEF complex, which stimulates nucleotide exchange and activation of Ypt7p	3.01
YPT32	Rab family GTPase involved in the exocytic pathway; mediates intra-Golgi traffic or the budding of post-Golgi vesicles from the trans-Golgi; protein abundance increases in response to DNA replication stress	3.01
CUE5	Ubiquitin-binding protein; functions as ubiquitin-Atg8p adaptor in ubiquitin-dependent autophagy	3.03
HSE1	Subunit of the endosomal Vps27p-Hse1p complex; complex is required for sorting of ubiquitinated membrane proteins into intraluminal vesicles prior to vacuolar degradation, as well as for recycling of Golgi proteins and formation of luminal membranes	3.07
ATG4	Conserved cysteine protease required for autophagy; cleaves Atg8p to a form required for autophagosome and Cvt vesicle generation	3.16
RTT10	WD40 domain-containing protein involved in endosomal recycling	3.18
YPT31	Rab family GTPase; involved in the exocytic pathway	3.23
SYN8	Endosomal SNARE related to mammalian syntaxin 8	3.36
MVB12	ESCRT-I subunit required to stabilize ESCRT-I core complex oligomers	3.36
MON1	Subunit of a heterodimeric guanine nucleotide exchange factor (GEF); subunit of the Mon1-Ccz1 GEF complex which stimulates nucleotide exchange and activation of Ypt7p	3.43
RDI1	Rho GDP dissociation inhibitor	3.48
GCS1	ADP-ribosylation factor GTPase activating protein (ARF GAP); involved in ER-Golgi transport	3.53
VID24	GID Complex regulatory subunit	3.53
GID8	Subunit of GID Complex, binds strongly to central component Vid30	3.61
YPT53	Stress-induced Rab family GTPase; required for vacuolar protein sorting and endocytosis	3.61
TRS33	Core component of TRAPP complexes I, II and IV	3.68
VPS3	Component of CORVET membrane tethering complex	3.71
DOA1	WD repeat protein required for ubiquitin-mediated protein degradation; ubiquitin binding cofactor that complexes with Cdc48p; required for ribophagy	3.76
PEP12	Target membrane receptor (t-SNARE); for vesicular intermediates traveling between the Golgi apparatus and the vacuole	3.89
EGD1	Subunit beta1 of the nascent polypeptide-associated complex (NAC); involved in protein targeting, associated with cytoplasmic ribosomes	3.92
GYL1	Putative GTPase activating protein (GAP) with a role in exocytosis	3.94
VPS16	Subunit of the HOPS and the CORVET complexes	3.94
ATG16	Conserved protein involved in autophagy	4.03
UBC8	Ubiquitin-conjugating enzyme that regulates gluconeogenesis	4.08
VTC2	Regulatory subunit of the vacuolar transporter chaperone (VTC) complex; involved in membrane trafficking, vacuolar polyphosphate accumulation, microautophagy and non-autophagic vacuolar fusion	4.14
MAK10	Non-catalytic subunit of the NatC N-terminal acetyltransferase	4.32
VPS8	Membrane-binding component of the CORVET complex	4.96
VID28	GID Complex subunit, serves as adaptor for regulatory subunit Vid24p	5.06
VTC4	Vacuolar membrane polyphosphate polymerase; subunit of the vacuolar transporter chaperone (VTC) complex involved in synthesis and transfer of polyP to the vacuole	5.10

BRE5	Ubiquitin protease cofactor; forms deubiquitination complex with Ubp3p that coregulates anterograde and retrograde transport between the endoplasmic reticulum and Golgi compartments	5.21
OSH6	Member of an oxysterol-binding protein family; family members have overlapping, redundant functions in sterol metabolism and collectively perform a function essential for viability	5.31
HSV2	Phosphatidylinositol 3,5-bisphosphate-binding protein; plays a role in micronucleophagy	6.11
VPS55	Late endosomal protein involved in late endosome to vacuole transport	6.11
RMD5	Component of GID Complex that confers ubiquitin ligase (U3) activity	6.19
YVH1	Dual specificity protein phosphatase; regulates growth, sporulation, and glycogen accumulation in a cAMP-dependent protein kinase cascade dependent manner	6.63
COS6	Endosomal protein involved in turnover of plasma membrane proteins	6.68
YPT7	Rab family GTPase; GTP-binding protein of the rab family	6.82
FYV10	Subunit of GID complex; involved in proteasome-dependent catabolite inactivation of gluconeogenic enzymes FBpase, PEPCK, and c-MDH	7.78
PEP3	Component of CORVET membrane tethering complex	7.89
TDA3	Putative oxidoreductase involved in late endosome to Golgi transport	8.51
SMF2	Divalent metal ion transporter involved in manganese homeostasis	9.85
GVP36	BAR domain protein that localizes to early and late Golgi vesicles	10.34
TRX1	Cytoplasmic thioredoxin isoenzyme; part of thioredoxin system which protects cells against oxidative and reductive stress	12.13
GTR2	Subunit of a TORC1-stimulating GTPase complex	12.82
VAM6	Guanine nucleotide exchange factor for the GTPase Gtr1p; subunit of the HOPS endocytic tethering complex; vacuole membrane protein	13.45
VPS27	Endosomal protein that forms a complex with Hse1p	15.67
DID4	Class E Vps protein of the ESCRT-III complex	16.00
VID30	Central component of GID Complex, involved in FBpase degradation	18.77
SNN1	Subunit of the BLOC-1 complex involved in endosomal maturation	19.03
ATG41	Protein of unknown function; required for selective and nonselective autophagy, and mitophagy	21.56
MEH1	Component of the EGO and GSE complexes	27.28
NPR2	Subunit of the Iml1p/SEACIT complex; SEACIT (Iml1p-Npr2p-Npr3p) is a subcomplex of the SEA complex	27.86
GTR1	Subunit of a TORC1-stimulating GTPase complex	36.00
NPR3	Subunit of the Iml1p/SEACIT complex; SEACIT (Iml1p-Npr2p-Npr3p) is a subcomplex of SEAC	99.04

**Table 8: A shortened list of genes considered during the GO enrichment analysis.**

## 1.4: DISCUSSION AND CONCLUSIONS

This chapter explains how we successfully applied two different genetic screens to identify potential regulators affecting the TORC1 signaling pathway. For both screens, we took advantage of the growth inhibition caused by the overexpression of the Gtr1<sup>S20L</sup> variant. First, we performed a classical genetic screen where spontaneous suppressors were selected within a population. Notably, roughly 30% of the mutations identified during the classical genetic screen affected well-known TORC1 pathway components

such as the EGOC components, the TORC1 members Tor1 and Tco89, and Vam6. Further experiments led us to conclude that the isolated mutations in EGOC and *TCO89* can be classified as loss of function mutations (Figure 3).

Concerning the TOR1 variants, we characterized the Tor1<sup>A1928D</sup> variant and observed that it behaved like a gain of function mutant (Figure 3). We hypothesize that this mutation either enhances the Tor1 kinase activity, its accessibility to substrates or detaches TORC1 from the upstream EGOC-dependent regulation. The study of the Tor1 mutants could unveil different aspects of Tor1 regulation or TORC1 assembly. Notably, the Vam6 variants presented a more complex picture. Even though the loss of the other HOPS complex components suppressed the Gtr1<sup>S20L</sup>-mediated growth inhibition, loss of Vam6, which affects both the HOPS complex formation and the EGOC regulation (Binda et al., 2009), did not do so (Figure 3B). It is possible that some Vam6 variants selectively affect the HOPS complex formation, but not the EGOC regulation; hence, by deleting *VAM6*, we would impair both functions, which in the context of Gtr1<sup>S20L</sup> overexpression could be deleterious.

Importantly, thanks to the classical genetic screen, we also identified loss of function mutants affecting the HOPS and AP-3 complexes. Further experiments showed us that loss of AP-3 or of HOPS components diverted Ego1-GFP and GFP-Gtr1, but not GFP-Tor1, to the plasma membrane and that loss of HOPS components even dispersed Ego1-GFP and GFP-Gtr1 from the vacuolar membrane (Figure 4). These results lead us to conclude that EGOC, but not TORC1, travels from the TGN to the vacuoles principally through the AP-3 pathway (Hatakeyama et al., 2019). Besides, we also identified loss of function mutations affecting the palmitoyl transferase Akr1, which palmitoylates Ego1, enabling its association to membranes. Therefore, we can also conclude that Gtr1<sup>S20L</sup> needs to correctly assemble in a vacuolar membrane-associated EGOC to inhibit the TORC1 kinase (Hatakeyama et al., 2019).

Besides identifying variants for well-known TORC1 regulators and characterizing Akr1 and the HOPS and AP-3 complexes as new players affecting the TORC1 signaling pathway, the classical genetic screen provided us with many potential TORC1 regulators (Table 5). Due to time constraints, among all these potential TORC1 regulators, we only further characterized the protein Opy1. Opy1 has been described to inhibit Mss4 - the Phosphatidylinositol-4-phosphate 5-kinase - in response to high levels of Phosphatidylinositol-4,5-bisphosphate (PI(4,5)P<sub>2</sub>) at the plasma membrane (Ling et al., 2012). Surprisingly, the overexpression of Opy1 was sufficient to suppress the

Gtr1<sup>S20L</sup>-dependent growth inhibition (Figure 5A), which indicates that Opy1 function affects the TORC1 pathway. Even though the exact mechanism by which Opy1 affects TORC1 remains elusive, we can entertain two hypotheses, either Opy1 is a regulator within the TORC1 pathway, or it affects, indirectly, the subcellular localization of TORC1 pathway components by altering the ratio at cellular membranes of PI4P:PI(4,5)P<sub>2</sub>. In agreement with this, phosphatidylinositol-4-phosphate (PI4P) and PI(4,5)P<sub>2</sub> have been shown to regulate different steps of the vacuole fusion cycle (Starr & Fratti, 2019, and references therein); therefore, a misbalanced ratio of PI4P:PI(4,5)P<sub>2</sub> may alter the cellular trafficking and delivery of cargo proteins to their proper subcellular compartments.

We also performed a SATurated Transposon Analysis in Yeast (SATAY) screen in parallel to the classical genetic screen. In this case, we selected suppressors within a previously generated library of transposon mutants, and then we quantified the number of Transposons Per Gene (TPG) and Reads Per Gene (RPG) in wild-type and a Gtr1<sup>S20L</sup> overexpressing population. As a control, we first analyzed the TPG and RPG quantified for well-known TORC1 pathway components. As expected, in the Gtr1<sup>S20L</sup> population, genes coding for the EGO, HOPS, and AP-3 components accumulated more transposition events (both TPG and RPG) while the *TOR1* locus was less disrupted by transposition events (Table 6).

Surprisingly, in the Gtr1<sup>S20L</sup> population, the *TCO89* and *AKR1* loci were less interrupted by transposons (Table 6). Since we previously observed that loss of function mutations in *TCO89* suppressed the Gtr1<sup>S20L</sup> overexpression (Binda et al., 2009; Hatakeyama et al., 2019), we expected to have more transposons interrupting the *TCO89* gene in the Gtr1<sup>S20L</sup> overexpressing population, but this was not the case. Nevertheless, analysis of the transposition pattern within the *TCO89* locus revealed that the Gtr1<sup>S20L</sup> overexpressing population was enriched with mutants harboring a transposon insertion in the sequence that codes for the Serine 73 of Tco89 (data not shown). Indeed, the phosphorylation of this residue, which has been proposed to be a potential TORC1 phosphosite (Hu et al., 2019), could be somehow involved in the Gtr1<sup>S20L</sup>-mediated TORC1 inhibition. Still, the fact that, in the Gtr1<sup>S20L</sup> overexpression population, we identified fewer transposons within the *TCO89* locus remains to some extent enigmatic.

Concerning *Akr1*, in the Gtr1<sup>S20L</sup> overexpressing population, there was a higher variability (high TPG) but fewer transposon mutants (RPG) interrupting the *AKR1* locus

(Table 6). Notably, we identified an enormous number of transposon insertions in the sequence coding for the proline 9 of Akr1 (data not shown) which, most probably, disrupt the expression of Akr1, hence the proper targeting of the EGOc to cellular membranes.

Moreover, we also analyzed the TPG and RPG values for the potential TORC1 regulators identified during the classical genetic screen (Table 5). Cyc8, Cts1, Kex2, and Opy1 are particularly interesting potential TORC1 regulators (Figure 7). From the TPG and RPG values, we could infer that the Cyc8 and Cts1 mutants are likely to be loss of function mutants (more TPG and RPG), while the Kex2 and Opy1 mutants could be gain of function mutants (less TPG and RPG).

Cyc8 functions with Tup1 as a transcriptional co-activator of the Stp1/2 activator (Tanaka & Mukai, 2015). The Stp1/2 activator upregulates the transcription of amino acid permeases (*i.e.*, Bap3, Gnp1, Mup1, Lyp1, Tat2, Dip5, Bap2, and Tat1) (Tanaka & Mukai, 2015). The identification of Cyc8 variants (*i.e.*, Cyc8<sup>A540P</sup> and Cyc8<sup>Q547H</sup>) and the enrichment of transposition-induced mutants within the prion domain of Cyc8 (*i.e.*, Cyc8<sup>A554</sup>) suggest that the loss of this domain may be somehow sufficient to suppress the Gtr1<sup>S20L</sup>-dependent growth inhibition. In line with this, it may be possible that the prion domain mediates positively or negatively the interaction of the Cyc8-Tup1 co-activator with the Stp1/2 activator; thus, mutations within this region may trigger an altered expression of amino acid transporters which may help suppress the Gtr1<sup>S20L</sup>-dependent growth inhibition. Notably, the *STP1* and *STP2* genes showed higher RPG (8.5 times more, and 2.4 times more, respectively) in the Gtr1<sup>S20L</sup> overexpression population.

Cts1 is an endochitinase required for cell separation after mitosis (Molon et al., 2018). The identification of a Cts1 variant (Cts1<sup>G477D</sup>) and many transposon-disrupted mutants (Cts1<sup>N552</sup>) nearby the chitin domain of Cts1 suggests that this domain may be necessary for the Gtr1<sup>S20L</sup>-dependent growth inhibition. Interestingly, Cts1 has been shown to play an important role in cellular lifespan (Molon et al., 2018), something that may link Cts1 with the TORC1 pathway.

The subtilisin-like serine proteinase Kex2 has been shown to be involved in processing  $\alpha$ -pheromone precursors, killer toxin precursors, and aspartic proteinase propeptides (Bader et al., 2008). However, since the loss of Kex2 displays such a pleiotropic phenotype (Bader et al., 2008, and references therein), it may be possible



that unknown substrates for Kex2 have yet to be discovered. It would be interesting to look for these new substrates using the identified Kex2 variants and disclose whether they play any role within the TORC1 signaling pathway.

Finally, we performed a GO enrichment analysis to understand which biological processes involve the genes accumulating more and fewer transposons in the Gtr1<sup>S20L</sup> overexpressing population (Figure 8). Interestingly, more transposons interrupted genes coding for members of the GID complex (Table 7: GO:0034657) in the Gtr1<sup>S20L</sup> overexpressing population. The GID complex is involved in the regulation of the carbon metabolism by marking for degradation gluconeogenic enzymes such as FBPase (Fructose-1,6-biphosphatase) and Mdh2 (Malate dehydrogenase) in cells growing in glucose-containing medium (Hung et al., 2004; Nakatsukasa et al., 2015; Santt et al., 2008). Although it is unclear how impairment of the GID complex may lead to the suppression of the Gtr1<sup>S20L</sup>-mediated growth inhibition, it could be possible that this ubiquitin ligase also marks proteins functioning within the TORC1 signaling pathway for degradation. Alternatively, preservation, in the presence of glucose, of the gluconeogenic enzymes may lead to the accumulation of glucose. Therefore, an alteration of the carbon metabolism may be accompanied by a subsequent alteration of the nitrogen metabolism, thereby affecting the TORC1 pathway.

In contrast, genes coding for members of the histone deacetylase Set3 complex (Lenstra et al., 2011) accumulated less transposons in the Gtr1<sup>S20L</sup> overexpressing population (Table 7: GO:0034967). Histone deacetylases are crucial for proper transcription regulation; therefore, it could be possible that the Set3 complex, similar to what has been described for the INO-80 complex (Beckwith et al., 2018), promotes, downstream the TORC1 signaling pathway, the transcription of TORC1-responsive genes.

## 1.5: BIBLIOGRAPHY

- Algret, R., Fernandez-Martinez, J., Shi, Y., Kim, S. J., Pellarin, R., Cimerancic, P., Cochet, E., Sali, A., Chait, B. T., Rout, M. P., & Dokudovskaya, S. (2014). Molecular Architecture and Function of the SEA Complex, a Modulator of the TORC1 Pathway. *Molecular & Cellular Proteomics*, 13(11), 2855–2870. <https://doi.org/10.1074/mcp.M114.039388>
- Averous, J., Lambert-Langlais, S., Carraro, V., Goubeyre, O., Parry, L., B'Chir, W., Muranishi, Y., Jousse, C., Bruhat, A., Maurin, A.-C., Proud, C. G., & Fournoux, P. (2014). Requirement for lysosomal localization of mTOR for its activation differs between leucine and other amino acids. *Cellular Signalling*, 26(9), 1918–1927. <https://doi.org/10.1016/j.cellsig.2014.04.019>



- Babu, P., Deschenes, R. J., & Robinson, L. C. (2004). Akr1p-dependent Palmitoylation of Yck2p Yeast Casein Kinase 1 Is Necessary and Sufficient for Plasma Membrane Targeting. *Journal of Biological Chemistry*, 279(26), 27138–27147. <https://doi.org/10.1074/jbc.M403071200>
- Bader, O., Krauke, Y., & Hube, B. (2008). Processing of predicted substrates of fungal Kex2 proteinases from *Candida albicans*, *C. glabrata*, *Saccharomyces cerevisiae* and *Pichia pastoris*. *BMC Microbiology*, 8(1), 116. <https://doi.org/10.1186/1471-2180-8-116>
- Bar-Peled, L., Chantranupong, L., Cherniack, A. D., Chen, W. W., Ottina, K. A., Grabiner, B. C., Spear, E. D., Carter, S. L., Meyerson, M., & Sabatini, D. M. (2013). A Tumor Suppressor Complex with GAP Activity for the Rag GTPases That Signal Amino Acid Sufficiency to mTORC1. *Science*, 340(6136), 1100–1106. <https://doi.org/10.1126/science.1232044>
- Bar-Peled, L., Schweitzer, L. D., Zoncu, R., & Sabatini, D. M. (2012). Ragulator Is a GEF for the Rag GTPases that Signal Amino Acid Levels to mTORC1. *Cell*, 150(6), 1196–1208. <https://doi.org/10.1016/j.cell.2012.07.032>
- Beckwith, S. L., Schwartz, E. K., García-Nieto, P. E., King, D. A., Gowans, G. J., Wong, K. M., Eckley, T. L., Paraschuk, A. P., Peltan, E. L., Lee, L. R., Yao, W., & Morrison, A. J. (2018). The INO80 chromatin remodeler sustains metabolic stability by promoting TOR signaling and regulating histone acetylation. *PLOS Genetics*, 14(2), e1007216. <https://doi.org/10.1371/journal.pgen.1007216>
- Binda, M., Péli-Gulli, M.-P., Bonfils, G., Panchaud, N., Urban, J., Sturgill, T. W., Loewith, R., & De Virgilio, C. (2009). The Vam6 GEF Controls TORC1 by Activating the EGO Complex. *Molecular Cell*, 35(5), 563–573. <https://doi.org/10.1016/j.molcel.2009.06.033>
- Bonfils, G., Jaquenoud, M., Bontron, S., Ostrowicz, C., Ungermann, C., & De Virgilio, C. (2012). Leucyl-tRNA Synthetase Controls TORC1 via the EGO Complex. *Molecular Cell*, 46(1), 105–110. <https://doi.org/10.1016/j.molcel.2012.02.009>
- Bowers, K., & Stevens, T. H. (2005). Protein transport from the late Golgi to the vacuole in the yeast *Saccharomyces cerevisiae*. *Biochimica et Biophysica Acta (BBA) - Molecular Cell Research*, 1744(3), 438–454. <https://doi.org/10.1016/j.bbamcr.2005.04.004>
- Brown, E. J., Albers, M. W., Bum Shin, T., Ichikawa, K., Keith, C. T., Lane, W. S., & Schreiber, S. L. (1994). A mammalian protein targeted by G1-arresting rapamycin–receptor complex. *Nature*, 369(6483), 756–758. <https://doi.org/10.1038/369756a0>
- Burd, C. G., & Emr, S. D. (1998). Phosphatidylinositol(3)-Phosphate Signaling Mediated by Specific Binding to RING FYVE Domains. *Molecular Cell*, 2(1), 157–162. [https://doi.org/10.1016/S1097-2765\(00\)80125-2](https://doi.org/10.1016/S1097-2765(00)80125-2)
- Cafferkey, R., Young, P. R., McLaughlin, M. M., Bergsma, D. J., Koltin, Y., Sathe, G. M., Faucette, L., Eng, W. K., Johnson, R. K., & Livi, G. P. (1993). Dominant missense mutations in a novel yeast protein related to mammalian phosphatidylinositol 3-kinase and VPS34 abrogate rapamycin cytotoxicity. *Molecular and Cellular Biology*, 13(10), 6012–6023. <https://doi.org/10.1128/MCB.13.10.6012>
- Caplan, S., Hartnell, L. M., Aguilar, R. C., Naslavsky, N., & Bonifacio, J. S. (2001). Human Vam6p promotes lysosome clustering and fusion in vivo. *Journal of Cell Biology*, 154(1), 109–122. <https://doi.org/10.1083/jcb.200102142>
- Chiu, M. I., Katz, H., & Berlin, V. (1994). RAPT1, a mammalian homolog of yeast Tor, interacts with the FKBP12/rapamycin complex. *Proceedings of the National Academy of Sciences*, 91(26), 12574–12578. <https://doi.org/10.1073/pnas.91.26.12574>
- Conrad, M., Schothorst, J., Kankipati, H. N., Van Zeebroeck, G., Rubio-Texeira, M., & Thevelein, J. M. (2014). Nutrient sensing and signaling in the yeast *Saccharomyces cerevisiae*. *FEMS Microbiology Reviews*, 38(2), 254–299. <https://doi.org/10.1111/1574-6976.12065>
- Cornu, M., Albert, V., & Hall, M. N. (2013). mTOR in aging, metabolism, and cancer. *Current Opinion in Genetics & Development*, 23(1), 53–62. <https://doi.org/10.1016/j.gde.2012.12.005>
- Cowles, C. R., Odorizzi, G., Payne, G. S., & Emr, S. D. (1997). The AP-3 Adaptor Complex Is Essential for Cargo-Selective Transport to the Yeast Vacuole. *Cell*, 91(1), 109–118. [https://doi.org/10.1016/S0092-8674\(01\)80013-1](https://doi.org/10.1016/S0092-8674(01)80013-1)
- Demetriades, C., Doumpas, N., & Teleman, A. A. (2014). Regulation of TORC1 in Response to Amino Acid Starvation via Lysosomal Recruitment of TSC2. *Cell*, 156(4), 786–799. <https://doi.org/10.1016/j.cell.2014.01.024>

- Dokudovskaya, S., & Rout, M. P. (2015). SEA you later alli-GATOR – a dynamic regulator of the TORC1 stress response pathway. *Journal of Cell Science*, 128(12), 2219–2228. <https://doi.org/10.1242/jcs.168922>
- Dokudovskaya, S., Waharte, F., Schlessinger, A., Pieper, U., Devos, D. P., Cristea, I. M., Williams, R., Salamero, J., Chait, B. T., Sali, A., Field, M. C., Rout, M. P., & Dargemont, C. (2011). A Conserved Coatomer-related Complex Containing Sec13 and Seh1 Dynamically Associates With the Vacuole in *Saccharomyces cerevisiae*. *Molecular & Cellular Proteomics*, 10(6), M110.006478. <https://doi.org/10.1074/mcp.M110.006478>
- Eltschinger, S., & Loewith, R. (2016). TOR Complexes and the Maintenance of Cellular Homeostasis. *Trends in Cell Biology*, 26(2), 148–159. <https://doi.org/10.1016/j.tcb.2015.10.003>
- Farnsworth, C. L., & Feig, L. A. (1991). Dominant inhibitory mutations in the Mg(2+)-binding site of RasH prevent its activation by GTP. *Molecular and Cellular Biology*, 11(10), 4822–4829. <https://doi.org/10.1128/MCB.11.10.4822>
- Fawal, M.-A., Brandt, M., & Djouder, N. (2015). MCRS1 Binds and Couples Rheb to Amino Acid-Dependent mTORC1 Activation. *Developmental Cell*, 33(1), 67–81. <https://doi.org/10.1016/j.devcel.2015.02.010>
- Forsberg, H., & Ljungdahl, P. O. (2001). Genetic and Biochemical Analysis of the Yeast Plasma Membrane Ssy1p-Ptr3p-Ssy5p Sensor of Extracellular Amino Acids. *Molecular and Cellular Biology*, 21(3), 814–826. <https://doi.org/10.1128/MCB.21.3.814-826.2001>
- Fromm, S. A., Lawrence, R. E., & Hurley, J. H. (2020). Structural mechanism for amino acid-dependent Rag GTPase nucleotide state switching by SLC38A9. *Nature Structural & Molecular Biology*, 27(11), 1017–1023. <https://doi.org/10.1038/s41594-020-0490-9>
- Gao, M., & Kaiser, C. A. (2006). A conserved GTPase-containing complex is required for intracellular sorting of the general amino-acid permease in yeast. *Nature Cell Biology*, 8(7), 657–667. <https://doi.org/10.1038/ncb1419>
- Gaubitz, C., Prouteau, M., Kusmider, B., & Loewith, R. (2016). TORC2 Structure and Function. *Trends in Biochemical Sciences*, 41(6), 532–545. <https://doi.org/10.1016/j.tibs.2016.04.001>
- Gong, R., Li, L., Liu, Y., Wang, P., Yang, H., Wang, L., Cheng, J., Guan, K.-L., & Xu, Y. (2011). Crystal structure of the Gtr1p-Gtr2p complex reveals new insights into the amino acid-induced TORC1 activation. *Genes & Development*, 25(16), 1668–1673. <https://doi.org/10.1101/gad.16968011>
- Gu, X., Orozco, J. M., Saxton, R. A., Condon, K. J., Liu, G. Y., Krawczyk, P. A., Scaria, S. M., Harper, J. W., Gygi, S. P., & Sabatini, D. M. (2017). SAMTOR is an S-adenosylmethionine sensor for the mTORC1 pathway. *Science*, 358(6364), 813–818. <https://doi.org/10.1126/science.aao3265>
- Han, J. M., Jeong, S. J., Park, M. C., Kim, G., Kwon, N. H., Kim, H. K., Ha, S. H., Ryu, S. H., & Kim, S. (2012). Leucyl-tRNA Synthetase Is an Intracellular Leucine Sensor for the mTORC1-Signaling Pathway. *Cell*, 149(2), 410–424. <https://doi.org/10.1016/j.cell.2012.02.044>
- Hatakeyama, R., & De Virgilio, C. (2016). Unsolved mysteries of Rag GTPase signaling in yeast. *Small GTPases*, 7(4), 239–246. <https://doi.org/10.1080/21541248.2016.1211070>
- Hatakeyama, R., Péli-Gulli, M.-P., Hu, Z., Jaquenoud, M., Garcia Osuna, G. M., Sardu, A., Dengjel, J., & De Virgilio, C. (2019). Spatially Distinct Pools of TORC1 Balance Protein Homeostasis. *Molecular Cell*, 73(2), 325–338.e8. <https://doi.org/10.1016/j.molcel.2018.10.040>
- Hayakawa, A., Hayes, S. J., Lawe, D. C., Sudharshan, E., Tuft, R., Fogarty, K., Lambright, D., & Corvera, S. (2004). Structural Basis for Endosomal Targeting by FYVE Domains. *Journal of Biological Chemistry*, 279(7), 5958–5966. <https://doi.org/10.1074/jbc.M310503200>
- Heitman, J., Movva, N., & Hall, M. (1991). Targets for cell cycle arrest by the immunosuppressant rapamycin in yeast. *Science*, 253(5022), 905–909. <https://doi.org/10.1126/science.1715094>
- Helliwell, S. B., Wagner, P., Kunz, J., Deuter-Reinhard, M., Henriquez, R., & Hall, M. N. (1994). TOR1 and TOR2 are structurally and functionally similar but not identical phosphatidylinositol kinase homologues in yeast. *Molecular Biology of the Cell*, 5(1), 105–118. <https://doi.org/10.1091/mbc.5.1.105>
- Hinnebusch, A. G. (2005). TRANSLATIONAL REGULATION OF GCN4 AND THE GENERAL AMINO ACID CONTROL OF YEAST. *Annual Review of Microbiology*, 59(1), 407–450. <https://doi.org/10.1146/annurev.micro.59.031805.133833>
- Hofman-Bang, J. (1999). Nitrogen Catabolite Repression in *Saccharomyces cerevisiae*. *Molecular Biotechnology*, 12(1), 35–74. <https://doi.org/10.1385/MB:12:1:35>

- Hu, Z., Raucci, S., Jaquenoud, M., Hatakeyama, R., Stumpe, M., Rohr, R., Reggiori, F., De Virgilio, C., & Dengjel, J. (2019). Multilayered Control of Protein Turnover by TORC1 and Atg1. *Cell Reports*, 28(13), 3486–3496.e6. <https://doi.org/10.1016/j.celrep.2019.08.069>
- Hung, G.-C., Brown, C. R., Wolfe, A. B., Liu, J., & Chiang, H.-L. (2004). Degradation of the Gluconeogenic Enzymes Fructose-1,6-bisphosphatase and Malate Dehydrogenase Is Mediated by Distinct Proteolytic Pathways and Signaling Events. *Journal of Biological Chemistry*, 279(47), 49138–49150. <https://doi.org/10.1074/jbc.M404544200>
- Jewell, J. L., Kim, Y. C., Russell, R. C., Yu, F.-X., Park, H. W., Plouffe, S. W., Tagliabracci, V. S., & Guan, K.-L. (2015). Differential regulation of mTORC1 by leucine and glutamine. *Science*, 347(6218), 194–198. <https://doi.org/10.1126/science.1259472>
- John, J., Rensland, H., Schlichting, I., Vetter, I., Borasio, G. D., Goody, R. S., & Wittinghofer, A. (1993). Kinetic and structural analysis of the Mg(2+)-binding site of the guanine nucleotide-binding protein p21H-ras. *The Journal of Biological Chemistry*, 268(2), 923–929.
- Kim, A., & Cunningham, K. W. (2015). A LAPF/phafin1-like protein regulates TORC1 and lysosomal membrane permeabilization in response to endoplasmic reticulum membrane stress. *Molecular Biology of the Cell*, 26(25), 4631–4645. <https://doi.org/10.1091/mbc.E15-08-0581>
- Kim, E., Goraksha-Hicks, P., Li, L., Neufeld, T. P., & Guan, K.-L. (2008). Regulation of TORC1 by Rag GTPases in nutrient response. *Nature Cell Biology*, 10(8), 935–945. <https://doi.org/10.1038/ncb1753>
- Kim, J., & Guan, K.-L. (2019). MTOR as a central hub of nutrient signalling and cell growth. *Nature Cell Biology*, 21(1), 63–71. <https://doi.org/10.1038/s41556-018-0205-1>
- Kim, J., & Kim, E. (2016). Rag GTPase in amino acid signaling. *Amino Acids*, 48(4), 915–928. <https://doi.org/10.1007/s00726-016-2171-x>
- Kingsbury, J. M., Sen, N. D., & Cardenas, M. E. (2015). Branched-Chain Aminotransferases Control TORC1 Signaling in *Saccharomyces cerevisiae*. *PLOS Genetics*, 11(12), e1005714. <https://doi.org/10.1371/journal.pgen.1005714>
- Kira, S., Tabata, K., Shirahama-Noda, K., Nozoe, A., Yoshimori, T., & Noda, T. (2014). Reciprocal conversion of Gtr1 and Gtr2 nucleotide-binding states by Npr2-Npr3 inactivates TORC1 and induces autophagy. *Autophagy*, 10(9), 1565–1578. <https://doi.org/10.4161/auto.29397>
- Kuhlee, A., Raunser, S., & Ungermann, C. (2015). Functional homologies in vesicle tethering. *FEBS Letters*, 589(19PartA), 2487–2497. <https://doi.org/10.1016/j.febslet.2015.06.001>
- Kunz, J., Henriquez, R., Schneider, U., Deuter-Reinhard, M., Movva, N. R., & Hall, M. N. (1993). Target of rapamycin in yeast, TOR2, is an essential phosphatidylinositol kinase homolog required for G1 progression. *Cell*, 73(3), 585–596. [https://doi.org/10.1016/0092-8674\(93\)90144-F](https://doi.org/10.1016/0092-8674(93)90144-F)
- Laplante, M., & Sabatini, D. M. (2012). MTOR Signaling in Growth Control and Disease. *Cell*, 149(2), 274–293. <https://doi.org/10.1016/j.cell.2012.03.017>
- Lenstra, T. L., Benschop, J. J., Kim, T., Schulze, J. M., Brabers, N. A. C. H., Margaritis, T., van de Pasch, L. A. L., van Heesch, S. A. A. C., Brok, M. O., Groot Koerkamp, M. J. A., Ko, C. W., van Leenen, D., Sameith, K., van Hooff, S. R., Lijnzaad, P., Kemmeren, P., Hentrich, T., Kobor, M. S., Buratowski, S., & Holstege, F. C. P. (2011). The Specificity and Topology of Chromatin Interaction Pathways in Yeast. *Molecular Cell*, 42(4), 536–549. <https://doi.org/10.1016/j.molcel.2011.03.026>
- Ling, Y., Stefan, C. J., MacGurn, J. A., Audhya, A., & Emr, S. D. (2012). The dual PH domain protein Opy1 functions as a sensor and modulator of PtdIns(4,5)P<sub>2</sub> synthesis: Opy1 regulates Mss4 lipid kinase activity. *The EMBO Journal*, 31(13), 2882–2894. <https://doi.org/10.1038/emboj.2012.127>
- Liu, G. Y., & Sabatini, D. M. (2020). MTOR at the nexus of nutrition, growth, ageing and disease. *Nature Reviews Molecular Cell Biology*, 21(4), 183–203. <https://doi.org/10.1038/s41580-019-0199-y>
- Loewith, R., Jacinto, E., Wullschleger, S., Lorberg, A., Crespo, J. L., Bonenfant, D., Oppliger, W., Jenoe, P., & Hall, M. N. (2002). Two TOR Complexes, Only One of which Is Rapamycin Sensitive, Have Distinct Roles in Cell Growth Control. *Molecular Cell*, 10(3), 457–468. [https://doi.org/10.1016/S1097-2765\(02\)00636-6](https://doi.org/10.1016/S1097-2765(02)00636-6)
- Magasanik, B., & Kaiser, C. A. (2002). Nitrogen regulation in *Saccharomyces cerevisiae*. *Gene*, 290(1–2), 1–18. [https://doi.org/10.1016/S0378-1119\(02\)00558-9](https://doi.org/10.1016/S0378-1119(02)00558-9)
- Masson, G. R. (2019). Towards a model of GCN2 activation. *Biochemical Society Transactions*, 47(5), 1481–1488. <https://doi.org/10.1042/BST20190331>



- Meng, D., Yang, Q., Wang, H., Melick, C. H., Navlani, R., Frank, A. R., & Jewell, J. L. (2020). Glutamine and asparagine activate mTORC1 independently of Rag GTPases. *Journal of Biological Chemistry*, 295(10), 2890–2899. <https://doi.org/10.1074/jbc.AC119.011578>
- Michel, A. H., Hatakeyama, R., Kimmig, P., Arter, M., Peter, M., Matos, J., De Virgilio, C., & Kornmann, B. (2017). Functional mapping of yeast genomes by saturated transposition. *ELife*, 6, e23570. <https://doi.org/10.7554/eLife.23570>
- Michel, A. H., van Schie, S., Mosbach, A., Scalliet, G., & Kornmann, B. (2019). *Exploiting homologous recombination increases SATAY efficiency for loss- and gain-of-function screening* [Preprint]. *Cell Biology*. <https://doi.org/10.1101/866483>
- Molon, M., Woznicka, O., & Zebrowski, J. (2018). Cell wall biosynthesis impairment affects the budding lifespan of the *Saccharomyces cerevisiae* yeast. *Biogerontology*, 19(1), 67–79. <https://doi.org/10.1007/s10522-017-9740-6>
- Nada, S., Hondo, A., Kasai, A., Koike, M., Saito, K., Uchiyama, Y., & Okada, M. (2009). The novel lipid raft adaptor p18 controls endosome dynamics by anchoring the MEK–ERK pathway to late endosomes. *The EMBO Journal*, 28(5), 477–489. <https://doi.org/10.1038/emboj.2008.308>
- Nadolski, M. J., & Linder, M. E. (2009). Molecular recognition of the palmitoylation substrate Vac8 by its palmitoyltransferase Pfa3. *The Journal of Biological Chemistry*, 284(26), 17720–17730. <https://doi.org/10.1074/jbc.M109.005447>
- Nakashima, N., Noguchi, E., & Nishimoto, T. (1999). *Saccharomyces cerevisiae* putative G protein, Gtr1p, which forms complexes with itself and a novel protein designated as Gtr2p, negatively regulates the Ran/Gsp1p G protein cycle through Gtr2p. *Genetics*, 152(3), 853–867.
- Nakatsukasa, K., Okumura, F., & Kamura, T. (2015). Proteolytic regulation of metabolic enzymes by E3 ubiquitin ligase complexes: Lessons from yeast. *Critical Reviews in Biochemistry and Molecular Biology*, 50(6), 489–502. <https://doi.org/10.3109/10409238.2015.1081869>
- Nassar, N., Singh, K., & Garcia-Diaz, M. (2010). Structure of the Dominant Negative S17N Mutant of Ras. *Biochemistry*, 49(9), 1970–1974. <https://doi.org/10.1021/bi9020742>
- Natarajan, K., Meyer, M. R., Jackson, B. M., Slade, D., Roberts, C., Hinnebusch, A. G., & Marton, M. J. (2001). Transcriptional Profiling Shows that Gcn4p Is a Master Regulator of Gene Expression during Amino Acid Starvation in Yeast. *Molecular and Cellular Biology*, 21(13), 4347–4368. <https://doi.org/10.1128/MCB.21.13.4347-4368.2001>
- Nicastro, R., Sardu, A., Panchaud, N., & De Virgilio, C. (2017). The Architecture of the Rag GTPase Signaling Network. *Biomolecules*, 7(4), 48. <https://doi.org/10.3390/biom7030048>
- Ostrowicz, C. W., Meiringer, C. T. A., & Ungermann, C. (2008). Yeast vacuole fusion: A model system for eukaryotic endomembrane dynamics. *Autophagy*, 4(1), 5–19. <https://doi.org/10.4161/auto.5054>
- Panchaud, N., Péli-Gulli, M.-P., & De Virgilio, C. (2013a). Amino Acid Deprivation Inhibits TORC1 Through a GTPase-Activating Protein Complex for the Rag Family GTPase Gtr1. *Science Signaling*, 6(277), ra42–ra42. <https://doi.org/10.1126/scisignal.2004112>
- Panchaud, N., Péli-Gulli, M.-P., & De Virgilio, C. (2013b). SEACing the GAP that nEGOCIates TORC1 activation: Evolutionary conservation of Rag GTPase regulation. *Cell Cycle*, 12(18), 2948–2952. <https://doi.org/10.4161/cc.26000>
- Péli-Gulli, M.-P., Raucchi, S., Hu, Z., Dengjel, J., & De Virgilio, C. (2017). Feedback Inhibition of the Rag GTPase GAP Complex Lst4-Lst7 Safeguards TORC1 from Hyperactivation by Amino Acid Signals. *Cell Reports*, 20(2), 281–288. <https://doi.org/10.1016/j.celrep.2017.06.058>
- Peng, M., Yin, N., & Li, M. O. (2017). SZT2 dictates GATOR control of mTORC1 signalling. *Nature*, 543(7645), 433–437. <https://doi.org/10.1038/nature21378>
- Petit, C. S., Roczniak-Ferguson, A., & Ferguson, S. M. (2013). Recruitment of folliculin to lysosomes supports the amino acid-dependent activation of Rag GTPases. *Journal of Cell Biology*, 202(7), 1107–1122. <https://doi.org/10.1083/jcb.201307084>
- Powis, K., Zhang, T., Panchaud, N., Wang, R., Virgilio, C. D., & Ding, J. (2015). Crystal structure of the Ego1-Ego2-Ego3 complex and its role in promoting Rag GTPase-dependent TORC1 signaling. *Cell Research*, 25(9), 1043–1059. <https://doi.org/10.1038/cr.2015.86>
- Roth, A. F., Wan, J., Bailey, A. O., Sun, B., Kuchar, J. A., Green, W. N., Phinney, B. S., Yates, J. R., & Davis, N. G. (2006). Global Analysis of Protein Palmitoylation in Yeast. *Cell*, 125(5), 1003–1013. <https://doi.org/10.1016/j.cell.2006.03.042>

- Sabatini, D. M., Erdjument-Bromage, H., Lui, M., Tempst, P., & Snyder, S. H. (1994). RAFT1: A mammalian protein that binds to FKBP12 in a rapamycin-dependent fashion and is homologous to yeast TORs. *Cell*, 78(1), 35–43. [https://doi.org/10.1016/0092-8674\(94\)90570-3](https://doi.org/10.1016/0092-8674(94)90570-3)
- Sabers, C. J., Martin, M. M., Brunn, G. J., Williams, J. M., Dumont, F. J., Wiederrecht, G., & Abraham, R. T. (1995). Isolation of a Protein Target of the FKBP12-Rapamycin Complex in Mammalian Cells. *Journal of Biological Chemistry*, 270(2), 815–822. <https://doi.org/10.1074/jbc.270.2.815>
- Sancak, Y., Bar-Peled, L., Zoncu, R., Markhard, A. L., Nada, S., & Sabatini, D. M. (2010). Ragulator-Rag Complex Targets mTORC1 to the Lysosomal Surface and Is Necessary for Its Activation by Amino Acids. *Cell*, 141(2), 290–303. <https://doi.org/10.1016/j.cell.2010.02.024>
- Sancak, Y., Peterson, T. R., Shaul, Y. D., Lindquist, R. A., Thoreen, C. C., Bar-Peled, L., & Sabatini, D. M. (2008). The Rag GTPases Bind Raptor and Mediate Amino Acid Signaling to mTORC1. *Science*, 320(5882), 1496–1501. <https://doi.org/10.1126/science.1157535>
- Santt, O., Pfirrmann, T., Braun, B., Juretschke, J., Kimmig, P., Scheel, H., Hofmann, K., Thumm, M., & Wolf, D. H. (2008). The Yeast GID Complex, a Novel Ubiquitin Ligase (E3) Involved in the Regulation of Carbohydrate Metabolism. *Molecular Biology of the Cell*, 19(8), 3323–3333. <https://doi.org/10.1091/mbc.e08-03-0328>
- Sarbassov, D. D., Ali, S. M., & Sabatini, D. M. (2005). Growing roles for the mTOR pathway. *Current Opinion in Cell Biology*, 17(6), 596–603. <https://doi.org/10.1016/j.ceb.2005.09.009>
- Saxton, R. A., Chantranupong, L., Knockenhauer, K. E., Schwartz, T. U., & Sabatini, D. M. (2016). Mechanism of arginine sensing by CASTOR1 upstream of mTORC1. *Nature*, 536(7615), 229–233. <https://doi.org/10.1038/nature19079>
- Saxton, R. A., & Sabatini, D. M. (2017). mTOR Signaling in Growth, Metabolism, and Disease. *Cell*, 168(6), 960–976. <https://doi.org/10.1016/j.cell.2017.02.004>
- Schürmann, A., Brauers, A., Maßmann, S., Becker, W., & Joost, H.-G. (1995). Cloning of a Novel Family of Mammalian GTP-binding Proteins (RagA, RagBs, RagB1) with Remote Similarity to the Ras-related GTPases. *Journal of Biological Chemistry*, 270(48), 28982–28988. <https://doi.org/10.1074/jbc.270.48.28982>
- Sekiguchi, T., Hirose, E., Nakashima, N., Ii, M., & Nishimoto, T. (2001). Novel G Proteins, Rag C and Rag D, Interact with GTP-binding Proteins, Rag A and Rag B. *Journal of Biological Chemistry*, 276(10), 7246–7257. <https://doi.org/10.1074/jbc.M004389200>
- Shen, K., & Sabatini, D. M. (2018). Ragulator and SLC38A9 activate the Rag GTPases through noncanonical GEF mechanisms. *Proceedings of the National Academy of Sciences*, 115(38), 9545–9550. <https://doi.org/10.1073/pnas.1811727115>
- Starr, M. L., & Fratti, R. A. (2019). The Participation of Regulatory Lipids in Vacuole Homotypic Fusion. *Trends in Biochemical Sciences*, 44(6), 546–554. <https://doi.org/10.1016/j.tibs.2018.12.003>
- Stracka, D., Jozefczuk, S., Rudroff, F., Sauer, U., & Hall, M. N. (2014). Nitrogen Source Activates TOR (Target of Rapamycin) Complex 1 via Glutamine and Independently of Gtr/Rag Proteins. *Journal of Biological Chemistry*, 289(36), 25010–25020. <https://doi.org/10.1074/jbc.M114.574335>
- Sturgill, T. W., Cohen, A., Diefenbacher, M., Trautwein, M., Martin, D. E., & Hall, M. N. (2008). TOR1 and TOR2 Have Distinct Locations in Live Cells. *Eukaryotic Cell*, 7(10), 1819–1830. <https://doi.org/10.1128/EC.00088-08>
- Tafur, L., Kefauver, J., & Loewith, R. (2020). Structural Insights into TOR Signaling. *Genes*, 11(8), 885. <https://doi.org/10.3390/genes11080885>
- Tanaka, N., & Mukai, Y. (2015). Yeast Cyc8p and Tup1p proteins function as coactivators for transcription of Stp1/2p-dependent amino acid transporter genes. *Biochemical and Biophysical Research Communications*, 468(1–2), 32–38. <https://doi.org/10.1016/j.bbrc.2015.11.001>
- Tanigawa, M., & Maeda, T. (2017). An *In Vitro* TORC1 Kinase Assay That Recapitulates the Gtr-Independent Glutamine-Responsive TORC1 Activation Mechanism on Yeast Vacuoles. *Molecular and Cellular Biology*, 37(14). <https://doi.org/10.1128/MCB.00075-17>
- Thoms, M., Mitterer, V., Kater, L., Falquet, L., Beckmann, R., Kressler, D., & Hurt, E. (2018). Suppressor mutations in Rpf2–Rrs1 or Rpl5 bypass the Cgr1 function for pre-ribosomal 5S RNP-rotation. *Nature Communications*, 9(1), 4094. <https://doi.org/10.1038/s41467-018-06660-w>
- Tsun, Z.-Y., Bar-Peled, L., Chantranupong, L., Zoncu, R., Wang, T., Kim, C., Spooner, E., & Sabatini, D. M. (2013). The Folliculin Tumor Suppressor Is a GAP for the RagC/D GTPases That

- Signal Amino Acid Levels to mTORC1. *Molecular Cell*, 52(4), 495–505. <https://doi.org/10.1016/j.molcel.2013.09.016>
- Ukai, H., Araki, Y., Kira, S., Oikawa, Y., May, A. I., & Noda, T. (2018). Gtr/Ego-independent TORC1 activation is achieved through a glutamine-sensitive interaction with Pib2 on the vacuolar membrane. *PLOS Genetics*, 14(4), e1007334. <https://doi.org/10.1371/journal.pgen.1007334>
- Valbuena, N., Guan, K.-L., & Moreno, S. (2012). The Vam6-Gtr1/Gtr2 pathway activates TORC1 in response to amino acids in fission yeast. *Journal of Cell Science*, jcs.094219. <https://doi.org/10.1242/jcs.094219>
- Varlakhanova, N. V., Mihalevic, M., Bernstein, K. A., & Ford, M. G. J. (2017). Pib2 and EGO Complex are both required for activation of TORC1. *Journal of Cell Science*, jcs.207910. <https://doi.org/10.1242/jcs.207910>
- Wedaman, K. P., Reinke, A., Anderson, S., Yates, J., McCaffery, J. M., & Powers, T. (2003). Tor Kinases Are in Distinct Membrane-associated Protein Complexes in *Saccharomyces cerevisiae*. *Molecular Biology of the Cell*, 14(3), 1204–1220. <https://doi.org/10.1091/mbc.e02-09-0609>
- Wolfson, R. L., Chantranupong, L., Saxton, R. A., Shen, K., Scaria, S. M., Cantor, J. R., & Sabatini, D. M. (2016). Sestrin2 is a leucine sensor for the mTORC1 pathway. *Science*, 351(6268), 43–48. <https://doi.org/10.1126/science.aab2674>
- Wolfson, R. L., Chantranupong, L., Wyant, G. A., Gu, X., Orozco, J. M., Shen, K., Condon, K. J., Petri, S., Kedir, J., Scaria, S. M., Abu-Remaileh, M., Frankel, W. N., & Sabatini, D. M. (2017). KICSTOR recruits GATOR1 to the lysosome and is necessary for nutrients to regulate mTORC1. *Nature*, 543(7645), 438–442. <https://doi.org/10.1038/nature21423>
- Wullschleger, S., Loewith, R., & Hall, M. N. (2006). TOR Signaling in Growth and Metabolism. *Cell*, 124(3), 471–484. <https://doi.org/10.1016/j.cell.2006.01.016>
- Zaman, S., Lippman, S. I., Zhao, X., & Broach, J. R. (2008). How *Saccharomyces* Responds to Nutrients. *Annual Review of Genetics*, 42(1), 27–81. <https://doi.org/10.1146/annurev.genet.41.110306.130206>
- Zhang, T., Péli-Gulli, M.-P., Zhang, Z., Tang, X., Ye, J., De Virgilio, C., & Ding, J. (2019). Structural insights into the EGO-TC-mediated membrane tethering of the TORC1-regulatory Rag GTPases. *Science Advances*, 5(9), eaax8164. <https://doi.org/10.1126/sciadv.aax8164>
- Zhang, W., Du, G., Zhou, J., & Chen, J. (2018). Regulation of Sensing, Transportation, and Catabolism of Nitrogen Sources in *Saccharomyces cerevisiae*. *Microbiology and Molecular Biology Reviews*, 82(1). <https://doi.org/10.1128/MMBR.00040-17>

## **CHAPTER 2: STUDY OF THE CROSSTALK BETWEEN TORC1 AND THE GAAC SIGNALING PATHWAYS**

## 2.1: INTRODUCTION

### 2.1.1: General introduction to the ISR/GAAC pathway

The Integrated Stress Response (ISR) pathway in mammalian cells or the General Amino Acid Control (GAAC) pathway in yeast is a conserved prosurvival pathway, which senses the availability of intracellular amino acids in parallel to the mTORC1/TORC1 pathway (Figure 1) (Masson, 2019, and references therein). Under stressful conditions, such as amino acid starvation, the Gcn2 (General Control Nonderepressible 2) protein kinase phosphorylates serine 52 of eIF2 $\alpha$  (translation initiation factor eIF2 subunit alpha, called Sui2 (SUppressor of Initiator codon) in yeast). This leads to the general repression of protein translation initiation and to the assembly of stress granules and the translation of stress-responsive mRNAs that possess a specific short open reading frame in their 5'-untranslated region (5'UTR) (Figure 1) (Advani & Ivanov, 2019, and references therein).

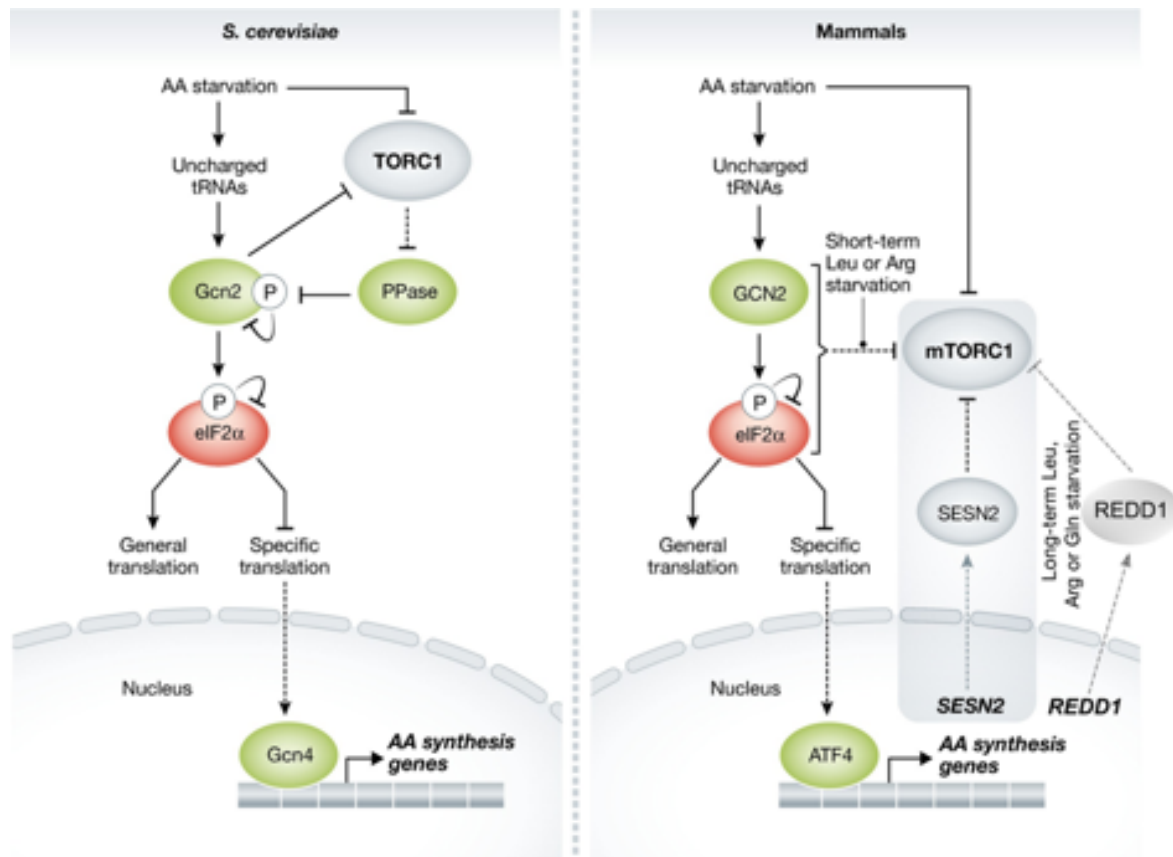


Figure 1: Amino acid-dependent activation of the GAAC (left) and ISR (right) pathways in *S.cerevisiae* and mammalian cells, respectively. Adapted from González & Hall, 2017.



Among these stress-responsive mRNAs, the *GCN4* mRNA in yeast and *ATF4* mRNA in mammals encode leucine zipper transcription factors that coordinate the expression of genes related to amino acid biosynthesis, nitrogen utilization, and signaling (Figure 1) (Hinnebusch, 2005; Pakos-Zebrucka et al., 2016; Wek, 2018). Therefore, activating the protein kinase Gcn2 after amino acid deprivation is essential for rewiring the cellular gene expression profile (Pakos-Zebrucka et al., 2016; Wek, 2018). Apart from amino acid deprivation, the Gcn2 kinase has been proposed to get active in response to other stimuli such as UV damage and stalled ribosomes (Anda et al., 2017; Masson, 2019).

### **2.1.2: The Gcn1-Gcn20 Gcn2 regulatory complex**

The Gcn1-Gcn20 heterodimer is critical for Gcn2 activation in response to amino acid starvation (Marton et al., 1993, 1997; Sattlegger & Hinnebusch, 2005). Gcn1 mediates the Gcn2-Gcn1-Gcn20 complex formation through interactions with both Gcn2 and Gcn20 (Garcia-Barrio, 2000; Kubota et al., 2000). In particular, the C-terminus of Gcn1 interacts with the RWD domain of Gcn2 (Sattlegger, 2000), while the HEAT repeats of Gcn1 bind the N-terminus of Gcn20 (Vazquez de Aldana et al., 1995). Notably, Gcn1 and Gcn20 have been shown to bind ribosomes (Marton et al., 1997; Sattlegger, 2000) and to share sequence homology with the translation elongation factor 3 (eEF3), which is in charge of promoting, during active translation, the release of uncharged tRNA from the E-site of ribosomes. Although the exact mechanism is still unclear, it might be possible that Gcn1 and Gcn20 promote the release of uncharged tRNAs from the A site of ribosomes to channel them to Gcn2 (Inglis et al., 2019; Marton et al., 1993; Sattlegger & Hinnebusch, 2005).

### **2.1.3: Activation of Gcn2 by tRNAs**

In nutrient-rich conditions, Gcn2 activation is mainly repressed by several autoinhibitory molecular interactions (Dey et al., 2007; Gárriz et al., 2009; Padyana et al., 2005; Qiu et al., 2001). Following amino acid deprivation, there is an increase in the pool of deacylated tRNAs that bind and activate the Gcn2 kinase activity (Lageix et al., 2015). The lysines 1552, 1553, and 1556 of the C-terminal domain (CTD) of Gcn2 and the m2 motif within the HisRS-like domain of Gcn2 mediate the binding of deacetylated tRNAs (Dong et al., 2000; Masson, 2019; Qiu et al., 2001; Wek et al., 1995). Besides,

dimerization of the HisRS-like domain of Gcn2 is crucial for tRNA binding and activation (Qiu et al., 2001). The binding of deacetylated tRNAs triggers a rearrangement of the Gcn2 structure that leads to the autophosphorylation of the Gcn2 activation loop within the protein kinase domain (*i.e.*, in yeast, Gcn2<sup>T882</sup> and Gcn2<sup>T887</sup>; and in mammals, Gcn2<sup>T898</sup>, and Gcn2<sup>T903</sup>) and the formation of a trans-dimer salt bridge (Dey et al., 2007; Lageix et al., 2014, 2015; Padyana et al., 2005; Romano et al., 1998).

#### **2.1.4: Activation of Gcn2 by the P-stalk**

The P-stalk, a heteropentameric complex composed of one copy of P0 ( $\mu$ L10) and two copies of P1 and P2, is proposed to lay around the A-site of the ribosome where it interacts with translation factors (Inglis et al., 2019 and references therein). Different *in vitro* studies have shown that Gcn2 interacts with the ribosomal P-stalk and that this interaction can activate Gcn2 even in the absence of deacetylated tRNAs (Inglis et al., 2019; Jiménez-Díaz et al., 2013). The surface of the Gcn2-P-stalk interaction would include, on one side, the pseudokinase, the kinase, and the HisRS-like domains of Gcn2 and, on the other side, the domain II of P0 plus the C-terminal tails of P0, P1, and P2 (Inglis et al., 2019 and references therein). Though the exact mechanism by which the P-stalk regulates the *in vivo* Gcn2 activity remains elusive, it has been proposed that ribosome stalling enhances the affinity of the Gcn2-Gcn1-Gcn20 complex for the P-stalk where then Gcn1 and Gcn20 would transfer uncharged tRNAs from the A site of ribosomes to the HisRS-like domain of Gcn2 (Inglis et al., 2019; Marton et al., 1993; Sattlegger & Hinnebusch, 2005).

#### **2.1.5: Regulation of the protein translation initiation**

eIF2 $\alpha$  associates with eIF2 $\beta$  (translation initiation factor eIF2 subunit beta; Sui3 (SUppressor of Initiator codon 3) in yeast) and eIF2 $\gamma$  (translation initiation factor eIF2 subunit gamma; Gcd11 (General Control Derepressed 11) in yeast) to form a trimeric complex with nucleotide-binding capacity called translation initiation factor eIF2 (Merrick & Pavitt, 2018, and references therein). In favorable nutritional conditions, the GTP-loaded eIF2 complex (eIF2-GTP) binds methionyl-charged tRNA (Met-tRNA<sup>i</sup>) to form the ternary complex (TC) eIF2-GTP-Met-tRNA<sup>i</sup> (Adomavicius et al., 2019, Merrick & Pavitt, 2018). Later, the TC associates with the 40S ribosomal subunit, and other eIFs,

to constitute the 43S preinitiation complex (PIC), which travels through the mRNA strand until it finds an AUG start codon (Adomavicius et al., 2019, Merrick & Pavitt, 2018). Once the AUG start codon is found, the GTPase-Activating Protein (GAP) eIF5 promotes, within the PIC, the hydrolysis of the GTP bound to the eIF2 complex (eIF2-GTP), thereby triggering the release of the eIF5-bound eIF2-GDP complex, while the Met-tRNA<sub>i</sub> remains bound to the 40S ribosomal subunit (Adomavicius et al., 2019, and references therein). Finally, the 60S ribosomal subunit is recruited by the Met-tRNA<sub>i</sub>-bound 40S ribosomal subunit forming the 80S initiation complex, which continues with protein translation (Adomavicius et al., 2019, and references therein). eIF5 not only promotes the hydrolysis of the GTP bound to eIF2 but also acts as a Guanosine Dissociation Inhibitor (GDI) by blocking the release of the GDP from the eIF2 complex (eIF2-GDP) (Adomavicius et al., 2019, and references therein). It is only by the action of the Guanine Exchange Factor (GEF) eIF2B that eIF5 is displaced and eIF2 can exchange GDP by GTP, thereby activating the eIF2 complex for another round of protein synthesis initiation (Adomavicius et al., 2019, and references therein).

As mentioned above, Gcn2 has been shown to phosphorylate the  $\alpha$  subunit of eIF2 (eIF2 $\alpha$ ) in response to amino acid starvation. While in *S. cerevisiae*, only Gcn2 has been shown to phosphorylate the serine 52 of eIF2 $\alpha$ , in mammalian cells, three more kinases can phosphorylate this residue in response to different stresses: HRI (Heme-Regulated eIF2 $\alpha$  kinase) in response to oxidative stress, PKR (double-stranded RNA-dependent Protein Kinase) in response to viral infection, and PERK (PKR-like ER Kinase) in response to Endoplasmic Reticulum stress (ER stress) (Masson, 2019; Pakos-Zebrucka et al., 2016; Wek et al., 2006).

#### **2.1.6: Crosstalk between the ISR/GAAC and the mTORC1/TORC1 pathways**

Some examples of crosstalk between the ISR/GAAC and the mTORC1/TORC1 signaling pathways have been reported (Figure 1). For instance, in *S. cerevisiae*, the dephosphorylation of the serine 577 of Gcn2 (Gcn2<sup>pS577</sup>), which keeps Gcn2 inactive, has been shown to be regulated by the TORC1 activity (Cherkasova, 2003; Kubota et al., 2003). In rich conditions, TORC1 is active, and Tap42 (Two A phosphatase associated protein 42) associates with and inhibits Sit4 and the PP2A phosphatases. Upon amino acid starvation, TORC1 inhibition favors the dissociation of Tap42 from Sit4 and the PP2A phosphatases, which then catalyze the dephosphorylation of

Gcn2<sup>pS577</sup>, thereby promoting Gcn2 activation (Cherkasova, 2003; Kubota et al., 2003). Notably, Gcn2 activation by dephosphorylation of its serine 577 seems to require the binding of deacetylated tRNAs (Cherkasova, 2003; Kubota et al., 2003). Importantly, *in vivo* data show that substituting the serine 577 by alanine leads to constitutive Gcn2 autophosphorylation and activation (Cherkasova, 2003; Garcia-Barrio et al., 2002).

In mammalian cells, Gcn2 has been proposed to inhibit mTORC1 upon amino acid deprivation through both ATF4-dependent and independent mechanisms (Averous et al., 2016; Rasmussen & Adams, 2020; Xu et al., 2020; Ye et al., 2015). On the one hand, the ATF4-independent mechanism seems to be mediated by an increase of eIF2 $\alpha$  phosphorylation upon leucine or arginine starvation (Averous et al., 2016). On the other hand, the ATF-dependent mechanism requires prolonged amino acid deprivation and involves the expression of Sestrin2 and REDD1 (Rasmussen & Adams, 2020; Xu et al., 2020; Ye et al., 2015).

In *S. cerevisiae*, Gcn2 has been proposed to phosphorylate the RNC (Raptor-like N-terminal–Conserved) domain of Kog1, thereby inhibiting the TORC1 activity in response to leucine or histidine starvation (Yuan et al., 2017). Recently, in *S. pombe*, Gcn2 has also been shown to inhibit TORC1 upon leucine starvation; however, in this case, the downstream Gcn2 effectors (*i.e.*, eIF2 $\alpha$ , Gcn3, and Fil1) are needed (Fukuda et al., 2021).

### **2.1.7: The Gcn2 kinase in disease**

The ISR/GAAC pathway is a prosurvival pathway essential for rewiring the cellular gene expression profile under different stresses (Pakos-Zebrucka et al., 2016; Wek, 2018). In particular, the Gcn2 kinase has been shown to sense amino acid scarcity, thereby getting active and regulating critical cellular processes such as protein translation, autophagy, and amino acid metabolism. Therefore, deregulation or malfunction of the Gcn2 kinase is linked to malignancy, metabolic disorders, oxidative stress, and neurodegeneration (Castilho et al., 2014; Falcón et al., 2019; Moradi Majd et al., 2020).

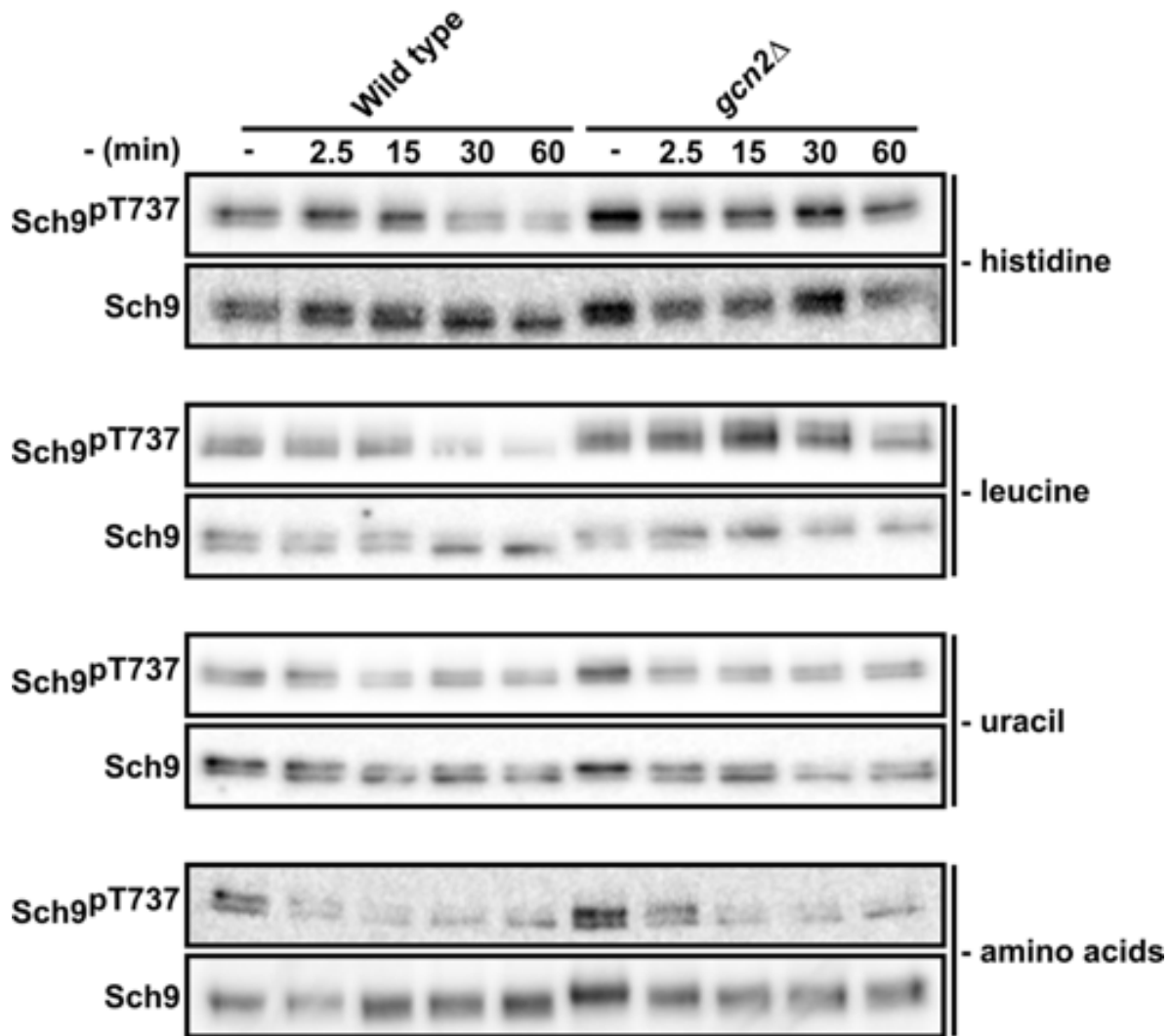
## **2.2: AIM OF THE CHAPTER**

In *S. cerevisiae*, the TORC1 and Gcn2 kinases respond antagonistically to amino acids availability. An excess of amino acids activates TORC1, thereby promoting anabolic and repressing catabolic processes, while amino acids scarcity activates Gcn2, thereby inhibiting general protein translation, promoting the translation of stress-responsive mRNAs and the activation of degradative pathways. Notably, the TORC1 and GAAC pathways interplay is crucial for cellular proteostasis, as exemplified by the reported crosstalk between the mTORC1/TORC1 and Gcn2 kinases. Interestingly, Yuan and colleagues in 2017 proposed that Gcn2 phosphorylates Kog1, thereby inhibiting TORC1, in response to histidine or leucine starvation (Yuan et al., 2017). Following this lead, this chapter aims to further characterize the regulation of TORC1 by the Gcn2 kinase.

## **2.3: RESULTS**

### **2.3.1: The Gcn2 expression is necessary for inhibiting TORC1 in leucine- or histidine-, but not nitrogen-starved cells**

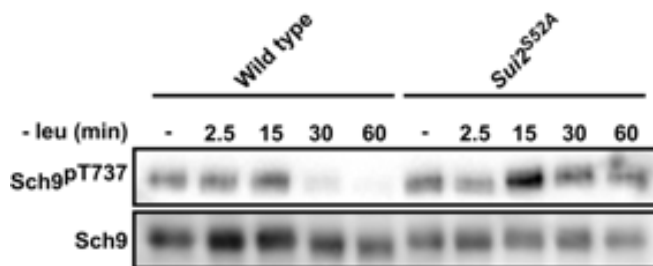
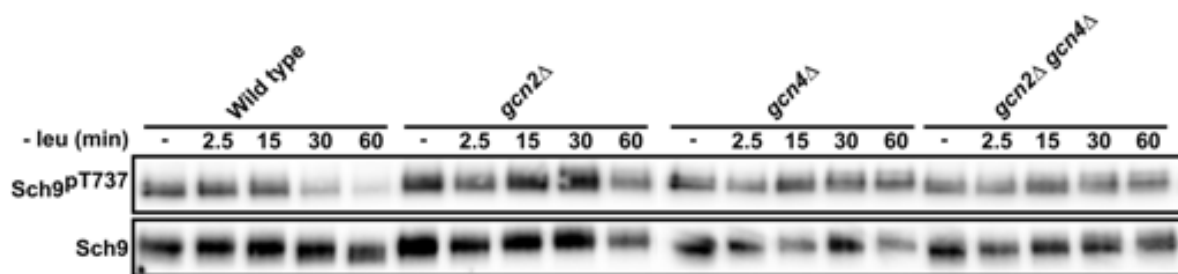
In *S. cerevisiae*, loss of Gcn2 has been proposed to prevent TORC1 inactivation upon leucine or histidine starvation (Yuan et al., 2017). We first validated that Gcn2 expression is necessary for inhibiting TORC1 upon leucine or histidine, but not upon nitrogen starvation (Figure 2). Notably, Gcn2 has been proposed to inhibit the TORC1 activity by phosphorylating the RNC domain of Kog1 (Yuan et al., 2017). Nonetheless, we wondered whether, apart from this direct Gcn2-dependent TORC1 regulation, downstream targets of Gcn2 affect the TORC1 activity.



**Figure 2: Gcn2 expression is necessary for inhibiting TORC1 in leucine- or histidine-, but not nitrogen-starved cells.** For histidine starvation (- histidine), we made use of WT and *gcn2*Δ cells auxotrophic for tryptophan and histidine; for leucine starvation (- leucine), WT and *gcn2*Δ cells auxotrophic for tryptophan and leucine were used; and for uracil starvation (- uracil), we made use of WT and *gcn2*Δ cells auxotrophic for tryptophan and uracil. Cells were grown exponentially in SC and then starved of the mentioned compound for the indicated times. In the all amino acid starvation experiment, WT and *gcn2*Δ cells auxotrophic for tryptophan were grown exponentially in SC and then starved for all amino acids (- amino acids) for the indicated times. Protein extracts were analyzed by SDS-PAGE and probed with anti-Sch9-pThr737 and anti-Sch9 antibodies.

### 2.3.2: The transcription factor Gcn4 also mediates TORC1 inhibition in leucine-starved cells

Hence, we decided to assess the TORC1 activity in leucine-starved (- leu) cells expressing the non-phosphorylatable variant of eIF2α (*sui2*<sup>S52A</sup>; Dever et al., 1992) (Figure 3A) and in leucine-starved (- leu) *gcn4*Δ and *gcn2*Δ *gcn4*Δ cells (Figure 3B).

**A****B**

**Figure 3: Gcn2 and Gcn4 mediate TORC1 inhibition in leucine-starved cells.** In (A) and (B), WT, *sui2<sup>S52A</sup>*, *gcn2Δ*, *gcn4Δ*, and *gcn2Δ gcn4Δ* cells (auxotrophic for tryptophan and leucine) were grown exponentially in SC and then starved for leucine for the indicated times. Protein extracts were analyzed by SDS-PAGE and probed with anti-Sch9-pThr737 and anti-Sch9 antibodies. Figure 3B adapted from Dokládál et al., 2021.

Interestingly, even in cells expressing Gcn2, expression of the non-phosphorylatable variant of eIF2 $\alpha$  (*sui2<sup>S52A</sup>*) or loss of Gcn4 protected the TORC1 activity from inactivation upon leucine starvation (Figure 3). Notably, the simultaneous loss of Gcn2 and Gcn4 did not further enhance this protection (Figure 3B). Therefore, we can conclude that, apart from the previously described Gcn2-dependent branch of TORC1 regulation, there exists a Gcn2-independent branch of TORC1 regulation that implicates the Gcn2 downstream effectors Sui2 and Gcn4 (Figure 3) (Dokládál et al., 2021).

### 2.3.3: Discovery of new Gcn2 targets in *S. cerevisiae*

As previously described, Gcn2 has been proposed to inhibit TORC1 through direct phosphorylation of Kog1 (Yuan et al., 2017). To confirm this result and to potentially find new Gcn2 targets within the TORC1 signaling pathway, we performed a set of quantitative phosphoproteomic experiments (an independent duplicate) using leucine-starved WT and *gcn2Δ* cells. For one replicate, we used the Stable Isotope Labeling by Amino acids in Cell culture (SILAC) method (as described in Hu et al., 2019), and for the other, the stable isotope DiMethyl Labeling (DML) at the peptide level method (Boersema et al., 2009; Tolonen & Haas, 2014). In *gcn2Δ* cells, a total of 46 significant

( $p$ -value < 0.05) hypophosphorylated and hyperphosphorylated residues were commonly identified between SILAC and DML phosphoproteomic experiments (Table 1).

Gene names	Protein names	SILAC log <sub>2</sub> (Fold change)	DML log <sub>2</sub> (Fold change)	Identified residue	Amino acid
<i>GCN2</i>	Serine/threonine-protein kinase GCN2	-5.87	-4.65	577	S
<i>GCN20</i>	Protein GCN20	-4.69	-3.77	95	S
<i>NCS2</i>	Cytoplasmic tRNA 2-thiolation protein 2	-4.64	-4.25	177	S
<i>TIF4631</i>	Eukaryotic initiation factor 4F subunit p150	-4.61	-2.54	920	S
<i>DED1</i>	ATP-dependent RNA helicase DED1	-3.97	-4.43	539	S
<i>DED1</i>	ATP-dependent RNA helicase DED1	-3.95	-4.41	543	S
<i>DED1</i>	ATP-dependent RNA helicase DED1	-3.87	-4.07	535	S
<i>DED1</i>	ATP-dependent RNA helicase DED1	-3.87	-5.75	541	S
<i>NUP1</i>	Nucleoporin NUP1	-3.86	-4.38	6	S
<i>RPS6B</i> ; <i>RPS6A</i>	40S ribosomal protein S6-B;40S ribosomal protein S6-A	-3.59	-4.60	232;232	S
<i>CBK1</i>	Serine/threonine-protein kinase CBK1	-3.57	-2.80	559	T
<i>YHR020W</i>	Putative proline-tRNA ligase YHR020W	-3.47	-3.87	149	S
<i>TIF4631</i>	Eukaryotic initiation factor 4F subunit p150	-3.46	-5.63	502	S
<i>TFG1</i>	Transcription initiation factor IIF subunit alpha	-3.05	-2.80	673	T
<i>HOS4</i>	Protein HOS4	-3.00	-3.36	688	T
<i>TIF4632</i>	Eukaryotic initiation factor 4F subunit p130	-2.98	-3.52	485	S
<i>SUI3</i>	Eukaryotic translation initiation factor 2 subunit beta	-2.72	-2.88	80	S
<i>SUM1</i>	Suppressor of mar1-1 protein	-2.55	-3.87	614	S
<i>MTC1</i>	Maintenance of telomere capping protein 1	-2.33	-2.54	72	S
<i>GCD6</i>	Translation initiation factor eIF-2B subunit epsilon	-2.26	-4.34	538	S
<i>GCN2</i>	Serine/threonine-protein kinase GCN2	-2.21	-5.97	572	S
<i>BAS1</i>	Myb-like DNA-binding protein BAS1	-2.20	-3.49	317	S
<i>SND1</i>	Srp-independent targeting	-2.17	-2.85	605	T
<i>DEF1</i>	RNA polymerase II degradation factor 1	-2.13	-6.26	227	S
<i>TIF4631</i>	Eukaryotic initiation factor 4F subunit p150	-2.02	-4.30	553	S
<i>ATG13</i>	Autophagy-related protein 13	-1.89	-2.65	577	S
<i>DEF1</i>	RNA polymerase II degradation factor 1	-1.56	-2.82	108	S
<i>SND1</i>	Srp-independent targeting	-1.55	-4.17	603	S
<i>SND1</i>	Srp-independent targeting	-1.52	-2.53	516	S
<i>DAT1</i>	Oligo(A)/oligo(T)-binding protein	-1.47	-3.27	230	S
<i>TIF5</i>	Eukaryotic translation initiation factor 5	-1.47	-5.10	228	S
<i>SUI2</i>	Eukaryotic translation initiation factor 2 subunit alpha	-1.42	-2.59	52	S
<i>YBT1</i>	ATP-dependent bile acid permease	-1.35	-3.42	945	S
<i>RRP15</i>	Ribosomal RNA-processing protein 15	-1.19	-3.03	233	S
<i>KCS1</i>	Inositol hexakisphosphate kinase 1	1.24	2.93	638	S
<i>TPS3</i>	Trehalose synthase complex regulatory subunit TPS3	1.70	2.17	195	S
<i>PUF6</i>	Pumilio homology domain family member 6	1.74	2.16	34	S



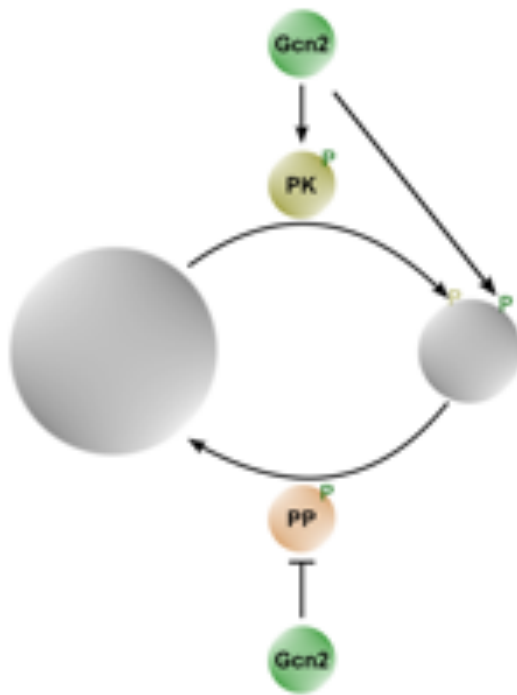
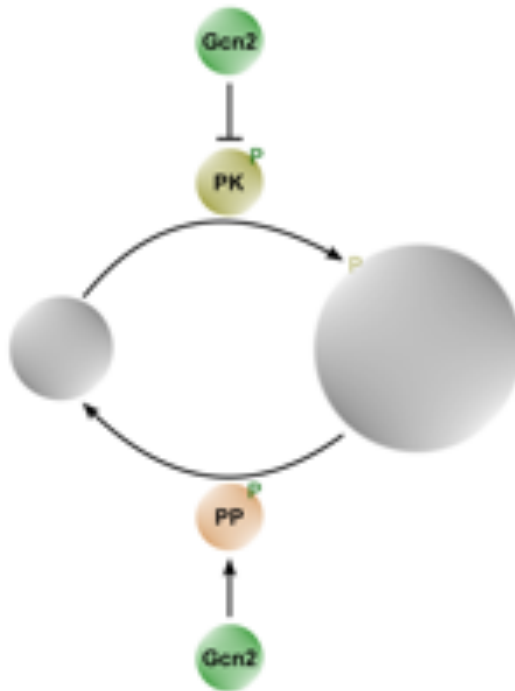
<i>RPS17B</i> ; <i>RPS17A</i>	40S ribosomal protein S17-B;40S ribosomal protein S17-A	1.86	2.66	89;89	S
<i>GCD1</i>	Translation initiation factor eIF-2B subunit gamma	1.95	2.76	296	S
<i>IST1</i>	Vacuolar protein sorting-associated protein IST1	1.99	2.20	244	S
<i>NOP13</i>	Nucleolar protein 13	2.15	6.76	4	T
<i>SCH9</i>	Serine/threonine-protein kinase SCH9	2.43	2.90	300	S
<i>POM152</i>	Nucleoporin POM152	2.65	2.54	11	T
<i>KCS1</i>	Inositol hexakisphosphate kinase 1	2.65	2.33	97	S
<i>YPK3</i>	AGC kinase YPK3	2.66	3.35	82	T
<i>KSP1</i>	Serine/threonine-protein kinase KSP1	2.82	2.59	909	S

**Table 1: Significantly (p-value < 0.05) hypophosphorylated (negative values) and hyperphosphorylated (positive values) residues identified simultaneously in both phosphoproteomic experiments (i.e., SILAC and DML).** The data was sorted from the most hypophosphorylated to the most hyperphosphorylated residues identified using SILAC.

In short, we have a list of hypophosphorylated (negative values) or hyperphosphorylated (positive values) residues in leucine-starved *gcn2Δ* cells (Table 1). Possibly then, a hypophosphorylated residue in leucine-starved *gcn2Δ* cells may be a direct target of Gcn2 or of a Gcn2-activated protein kinase. Alternatively, it may be a target of a protein phosphatase that is directly or indirectly downregulated by Gcn2 (Figure 4A). In contrast, we may hypothesize that a hyperphosphorylated residue in leucine-starved *gcn2Δ* cells may be a target of a Gcn2-inhibited protein kinase or a Gcn2-activated protein phosphatase (Figure 4B). Therefore, the only putative direct Gcn2 targets are those hypophosphorylated in leucine-starved *gcn2Δ* cells.

Even though we did not identify Gcn2 targets within well-known TORC1 pathway components (Table 1), Gcn2 may still regulate TORC1 through hitherto unknown TORC1 regulators. In line with this, the threonine 688 of Hos4 and the residues threonine 605, serine 603, and serine 516 of Snd1 caught our attention.

Moreover, these phosphoproteomic experiments - along with similar experiments performed by Dr. Dokládál from our research group- led us to identify Sui3<sup>S80</sup> and Gcn20<sup>S95</sup> as new interesting Gcn2 targets working in protein translation regulation (Dokládál et al., 2021). Subsequent experiments performed by Dokládál and colleagues led us to conclude that, in response to amino acid starvation, Gcn2 regulates protein translation through the phosphorylation of not only Sui2<sup>S52</sup> but also of Sui3<sup>S80</sup> and Gcn20<sup>S95</sup>.

**A****B**

hypophosphorylated in  
leucine-starved *gcn2Δ* cells

 Protein Kinase



hyperphosphorylated in  
leucine-starved *gcn2Δ* cells

 Protein Phosphatase

**Figure 4: Interpretation of the phosphoproteomic results listed in Table 1.** (A) Conditions leading to the accumulation of hypophosphorylated protein residues in leucine-starved *gcn2Δ* cells. (B) Conditions leading to the accumulation of hyperphosphorylated protein residues in leucine-starved *gcn2Δ* cells.

## 2.4: DISCUSSION AND CONCLUSIONS

In this chapter, we tried to elucidate how Gcn2 and other GAAC pathway members affect the TORC1 activity. We first confirmed that Gcn2 expression is needed to inhibit TORC1 upon leucine or histidine starvation (Yuan et al., 2017) (Figure 2). Notably, in Gcn2 expressing cells, expression of the non-phosphorylatable eIF2 $\alpha$  variant (Sui2<sup>S52A</sup>) or loss of Gcn4 protected the TORC1 activity from inactivation upon leucine starvation (Figure 3). Since eIF2 $\alpha$  phosphorylation (Sui2<sup>pS52</sup>) by active Gcn2 leads to an increase in Gcn4 translation (Hinnebusch, 2005; Wek, 2018), Gcn4 levels remain low in Sui2<sup>S52A</sup>-expressing cells when they are starved for leucine and Gcn2 is active. Therefore, we can conclude that, apart from the previously described Gcn2-dependent branch of TORC1 regulation, there also exists a Gcn4-dependent branch of TORC1 regulation (Figure 3) (Dokládál et al., 2021). Even though the exact mechanism by which Gcn4 regulates TORC1 remains still elusive, possibly, and in analogy with the mammalian transcription factor ATF4 (Gcn4 homolog), the Gcn4-dependent branch of TORC1 regulation may involve the expression of a functional homolog of Sestrin2 or REDD1.

Concerning the Gcn2-dependent branch of TORC1 regulation, Gcn2 has been proposed to directly regulate the TORC1 activity through the phosphorylation of the RNC (Raptor-like N-terminal–Conserved) domain of Kog1 (Yuan et al., 2017). To confirm this result and find potential Gcn2 targets within the TORC1 signaling pathway, we performed a set of quantitative phosphoproteomic experiments using leucine-starved WT and *gcn2Δ* cells. In these experiments, we did not identify significant Gcn2 target sites neither in Kog1 nor in well-known TORC1 regulators. Nonetheless, the threonine 688 of Hos4 and the residues serine 516, serine 603, and threonine 605 of Snd1 were identified as putative Gcn2 targets with a potential role in the regulation of the TORC1 activity. On one side, Hos4 is a subunit of the Set3 complex, which when impaired showed a negative genetic interaction with Gtr1<sup>S20L</sup> overexpression (Chapter 1). As discussed in Chapter 1, it may be possible that the Set3 complex promotes, downstream the TORC1 signaling pathway, the transcription of TORC1-responsive genes. Therefore, it would be interesting to study the phosphorylation of the threonine 688 of Hos4 and its effects on the TORC1 pathway functionality.

On the other side, *SND1* deletion was reported to display (i) a negative genetic interaction with deletion of *NPR3*, which codes for a negative TORC1 regulator in cells growing in poor nitrogen media, and (ii) a positive genetic interaction with deletions of *EGO1*, *LST4*, and *GTR1*, which code for positive TORC1 regulators in cells growing in rich nitrogen media (Costanzo et al., 2016). These results suggest that Snd1 may share a functional relationship with the mentioned upstream TORC1 regulators. Interestingly, Snd1, along with Snd2 and Snd3, is proposed to constitute a Srp-independent pathway mediating protein import into the ER that functions similarly and in parallel to the Get pathway (Aviram et al., 2016; Farkas & Bohnsack, 2021). In brief, cytosolic Snd1 has been proposed to capture nascent proteins with Transmembrane Domains (TMDs) or downstream hydrophobic motifs (Aviram et al., 2016). Later Snd1 has been suggested to deliver these substrates to the Sec61 translocon associated with the ER transmembrane proteins Snd2-Snd3 (Aviram et al., 2016). The import of nascent proteins to the ER is essential for the proper folding, processing, sorting, and subcellular trafficking of approximately one-third of all cellular proteins (Aviram et al., 2016; Farkas & Bohnsack, 2021). Hence, it is possible that, by phosphorylating Snd1, Gcn2 regulates the import of nascent TORC1 pathway components to the ER. Therefore, it would be interesting to study the phosphorylation of the residues 516, 603, and 605 of Snd1 and their effects on protein levels and subcellular localization of TORC1 pathway components.

Finally, the phosphoproteomic experiments presented here contributed to uncovering that Gcn2 regulates protein translation through the phosphorylation of not only Sui2<sup>S52</sup> but also Sui3<sup>S80</sup> and Gcn20<sup>S95</sup> (Dokládál et al., 2021). In brief, experiments performed by Dr. Dokládál and colleagues unveiled that phosphorylation of serine 80 of eIF2 $\beta$  (Sui3<sup>pS80</sup>) promotes the GDI (guanosine dissociation inhibitor) activity of eIF5 toward the GDP-loaded eIF2, thereby inhibiting protein synthesis by blocking the recycling of the eIF2 ternary complex (Dokládál et al., 2021). In addition, they discovered that phosphorylation of Gcn20<sup>S95</sup> (Gcn20<sup>pS95</sup>) antagonizes the formation of the Gcn2-Gcn1-Gcn20 activatory complex, thereby acting in a negative feedback loop for the activation of Gcn2 (Dokládál et al., 2021).

## 2.5: BIBLIOGRAPHY

- Adomavicius, T., Guaita, M., Zhou, Y., Jennings, M. D., Latif, Z., Roseman, A. M., & Pavitt, G. D. (2019). The structural basis of translational control by eIF2 phosphorylation. *Nature Communications*, 10(1), 2136. <https://doi.org/10.1038/s41467-019-10167-3>
- Advani, V. M., & Ivanov, P. (2019). Translational Control under Stress: Reshaping the Translatome. *BioEssays*, 41(5), 1900009. <https://doi.org/10.1002/bies.201900009>
- Anda, S., Zach, R., & Grallert, B. (2017). Activation of Gcn2 in response to different stresses. *PLOS ONE*, 12(8), e0182143. <https://doi.org/10.1371/journal.pone.0182143>
- Averous, J., Lambert-Langlais, S., Mesclon, F., Carraro, V., Parry, L., Jousse, C., Bruhat, A., Maurin, A.-C., Pierre, P., Proud, C. G., & Fournoux, P. (2016). GCN2 contributes to mTORC1 inhibition by leucine deprivation through an ATF4 independent mechanism. *Scientific Reports*, 6(1), 27698. <https://doi.org/10.1038/srep27698>
- Boersema, P. J., Raijmakers, R., Lemeer, S., Mohammed, S., & Heck, A. J. R. (2009). Multiplex peptide stable isotope dimethyl labeling for quantitative proteomics. *Nature Protocols*, 4(4), 484–494. <https://doi.org/10.1038/nprot.2009.21>
- Castilho, B. A., Shanmugam, R., Silva, R. C., Ramesh, R., Himme, B. M., & Sattlegger, E. (2014). Keeping the eIF2 alpha kinase Gcn2 in check. *Biochimica et Biophysica Acta (BBA) - Molecular Cell Research*, 1843(9), 1948–1968. <https://doi.org/10.1016/j.bbamcr.2014.04.006>
- Cherkasova, V. A. (2003). Translational control by TOR and TAP42 through dephosphorylation of eIF2alpha kinase GCN2. *Genes & Development*, 17(7), 859–872. <https://doi.org/10.1101/gad.1069003>
- Dever, T. E., Feng, L., Wek, R. C., Cigan, A. M., Donahue, T. F., & Hinnebusch, A. G. (1992). Phosphorylation of initiation factor 2 alpha by protein kinase GCN2 mediates gene-specific translational control of GCN4 in yeast. *Cell*, 68(3), 585–596. [https://doi.org/10.1016/0092-8674\(92\)90193-g](https://doi.org/10.1016/0092-8674(92)90193-g)
- Dey, M., Cao, C., Sicheri, F., & Dever, T. E. (2007). Conserved Intermolecular Salt Bridge Required for Activation of Protein Kinases PKR, GCN2, and PERK. *Journal of Biological Chemistry*, 282(9), 6653–6660. <https://doi.org/10.1074/jbc.M607897200>
- Dokládál, L., Stumpe, M., Pillet, B., Hu, Z., García Osuna, G. M., Kressler, D., Dengjel, J., & De Virgilio, C. (2021). Global phosphoproteomics pinpoints uncharted Gcn2-mediated mechanisms of translational control. *Molecular Cell*, 81(9), 1879–1889.e6. <https://doi.org/10.1016/j.molcel.2021.02.037>
- Dong, J., Qiu, H., Garcia-Barrio, M., Anderson, J., & Hinnebusch, A. G. (2000). Uncharged tRNA Activates GCN2 by Displacing the Protein Kinase Moiety from a Bipartite tRNA-Binding Domain. *Molecular Cell*, 6(2), 269–279. [https://doi.org/10.1016/S1097-2765\(00\)00028-9](https://doi.org/10.1016/S1097-2765(00)00028-9)
- Falcón, P., Escandón, M., Brito, Á., & Matus, S. (2019). Nutrient Sensing and Redox Balance: GCN2 as a New Integrator in Aging. *Oxidative Medicine and Cellular Longevity*, 2019, 1–9. <https://doi.org/10.1155/2019/5730532>
- Fukuda, T., Sofyantoro, F., Tai, Y. T., Chia, K. H., Matsuda, T., Murase, T., Morozumi, Y., Tatebe, H., Kanki, T., & Shiozaki, K. (2021). Tripartite suppression of fission yeast TORC1 signaling by the GATOR1-Sea3 complex, the TSC complex, and Gcn2 kinase. *ELife*, 10, e60969. <https://doi.org/10.7554/eLife.60969>
- Garcia-Barrio, M. (2000). Association of GCN1-GCN20 regulatory complex with the N-terminus of eIF2alpha kinase GCN2 is required for GCN2 activation. *The EMBO Journal*, 19(8), 1887–1899. <https://doi.org/10.1093/emboj/19.8.1887>
- Garcia-Barrio, M., Dong, J., Cherkasova, V. A., Zhang, X., Zhang, F., Ufano, S., Lai, R., Qin, J., & Hinnebusch, A. G. (2002). Serine 577 Is Phosphorylated and Negatively Affects the tRNA Binding and eIF2 $\alpha$  Kinase Activities of GCN2. *Journal of Biological Chemistry*, 277(34), 30675–30683. <https://doi.org/10.1074/jbc.M203187200>
- Gárriz, A., Qiu, H., Dey, M., Seo, E.-J., Dever, T. E., & Hinnebusch, A. G. (2009). A Network of Hydrophobic Residues Impeding Helix  $\alpha$ C Rotation Maintains Latency of Kinase Gcn2, Which Phosphorylates the  $\alpha$  Subunit of Translation Initiation Factor 2. *Molecular and Cellular Biology*, 29(6), 1592–1607. <https://doi.org/10.1128/MCB.01446-08>
- González, A., & Hall, M. N. (2017). Nutrient sensing and TOR signaling in yeast and mammals. *The EMBO Journal*, 36(4), 397–408. <https://doi.org/10.15252/embj.201696010>

- Hinnebusch, A. G. (2005). TRANSLATIONAL REGULATION OF GCN4 AND THE GENERAL AMINO ACID CONTROL OF YEAST. *Annual Review of Microbiology*, 59(1), 407–450. <https://doi.org/10.1146/annurev.micro.59.031805.133833>
- Hu, Z., Raucci, S., Jaquenoud, M., Hatakeyama, R., Stumpe, M., Rohr, R., Reggiori, F., De Virgilio, C., & Dengjel, J. (2019). Multilayered Control of Protein Turnover by TORC1 and Atg1. *Cell Reports*, 28(13), 3486–3496.e6. <https://doi.org/10.1016/j.celrep.2019.08.069>
- Inglis, A. J., Masson, G. R., Shao, S., Perisic, O., McLaughlin, S. H., Hegde, R. S., & Williams, R. L. (2019). Activation of GCN2 by the ribosomal P-stalk. *Proceedings of the National Academy of Sciences*, 116(11), 4946–4954. <https://doi.org/10.1073/pnas.1813352116>
- Kubota, H., Obata, T., Ota, K., Sasaki, T., & Ito, T. (2003). Rapamycin-induced Translational Derepression of GCN4 mRNA Involves a Novel Mechanism for Activation of the eIF2 $\alpha$  Kinase GCN2. *Journal of Biological Chemistry*, 278(23), 20457–20460. <https://doi.org/10.1074/jbc.C300133200>
- Kubota, H., Sakaki, Y., & Ito, T. (2000). GI Domain-mediated Association of the Eukaryotic Initiation Factor 2 $\alpha$  Kinase GCN2 with Its Activator GCN1 Is Required for General Amino Acid Control in Budding Yeast. *Journal of Biological Chemistry*, 275(27), 20243–20246. <https://doi.org/10.1074/jbc.C000262200>
- Lageix, S., Rothenburg, S., Dever, T. E., & Hinnebusch, A. G. (2014). Enhanced interaction between pseudokinase and kinase domains in Gcn2 stimulates eIF2 $\alpha$  phosphorylation in starved cells. *PLoS Genetics*, 10(5), e1004326. <https://doi.org/10.1371/journal.pgen.1004326>
- Lageix, S., Zhang, J., Rothenburg, S., & Hinnebusch, A. G. (2015). Interaction between the tRNA-Binding and C-Terminal Domains of Yeast Gcn2 Regulates Kinase Activity In Vivo. *PLOS Genetics*, 11(2), e1004991. <https://doi.org/10.1371/journal.pgen.1004991>
- Marton, M. J., Crouch, D., & Hinnebusch, A. G. (1993). GCN1, a translational activator of GCN4 in *Saccharomyces cerevisiae*, is required for phosphorylation of eukaryotic translation initiation factor 2 by protein kinase GCN2. *Molecular and Cellular Biology*, 13(6), 3541–3556. <https://doi.org/10.1128/mcb.13.6.3541-3556.1993>
- Marton, M. J., Vazquez de Aldana, C. R., Qiu, H., Chakraborty, K., & Hinnebusch, A. G. (1997). Evidence that GCN1 and GCN20, translational regulators of GCN4, function on elongating ribosomes in activation of eIF2 $\alpha$  kinase GCN2. *Molecular and Cellular Biology*, 17(8), 4474–4489. <https://doi.org/10.1128/MCB.17.8.4474>
- Masson, G. R. (2019). Towards a model of GCN2 activation. *Biochemical Society Transactions*, 47(5), 1481–1488. <https://doi.org/10.1042/BST20190331>
- Merrick, W. C., & Pavitt, G. D. (2018). Protein Synthesis Initiation in Eukaryotic Cells. *Cold Spring Harbor Perspectives in Biology*, 10(12), a033092. <https://doi.org/10.1101/cshperspect.a033092>
- Moradi Majd, R., Mayeli, M., & Rahmani, F. (2020). Pathogenesis and promising therapeutics of Alzheimer disease through eIF2 $\alpha$  pathway and correspondent kinases. *Metabolic Brain Disease*, 35(8), 1241–1250. <https://doi.org/10.1007/s11011-020-00600-8>
- Padyana, A. K., Qiu, H., Roll-Mecak, A., Hinnebusch, A. G., & Burley, S. K. (2005). Structural Basis for Autoinhibition and Mutational Activation of Eukaryotic Initiation Factor 2 $\alpha$  Protein Kinase GCN2\*[boxes]. *Journal of Biological Chemistry*, 280(32), 29289–29299. <https://doi.org/10.1074/jbc.M504096200>
- Pakos-Zebrucka, K., Koryga, I., Mnich, K., Ljubic, M., Samali, A., & Gorman, A. M. (2016). The integrated stress response. *EMBO Reports*, 17(10), 1374–1395. <https://doi.org/10.15252/embr.201642195>
- Qiu, H., Dong, J., Hu, C., Francklyn, C. S., & Hinnebusch, A. G. (2001a). The tRNA-binding moiety in GCN2 contains a dimerization domain that interacts with the kinase domain and is required for tRNA binding and kinase activation. *The EMBO Journal*, 20(6), 1425–1438. <https://doi.org/10.1093/emboj/20.6.1425>
- Qiu, H., Dong, J., Hu, C., Francklyn, C. S., & Hinnebusch, A. G. (2001b). The tRNA-binding moiety in GCN2 contains a dimerization domain that interacts with the kinase domain and is required for tRNA binding and kinase activation. *The EMBO Journal*, 20(6), 1425–1438. <https://doi.org/10.1093/emboj/20.6.1425>
- Rasmussen, B. B., & Adams, C. M. (2020). ATF4 Is a Fundamental Regulator of Nutrient Sensing and Protein Turnover. *The Journal of Nutrition*, 150(5), 979–980. <https://doi.org/10.1093/jn/nxaa067>

- Romano, P. R., Garcia-Barrio, M. T., Zhang, X., Wang, Q., Taylor, D. R., Zhang, F., Herring, C., Mathews, M. B., Qin, J., & Hinnebusch, A. G. (1998). Autophosphorylation in the Activation Loop Is Required for Full Kinase Activity In Vivo of Human and Yeast Eukaryotic Initiation Factor 2 $\alpha$  Kinases PKR and GCN2. *Molecular and Cellular Biology*, 18(4), 2282–2297. <https://doi.org/10.1128/MCB.18.4.2282>
- Sattlegger, E. (2000). Separate domains in GCN1 for binding protein kinase GCN2 and ribosomes are required for GCN2 activation in amino acid-starved cells. *The EMBO Journal*, 19(23), 6622–6633. <https://doi.org/10.1093/emboj/19.23.6622>
- Sattlegger, E., & Hinnebusch, A. G. (2005). Polyribosome binding by GCN1 is required for full activation of eukaryotic translation initiation factor 2{alpha} kinase GCN2 during amino acid starvation. *The Journal of Biological Chemistry*, 280(16), 16514–16521. <https://doi.org/10.1074/jbc.M414566200>
- Vazquez de Aldana, C. R., Marton, M. J., & Hinnebusch, A. G. (1995). GCN20, a novel ATP binding cassette protein, and GCN1 reside in a complex that mediates activation of the eIF-2 alpha kinase GCN2 in amino acid-starved cells. *The EMBO Journal*, 14(13), 3184–3199.
- Wek, R. C. (2018). Role of eIF2 $\alpha$  Kinases in Translational Control and Adaptation to Cellular Stress. *Cold Spring Harbor Perspectives in Biology*, 10(7), a032870. <https://doi.org/10.1101/cshperspect.a032870>
- Wek, S. A., Zhu, S., & Wek, R. C. (1995). The histidyl-tRNA synthetase-related sequence in the eIF-2 alpha protein kinase GCN2 interacts with tRNA and is required for activation in response to starvation for different amino acids. *Molecular and Cellular Biology*, 15(8), 4497–4506. <https://doi.org/10.1128/MCB.15.8.4497>
- Xu, D., Dai, W., Kutzler, L., Lacko, H. A., Jefferson, L. S., Dennis, M. D., & Kimball, S. R. (2020). ATF4-Mediated Upregulation of REDD1 and Sestrin2 Suppresses mTORC1 Activity during Prolonged Leucine Deprivation. *The Journal of Nutrition*, 150(5), 1022–1030. <https://doi.org/10.1093/jn/nxz309>
- Ye, J., Palm, W., Peng, M., King, B., Lindsten, T., Li, M. O., Koumenis, C., & Thompson, C. B. (2015). GCN2 sustains mTORC1 suppression upon amino acid deprivation by inducing Sestrin2. *Genes & Development*, 29(22), 2331–2336. <https://doi.org/10.1101/gad.269324.115>
- Yuan, W., Guo, S., Gao, J., Zhong, M., Yan, G., Wu, W., Chao, Y., & Jiang, Y. (2017). General Control Nonderepressible 2 (GCN2) Kinase Inhibits Target of Rapamycin Complex 1 in Response to Amino Acid Starvation in *Saccharomyces cerevisiae*. *Journal of Biological Chemistry*, 292(7), 2660–2669. <https://doi.org/10.1074/jbc.M116.772194>

**CHAPTER 3: RIBOSOMAL PROTEIN DEFECTS UNRAVEL A  
FUNCTION OF THE ARF1 GTPASE IN CONTROLLING TORC1  
ACTIVITY**



### **3.1: INTRODUCTION**

The TORC1 pathway plays a fundamental role in balancing, mainly in response to amino acids availability, cellular anabolism, and catabolism. The primary anabolic process is protein translation with the ribosome as its principal player. A eukaryotic ribosome is a ribonucleoprotein machine made up of four ribosomal RNAs (rRNAs) and 79-80 ribosomal proteins (RPs) that is able to translate mRNA to proteins (Woolford & Baserga, 2013).

Ribosome biogenesis is a multi-step and multi-compartmentalized pathway. It starts at the nucleolus, continues at the nucleoplasm, and finishes in the cytoplasm. During this journey, orchestrated by alternative ribosome assembly factors, different pre-ribosomal particles, composed of specific ribosomal proteins, follow one another, and end up with the maturation of the pre-rRNAs and the formation of the small and big ribosomal subunits (de la Cruz et al., 2015).

In numbers, ribosomal biogenesis is a costly process that produces around 200,000 ribosomes per cell in a fast-growing haploid strain (von der Haar, 2008) and, only for the transcription of rRNA, engage 60% of the global cellular transcription (Warner, 1999). Therefore, eukaryotic cells need to fine-tune ribosome biogenesis in response to different intracellular and extracellular stimuli to attain an equimolar expression of pre-rRNAs, r-proteins, and ribosome assembly factors (Gallagher, 2004; Kief & Warner, 1981). Notably, TORC1 regulates, at different levels, the ribosome biogenesis pathway.

#### **3.1.1: Transcriptional regulation of the ribosomal components**

In yeast, the rRNA is encoded by 100-200 gene copies whose expression are determined mainly by, on the one hand, the RNAPI (RNA Polymerase I) activation (French et al., 2003; Zhang et al., 2010) and, on the other hand, the histone deacetylase Rpd3 and FACT complex activities (Dammann et al., 1993). Ribosome biogenesis starts with the coordinated and interdependent action of RNAPI, II, and III, where RNAPI transcribes the 35S pre-rRNA (precursor of the mature 5.8, 18, and 25S rRNAs), RNAPII transcribes mRNAs coding for ribosomal proteins and ribosome assembly factors, and RNAPIII transcribes the pre-5S rRNA (Laferte, 2006).

TORC1 inhibition negatively regulates the pre-rRNA synthesis by promoting the degradation, through the ubiquitin-proteasome system, of Rrn3, which mediates the

recruitment of the RNAPII initiation factor to the rRNA encoding genes (Philippi et al., 2010). Additionally, TORC1 or PKA inhibition leads to the dephosphorylation of cytoplasmic Maf1, which then relocates to the nucleus and inhibits RNAPIII activity (Wei & Zheng, 2010). Moreover, the transcription of RPs and RiBi genes by RNAPII is positively regulated, at least partially, by Sfp1 (zinc-coordinating transcription factor Split Finger Protein 1) and Sch9 in response to TORC1 and PKA activity levels (Jorgensen, 2004; Urban et al., 2007).

### 3.1.2: 35S pre-rRNA processing

Ribosome assembly starts co-transcriptionally with the formation of a pre-ribosome (around the 35S pre-rRNA) that comprises several 40S ribosomal proteins and that, eventually, leads to the formation of a 90S pre-ribosomal particle (de la Cruz et al., 2015; Mougey et al., 1993). Even though 35S pre-rRNA processing can occur co-transcriptionally or post-transcriptionally, in exponentially growing cells, 35S pre-rRNA processing occurs mainly co-transcriptionally (Koř & Tollervey, 2010; Osheim et al., 2004). Notably, co-transcriptional processing (characterized by cleavage at site A2) of 35S pre-rRNA (Figure 1) is inhibited upon heat or cold shock, low pH, osmotic or oxidative stress, growth arrest, rapamycin treatment, and loss or inactivation of specific 60S ribosomal biogenesis factors (*i.e.*, Drs1, Rrp5, and Rat1), thus leading to a non-productive pre-rRNA processing pathway (Axt et al., 2014; Kos-Braun et al., 2017; Lebaron et al., 2013; Osheim et al., 2004; Talkish et al., 2016).

In 2017 Kos-Braun and colleagues revealed that the alternation between productive (cleavage at sites A2 and A3) and non-productive (cleavage almost exclusively at site A3) pre-rRNA processing pathways is mainly determined by TORC1 and CK2 (Casein Kinase) activities. Especially, TORC1 inhibition seems to promote the non-productive 35S pre-rRNA processing pathway via the transcriptional repression of RPs (Ribosomal Proteins) and RiBi (Ribosome Biogenesis) factors and through the inhibition of the RNAPII activity (Kos-Braun et al., 2017). The cleavage at site A2, which is part of the co-transcriptional 35S pre-rRNA processing pathway, is crucial for the ribosome assembly pathway since it divides the 90S pre-ribosomal particle (SSU processome) into two independent precursors: the 43S pre-ribosome with 20S pre-rRNA and the 66S pre-ribosome with 27S pre-rRNA, that will mature to form the small and big ribosomal subunits, respectively (Fernández-Pevida et al., 2015) (Figure 1). Besides the cleavage

at A2, several endo- and exonucleolytic cleavages eliminate spacer sequences within the pre-rRNA, thus generating mature 18S (an integral part of the 40S small subunit), 5.8S, and 25S rRNAs (integral parts of the 60S large subunit) (Fernández-Pevida et al., 2015) (Figure 1).

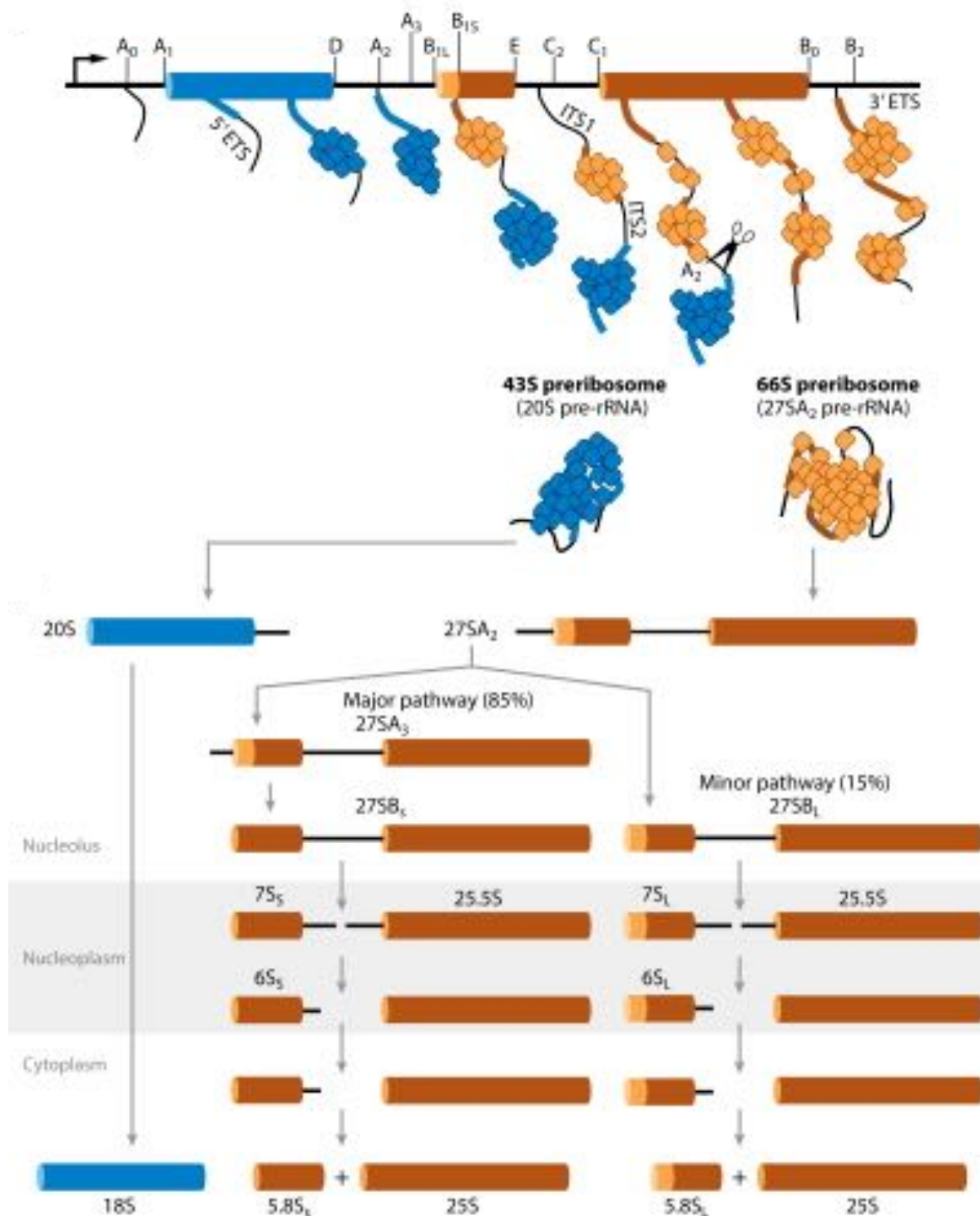


**Figure 1: Co-transcriptional precursor rRNA (pre-rRNA) processing in *Saccharomyces cerevisiae*.** The cleavage at site A2 divides the 90S pre-ribosomal particle (SSU processome) into two independent precursors; the 43S pre-ribosome with 20S pre-rRNA and the 66S pre-ribosome with 27S pre-rRNA (de la Cruz et al., 2015).

### **3.1.3: Pre-ribosomal particles nucleocytoplasmic export**

In response to nutrients availability and stressful insults, the TORC1 pathway controls the export of pre-ribosomal particles from the nucleus to the cytoplasm. For instance, the Nog1 GTPase is a nucleocytoplasmic shuttling protein that plays a crucial role in the late cytoplasmic stages of ribosomal maturation; following TORC1 inhibition, the Nog1 GTPase gets trapped in the nucleus, thus impairing the 60S ribosomal subunit export and maturation (Honma et al., 2006). Similarly, TORC1 inhibition also leads to the nucleolar trapping of the nucleocytoplasmic shuttling proteins Dim2 and Rrp12, which are necessary for several steps of the ribosome assembly pathway such as the co-transcriptional ribosome assembly, pre-rRNA processing, and the export of the pre-40S ribosomal subunit from the nucleus to the cytoplasm (Vanrobays et al., 2008).

### **3.1.4: RP and RiBi regulons**

Apart from the enzymes involved in pre-rRNA processing, ribosome biogenesis requires the synchronized action of ribosomal proteins and ribosome assembly factors. Especially, TORC1 and PKA pathways govern, in response to different stimuli, the transcription of RP (Ribosomal protein) and RiBi (Ribosomal Biogenesis) regulons (Ho & Gasch, 2015; Lempiäinen & Shore, 2009; Loewith & Hall, 2011; Martin et al., 2004; Powers & Walter, 1999). While the RP regulon includes the genes coding for the ribosomal proteins (Warner 1989; Warner 1999; Warner et al., 1985), the RiBi regulon, besides ribosome assembly factors, comprises the genes coding for proteins that, even if they are not directly related to ribosome assembly, play a crucial role in ribosome biogenesis and function (*i.e.*, translation factors, aminoacyl-tRNA synthetases, tRNA-modifying factors, nucleotide metabolic enzymes, and subunits of RNAPI and III) (Jorgensen, 2002, 2004; Wade et al., 2006).

### **3.1.5: Transcriptional regulation of the RP genes**

The transcription of the RP regulon is principally regulated by the DNA binding activators Rap1, Fhl1, and the transcriptional activator and repressor Iyh1 and Cfr1, respectively. According to the conditions, TORC1 and PKA kinases (Martin et al., 2004; Schawalder et al., 2004; Zhao et al., 2006) and their downstream targets Sch9 and Sfp1 (Fingerman et al., 2003; Jorgensen, 2004; Lempiäinen & Shore, 2009; Marion et al.,

2004) shape the transcription profile of the RP regulon. In the nucleus, Rap1 and Fhl1 constitutively bind the RP promoters (Rudra et al., 2007). In rich conditions, TORC1 phosphorylates Ifh1 and promotes its nuclear localization and binding to the Fhl1-Rap1 complex, thus promoting the activation of RP gene transcription, while, in these same conditions, Crf1 stays in the cytoplasm. (Schawalder et al., 2004). In contrast, Yak1 kinase activation, followed by TORC1 inhibition, results in Crf1 phosphorylation, which relocates from the cytoplasm to the nucleus and downregulates RP gene transcription by displacing Ifh1 from the Fhl1-Rap1 DNA binding complex (Martin et al. 2004). Further, also in poor conditions, the RP gene transcription is actively repressed by the Rpd13 histone deacetylase, whose binding to the RP gene promoters is mediated by the Stb3 repressor, which is also involved in the RiBi regulon transcriptional regulation (Liko et al., 2007).

### **3.1.6. Transcriptional regulation of the RiBi genes**

As for the RP regulon, TORC1 and PKA kinases, and their downstream targets Sch9 and Sfp1, also govern the transcription of the RiBi regulon (Kunkel et al., 2019; Lippman & Broach, 2009). Transcription of RiBi genes is driven by a balance between transcription activators, also called General Regulatory Factors (GRFs), (*i.e.*, Abf1, Reb1, and, less frequently, Rap1 and Tbf1) and repressors (*i.e.*, Dot6/Tod6 and Stb3) (Bosio et al., 2017; Huber et al., 2011).

In rich conditions, following TORC1 and PKA activation, Sch9 and Sfp1 operate, in parallel, to positively regulate the transcription of the RiBi genes; in particular, Sch9 phosphorylates the transcription repressors Dot6/Tod6 and Stb3, impeding their association with the RiBi gene promoters, thereby promoting, with the participation of the GRFs (*i.e.*, Abf1, Reb1, and, less frequently, Rap1 and Tbf1), the transcription of the RiBi genes (Bosio et al., 2017). Under poor conditions, de-phosphorylation of the Dot6/Tod6 and Stb3 transcription repressors allows them to bind the PAC (RNA Polymerase A and C) and RRPE (Ribosomal RNA-Processing Element) sequence elements at the RiBi gene promoters, respectively, where then they recruit the histone acetyltransferase Rpd13 to repress the transcription of the RiBi genes (Badis et al., 2008; Freckleton et al., 2009; Huber et al., 2011; Liko et al., 2007; Lippman & Broach, 2009; McKnight et al., 2015; Zhu et al., 2009).

### 3.1.7: The crosstalk between rRNA and RPs expression

TORC1 regulates the transcription of rRNA and RP genes by Sch9-dependent and Sch9-independent mechanisms. Additionally, in optimal conditions, the HMG (High Mobility Protein) Hmo1 has been shown to simultaneously activate the transcription of rRNA and a subset of RP genes, which requires its interaction with Rap1 when TORC1 is active (Berger et al., 2007; Hall et al., 2006). In line with this, transcriptional inhibition of this RP gene subset following TORC1 inactivation requires the detachment of Hmo1 from the RP gene promoters (Berger et al., 2007).

Another example is the formation of the CURl complex that follows Sch9 inhibition (Albert et al., 2016; Rudra et al., 2007). The CURl complex comprises Lfh1 and the UTP-C subcomplex. The latter consists of the four subunits of CK2 kinase (*i.e.*, CKA1/2, CKB1/2) and the ribosome assembly factors Utp22 and Rrp7 (Rudra et al., 2007). Under rich conditions, the UTP-C subcomplex has been shown to play a positive role in the transcription and processing of the 35S pre-rRNA (Rudra et al., 2007), while Lfh1 promotes the RP genes transcription (Schawalder et al., 2004). In contrast, in poor conditions, Sch9 inactivation following TORC1 inhibition promotes the simultaneous disengagement of, on the one hand, the UTP-C subcomplex from the 35S pre-rRNA and, on the other hand, Lfh1 from RP promoters, thus leading to the stable formation of the CURl complex (Albert et al., 2016; Rudra et al., 2007).

### 3.1.8: Turnover of pre-ribosomal particles and ribosomes

In eukaryotic cells, quality control mechanisms ensure proper ribosome assembly and function so that defective ribosomal components and ribosomes are rapidly degraded. First, the rRNA decay pathway involves different quality control mechanisms that function at subsequent steps of the ribosome assembly pathway. Already in the nucleolus, nascent rRNA molecules or rRNA molecules included in early-stage pre-rRNA particles are degraded by the TRAMP-exosome complex (Houseley et al., 2006). On one side, The TRAMP complex is composed of the poly(A) polymerase catalytic subunit (Trf4 or Trf5), a putative RNA-binding protein (Air1 or Air2), and the DEVH helicase Mtr4 (LaCava et al., 2005; Vaňáčová et al., 2005; Wyers et al., 2005), while the exosome complex comprises Rrp41 (Ski6), Rrp42, Rrp46, Rrp43, Mtr3, and Rrp45 (Anderson, 1998; Schmid & Jensen, 2008). The TRAMP complex is a poly(A)

polymerase that marks RNA molecules for degradation, including aberrant tRNAs, pre-snrRNAs, pre-snoRNAs, pre-mRNAs, cryptic unstable transcripts (CUTs), and pre-rRNAs. At the same time, the exosome is a ribonuclease complex with exo- and possibly endoribonuclease activity that rapidly degrades poly(A) marked molecules (Houseley et al., 2006).

In the cytoplasm, the non-functional rRNA decay (NRD) pathway is a highly complex surveillance mechanism including more than 20 different proteins that degrade defective rRNAs by detecting translationally defective ribosomes (Cole et al., 2009; Fujii et al., 2009; LaRiviere et al., 2006; Schmid & Jensen, 2008). NRD encompasses two distinct pathways, the 18S NRD, which shares key players with the mRNA no-go decay pathway (NGD) (Cole et al., 2009), and the 25S NRD (LaRiviere et al., 2006). The 18S NRD substrates, as well as the NGD ones, are sent to P-bodies and degraded by the cytoplasmic Ski complex/Ski7-exosome complex (Cole et al., 2009), while those of the 25S pathway accumulate in cytosolic peri-nuclear foci and are degraded by the ubiquitin-proteasome system (Fujii et al., 2009).

In response to nutrient limitations or stress, ribosomes were proposed to be destroyed by bulk autophagy (micro and macroautophagy). However, in yeast, ribosome degradation occurs principally through selective autophagy, also called ribophagy (Beau et al., 2008; Kraft et al., 2008). During ribophagy, the Ubp3-Bre5 complex, in collaboration with Cdc48, Ufd3, and the  $\gamma$ -Glutamyl kinase, de-ubiquitinates the lysine 74 of Rpl25 which, previously, was ubiquitinated by the E3 ligase Ltn1 (Kraft et al., 2008; Ossareh-Nazari et al., 2014; Tatehashi et al., 2016). Finally, excess of ribosomal proteins has been proposed to be degraded by the ubiquitin-proteasome system (An & Harper, 2020; Sung et al., 2016). Notably, TORC1 inhibition has been shown to promote both ribophagy and NRD pathways (Pestov & Shcherbik, 2012; Waliullah et al., 2017), playing an essential role in the cytoplasmatic turnover of mature ribosomes, and therefore in proteostasis.

Therefore, it is clear that TORC1 plays a crucial role in ribosome biogenesis and turnover; however, how ribosome biogenesis may impinge on the TORC1 pathway remains unclear.

## 3.2: AIM OF THE CHAPTER

In 2015, Péli-Gulli and colleagues showed that, among amino acids, aspartate (Asp), asparagine (Asn), cysteine (Cys), glutamine (Gln), and methionine (Met) are more potent inducers of the TORC1 activity than other amino acids in yeast (Péli-Gulli et al., 2015). Later, in 2016, Mülleder and colleagues reported the intracellular amino acid concentration of the whole haploid knockout collection of yeast mutants (Mülleder et al., 2016). Considering the results published by Péli-Gulli and colleagues, we decided to analyze further the Asp, Asn, Gln, and Met values (Cys values were not quantified in the study) reported by Mülleder and colleagues in 2016. Cluster analyses indicated that some ribosomal protein gene mutants (*i.e.*, *rps10A* $\Delta$ , *rpl20B* $\Delta$ , and *rps12* $\Delta$ ), as well as *ygl188C-a* $\Delta$ , a deletion of an uncharacterized ORF located within the 5' untranslated region (5'UTR) of *RPS26A*, exhibited a similar amino acid profile signature to TORC1 pathway mutants, suggesting a functional link between ribosomal proteins and TORC1. An initial analysis led us to understand that deletion of *YGL188C-A* dampens the protein levels of Rps26A. In mammals, hypomorphic mutations in the *RPS26* locus are linked to the development of Diamond-Blackfan-Anemia (DBA) (Stenson et al., 2017), which increases the risk of cancer development (Alter et al., 2018; Vlachos et al., 2001; Vlachos et al., 2018). As in mammals, we might speculate that mutations in the *RPS26A* yeast locus may affect the signaling pathways governing cell growth and proliferation in yeast. Interestingly, in yeast, Rps26a has been proposed to be an integral part of a specialized pool of ribosomes that favors the expression of specific mRNAs (Ferretti et al., 2017). This chapter employs an *RPS26A* null mutant as a case study to explore how the impairment of ribosome biogenesis impacts the TORC1 pathway functionality. Considering all the information reported within this chapter, we will discuss how a ribosomopathy (a disease caused by mutations in genes coding for ribosomal components) may create the necessary context for a hypoproliferative cell to become hyperproliferative.

## 3.3: RESULTS

### 3.3.1: Bioinformatic analysis of Mülleder's dataset

In Mülleder's dataset, the mean and variance among the Asp (Aspartate), Asn (Asparagine), Gln (Glutamine), and Met (Methionine) variables strongly differ, making



further analysis difficult. For this reason, we applied a z-score normalization transforming for each variable (Asp, Asn, Gln, or Met) the mean and variance to 0 (or very close to 0) and 1, respectively (Table 1). We then clustered the normalized dataset (4680 mutants) into 50 groups based on the Asp, Asn, Gln, and Met intracellular accumulation profile signatures.

Amino acid	Raw Data		Normalized Data	
	Mean (mM)	Variance	Z-score	Variance
Asp	5.11E+00	4.76E-01	-2.34E-14	1.00E+00
Asn	1.23E+00	1.97E-02	-8.69E-15	1.00E+00
Gln	2.80E+01	1.47E+01	3.00E-14	1.00E+00
Met	1.24E-01	5.26E-04	-3.33E-14	1.00E+00

**Table 1: Z-score normalization of Müllender's dataset.** On the left, mean and variance for Asp, Asn, Gln and Met measurements from Müllender's study (Raw Data). On the right, mean and variance for Asp, Asn, Gln and Met measurements from Müllender's study after Z-score normalization (Normalized Data).

Interestingly, the *TCO89* deletion mutant cluster (*tco89Δ* cluster) displayed high levels of intracellular asparagine and glutamine (Figure 2A). The *tco89Δ* cluster contained a total of 27 members (Table 2), among which we found other TORC1 pathway regulator mutants such as *sea4Δ* and *ego2Δ* - although *ego2Δ*, *per se*, is not in the knockout collection, our group identified a loss of function mutation in *EGO2* in the *snx4Δ* strain (Puddu et al., 2019). A GO enrichment analysis was performed to understand which biological processes may be affected in the mutants included in the *tco89Δ* cluster (Figure 2B and Table 3). Mostly, the mutants included in the *tco89Δ* cluster mediated the intracellular transport, the TORC1 signaling pathway, or the proteasome-mediated degradation.

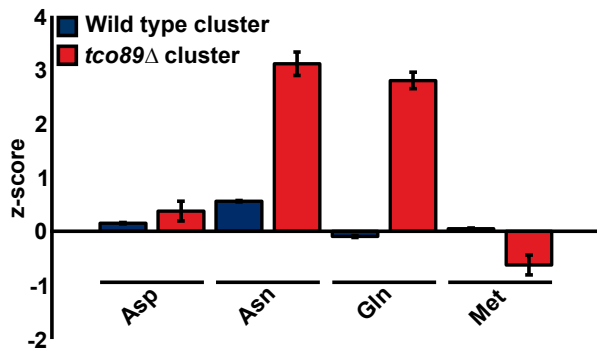
Deletion mutant	ORF	Asp	Asn	Gln	Met
<i>TCO89</i>	<i>YPL180W</i>	-8.1E-01	4.2E+00	2.6E+00	-1.1E+00
<i>SEA4</i>	<i>YBL104C</i>	1.1E+00	4.1E+00	2.4E+00	-4.9E-02
<i>SNX4</i>	<i>YJL036W</i>	1.9E+00	4.5E+00	2.8E+00	5.4E-01
<i>RPS10A</i>	<i>YOR293W</i>	-1.0E-01	3.6E+00	2.2E+00	-2.1E+00
<i>RPL20B</i>	<i>YOR312C</i>	-4.3E-01	3.9E+00	3.8E+00	1.1E-01
<i>RPS12</i>	<i>YOR369C</i>	9.5E-01	2.0E+00	2.0E+00	-6.6E-01
	<i>YGL188C-A</i>	-4.0E-01	3.2E+00	3.2E+00	-1.7E-01
<i>UMP1</i>	<i>YBR173C</i>	-8.9E-01	6.0E+00	2.1E+00	3.7E-01
<i>VPS61</i>	<i>YDR136C</i>	1.3E+00	2.9E+00	2.8E+00	-4.6E-01
<i>VPS3</i>	<i>YDR495C</i>	2.0E+00	2.7E+00	3.2E+00	-1.3E+00
<i>GET2</i>	<i>YER083C</i>	1.1E+00	2.3E+00	3.2E+00	-6.1E-01
<i>PRE9</i>	<i>YGR135W</i>	3.1E-01	4.0E+00	1.2E+00	9.5E-02
<i>EFG1</i>	<i>YGR271C-A</i>	-1.2E+00	3.2E+00	1.4E+00	-1.6E+00
<i>PEP8</i>	<i>YJL053W</i>	5.9E-01	2.4E+00	3.7E+00	3.7E-01
<i>VPS35</i>	<i>YJL154C</i>	2.5E+00	3.0E+00	3.4E+00	-3.5E-01

<i>ATG36</i>	<i>YJL185C</i>	1.1E+00	4.3E+00	3.0E+00	1.1E-01
<i>DEF1</i>	<i>YKL054C</i>	-1.4E+00	4.4E+00	1.7E+00	-1.6E+00
<i>OPI8</i>	<i>YKR035C</i>	-1.0E-01	1.8E+00	3.3E+00	2.3E-01
<i>RIC1</i>	<i>YLR039C</i>	6.2E-01	2.8E+00	2.4E+00	-5.9E-01
<i>SWI6</i>	<i>YLR182W</i>	-1.0E-01	1.4E+00	3.5E+00	-1.2E+00
<i>YKE2</i>	<i>YLR200W</i>	-6.0E-02	2.5E+00	3.3E+00	-2.7E+00
<i>ORM2</i>	<i>YLR350W</i>	1.3E+00	2.3E+00	2.3E+00	-1.4E-01
<i>YDJ1</i>	<i>YNL064C</i>	-5.7E-01	3.0E+00	2.4E+00	-2.5E+00
	<i>YNR005C</i>	4.3E-01	3.0E+00	3.1E+00	1.1E-01
<i>VPS27</i>	<i>YNR006W</i>	6.4E-01	2.7E+00	2.3E+00	3.8E-01
<i>NGL1</i>	<i>YOL042W</i>	4.4E-01	2.9E-01	5.0E+00	-2.4E+00
<i>BFR1</i>	<i>YOR198C</i>	-1.0E-01	3.3E+00	3.4E+00	3.2E-01

**Table 2: Z-scored normalized Asp, Asn, Gln, and Met measurements for the *tco89*Δ cluster members.**

Moreover, this cluster also included some ribosomal protein gene mutants (*i.e.*, *rps10a*Δ, *rpl20b*Δ, and *rps12*Δ), as well as *ygl188C-a*Δ that carries a deletion of an uncharacterized ORF in the 5'UTR of *RPS26A* - which was not included in the yeast haploid knockout collection (Nagalakshmi et al., 2008). We first got very interested in the putative uncharacterized ORF *YGL188C-A*. However, the fact that it lies within the 5'UTR of *RPS26A* led us to suspect that it may be affecting the *RPS26A* mRNA stability or translation.

**A**



**B**

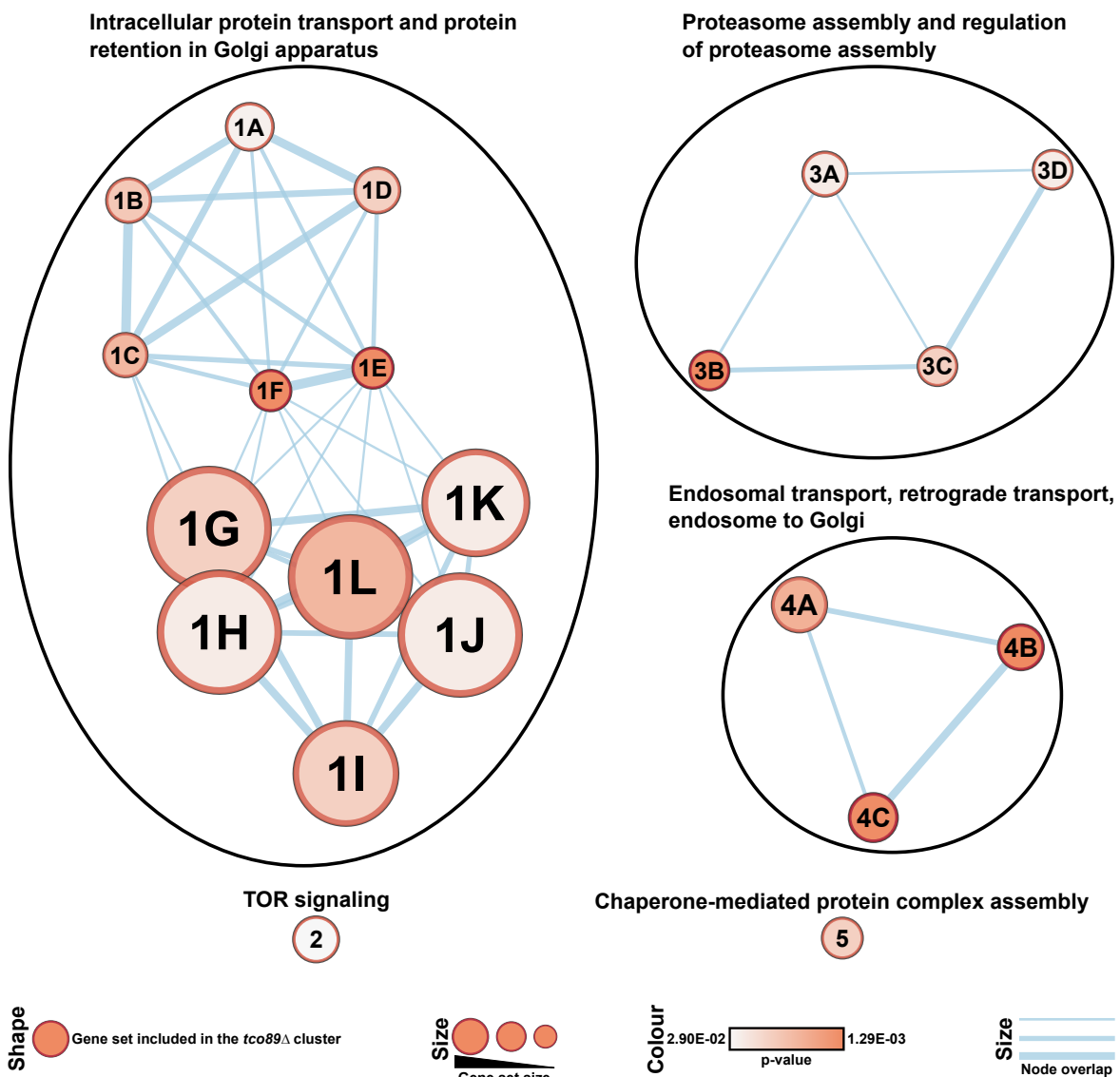


**Figure 2: GO enrichment analysis of the *tco89*Δ cluster which is characterized by high levels of intracellular asparagine and glutamine.** (A) The amino acid profile of the mutants included within the *tco89*Δ cluster is characterized by glutamine and asparagine intracellular accumulation. In (A), the intracellular concentration of amino acids was measured in prototrophic strains growing exponentially in minimal synthetic medium (SD), which lacks amino acids but contains ammonium sulfate (Mülleder et al., 2016). (B) GO enrichment analysis of the mutants included in the *tco89*Δ cluster. In (B) a functional enrichment analysis was performed using gprofiler applying a p-

value < 0.05. A publication-ready enrichment map was generated using Cytoscape. Node cut-off FDR Q value < 0.05 and edge cut-off < 0.5.

Node	GO term	Description	p-value
1A	GO:0051235	maintenance of location	2.72E-02
1B	GO:0045185	maintenance of protein location	1.71E-02
1C	GO:0032507	maintenance of protein location in cell	1.28E-02
1D	GO:0051651	maintenance of location in cell	1.92E-02
1E	GO:0045053	protein retention in Golgi apparatus	1.80E-03
1F	GO:0034067	protein localization to Golgi apparatus	1.80E-03
1G	GO:0070727	cellular macromolecule localization	1.92E-02
1H	GO:0034613	cellular protein localization	2.59E-02
1I	GO:0006886	intracellular protein transport	1.92E-02
1J	GO:0015031	protein transport	2.59E-02
1K	GO:0033365	protein localization to organelle	2.59E-02
1L	GO:0045184	establishment of protein localization	1.28E-02
2	GO:0031929	TOR signaling	2.90E-02
3A	GO:0043248	proteasome assembly	2.59E-02
3B	GO:0080129	proteasome core complex assembly	1.29E-03
3C	GO:0090363	regulation of proteasome core complex assembly	1.92E-02
3D	GO:0090364	regulation of proteasome assembly	2.59E-02
4A	GO:0016197	endosomal transport	1.12E-02
4B	GO:0042147	retrograde transport, endosome to Golgi	1.29E-03
4C	GO:0016482	cytosolic transport	2.03E-03
5	GO:0051131	chaperone-mediated protein complex assembly	1.92E-02

Table 3: GO terms depicted in Figure 2B.

### 3.3.2: Characterization of *YGL188C-A* and its effects on the downstream gene *RPS26A*

We undertook the characterization of this protein by first testing its expression levels using specific antibodies raised against a peptide deduced from the predicted *YGL188C-A* ORF. Notably, we were not able to detect any Ygl188c-a related protein in yeast extract except when a GFP tag sequence was fused to the *YGL188C-A* ORF (Figure 3A). As explained before, we noticed that the *YGL188C-A* sequence was part of the *RPS26A* mRNA (Nagalakshmi et al., 2008); therefore, we started analyzing how deletion of *YGL188C-A* may affect *RPS26A* mRNA and protein levels. Interestingly, loss of Ygl188c-a did not affect the *RPS26A* mRNA levels; in contrast, the *ygl188c-a* $\Delta$  strain displayed decreased levels of the Rps26a ribosomal protein (Figures 3B and 3C).

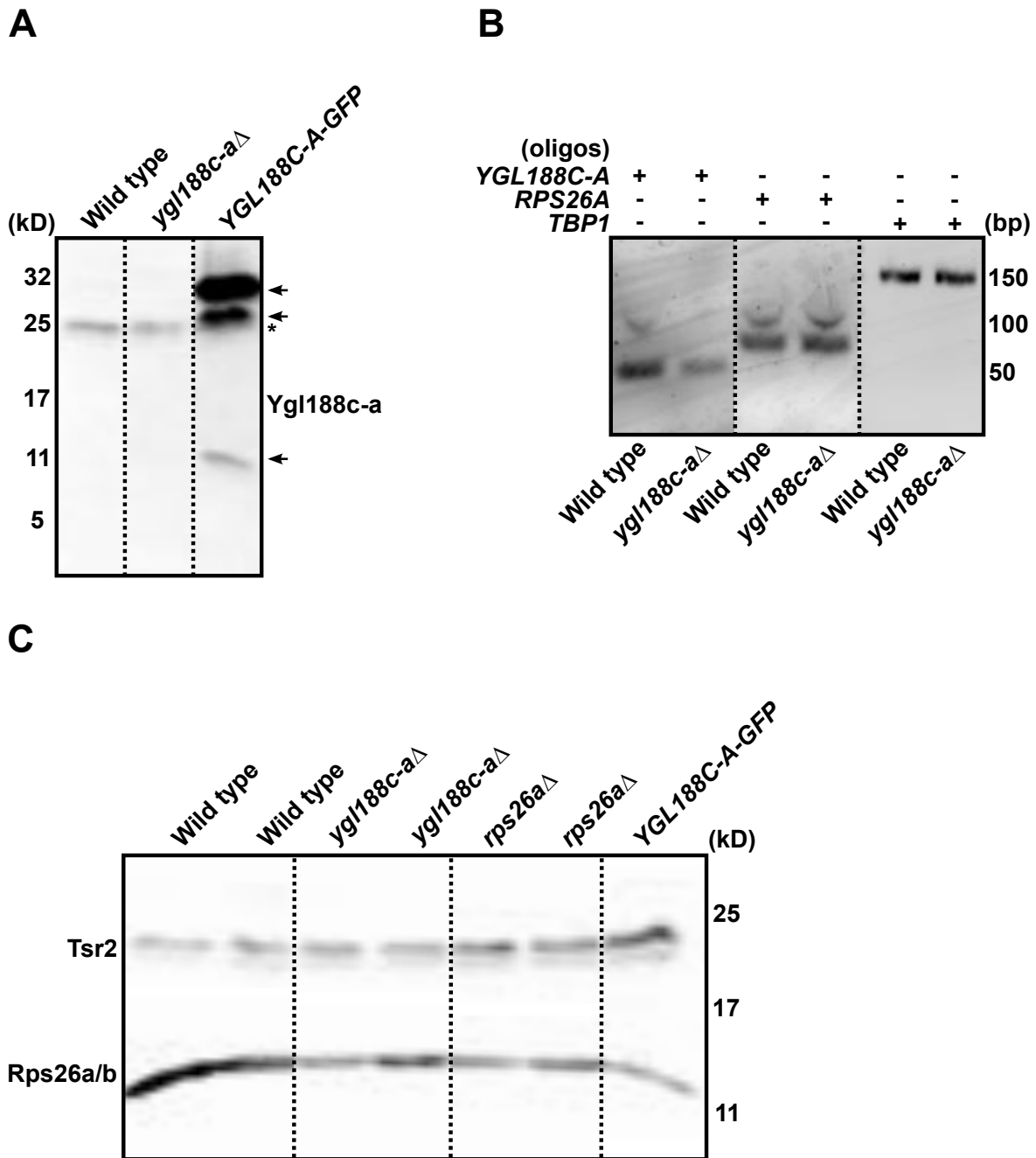


**Figure 3: Characterization of *YGL188C-A* and its effects on the downstream gene *RPS26A*.** (A) The *YGL188C-A* sequence is not expressed under physiological conditions. WT, *ygl188c-aΔ* cells, or cells expressing genomically tagged Ygl188c-a-GFP were grown exponentially in SC medium. Protein extracts were analyzed by SDS-PAGE and probed with an antibody specific to a synthetic peptide corresponding to a deduced sequence from Ygl188C-a. The single asterisk (\*) indicates a non-specific cross-reacting band while arrows indicate Ygl188c-a-GFP and degradation products. (B) *YGL188C-A* deletion does not affect the *RPS26A* transcription. WT and *ygl188c-aΔ* cells were grown exponentially in rich YPD medium. *YGL188C-A*, *RPS26A*, and *TBP1* (housekeeping gene) transcription levels were monitored by RT-PCR using specific oligo-pairs. (C) *YGL188C-A* deletion or c-terminal GFP tagging of Ygl188c-a leads to a downregulation of Rps26a protein levels. Independent clones of the strains with the indicated genotypes were grown exponentially in SC. Protein extracts were analyzed by western blot and probed with an  $\alpha$ -Rps26a antibody raised against the Tsr2/Rps26 complex (Schütz et al. 2014). Note that this antibody cross-reacts with the Rps26a paralogous protein Rps26b and also with the Rps26a/b dedicated chaperone Tsr2, which serves here as an internal loading control.

These data indicate that *YGL188C-A* does not code for any protein but is important for proper Rps26a translation, thus suggesting that the high levels of asparagine and

glutamine measured in the *yg188c-aΔ* strain were, most probably, caused by decreased levels of Rps26a. Hence, the previously described *tco89Δ* cluster includes not only the ribosomal mutants *rps10AΔ*, *rpl20BΔ*, and *rps12Δ* but also a mutant (*yg188c-aΔ*) with decreased Rps26a levels. Since a subset of TORC1 and ribosomal mutants accumulated asparagine and glutamine in a very similar manner, we decided to investigate the effects of ribosomal biogenesis defects on the TORC1 pathway by focusing particularly on one of these ribosomal mutants. In the next paragraph, you will find the arguments that led us to focus on Rps26a and the characterization of the *RPS26A* null mutant.

### 3.3.3: Introduction to *RPS26A* and characterization of its null mutant

In humans, Diamond-Blackfan-Anemia (DBA) is a ribosomopathy (Choesmel et al., 2008; Farrar et al., 2008; Gazda et al., 2006, 2008, 2012) typically characterized by anemia, malformations (in 50% of the cases), growth deficiency (30% of the cases), and malignancy (*i.e.*, acute myelogenous leukemia, myelodysplastic syndrome, and solid tumors) (Alter et al., 2018; Ball et al., 1996; Janov et al., 1996; Lipton et al., 2006; Ramenghi et al., 2000; Vlachos et al., 2001; Vlachos et al., 2018). The disease development is usually linked to hypomorphic missense variants spread in a total of 22 genes coding, primarily, for ribosomal proteins (*e.g.*, *RPS26A*, *RPS10*, *RPL5*, *RPL9*), but also in genes such as *TSR2* and *GATA1* (Stenson et al., 2017).

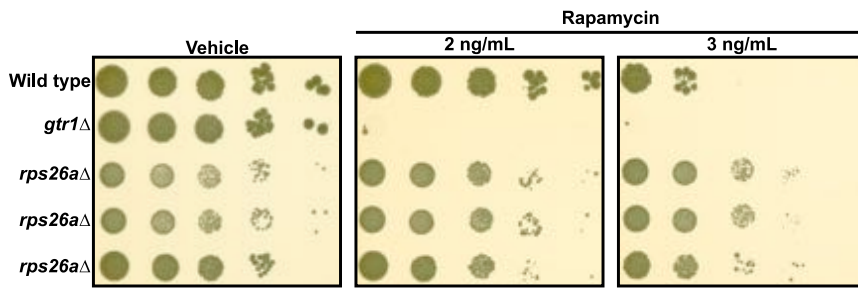
At the molecular level, these missense variants have been proposed to impair the ribosome assembly pathway at different stages, which eventually triggers the p53-mediated nucleolar stress response, thereby promoting cell cycle arrest and apoptosis (Danilova et al., 2008; Gazda et al., 2012). Besides, the decrease in the number of ribosomes may limit the formation of 43S translation preinitiation complexes (PICs) (*i.e.*, 40S SSU, eIF1A, eIF3, and eIF2-GTP-bound methionyl-initiator methionine tRNA), thus promoting, by a non-specific mechanism, the translation of "strong" mRNAs that are characterized by being abundant and stable, by having short coding and 5'UTRs sequences, and by encoding the Kozak consensus sequence (Gaikwad et al., 2021). Furthermore, In the particular case of Rps26, the yeast ortholog Rps26a has been proposed to be an integral part of a specialized pool of ribosomes that favors the expression of specific mRNAs (Ferretti et al., 2017). Considering that, in mammals, hypomorphic Rps26 variants are linked to the development of DBA and cancer and, in

yeast, Rps26a is part of a specialized pool of ribosomes, we got interested in the study of *RPS26A* null mutant and its effects on the TORC1 pathway.

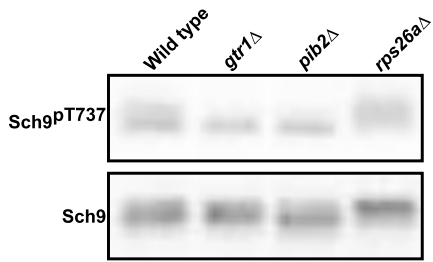
An initial drop spot analysis revealed that loss of Rps26a rendered cells more resistant to sublethal concentrations of the TORC1 inhibitor rapamycin (Figure 4A). This motivated us to further study the effects of loss of Rps26a, but this time, on the mechanism that fine-tunes TORC1 activity following nitrogen starvation plus asparagine or glutamine re-addition. Compared to wild-type (WT) cells, *gtr1* $\Delta$  and *pib2* $\Delta$  cells displayed significantly lower levels of TORC1 activity in exponentially growing cells, while exponentially growing *rps26a* $\Delta$  cells exhibited only moderately reduced TORC1 activity levels (Figures 4B and 4C). In wild-type cells, the TORC1 pathway sensed nitrogen scarcity quickly to strongly inhibit the TORC1 kinase activity upon 2.5 minutes of nitrogen starvation. In contrast, loss of Rps26a transiently kept Sch9<sup>T737</sup> phosphorylation levels (Sch9<sup>pT737</sup>) high up to 2.5 min of nitrogen starvation, even though, upon 15 minutes of nitrogen starvation, Sch9<sup>T737</sup> phosphorylation levels (Sch9<sup>pT737</sup>) were comparable between wild-type and *rps26a* $\Delta$  cells (Figures 4D and 4E). Asparagine re-addition quickly re-stimulated the TORC1 kinase activity in both wild-type and *rps26a* $\Delta$  cells, yet, loss of Rps26a promoted a more robust and stable peak of TORC1 re-activation (Figure 4E). Importantly, restoring Rps26a expression from an integrative plasmid in *rps26a* $\Delta$  cells fully complemented the observed effects on TORC1 activity in nitrogen-starved and glutamine re-stimulated cells (Figure 4F).

However, high Sch9<sup>T737</sup> phosphorylation levels (Sch9<sup>pT737</sup>) can result from either high TORC1 kinase activity or low phosphatase activity. To rule out the possibility that loss of Rps26a might delay the de-phosphorylation of Sch9<sup>pT737</sup>, we treated wild-type and *rps26a* $\Delta$  cells with a lethal concentration of rapamycin and monitored Sch9<sup>pT737</sup> de-phosphorylation dynamics. When cultured in a rich medium and treated with a fully inhibitory concentration of rapamycin, wild-type and *rps26a* $\Delta$  cells showed remarkably similar de-phosphorylation profiles. Thus, loss of Rps26a does not protect Sch9<sup>pT737</sup> from de-phosphorylation but, instead, protects TORC1 from inactivation (Figure 5). These results show that loss of Rps26a affects the TORC1 kinase regulation by delaying its inactivation following nitrogen starvation and enhancing its re-activation following asparagine or glutamine re-addition.

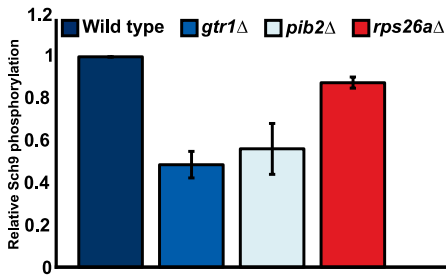
**A**



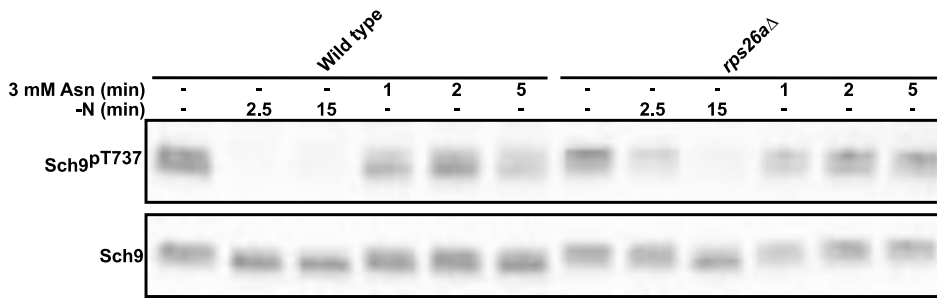
**B**



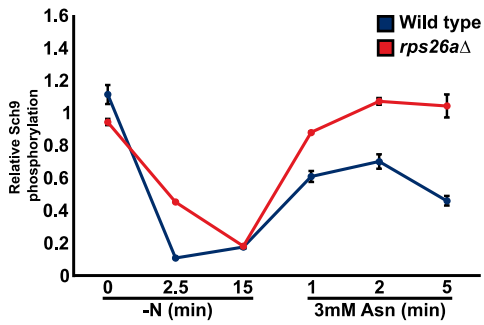
**C**



**D**



**E**



**F**

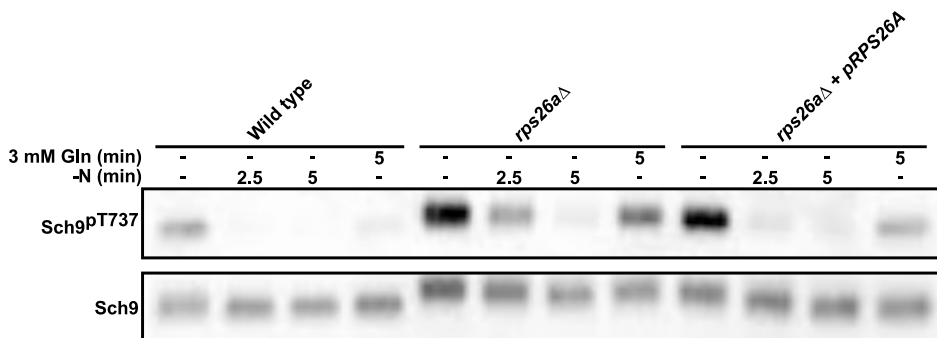
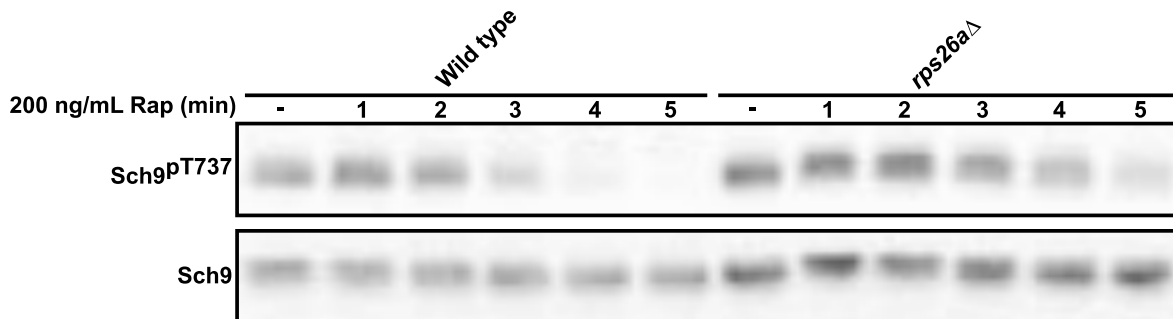




**Figure 4: Characterization of the effect of *RPS26A* deletion on the TORC1 pathway.** (A) *RPS26A* deletion renders cells partially resistant to sublethal concentrations of rapamycin, which directly inhibits the TORC1 kinase activity. WT, *gtr1Δ*, and *rps26aΔ* prototrophic cells (three independent clones) were grown exponentially in SC medium. Serial 10 fold dilutions were spotted on plates containing SC medium plus either ethanol (vehicle) or different concentrations of rapamycin. (B) and (C) *RPS26A* deletion decreases the TORC1 activity of cells growing exponentially. WT, *gtr1Δ*, *pib2Δ*, and *rps26aΔ* prototrophic cells were grown exponentially in SC medium. Protein extracts were analyzed by SDS-PAGE and probed with anti-Sch9-pThr<sup>737</sup> and anti-Sch9 antibodies. Relative TORC1 activities were determined as the ratio of Sch9-pThr<sup>737</sup>/Sch9 normalized to that of WT cells. (D) and (E) *RPS26A* deletion delays TORC1 inhibition upon nitrogen starvation and enhances TORC1 re-activation upon asparagine re-addition. WT and *rps26aΔ* prototrophic cells were grown exponentially in SC medium, then shifted to medium lacking nitrogen for 15 minutes, and finally re-fed with 3 mM asparagine for 5 minutes. Protein extracts were analyzed by SDS-PAGE and probed with anti-Sch9-pThr<sup>737</sup> and anti-Sch9 antibodies. Relative TORC1 activities were determined as the ratio of Sch9-pThr<sup>737</sup>/Sch9 normalized to that of WT cells. Data represent means ± SEM across subjects (N=3). (F) *rps26aΔ* cells expressing Rps26a from a single integration vector display starvation and re-addition patterns similar to WT cells. WT and *rps26aΔ* prototrophic cells were grown exponentially in SC medium, then shifted to medium lacking nitrogen for 5 minutes, and finally re-fed with 3 mM glutamine for 5 minutes. Protein extracts were analyzed by SDS-PAGE and probed with anti-Sch9-pThr<sup>737</sup> and anti-Sch9 antibodies.

**A**



**B**

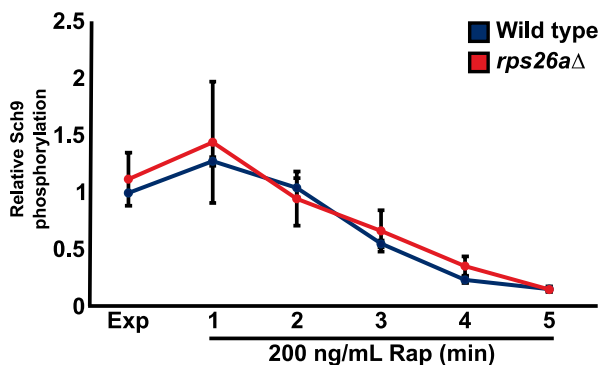


**Figure 5: Characterization of the effect of *RPS26A* deletion on the dynamics of Sch9 de-phosphorylation upon TORC1 inhibition with rapamycin.** (A) and (B) *RPS26A* deletion does not alter the dynamics of Sch9 de-phosphorylation upon rapamycin-mediated TORC1 inhibition. Wild-type and *rps26aΔ* prototrophic cells were grown exponentially in SC medium, then treated with a lethal concentration of rapamycin (200 ng/ml) for the indicated times. Protein extracts were analyzed as in Fig. 4. Relative TORC1 activities were determined as before and normalized to that of Wild-type cells. Data represent means ± SEM across subjects (N=3).

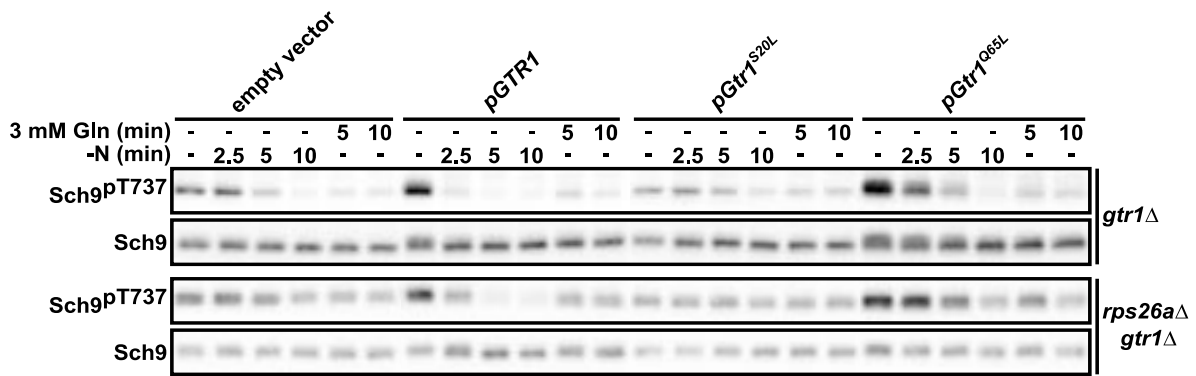
### 3.3.4: Genetic interaction analysis between *RPS26A* and well-known regulators within the TORC1 pathway in yeast

The EGO has been proved to be one of the most important TORC1 upstream regulators in response to the availability of amino acids. As part of the EGO, the

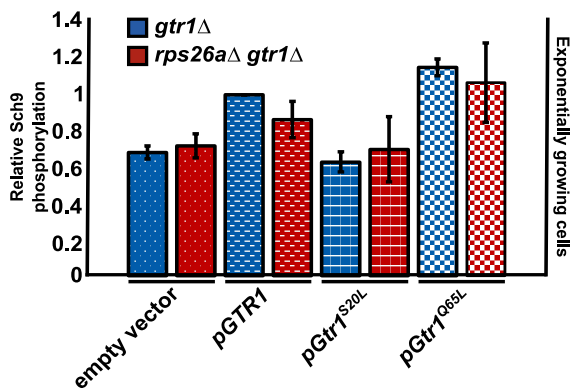
Gtr1/Gtr2 heterodimer impinges on TORC1 through a molecular mechanism that remains elusive; however, previous studies have shown that expression of the compromised Gtr1<sup>S20L</sup> or the GTP-locked Gtr1<sup>Q65L</sup> alleles impinges, respectively, negatively and positively on the TORC1 kinase (Binda et al., 2009; Gao & Kaiser, 2006; Nakashima et al., 1999). Trying to assess whether the effect caused by the loss of Rps26a is transmitted to TORC1 via the EGOC, expression of none or different Gtr1 alleles was carried out in *gtr1Δ* and *rps26aΔ gtr1Δ* cells. In exponentially growing cells, loss of Gtr1 or expression of Gtr1<sup>S20L</sup> downregulated while expression of Gtr1<sup>Q65L</sup> upregulated the TORC1 activity to similar extents in the single *gtr1Δ* and the double *gtr1Δ rps26aΔ* mutants (Figures 6A and 6B).

Following nitrogen starvation, single loss of Rps26a or Gtr1 protected TORC1 activity from inactivation up to 2.5 or 5 minutes, respectively (Figures 6A and 6C-D). Remarkably, the combined loss of Rps26A and Gtr1 led to longer protection of the TORC1 activity up to 10 min of N starvation (Figures 6A and 6C). In line with this, combined loss of Rps26A and Ego1 was also tested, resulting in the same protection as the one described for the *rps26aΔ gtr1Δ* mutant (Data not shown). Gtr1<sup>S20L</sup> or Gtr1<sup>Q65L</sup> expression, in *gtr1Δ* and *rps26aΔ gtr1Δ* cells, also protected TORC1 from inactivation (Figures 6A and 6E-F). Interestingly, upon glutamine re-addition, *rps26aΔ gtr1Δ* cells required Gtr1 or Gtr1<sup>Q65L</sup> expression to trigger TORC1 reactivation (Figures 6A, 6C-F). Altogether these results suggest that, upon nitrogen starvation, loss of Rps26a protects TORC1 from inactivation in parallel to the EGOC regulatory branch.

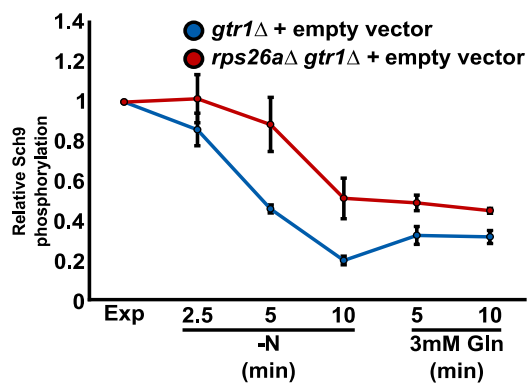
**A**



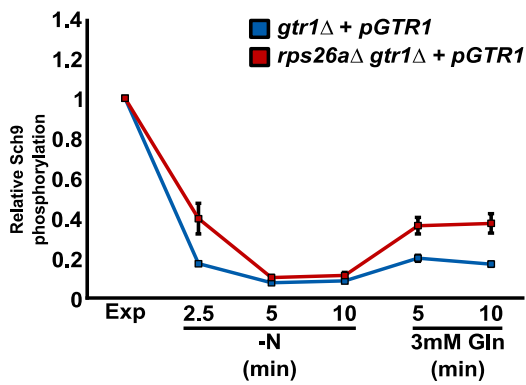
**B**



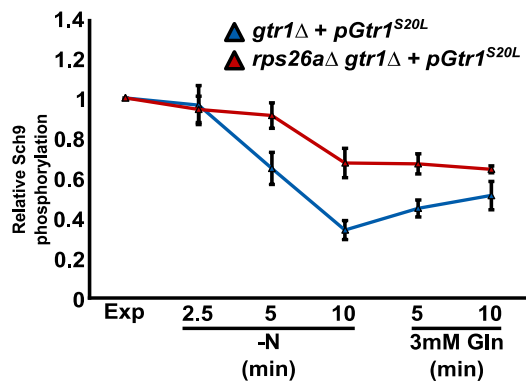
**C**



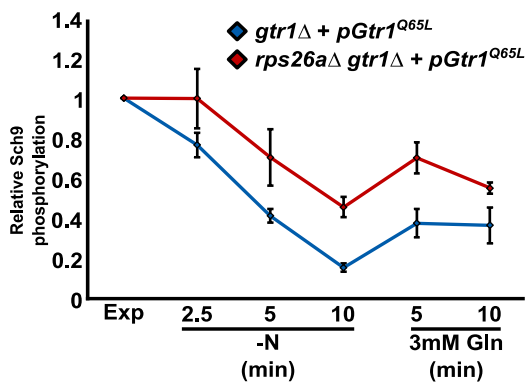
**D**



**E**



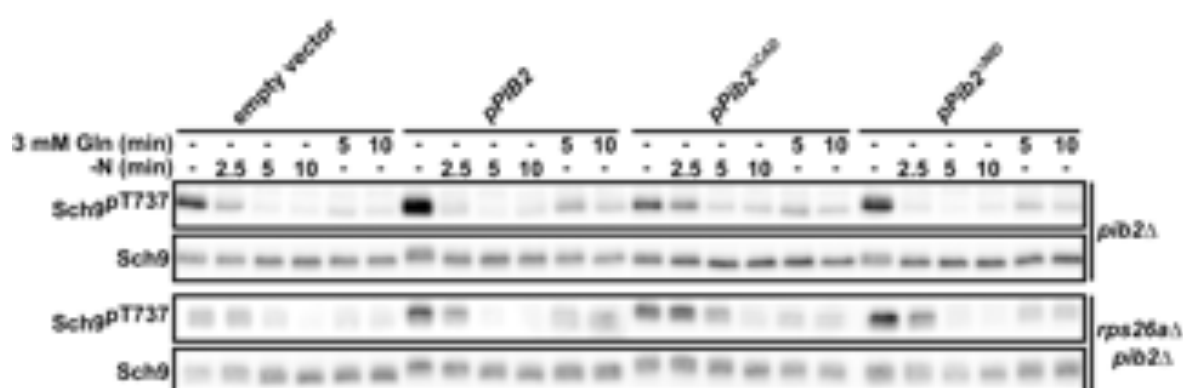
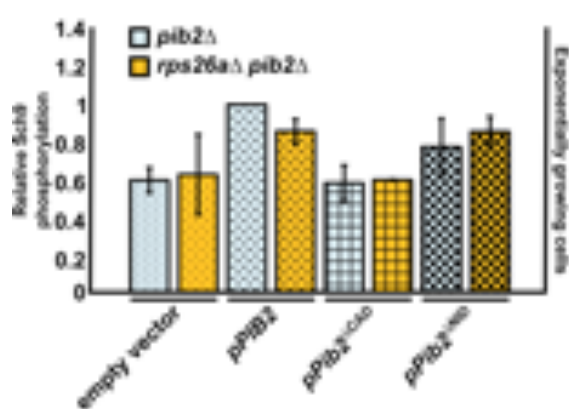
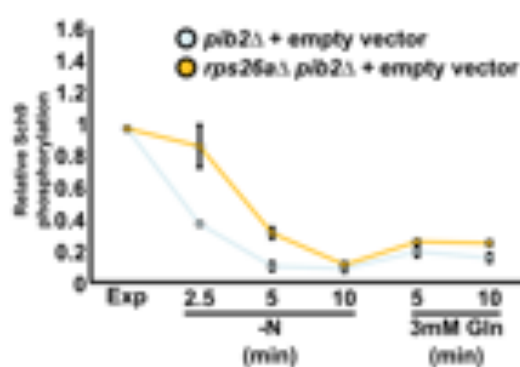
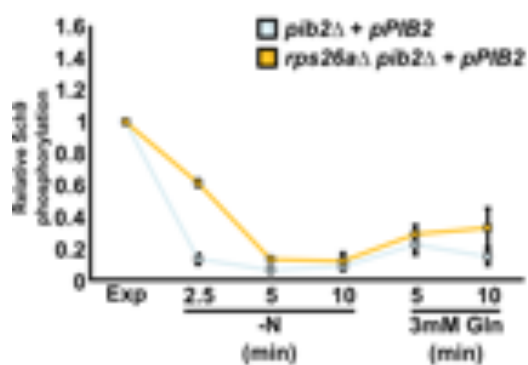
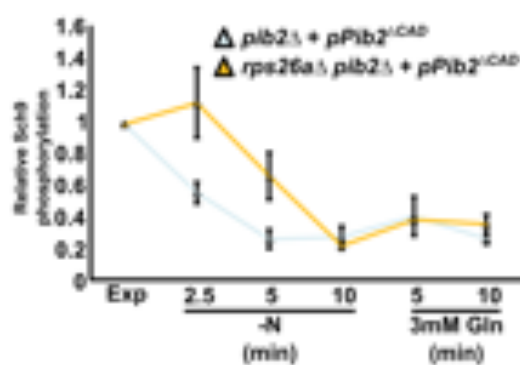
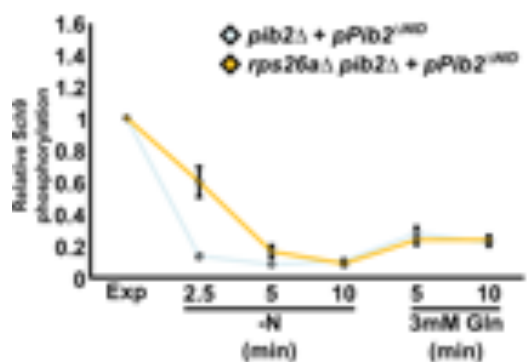
**F**



**Figure 6: Loss of Rps26a protects TORC1 from inactivation upon N starvation in parallel to Gtr1.** (A) Prototrophic *gtr1Δ* and *gtr1Δ rps26aΔ* cells expressing, or not (empty vector), the indicated Gtr1 variants from centromeric vectors were grown exponentially in SC medium (EXP). They were then shifted to a medium lacking nitrogen (-N), and re-fed with 3 mM glutamine for the indicated times. Protein extracts were analyzed as in Fig. 4. (B) Relative TORC1 activities in the exponential growth phase were determined as before and normalized to that of *gtr1Δ +pGTR1* cells. (C-F) Relative TORC1 activities of *gtr1Δ* and *gtr1Δ rps26aΔ* expressing empty vector (C), Gtr1 (D), Gtr1<sup>S20L</sup> (E), or Gtr1<sup>Q65L</sup> (F), were normalized to their respective TORC1 activities in EXP. Data represent means ± SEM across subjects (N=3).

Besides the EGO, Pib2 has been proposed to signal to TORC1 in response to the availability of amino acids, particularly in response to glutamine availability (Michel et al., 2017; Ukai et al., 2018; Varlakhanova et al., 2017). However, whether Pib2 regulates TORC1 independently (Michel et al., 2017; Ukai et al., 2018) or in cooperation with the EGO is unclear (Varlakhanova et al., 2017). Michel and colleagues in 2017 reported that Pib2 harbors, among others, a C-terminal TORC1-Activating Domain (CAD) and an N-terminal TORC1-Inhibiting domain (NID) (Michel et al., 2017). Accordingly, Michel and colleagues generated the Pib2<sup>ΔCAD</sup> and Pib2<sup>ΔNID</sup> alleles which were shown to impinge, respectively, negatively and positively towards TORC1 (Michel et al., 2017).

Trying to assess whether the effect caused by the loss of Rps26a is transmitted to TORC1 via Pib2, expression of none or different Pib2 alleles was carried out, respectively, in *pib2Δ* and *rps26aΔ pib2Δ* cells. In exponentially growing cells, loss of Pib2 or expression of the inhibitory allele Pib2<sup>ΔCAD</sup> reduced TORC1 activity levels in both *pib2Δ* and *rps26aΔ pib2Δ* cells (Figures 7A-7B). Similar to the loss of Rps26a, loss of Pib2 or expression of Pib2<sup>ΔCAD</sup> transiently protected TORC1 from inactivation up to 2.5 min of nitrogen starvation (Figures 7A, 7C-E). Remarkably, simultaneous loss of Rps26a and Pib2 caused, upon nitrogen starvation, more robust protection of the TORC1 activity from inactivation (Figures 7A, 7C-D). Surprisingly, the inhibitory allele Pib2<sup>ΔNID</sup> did not display any phenotype (compare Figures 7A, 7D, and 7F). Although Pib2 is required for high TORC1 activity levels (Figures 7A-B), in its absence, glutamine re-addition was still able to re-activate TORC1 in nitrogen-starved cells (Figures 7A and 7C-D). Considering these results, we can conclude that loss of Rps26a protects TORC1 from nitrogen starvation-induced inactivation independently of Pib2.

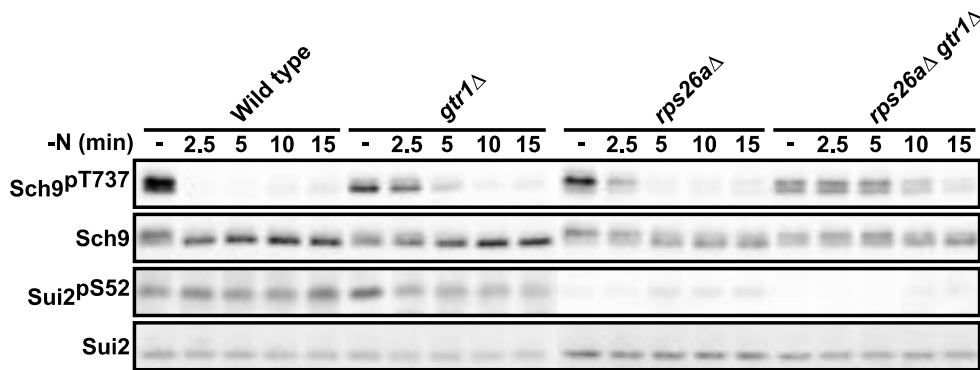
**A****B****C****D****E****F**

**Figure 7: Loss of Rps26a protects TORC1 from inactivation upon N starvation in parallel to Pib2.** (A) Prototrophic *pib2Δ* and *pib2Δ rps26aΔ* cells expressing, or not (empty vector), the indicated Pib2 variants from centromeric vectors were grown exponentially in SC medium (EXP). They were then shifted to a medium lacking nitrogen (-N), and re-fed with 3 mM glutamine for the indicated times. Protein extracts were analyzed as in Fig 4. (B) Relative TORC1 activities in the exponential growth phase were determined as before and normalized to that of *pib2Δ +pPIB2* cells. (C-F) Relative TORC1 activities of *pib2Δ* and *pib2Δ rps26aΔ* expressing nothing (empty vector) (C), Pib2 (D), Pib2<sup>ΔCAD</sup> (E), or Pib2<sup>ΔNID</sup> (F), were normalized to their respective TORC1 activities in EXP. Data represent means ± SEM across subjects (N=3).

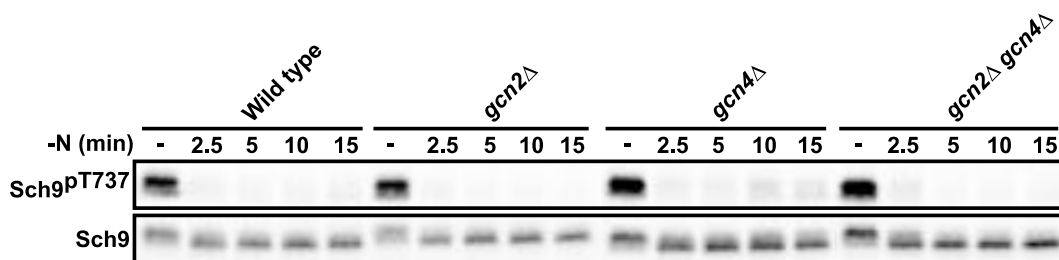
In parallel to the TORC1 pathway, the General Amino Acid Control (GAAC) pathway also senses the intracellular amino acid status, getting active upon amino acid deprivation. The master regulator of the GAAC pathway, the Gcn2 kinase, has been shown to inhibit the TORC1 kinase activity following histidine or leucine starvation (Yuan et al., 2017; Dokládál et al., 2021; Chapter 2, Figure 2). To evaluate whether the loss of Rps26a affects the Gcn2 activity, we first monitored the phosphorylation dynamics of Sui2 (Sui2<sup>pS52</sup>), the specific target of Gcn2, in wild-type, *gtr1Δ*, *rps26aΔ*, and *rps26aΔ gtr1Δ* cells grown in rich conditions and then shifted to a nitrogen lacking medium. Indeed, loss of Rps26a impaired the Gcn2 activity (Figure 8A). Since Gcn2 levels were similar in *rps26aΔ* and wild-type cells (data not shown), loss of Rps26a seems to impair Gcn2 activation.

Next, we examined whether loss of Gcn2, its downstream target Gcn4, or loss of both could recapitulate the phenotype observed in *rps26aΔ* cells. Notably, loss of Gcn2, Gcn4, or Gcn2 and Gcn4 did not protect TORC1 from inactivation upon short time points of nitrogen starvation (Figure 8B). Based on these results, we can conclude that Gcn2 does not mediate quick TORC1 inhibition upon nitrogen starvation in Rps26a expressing cells. However, to exclude the possibility that it may do so in the context of the *RPS26A* deletion mutant, we analyzed the consequences of restoring Gcn2 activity in the *rps26aΔ* cells, making use of the Gcn2<sup>F842L</sup> hyperactive allele. Since this allele induces cell growth arrest when constitutively expressed (Qiu, 2002), we employed a system by which the genomic expression of Gcn2<sup>F842L</sup> (*pGCN2<sup>F842L</sup>*) was finely tuned. In this system, Gcn2<sup>F842L</sup> expression was regulated by, on the one hand, the constitutive expression of an inactive transcription factor (*pTF*) and, on the other hand, the addition to the culture medium of  $\beta$ -estradiol (estradiol), which triggers the activation of this transcription factor in a concentration-dependent manner (Ottoz et al., 2014).

**A**



**B**



**C**

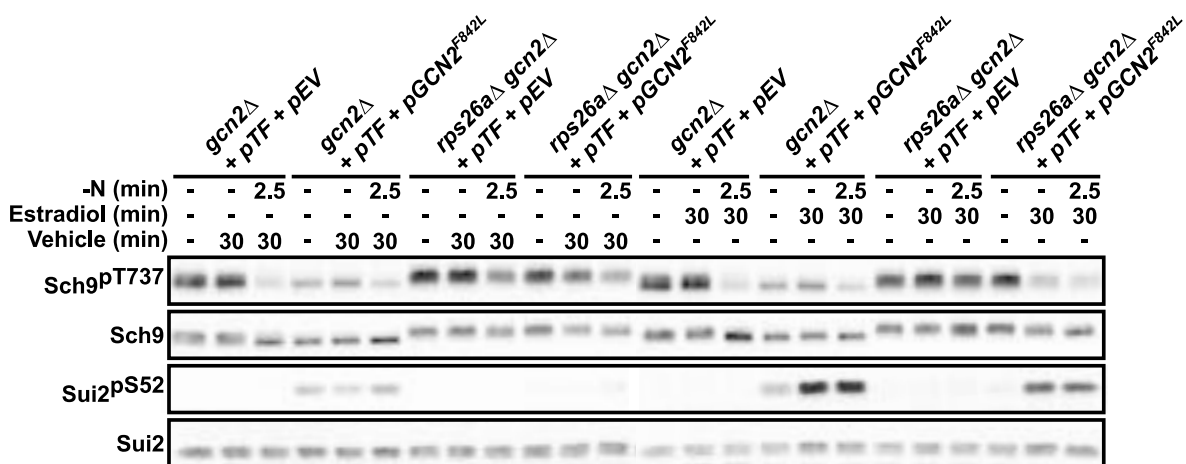


**Figure 8: Gcn2 plays no role in the protection of TORC1 from inactivation caused by loss of Rps26a.** (A) *RPS26A* deletion impairs Gcn2 activity. Prototrophic wild-type, *gtr1*Δ, *rps26a*Δ, and *rps26a*Δ *gtr1*Δ cells were grown exponentially in SC medium (-), then shifted to medium lacking nitrogen (-N). Protein extracts were probed with anti-Sch9-pThr<sup>737</sup> and anti-Sch9 antibodies to monitor TORC1 activity and with anti-Sui2-pS<sup>52</sup> and anti-Sui2 specific antibodies to assess Gcn2 activity. (B) GAAC pathway disruption does not protect TORC1 activity upon nitrogen starvation. Tryptophan auxotrophic wild-type, *gcn2*Δ, *gcn4*Δ, and *gcn2*Δ *gcn4*Δ cells were grown exponentially in SC medium (-), and then shifted to medium lacking nitrogen (-N). Protein extracts were analyzed as in Fig. 4. (C) Induced expression of the Gcn2<sup>F842</sup> hyperactive allele does not abolish, upon nitrogen starvation, the protection of TORC1 from inactivation caused by loss of Rps26a. Tryptophan auxotrophic *gcn2*Δ and *rps26a*Δ *gcn2*Δ cells were transformed, or not (empty vector; pEV), with an integrative vector constitutively expressing a transcription factor (pTF) able to induce the expression of Gcn2<sup>F842</sup> (pGcn2<sup>F842L</sup>) in the presence of estradiol. Cells were grown exponentially in SC medium (-). They were then treated with either vehicle (ethanol) or 2 μM estradiol for 30 minutes, and shifted to a medium lacking nitrogen (-N) for 2.5 minutes. Protein extracts were treated as in panel A.

Remarkably, in *gcn2Δ* cells, but not in *rps26aΔ gcn2Δ* cells, non-induced expression of the GCN2<sup>F842L</sup> allele was sufficient to inhibit the TORC1 activity in rich conditions (Figure 8C). Besides, estradiol treatment did not affect TORC1 or Gcn2 activities in *gcn2Δ* and *rps26aΔ gcn2Δ* cells lacking the GCN2<sup>F842L</sup>-inducible plasmid (Figure 8C). Following estradiol treatment, Gcn2<sup>F842L</sup> was strongly induced in both *gcn2Δ* and *rps26aΔ gcn2Δ* cells (Figure 8C). Notably, in the case of *gcn2Δ* cells, overexpression of Gcn2<sup>F842L</sup> did not decrease further the TORC1 activity levels when compared to leaky-expressing *gcn2Δ* cells (Figure 8C). Even though in *rps26aΔ gcn2Δ* cells overexpression of Gcn2<sup>F842L</sup> also led to TORC1 inhibition, the TORC1 activity levels before and after nitrogen starvation were largely identical. From these results, we conclude that, upon nitrogen starvation, Gcn2 plays no role in the protection of TORC1 from inactivation caused by the loss of Rps26a.

### **3.3.5: Genetic interaction analysis between RPS26A and potential regulators within the TORC1 pathway in yeast**

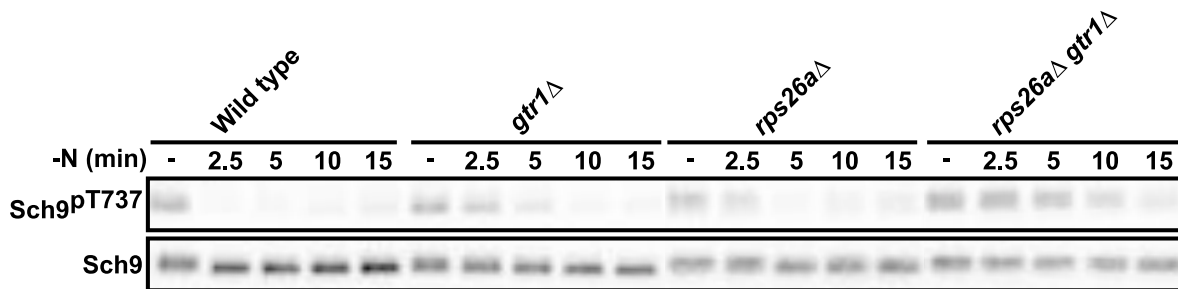
As mentioned before, loss of Rps26a negatively impacts the ribosome assembly pathway, which may lead to a higher degradation of rRNA and hence to the accumulation of adenine and uracil. Since the accumulation of these two compounds may impact the TORC1 activity, we tried to reduce their intracellular levels by growing cells in media lacking adenine and uracil. Removing adenine and uracil from the culture media did not abolish, upon nitrogen starvation, the protection of the TORC1 activity caused by loss of Rps26a (Figure 9A). However, removing adenine and uracil from the culture media may not sufficiently lower down the intracellular levels of these two compounds.

In humans, elevated erythrocyte adenosine deaminase (eADA) activity is used to diagnose Diamond-Blackfan-Anemia (DBA) (Fargo et al., 2013; Whitehouse et al., 1986). The enzyme adenosine deaminase plays a role in the purine salvage pathway, catalyzing the irreversible deamination of adenosine to inosine and 2' deoxyadenosine to 2' deoxyinosine (Hirschhorn & Ratech, 1980). As of today, the role of the adenosine deaminase in the development of DBA remains obscure, but, interestingly, a higher activity of this enzyme has also been measured, among others, in cells from breast, kidney, and colorectal tumors (Aghaei et al., 2005; Camici et al., 1990; Durak et al., 1997; Eroğlu et al., 2000; Mahajan et al., 2013). In yeast, the ortholog of the adenosine



deaminase is the adenine deaminase (*AAH1*) which is also involved in the yeast purine salvage pathway converting adenine to hypoxanthine (Guetsova et al., 1997; Woods et al., 1984).

**A**



**B**

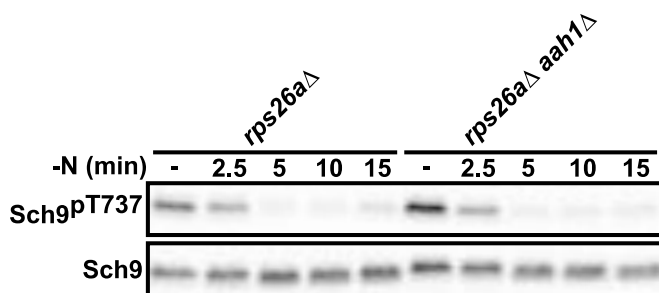


**Figure 9: Protection of the TORC1 activity upon nitrogen starvation does not seem to be linked to increased intracellular uracil and adenine levels or increased Aah1 enzymatic activity.** (A) Prototrophic wild-type, *gtr1*Δ, *rps26a*Δ, *rps26a*Δ *gtr1*Δ were grown exponentially in a rich medium lacking adenine and uracil (-), and then shifted to a medium lacking nitrogen (-N) for the indicated times. (B) Prototrophic *rps26a*Δ and *rps26a*Δ *aah1*Δ cells were grown exponentially in SC medium (-), and then shifted to medium lacking nitrogen (-N) for the indicated times. Protein extracts were analyzed as in Fig 4.

Interestingly, the loss of Rps26a caused a 34% increase in the levels of the Aah1 enzyme (data not shown). Therefore, we decided to study the adenine deaminase (*AAH1*) role on the TORC1 pathway. As depicted in Figure 9B, loss of Aah1 did not suppress the TORC1 protection caused by loss of Rps26a (Figure 9B). Although we cannot rule it out completely, it seems that increased rRNA catabolism, with the subsequent accumulation of intracellular adenine and uracil, is not responsible, upon nitrogen starvation, for the TORC1 activity protection that results from the loss of Rps26a.

All the previous results showed us that loss of Rps26a affects the TORC1 activity in parallel to well-known TORC1 regulators such as Gtr1, Pib2, and Gcn2. Therefore, to find hitherto unknown TORC1 regulators in yeast, we searched for well-established mTOR regulators in mammals. For example, the GTPase Arf1 has been proposed to

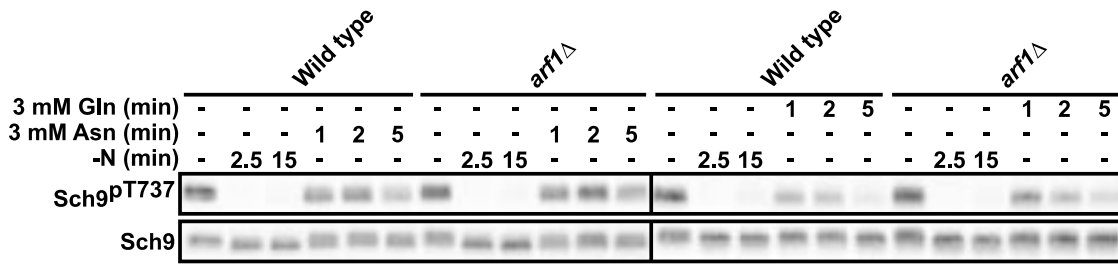
activate, in parallel to the Rag GTPases, lysosomal mTOR in response to increased glutamine and asparagine intracellular levels (Meng et al., 2020). Besides, in starved cells re-fed with amino acids, rapid re-localization of mTORC1 from Aster-c, which is a subdomain of the endoplasmic reticulum (ER), to the lysosomal membrane has been proposed to be mediated by COPI vesicles, and thus catalyzed by Arf1 (Zhang et al., 2020). These data prompted us to investigate whether, in yeast, Arf1 plays any role within the TORC1 pathway.

Analysis of the levels of TORC1 activity in exponentially growing cells revealed that loss of Arf1 reduced the TORC1 activity levels by around 20% (Figures 10A-B). Besides, loss of Arf1 did not abrogate the proper TORC1 inactivation upon nitrogen starvation (Figures 10A, and 10C-D). Interestingly, in comparison to wild-type cells, loss of Arf1 led to a more robust peak of TORC1 re-activation upon asparagine or glutamine re-addition (Figures 10C-D). These results suggest that Arf1 plays a role in TORC1 regulation.

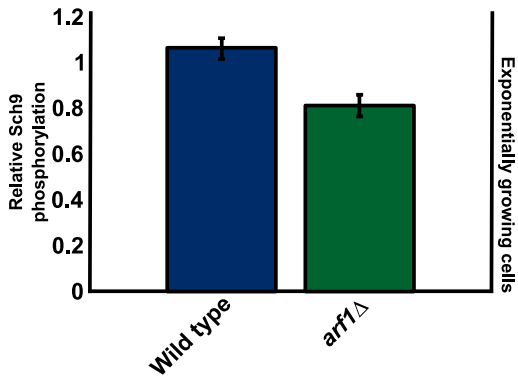
Then we wondered whether loss of Rps26a signals to TORC1 through Arf1. Loss of Gcs1 (the Arf1-GAP) and, to a lesser extent, Arf1 decreased the levels of TORC1 activity in *rps26a* $\Delta$  cells growing exponentially in SC (Figures 11A and 11B). Astonishingly, loss of Arf1 (but not Arf2) and Gcs1 abolished, upon nitrogen starvation, the TORC1 protection from inactivation typically described for *rps26a* $\Delta$  cells, yet, *gcs1* $\Delta$  cells displayed dramatic low levels of TORC1 activity already in exponentially growing cells (Figures 11A, C, and D).

Although the loss of Gtr1 protects TORC1 from inactivation upon nitrogen starvation, loss of Arf1 in *gtr1* $\Delta$  cells further enhanced this phenotype, and, loss of Arf1 in the double mutant *rps26a* $\Delta$  *gtr1* $\Delta$  reduced, upon nitrogen starvation, the TORC1 activity levels to those of the double mutant *gtr1* $\Delta$  *arf1* $\Delta$  (Figure 11A).

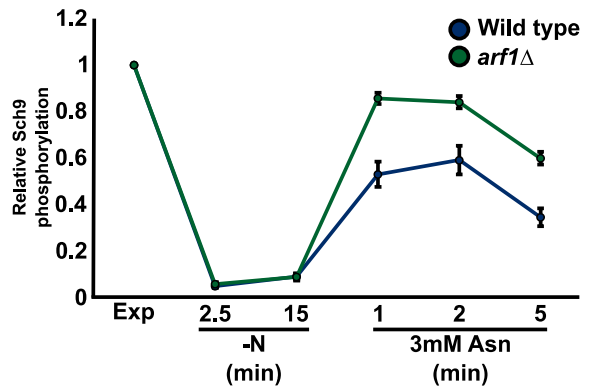
**A**



**B**



**C**



**D**

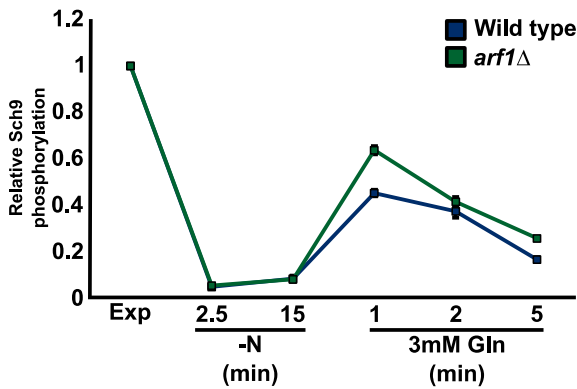
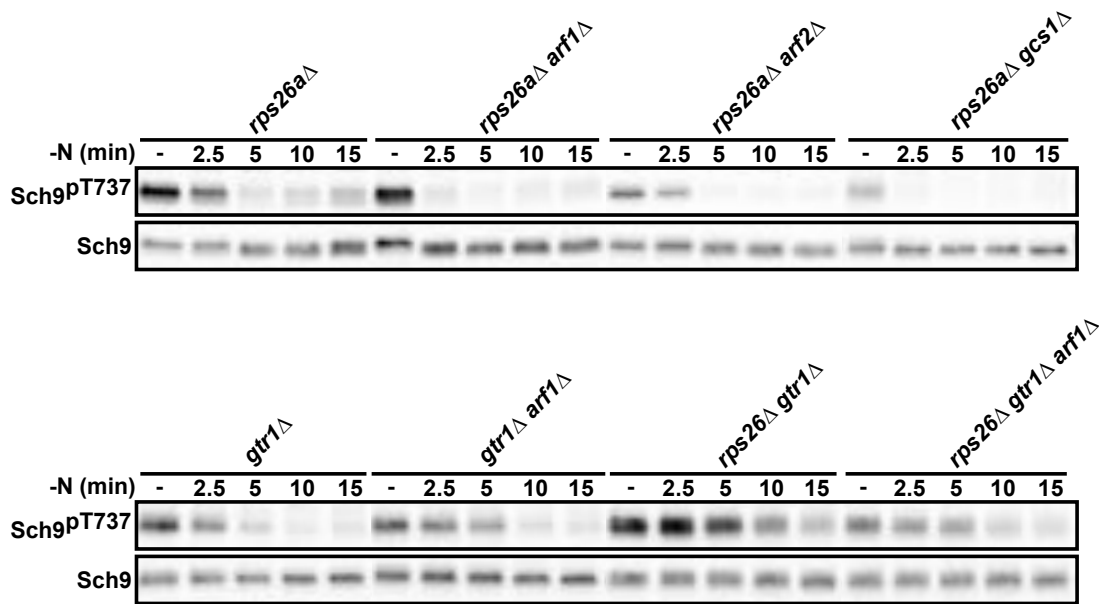
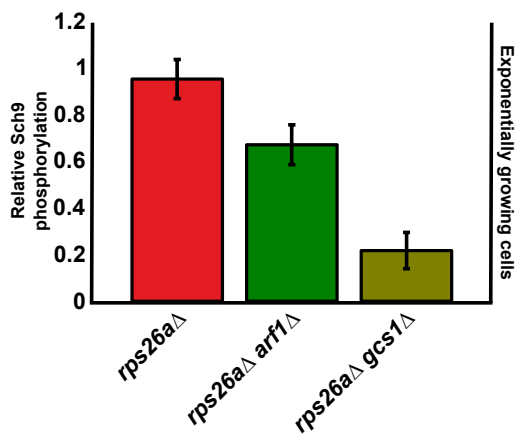


**Figure 10: The *arf1* $\Delta$  mutant shows normal TORC1 inactivation upon nitrogen starvation but stronger re-activation upon asparagine or glutamine re-addition.** (A) Prototrophic wild-type and *arf1* $\Delta$  cells were grown exponentially in SC medium (EXP). They were then shifted to a medium lacking nitrogen (-N), and re-fed with 3 mM asparagine or 3 mM glutamine for the indicated times. Protein extracts were analyzed as in Fig 4. (B) Relative TORC1 activities in the exponential growth phase were determined as before and normalized to that of wild-type cells. (C) and (D) Relative TORC1 activities of wild-type and *arf1* $\Delta$  cells were normalized to their respective TORC1 activities in EXP. Data represent means  $\pm$  SEM across subjects (N=6 for (B) and N=3 for (C) and (D)).

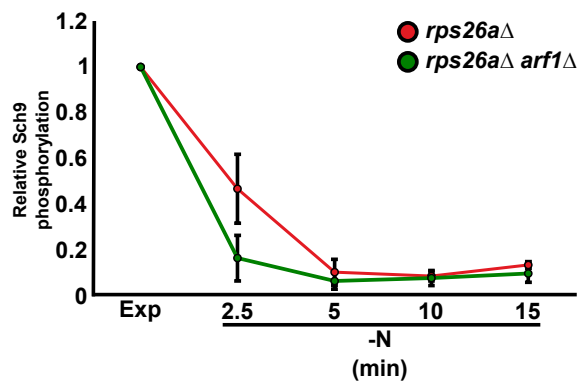
**A**



**B**



**C**



**D**

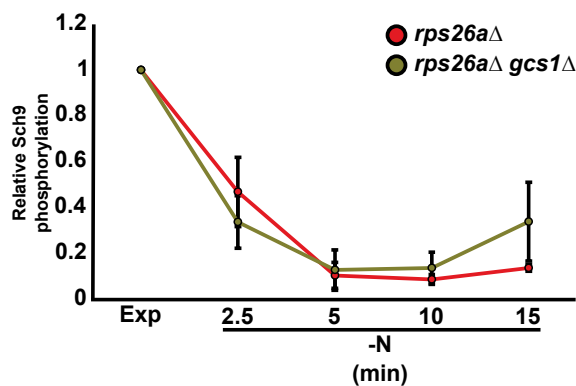


**Figure 11: Loss of Arf1 GTPase (but not Arf2) abolishes the protection of TORC1 from inactivation upon nitrogen starvation caused by loss of Rps26a.** (A) Prototrophic *rps26aΔ*, *rps26aΔ arf1Δ*, *rps26aΔ arf2Δ*, *rps26aΔ gcs1Δ*, *gtr1Δ*, *gtr1Δ arf1Δ*, *rps26aΔ gtr1Δ*, and *rps26aΔ gtr1Δ arf1Δ* cells were grown exponentially in SC medium (-), and then shifted to a medium lacking nitrogen (-N) for the indicated times. Protein extracts were analyzed as in Fig 4. (B) Relative TORC1 activities in the exponential growth phase were determined as before and normalized to that of *rps26aΔ* cells. (C) and (D) Relative TORC1 activities of *rps26aΔ* and *rps26aΔ arf1Δ* (D) or *rps26aΔ* and *rps26aΔ gcs1Δ*

*gcs1Δ* cells (E) were normalized to their respective TORC1 activities in EXP. Data represent means ± SEM across subjects (N=3).

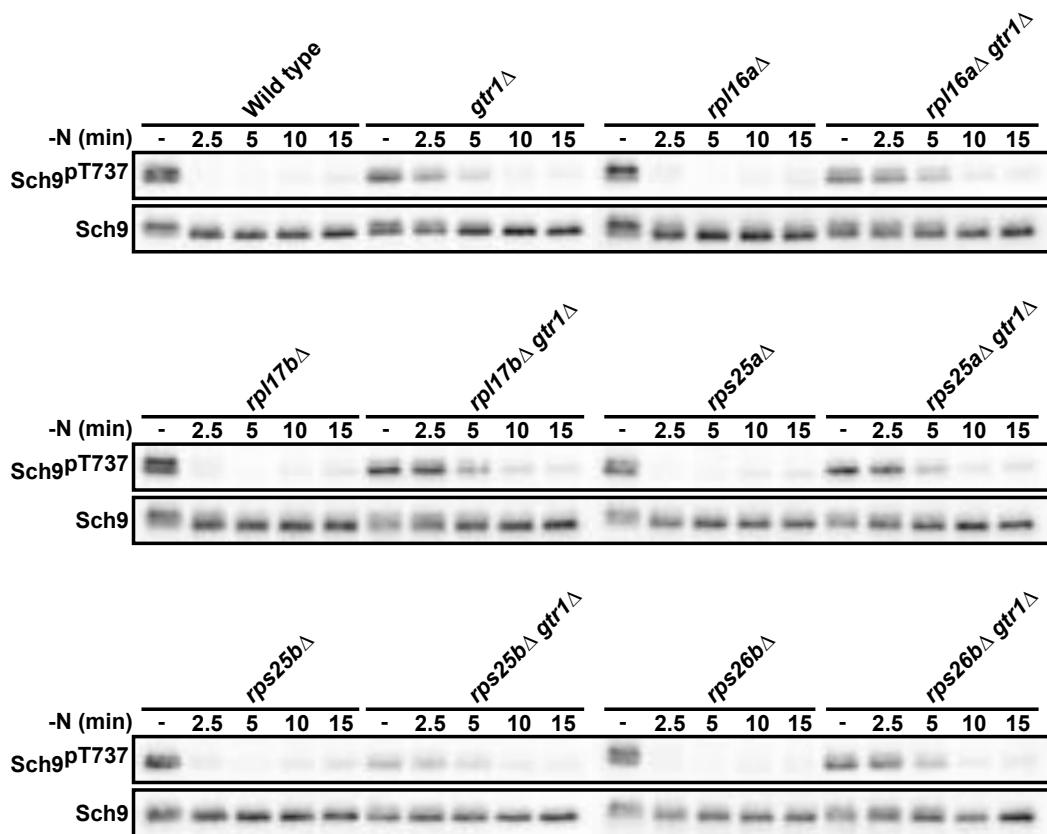
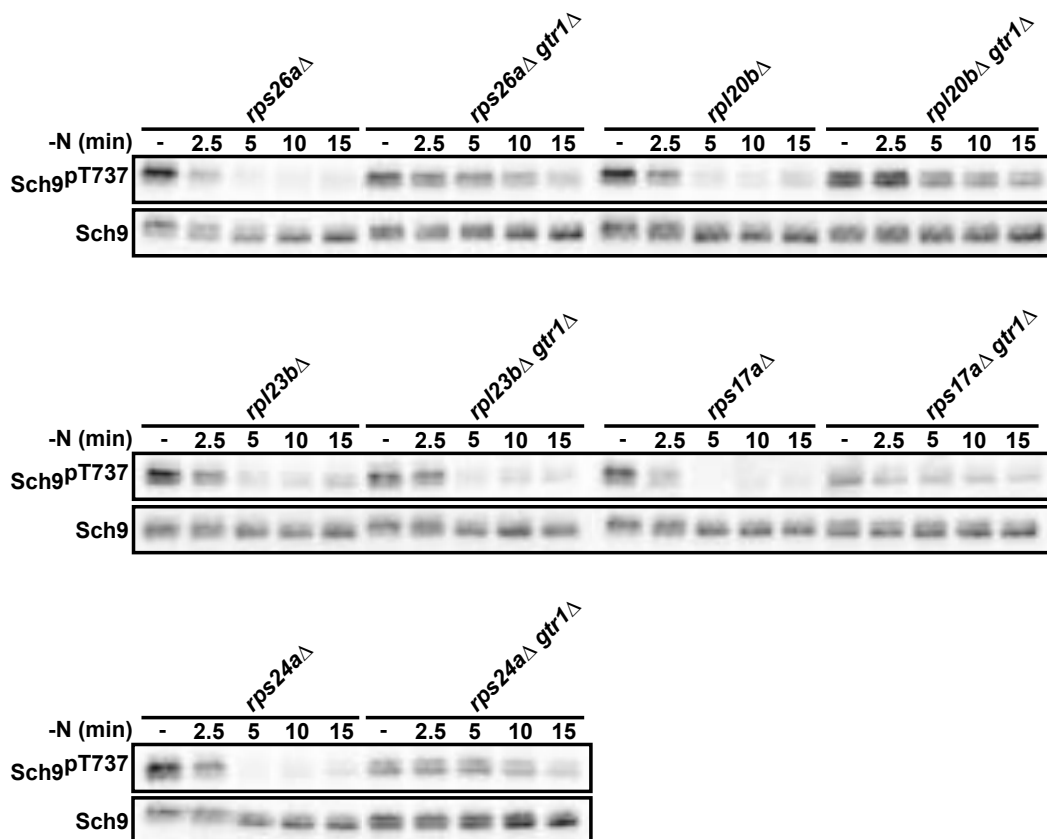
Considering these new results, we can conclude that Arf1 not only plays a role, in parallel to the EGO, in the TORC1 kinase regulation but also mediates, upon nitrogen starvation, TORC1 protection from inactivation in *rps26aΔ* cells. However, we still wondered how the loss of Rps26a may impact Arf1 activity. Interestingly, proteomic analysis revealed that loss of Rps26a altered the protein levels of some Arf1 regulators: Guanine nucleotide Exchange Factors (GEFs) Sec7 and Gea2, and the GTPase-Activating Proteins (GAPs) Gcs1 and Glo3 (Table 4). Therefore, loss of Rps26a may lead to Arf1 misregulation, which would eventually impact the TORC1 activity.

Protein	Description	Fold change	Significance
ARF1	ADP-ribosylation factor 1	-1.04	-
SEC7	GEF	1.16	+
GEA1	GEF	-1.07	-
GEA2	GEF	1.29	+
SYT1	GEF	NaN	-
GCS1	GAP	1.26	+
GLO3	GAP	2.01	+

**Table 4: Fold change of Arf1 and Arf1 regulators in *rps26aΔ* cells compared to wild-type cells.** Wild-type and *rps26aΔ* cells were grown, in sextuplicate, exponentially in a rich medium. Positive significance (+) is considered when p-value < 0.05.

### 3.3.6: Specificity of the *RPS26A* deletion mutant phenotype

At this point, we also wondered about the specificity of the phenotype caused by the loss of Rps26a. To address this, we generated, *de novo*, a subset of ribosomal protein mutants that (a) made part of either the small or the large ribosomal subunit, (b) displayed or not a slow-growth phenotype, or (c) did or did not show high levels of intracellular glutamine and asparagine based on Müllerer's measurements. Cells were cultured exponentially in a rich medium (-) and then starved for nitrogen (-N) (Figure 12). Loss of Rpl16a, Rpl17b, Rps25a, Rps25b, and Rps26b did neither render cells slow-growing nor impaired TORC1 inactivation upon nitrogen starvation (Figure 12A).

**A****B**

**Figure 12: The loss of ribosomal proteins that cause slow-growth phenotype protects TORC1 from inactivation upon nitrogen starvation.** (A) Prototrophic wild-type, *gtr1Δ*, *rpl16aΔ*, *rpl16aΔ gtr1Δ*, *rpl17bΔ*, *rpl17bΔ gtr1Δ*, *rps25aΔ*, *rps25aΔ gtr1Δ*, *rps25bΔ*, *rps25bΔ gtr1Δ*, *rps26bΔ*, and *rps26bΔ gtr1Δ* normal-growth strains were grown exponentially in SC medium (-) and then shifted to a medium lacking nitrogen (-N). Protein extracts were analyzed as in Fig 4. (B) Prototrophic *rps26aΔ*, *rps26aΔ gtr1Δ*, *rpl20bΔ*, *rpl20bΔ gtr1Δ*, *rpl23bΔ*, *rpl23bΔ gtr1Δ*, *rps17aΔ*, *rps17aΔ gtr1Δ*, *rps24aΔ*, and *rps24aΔ gtr1Δ* slow-growth strains were grown exponentially in SC medium (-) and then shifted to a medium lacking nitrogen (-N). Protein extracts were analyzed as in Fig 4.

In line with this, simultaneous loss of Rpl16a, Rpl17b, Rps25a, Rps25b, or Rps26b and Gtr1 caused the same phenotype as the single loss of Gtr1 (Figure 12A). In contrast, the loss of Rps26a, Rpl20b, Rpl23b, Rps17a, or Rps24a rendered cells slow-growing and protected TORC1 from inactivation upon 2.5 minutes of nitrogen starvation (Figure 12B). Interestingly, combined loss of Rps26a, Rpl20b, Rps17a, or Rps24a, but not Rpl23b, and Gtr1 led to a more robust TORC1 protection than the one observed in the single mutants (Figure 12B).

Interestingly, similar to human Rps26, mutations in Rps24 (ortholog of Rps24a/b) and Rps17 (ortholog of Rps17a/b) are linked to the development of Diamond Blackfan Anemia (DBA) (Choesmel et al., 2008; Stenson et al., 2017). Differently, Rpl23 has been shown to act as a tumor suppressor by activating p53 when the p19ARF-MDM2-p53 regulatory pathway is lost (Meng et al., 2016). According to these results, we can conclude that, upon nitrogen starvation, the protection of the TORC1 activity from inactivation is not a specific trait for *rps26aΔ* cells but rather for slow-growth ribosomal mutants. Interestingly, on one side, loss of Rps26a, Rps24a, Rps17a and, on the other side, Rpl23b seem to impinge on TORC1 via different branches; in the first case, this occurs in parallel to the EGOC, and, in the second case, through the EGOC.

### 3.3.7: Proteome analysis of the *rps26aΔ* strain

Although the eukaryotic ribosomal protein eS26 (Rps26a/b in yeast) is, along with the eS10, one of the last to be stably incorporated into the 18S pre-SSU (Small SubUnit) ribosomal particle in the cytoplasm (Ferreira-Cerca et al., 2007; Sturm et al., 2017), loss of eS26 has a strong negative impact on early-stage of 20S pre-rRNA processing at the nucleolus (Schütz et al., 2014). In line with this, Peña and colleagues observed that eS26, together with uS11, forms a complex that is transferred into the 90S pre-ribosomal particle by the ATPase Fap7 (Peña et al., 2016). Finally, recent evidence suggests that eS26, together with Rio1, is essential for the last cytoplasmic 18S rRNA processing step catalyzed by Nob1 (Plassart et al., 2021).

In the mature 80S ribosome, Rps26a is known to be located at the mRNA exit channel (Ben-Shem et al., 2011), where it interacts with the 5' UTR of the mRNAs (Graifer, 2004; Pisarev et al., 2008) and mediates, supposedly, translation initiation (Sharifulin et al., 2012). Especially significant for the mRNA-Rps26a interaction is the region between Y62 and K70 of Rps26a (Sharifulin et al., 2012). However, Belyy and colleagues in 2016 revealed that mutation or deletion of the sequence comprised between Y62 and K70 is not important for translation initiation but, instead, for the 40S subunit assembly (Belyy et al., 2016). These studies demonstrate the importance Rps26a has in both the early and late stages of the rRNA processing and, hence, in ribosome assembly.

Moreover, in 2017, Ferretti and colleagues co-purified, from *rps26b* $\Delta$  cells, the mRNAs that bind to Rps26a-containing and Rps26a-depleted ribosomes. They quantified the affinities of these two ribosomal pools against the same mRNAs and observed that Rps26a-depleted ribosomes bind strongly to mRNAs coding for members of the high salt (Hog1) and high pH (Rim101) stress response pathways. Analysis of the 5' UTR of mRNAs co-precipitating with these two different pools of ribosomes revealed that mRNAs associated with Rps26a-containing ribosomes are prone to contain the consensus Kozak sequence and adenine at positions -4 and -2. In contrast, mRNAs associated with Rps26a-depleted ribosomes usually lack the consensus Kozak sequence and have guanine at position -4 (Ferretti et al., 2017). This study shows that Rps26a forms an integral part of a specialized pool of ribosomes that favors the expression of specific mRNAs.

To gain further insights on how the loss of Rps26a may impact the ribosome biogenesis, the translome, and possibly TORC1, we undertook the comparison of the proteomes from wild-type and *rp26a* $\Delta$  mutant cells. Label-free quantification was followed by a GO enrichment analysis, using gprofiler and Cytoscape (Reimand et al., 2019), of the proteins that were significantly enriched or diminished (at least 1.5 times, p-value < 0.05) in the *rps26a* $\Delta$  proteome (Figure 13 and Table 5). Table 6 shows a shorter list of the proteins used during the GO enrichment analysis (at least 2 times, p-value < 0.05).



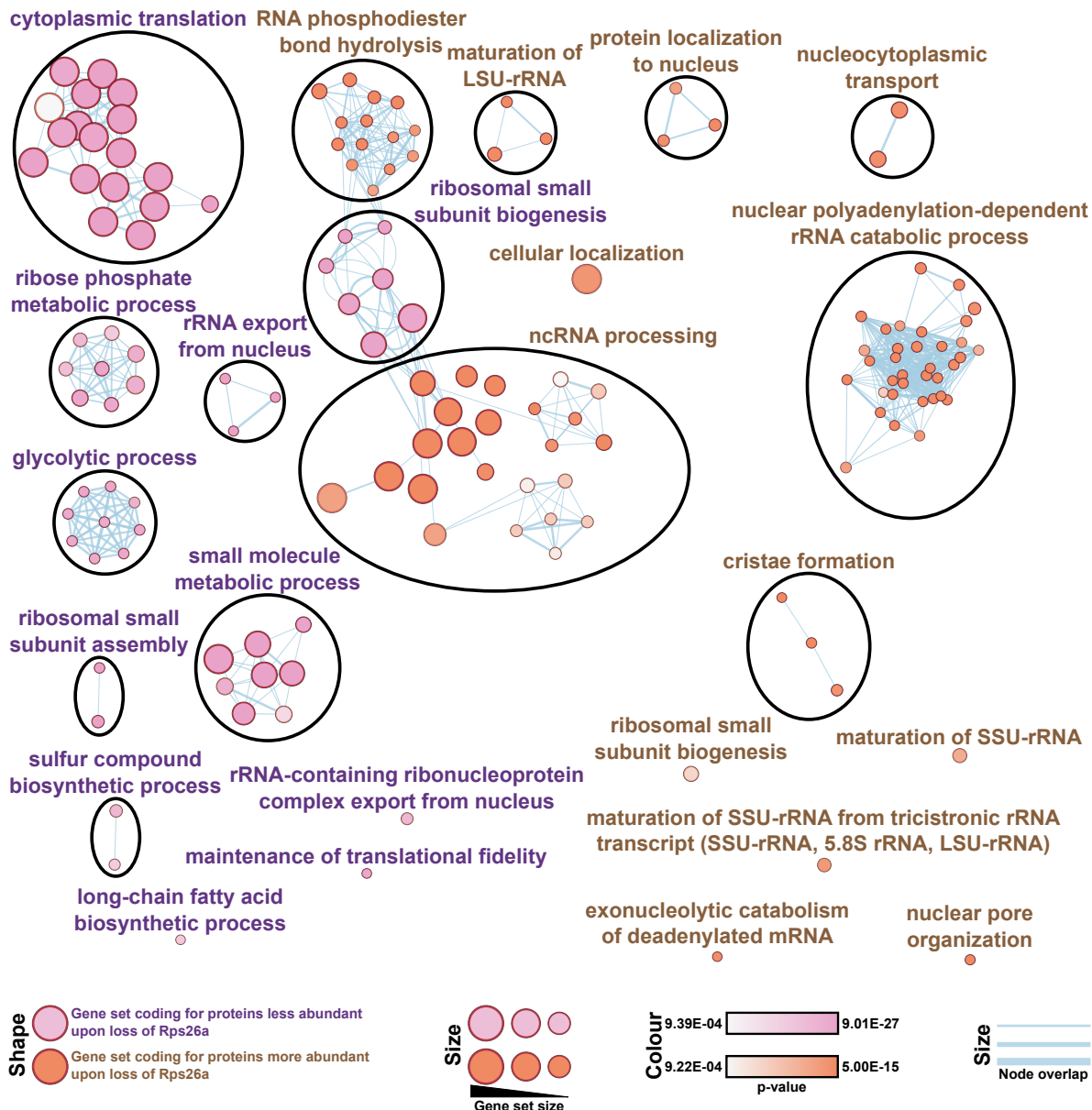


**Figure 13: GO enrichment analysis of the proteins enriched and diminished upon Rps26a loss.** For the analysis of GO terms, proteins whose levels increased or decreased by at least 50% were chosen. A functional enrichment analysis was performed using gprofiler applying a p-value < 0.05. A publication-ready enrichment map was generated using Cytoscape. Node cut-off FDR Q value < 0.05 and edge cut-off < 0.5.

GO term	Description	p-value
GO:0002181*	cytoplasmic translation	9.01E-27
GO:0043604	amide biosynthetic process	4.23E-23
GO:0043603	cellular amide metabolic process	5.82E-21
GO:1901566	organonitrogen compound biosynthetic process	7.12E-21
GO:0006412	translation	7.00E-20
GO:0043043	peptide biosynthetic process	1.39E-19
GO:0006518	peptide metabolic process	1.43E-17
GO:1901576	organic substance biosynthetic process	5.49E-13
GO:0009058	biosynthetic process	9.50E-13
GO:1901564	organonitrogen compound metabolic process	6.55E-11
GO:0044249	cellular biosynthetic process	1.71E-10
GO:0044271	cellular nitrogen compound biosynthetic process	2.95E-09
GO:0019538	protein metabolic process	1.80E-04
GO:0044267	cellular protein metabolic process	5.69E-04

GO:0034645	cellular macromolecule biosynthetic process	1.85E-03
GO:0009059	macromolecule biosynthetic process	3.48E-03
GO:0034641	cellular nitrogen compound metabolic process	3.76E-03
GO:0044237	cellular metabolic process	4.85E-02
GO:0042274*	ribosomal small subunit biogenesis	2.05E-09
GO:0030490	maturation of SSU-rRNA	1.24E-05
GO:0042254	ribosome biogenesis	2.99E-04
GO:0006364	rRNA processing	3.59E-04
GO:0000462	maturation of SSU-rRNA from tricistronic rRNA transcript (SSU-rRNA, 5.8S rRNA, LSU-rRNA)	9.39E-04
GO:0016072	rRNA metabolic process	1.10E-03
GO:0022613	ribonucleoprotein complex biogenesis	3.04E-03
GO:0019693*	ribose phosphate metabolic process	1.96E-03
GO:0009117	nucleotide metabolic process	3.66E-03
GO:0009259	ribonucleotide metabolic process	4.09E-03
GO:0006753	nucleoside phosphate metabolic process	6.47E-03
GO:0055086	nucleobase-containing small molecule metabolic process	7.28E-03
GO:0009150	purine ribonucleotide metabolic process	1.25E-02
GO:0006163	purine nucleotide metabolic process	1.60E-02
GO:0072521	purine-containing compound metabolic process	2.37E-02
GO:0006407*	rRNA export from nucleus	1.35E-08
GO:0051029	rRNA transport	1.35E-08
GO:0097064	ncRNA export from nucleus	1.93E-05
GO:0006096*	glycolytic process	2.22E-03
GO:0006757	ATP generation from ADP	2.22E-03
GO:0046031	ADP metabolic process	3.26E-03
GO:0046939	nucleotide phosphorylation	4.56E-03
GO:0009185	ribonucleoside diphosphate metabolic process	4.56E-03
GO:0006165	nucleoside diphosphate phosphorylation	4.56E-03
GO:0009135	purine nucleoside diphosphate metabolic process	4.56E-03
GO:0009179	purine ribonucleoside diphosphate metabolic process	4.56E-03
GO:0009132	nucleoside diphosphate metabolic process	8.44E-03
GO:0044281*	small molecule metabolic process	7.02E-07
GO:0044283	small molecule biosynthetic process	3.00E-06
GO:0019752	carboxylic acid metabolic process	3.06E-06
GO:0006082	organic acid metabolic process	4.41E-06
GO:0043436	oxoacid metabolic process	1.21E-05
GO:0032787	monocarboxylic acid metabolic process	7.22E-04
GO:0016053	organic acid biosynthetic process	7.47E-03
GO:0046394	carboxylic acid biosynthetic process	3.20E-02
GO:0000028*	ribosomal small subunit assembly	2.81E-07
GO:0042255	ribosome assembly	2.36E-04
GO:0044272*	sulfur compound biosynthetic process	1.19E-02
GO:0006555	methionine metabolic process	2.42E-02
GO:0071428*	rRNA-containing ribonucleoprotein complex export from nucleus	1.21E-02
GO:1990145*	maintenance of translational fidelity	2.04E-03
GO:0042759*	long-chain fatty acid biosynthetic process	2.26E-02
GO:0090501*	RNA phosphodiester bond hydrolysis	2.53E-10
GO:0000460	maturation of 5.8S rRNA	2.94E-10
GO:0000466	maturation of 5.8S rRNA from tricistronic rRNA transcript (SSU-rRNA, 5.8S rRNA, LSU-rRNA)	9.59E-10
GO:0000469	cleavage involved in rRNA processing	4.65E-09
GO:0090305	nucleic acid phosphodiester bond hydrolysis	3.57E-08
GO:0090502	RNA phosphodiester bond hydrolysis, endonucleolytic	3.09E-04
GO:0000479	endonucleolytic cleavage of tricistronic rRNA transcript (SSU-rRNA, 5.8S rRNA, LSU-rRNA)	6.03E-04
GO:0000478	endonucleolytic cleavage involved in rRNA processing	6.03E-04
GO:0000967	rRNA 5'-end processing	3.11E-03
GO:0034471	ncRNA 5'-end processing	4.99E-03

GO:0000447	endonucleolytic cleavage in ITS1 to separate SSU-rRNA from 5.8S rRNA and LSU-rRNA from tricistronic rRNA transcript (SSU-rRNA, 5.8S rRNA, LSU-rRNA)	5.05E-03
GO:0000472	endonucleolytic cleavage to generate mature 5'-end of SSU-rRNA from (SSU-rRNA, 5.8S rRNA, LSU-rRNA)	6.68E-03
GO:0000966	RNA 5'-end processing	7.82E-03
GO:0000480	endonucleolytic cleavage in 5'-ETS of tricistronic rRNA transcript (SSU-rRNA, 5.8S rRNA, LSU-rRNA)	1.27E-02
GO:0000470*	maturation of LSU-rRNA	2.81E-05
GO:0000463	maturation of LSU-rRNA from tricistronic rRNA transcript (SSU-rRNA, 5.8S rRNA, LSU-rRNA)	6.65E-04
GO:0042273	ribosomal large subunit biogenesis	6.90E-04
GO:0034504*	protein localization to nucleus	8.56E-04
GO:0006606	protein import into nucleus	2.54E-03
GO:0051170	import into nucleus	1.08E-02
GO:0006913*	nucleocytoplasmic transport	3.15E-03
GO:0051169	nuclear transport	3.15E-03
GO:0071035*	nuclear polyadenylation-dependent rRNA catabolic process	3.77E-07
GO:0071029	nuclear ncRNA surveillance	8.81E-07
GO:0043634	polyadenylation-dependent ncRNA catabolic process	8.81E-07
GO:0071046	nuclear polyadenylation-dependent ncRNA catabolic process	8.81E-07
GO:0000291	nuclear-transcribed mRNA catabolic process, exonucleolytic	2.40E-06
GO:0016078	tRNA catabolic process	2.85E-06
GO:0071038	nuclear polyadenylation-dependent tRNA catabolic process	2.85E-06
GO:0106354	tRNA surveillance	2.85E-06
GO:0043633	polyadenylation-dependent RNA catabolic process	3.97E-06
GO:0000459	exonucleolytic trimming involved in rRNA processing	2.70E-05
GO:0090503	RNA phosphodiester bond hydrolysis, exonucleolytic	2.70E-05
GO:0000467	exonucleolytic trimming to generate mature 3'-end of 5.8S rRNA from tricistronic rRNA transcript (SSU-rRNA, 5.8S rRNA, LSU-rRNA)	3.74E-05
GO:0016074	sno(s)RNA metabolic process	4.40E-05
GO:0071051	polyadenylation-dependent snoRNA 3'-end processing	7.36E-05
GO:0031126	sno(s)RNA 3'-end processing	1.08E-04
GO:0034427	nuclear-transcribed mRNA catabolic process, exonucleolytic, 3'-5'	2.01E-04
GO:0070478	nuclear-transcribed mRNA catabolic process, 3'-5' exonucleolytic nonsense-mediated decay	2.01E-04
GO:0016075	rRNA catabolic process	2.71E-04
GO:0043144	sno(s)RNA processing	4.20E-04
GO:0071027	nuclear RNA surveillance	4.79E-04
GO:0071025	RNA surveillance	4.79E-04
GO:0071042	nuclear polyadenylation-dependent mRNA catabolic process	6.20E-04
GO:0071047	polyadenylation-dependent mRNA catabolic process	6.20E-04
GO:0031125	rRNA 3'-end processing	7.19E-04
GO:0034661	ncRNA catabolic process	9.75E-04
GO:0071028	nuclear mRNA surveillance	1.21E-03
GO:0043628	ncRNA 3'-end processing	3.18E-03
GO:0031123	RNA 3'-end processing	3.79E-03
GO:0070481	nuclear-transcribed mRNA catabolic process, non-stop decay	7.01E-03
GO:0000184	nuclear-transcribed mRNA catabolic process, nonsense-mediated decay	1.07E-02
GO:0071034	CUT catabolic process	1.10E-02
GO:0071043	CUT metabolic process	1.10E-02
GO:0016073	snRNA metabolic process	1.43E-02
GO:0034475	U4 snRNA 3'-end processing	1.94E-02
GO:0071031	nuclear mRNA surveillance of mRNA 3'-end processing	3.16E-02
GO:0051641*	cellular localization	5.59E-03
GO:0034470*	ncRNA processing	5.00E-15
GO:0034660	ncRNA metabolic process	7.50E-13
GO:0016072	rRNA metabolic process	1.47E-12
GO:0006396	RNA processing	2.86E-12
GO:0006364	rRNA processing	3.77E-12
GO:0022613	ribonucleoprotein complex biogenesis	4.88E-09
GO:0042254	ribosome biogenesis	8.06E-09

GO:0016070	RNA metabolic process	1.35E-05
GO:0044085	cellular component biogenesis	2.04E-05
GO:0009451	RNA modification	2.34E-04
GO:0031167	rRNA methylation	4.06E-04
GO:0006399	tRNA metabolic process	1.91E-03
GO:0001510	RNA methylation	3.92E-03
GO:0000154	rRNA modification	3.99E-03
GO:0010467	gene expression	1.11E-02
GO:0016071	mRNA metabolic process	1.17E-02
GO:0000956	nuclear-transcribed mRNA catabolic process	2.97E-02
GO:0043414	macromolecule methylation	2.98E-02
GO:0050779	RNA destabilization	3.04E-02
GO:0061014	positive regulation of mRNA catabolic process	3.04E-02
GO:0061157	mRNA destabilization	3.04E-02
GO:1903313	positive regulation of mRNA metabolic process	4.43E-02
GO:0006402	mRNA catabolic process	4.63E-02
GO:0032259	methylation	4.98E-02
GO:0042407*	cristae formation	1.99E-05
GO:0007007	inner mitochondrial membrane organization	4.83E-04
GO:0007006	mitochondrial membrane organization	4.32E-03
GO:0042274*	ribosomal small subunit biogenesis	3.49E-02
GO:0030490*	maturation of SSU-rRNA	1.56E-02
GO:0000462*	maturation of SSU-rRNA from tricistronic rRNA transcript (SSU-rRNA, 5.8S rRNA, LSU-rRNA)	7.46E-03
GO:0043928*	exonucleolytic catabolism of deadenylated mRNA	2.65E-03
GO:0006999*	nuclear pore organization	5.33E-04

**Table 5: GO enrichment analysis plotted in Figure 13 of the proteins listed in table 6 using gprofiler and Cytoscape (Reimand et al., 2019).** Gene set coding for proteins less abundant upon loss of Rps26a and Gene set coding for proteins more abundant upon loss of Rps26a. The asterisk (\*) highlights the representative GO terms depicted in Figure 13.

Analysis of the *rps26a*Δ proteome revealed that loss of Rps26a dropped the levels of proteins involved in the cleavage at the site A2 of the 35S pre-rRNA (that produces 20S pre-rRNA) while increased the levels of proteins involved in the processing of the 27S pre-rRNA (Table 5: GO:0042274; GO:0030490; GO:0000462, GO:0000460, GO:0000466, GO:0000463). Moreover, loss of Rps26a decreased the levels of proteins involved in nucleocytoplasmic export of rRNA (Table 5: GO:0006407, GO:0097064) but increased the levels of those involved in the nuclear pore organization (GO:0006999). Interestingly, loss of Rps26a reduced the levels of proteins involved in glycolysis, biosynthesis of methionine, cysteine, and glutathione, and proteins involved in fatty acid biosynthesis (Table 5: GO:0006096, GO:0044272, GO:0042759). In contrast, loss of Rps26a increased the levels of proteins involved in the inner mitochondrial membrane organization and cristae formation (GO:0007007, GO:0042407). Further, *rps26a*Δ cells displayed increased levels of proteins involved in the RNA catabolism (Table 5: GO:0071035, GO:0043634, GO:0071046, GO:0000291, GO:0016078, GO:0071038). Finally, loss of Rps26a dampened the number of functional ribosomes (Table 5:

GO:0042254, GO:0000028, GO:0042255) therefore diminishing the translation capacity of the cell (Table 5: GO:0002181, GO:0006412).

As for the amino acid metabolism, loss of Rps26a did not significantly increase the levels of enzymes involved in amino acid biosynthesis and transport (data not shown) (except for Tat1 levels that increased 84% upon loss of Rps26a). Therefore, most probably, the accumulation of intracellular asparagine and glutamine is not caused by increased uptake or biosynthesis of these two amino acids. As for the TORC1 complex, except for Tco89, loss of Rps26a caused only a mild increase of the TORC1 components Tor1, Kog1, and Lst8 (data not shown). Therefore, the loss of Rps26a does not seem to dramatically affect the total number of TORC1 complexes.

Protein	Description	Fold Change
ATX1	Metal homeostasis factor ATX1	27.67
IGO1	mRNA stability protein IGO1	3.51
FUS3	Mitogen-activated protein kinase FUS3	3.48
VPS24	Vacuolar protein-sorting-associated protein 24	3.32
SPC3	Signal peptidase complex subunit SPC3	3.25
MAK16	Protein MAK16	3.23
SSA4	Heat shock protein SSA4	3.20
SEC15	Exocyst complex component SEC15	3.07
SLM1	Phosphatidylinositol 4,5-bisphosphate-binding protein SLM1	3.03
ECM22	Sterol regulatory element-binding protein ECM22	2.97
RPL22B	60S ribosomal protein L22-B	2.91
CDC14	Tyrosine-protein phosphatase CDC14	2.89
RTC3	Restriction of telomere capping protein 3	2.81
TRM2	tRNA (uracil(54)-C(5))-methyltransferase	2.79
IXR1	Intrastrand cross-link recognition protein	2.77
SKI8	Antiviral protein SKI8	2.64
RRP40	Exosome complex component RRP40	2.62
RIO1	Serine/threonine-protein kinase RIO1	2.58
RHO4	GTP-binding protein RHO4	2.58
PET100	Protein PET100, mitochondrial	2.53
POM33	Pore membrane protein of 33 kDa	2.48
CDC42	Cell division control protein 42	2.46
GPA1	Guanine nucleotide-binding protein alpha-1 subunit	2.45
RRT14	Regulator of rDNA transcription protein 14	2.45
COG3	Conserved oligomeric Golgi complex subunit 3	2.43
YAR1	Ankyrin repeat-containing protein YAR1	2.41
ARP6	Actin-like protein ARP6	2.41
IMP4	U3 small nucleolar ribonucleoprotein protein IMP4	2.41
SIF2	SIR4-interacting protein SIF2	2.41
SRP102	Signal recognition particle receptor subunit beta	2.38
RRP46	Exosome complex component RRP46	2.38
KIN28	Serine/threonine-protein kinase KIN28	2.38
FHL1	Pre-rRNA-processing protein FHL1	2.36
LSM7	U6 snRNA-associated Sm-like protein LSm7	2.36
HPM1	Histidine protein methyltransferase 1	2.35
SUA5	Threonylcarbamoyl-AMP synthase	2.33
SDH8	Succinate dehydrogenase assembly factor 4, mitochondrial	2.33
RRP43	Exosome complex component RRP43	2.31
ORM2	Protein ORM2	2.31
CKA1	Casein kinase II subunit alpha	2.31
CRZ1	Transcriptional regulator CRZ1	2.30
NOP9	Nucleolar protein 9	2.28



SPC72	Spindle pole component SPC72	2.28
ASG1	Activator of stress genes 1	2.28
SEC3	Exocyst complex component SEC3	2.27
EFM5	Protein-lysine N-methyltransferase EFM5	2.27
PEX19	Peroxisomal membrane protein import receptor PEX19	2.27
NUP157	Nucleoporin NUP157	2.25
DIG1	Down-regulator of invasive growth 1	2.25
TAF4	Transcription initiation factor TFIID subunit 4	2.25
NPC2	Phosphatidylglycerol/phosphatidylinositol transfer protein	2.25
SNF7	Vacuolar-sorting protein SNF7	2.25
SMD2	Small nuclear ribonucleoprotein Sm D2	2.23
CDC37	Hsp90 co-chaperone Cdc37	2.23
RDS3	Pre-mRNA-splicing factor RDS3	2.22
NOB1	20S-pre-rRNA D-site endonuclease NOB1	2.22
AST2	Protein AST2	2.22
NCS2	Cytoplasmic tRNA 2-thiolation protein 2	2.20
RRP45	Exosome complex component RRP45	2.20
RPC25	DNA-directed RNA polymerase III subunit RPC8	2.20
SNF5	SWI/SNF chromatin-remodeling complex subunit SNF5	2.20
PIN3	[PSI+] inducibility protein 3	2.19
UTP5	U3 small nucleolar RNA-associated protein 5	2.19
STE20	Serine/threonine-protein kinase STE20	2.19
PUS1	tRNA pseudouridine synthase 1	2.19
RHO1	GTP-binding protein RHO1	2.17
BUD21	Bud site selection protein 21	2.17
NOC2	Nucleolar complex protein 2	2.16
RBA50	RNA polymerase II-associated protein RBA50	2.16
KTI12	Protein KTI12	2.16
TRI1	Protein TRI1	2.16
NFU1	NifU-like protein, mitochondrial	2.14
PRP11	Pre-mRNA-splicing factor PRP11	2.14
RPC53	DNA-directed RNA polymerase III subunit RPC4	2.13
CIA1	Cytosolic iron-sulfur protein assembly protein 1	2.11
JIP5	WD repeat-containing protein JIP5	2.11
SYC1	Protein SYC1	2.11
RRP7	Ribosomal RNA-processing protein 7	2.11
SEG1	Eisosome protein SEG1	2.11
RPC10	DNA-directed RNA polymerases I, II, and III subunit RPABC4	2.11
UTP23	rRNA-processing protein UTP23	2.10
RRP4	Exosome complex component RRP4	2.08
NUP116	Nucleoporin NUP116/NSP116	2.07
SWD2	COMPASS component SWD2	2.07
NOP8	60S ribosome subunit biogenesis protein NOP8	2.07
VTI1	t-SNARE VTI1	2.07
ELF1	Transcription elongation factor 1	2.07
MDM20	N-terminal acetyltransferase B complex subunit MDM20	2.06
VRP1	Verprolin	2.06
NUP53	Nucleoporin NUP53	2.04
RPL37A	60S ribosomal protein L37-A	2.04
HAS1	ATP-dependent RNA helicase HAS1	2.04
HSK3	DASH complex subunit HSK3	2.03
UME1	Transcriptional regulatory protein UME1	2.03
YFR011C	MICOS complex subunit MIC19	2.03
TPM1	Tropomyosin-1	2.03
BRE1	E3 ubiquitin-protein ligase BRE1	2.01
ROD1	Protein ROD1	2.01
VTA1	Vacuolar protein sorting-associated protein VTA1	2.01
DBP6	ATP-dependent RNA helicase DBP6	2.01
GLO3	ADP-ribosylation factor GTPase-activating protein GLO3	2.00
CSR1	Phosphatidylinositol transfer protein CSR1	2.00
NUT1	Mediator of RNA polymerase II transcription subunit 5	2.00
PWP1	Periodic tryptophan protein 1	2.00
VAC8	Vacuolar protein 8	1.99

GET1	Golgi to ER traffic protein 1	1.99
AIR1	Protein AIR1	1.99
TRM44	tRNA (uracil-O(2)-)-methyltransferase	1.99
SLX9	Ribosome biogenesis protein SLX9	1.99
APL2	AP-1 complex subunit beta-1	1.97
BMH2	Protein BMH2	1.97
ERV46	ER-derived vesicles protein ERV46	1.97
YET1	Endoplasmic reticulum transmembrane protein 1	1.97
REB1	DNA-binding protein REB1	1.97
SNC1	Synaptobrevin homolog 1	1.97
CKB1	Casein kinase II subunit beta	1.97
TAF11	Transcription initiation factor TFIID subunit 11	1.97
RPF1	Ribosome production factor 1	1.96
SEC12	Guanine nucleotide-exchange factor SEC12	1.96
ESF2	Pre-rRNA-processing protein ESF2	1.96
PWP2	Periodic tryptophan protein 2	1.96
AIR2	Protein AIR2	1.96
PDC2	Protein PDC2	1.96
NAB6	RNA-binding protein NAB6	1.96
UTP11	U3 small nucleolar RNA-associated protein 11	1.96
MLC1	Myosin light chain 1	1.95
YPT32	GTP-binding protein YPT32/YPT11	1.95
COG5	Conserved oligomeric Golgi complex subunit 5	1.95
RSC8	Chromatin structure-remodeling complex protein RSC8	1.95
AI1	Putative COX1/OXI3 intron 1 protein	1.95
RHB1	Rheb-like protein RHB1	1.95
DIF1	Damage-regulated import facilitator 1	1.93
CSL4	Exosome complex component CSL4	1.93
SPC97	Spindle pole body component SPC97	1.93
SWI6	Regulatory protein SWI6	1.93
RBG2	Ribosome-interacting GTPase 2	1.92
GIM4	Prefoldin subunit 2	1.92
SMX2	Small nuclear ribonucleoprotein G	1.91
NGR1	Negative growth regulatory protein NGR1	1.91
APM3	AP-3 complex subunit mu	1.91
CET1	mRNA-capping enzyme subunit beta	1.91
YOP1	Protein YOP1	1.91
KRR1	KRR1 small subunit processome component	1.91
RPB7	DNA-directed RNA polymerase II subunit RPB7	1.91
RQC2	Ribosome quality control complex subunit 2	1.89
UBA4	Adenylyltransferase and sulfurtransferase UBA4 Adenylyltransferase UBA4 Sulfurtransferase UBA4	1.89
ADD66	Proteasome assembly chaperone 2	1.89
APL5	AP-3 complex subunit delta	1.89
GRX5	Monothiol glutaredoxin-5, mitochondrial	1.89
TOP1	DNA topoisomerase 1	1.89
KAP104	Importin subunit beta-2	1.88
TRM8	tRNA (guanine-N(7)-)-methyltransferase	1.88
TCD2	tRNA threonylcarbamoyladenosine dehydratase 2	1.88
MTR10	mRNA transport regulator MTR10	1.87
SDO1	Ribosome maturation protein SDO1	1.87
KEL1	Kelch repeat-containing protein 1	1.87
TCD1	tRNA threonylcarbamoyladenosine dehydratase 1	1.87
SEC1	Protein transport protein SEC1	1.87
TRM10	tRNA (guanine(9)-N1)-methyltransferase	1.87
RIX1	Pre-rRNA-processing protein RIX1	1.87
CIC1	Proteasome-interacting protein CIC1	1.85
CBP6	Cytochrome B pre-mRNA-processing protein 6	1.85
YSH1	Endoribonuclease YSH1	1.85
ATG7	Ubiquitin-like modifier-activating enzyme ATG7	1.85
YME2	Mitochondrial escape protein 2	1.85
NUP133	Nucleoporin NUP133	1.84
SPB4	ATP-dependent rRNA helicase SPB4	1.84

CAP2	F-actin-capping protein subunit beta	1.84
ASM4	Nucleoporin ASM4	1.84
NOP15	Ribosome biogenesis protein 15	1.84
REI1	Cytoplasmic 60S subunit biogenesis factor REI1	1.84
HEH2	Inner nuclear membrane protein HEH2	1.84
POP2	Poly(A) ribonuclease POP2	1.84
RRP8	25S rRNA (adenine(645)-N(1))-methyltransferase	1.84
SRP14	Signal recognition particle subunit SRP14	1.84
EXO84	Exocyst complex component EXO84	1.84
VPS27	Vacuolar protein sorting-associated protein 27	1.83
SLS1	Sigma-like sequence protein 1, mitochondrial	1.83
PTC1	Protein phosphatase 2C homolog 1	1.83
DIS3	Exosome complex exonuclease DIS3	1.83
IKI1	Elongator complex protein 5	1.83
VPS5	Vacuolar protein sorting-associated protein 5	1.82
CDC36	General negative regulator of transcription subunit 2	1.82
RPP1	Ribonuclease P/MRP protein subunit RPP1	1.82
MRN1	RNA-binding protein MRN1	1.82
SRP21	Signal recognition particle subunit SRP21	1.82
YKR023W	Uncharacterized protein YKR023W	1.82
RRP6	Exosome complex exonuclease RRP6	1.82
DPH6	Diphthine--ammonia ligase	1.82
VPS75	Vacuolar protein sorting-associated protein 75	1.80
MUK1	Protein MUK1	1.80
UTP13	U3 small nucleolar RNA-associated protein 13	1.80
POM34	Nucleoporin POM34	1.80
SAK1	SNF1-activating kinase 1	1.80
TRM112	Multifunctional methyltransferase subunit TRM112	1.80
SIN3	Transcriptional regulatory protein SIN3	1.80
JJJ1	J protein JJJ1	1.80
UPF3	Nonsense-mediated mRNA decay protein 3	1.80
GSP1	GTP-binding nuclear protein GSP1/CNR1	1.80
ARP5	Actin-related protein 5	1.80
ADH6	NADP-dependent alcohol dehydrogenase 6	-1.82
RPS21A	40S ribosomal protein S21-A	-1.82
RPS20	40S ribosomal protein S20	-1.82
LYS20	Homocitrate synthase, cytosolic isozyme	-1.82
RPL3	60S ribosomal protein L3	-1.83
FAS1	Fatty acid synthase subunit beta 3-hydroxyacyl-[acyl-carrier-protein] dehydratase Enoyl-[acyl-carrier-protein] reductase [NADH] [Acyl-carrier-protein] acetyltransferase [Acyl-carrier-protein] malonyltransferase S-acyl fatty acid synthase thioesterase	-1.83
MAK31	N-alpha-acetyltransferase 38, NatC auxiliary subunit	-1.84
ATP16	ATP synthase subunit delta, mitochondrial	-1.84
RPS5	40S ribosomal protein S5	-1.85
PDX3	Pyridoxamine 5-phosphate oxidase	-1.85
CDC19	Pyruvate kinase 1	-1.85
NOP1	rRNA 2-O-methyltransferase fibrillar	-1.85
RPL27B/A	60S ribosomal protein L27-B 60S ribosomal protein L27-A	-1.87
THI20	Hydroxymethylpyrimidine/phosphomethylpyrimidine kinase THI20	-1.88
HXK1	Hexokinase-1	-1.91
ERG11	Lanosterol 14-alpha demethylase	-1.91
CPA2	Carbamoyl-phosphate synthase arginine-specific large chain	-1.92
ILV5	Ketol-acid reductoisomerase, mitochondrial	-1.92
FAT1	Very long-chain fatty acid transport protein	-1.92
IDP1	Isocitrate dehydrogenase [NADP], mitochondrial	-1.92
IPP1	Inorganic pyrophosphatase	-1.93
PDI1	Protein disulfide-isomerase	-1.93
MED1	Mediator of RNA polymerase II transcription subunit 1	-1.95
RIB5	Riboflavin synthase	-1.95
TDA10	Probable ATP-dependent kinase TDA10	-1.96
EXG2	Glucan 1,3-beta-glucosidase 2	-1.97
TFC7	Transcription factor tau 55 kDa subunit	-1.99



ENO1	Enolase 1	-2.00
MKC7	Aspartic proteinase MKC7	-2.00
UBC6	Ubiquitin-conjugating enzyme E2 6	-2.00
NOP6	Nucleolar protein 6	-2.01
RPS18B/A	40S ribosomal protein S18-B 40S ribosomal protein S18-A	-2.01
RPS15	40S ribosomal protein S15	-2.04
MAG1	DNA-3-methyladenine glycosylase	-2.06
MRPL28	54S ribosomal protein L28, mitochondrial	-2.06
MRP49	54S ribosomal protein MRP49, mitochondrial	-2.08
RPL1B/A	60S ribosomal protein L1-B 60S ribosomal protein L1-A	-2.08
HTA1	Histone H2A.2 Histone H2A.1	-2.14
HTA2	Histone H2A.2 Histone H2A.1	-2.14
FUM1	Fumarate hydratase, mitochondrial	-2.14
ADO1	Adenosine kinase	-2.14
MRP13	37S ribosomal protein MRP13, mitochondrial	-2.16
RPS7B	40S ribosomal protein S7-B	-2.16
MRPL50	54S ribosomal protein L50, mitochondrial	-2.16
CDC55	Protein phosphatase PP2A regulatory subunit B	-2.19
RPL38	60S ribosomal protein L38	-2.19
FRK1	Fatty acyl-CoA synthetase and RNA processing-associated kinase 1	-2.20
MCR1	NADH-cytochrome b5 reductase 2 NADH-cytochrome b5 reductase p34 form NADH-cytochrome b5 reductase p32 form	-2.20
RPS9B	40S ribosomal protein S9-B	-2.22
YGP1	Protein YGP1	-2.22
SAM1	S-adenosylmethionine synthase 1	-2.23
SPE4	Spermine synthase	-2.27
HTZ1	Histone H2A.Z	-2.30
RPL23B/A	60S ribosomal protein L23-B 60S ribosomal protein L23-A	-2.30
HOM2	Aspartate-semialdehyde dehydrogenase	-2.36
URA3	Orotidine 5-phosphate decarboxylase	-2.36
YSA1	ADP-ribose pyrophosphatase	-2.39
RPS10A/B	40S ribosomal protein S10-A 40S ribosomal protein S10-B	-2.39
HPT1	Hypoxanthine-guanine phosphoribosyltransferase	-2.43
RPS14B	40S ribosomal protein S14-B	-2.43
RPS30B/A	40S ribosomal protein S30-B 40S ribosomal protein S30-A	-2.51
RPS1A	40S ribosomal protein S1-A	-2.51
AAC1	ADP,ATP carrier protein 1	-2.57
MET17	Protein MET17 O-acetylhomoserine sulfhydrylase O-acetylserine sulfhydrylase	-2.66
ARG3	Ornithine carbamoyltransferase	-2.68
RPS28A/B	40S ribosomal protein S28-A 40S ribosomal protein S28-B	-2.68
CYC1	Cytochrome c iso-1	-2.68
EGD1	Nascent polypeptide-associated complex subunit beta-1	-2.79
YKR070W	Uncharacterized protein YKR070W	-2.83
HNT1	Hit family protein 1	-2.87
CDC33	Eukaryotic translation initiation factor 4E	-2.97
FBA1	Fructose-bisphosphate aldolase	-3.01
ALT2	Probable alanine aminotransferase	-3.03
ARG1	Argininosuccinate synthase	-3.14
RPS11B/A	40S ribosomal protein S11-B 40S ribosomal protein S11-A	-3.16
BNA1	3-hydroxyanthranilate 3,4-dioxygenase	-3.20
YHB1	Flavoheмоprotein	-3.25
SPE3	Spermidine synthase	-3.25
RPS24B/A	40S ribosomal protein S24-B 40S ribosomal protein S24-A	-3.27
RPS29B	40S ribosomal protein S29-B	-3.46
RPS8B/A	40S ribosomal protein S8-B 40S ribosomal protein S8-A	-3.51
NAM2	Leucine--tRNA ligase, mitochondrial	-3.56
ATP5	ATP synthase subunit 5, mitochondrial	-3.61
YDJ1	Mitochondrial protein import protein MAS5	-3.61
RPS6B/A	40S ribosomal protein S6-B 40S ribosomal protein S6-A	-3.68
YMR31	37S ribosomal protein YMR-31, mitochondrial	-3.76
RPL35B/A	60S ribosomal protein L35-B 60S ribosomal protein L35-A	-3.78
RPL32	60S ribosomal protein L32	-3.97

RPS29A	40S ribosomal protein S29-A	-4.03
PBI2	Protease B inhibitor 2	-4.38
MRPL49	54S ribosomal protein L49, mitochondrial	-4.66
YRB1	Ran-specific GTPase-activating protein 1	-6.50
RPS25A/B	40S ribosomal protein S25-A 40S ribosomal protein S25-B	-6.63
RPL39	60S ribosomal protein L39	-7.16
RPL17A	60S ribosomal protein L17-A	-24.93

**Table 6:** List of proteins that were significantly enriched (at least 1.8 times, p-value < 0.05) and diminished (at least 1.8 times, p-value < 0.05) in the *rps26a*Δ proteome.

### 3.4: DISCUSSION AND CONCLUSIONS

This project started with the metanalysis of the dataset published by Mülleder and colleagues in 2016 (Mülleder et al., 2016). The analysis of this dataset revealed that some ribosomal protein gene mutants (*i.e.*, *rps10A*Δ, *rpl20B*Δ, and *rps12*Δ) as well as Rps26a depletion - indirectly caused by *YGL188C-A* deletion - exhibited a similar amino acid profile signature to some TORC1 pathway mutants, thus suggesting a functional link between ribosomal proteins and TORC1. In particular, this amino acid profile signature was characterized by high intracellular levels of asparagine, and glutamine, two potent TORC1 activators (Péli-Gulli et al., 2015). Since, on one side, hypomorphic missense mammalian Rps26 variants are linked to the development of DBA and cancer, and, on the other side, yeast Rps26a has been shown to mediate the specific translation of certain mRNAs, we decided to undertake the characterization of the *RPS26A* null mutant to uncover a potential ribosomal-dependent TORC1 pathway regulation.

The combined inhibition of protein synthesis and stimulation of cataplerotic reactions when TORC1 activity is low can explain the intracellular accumulation of asparagine and glutamine observed in TORC1 pathway mutants. Indeed, in cells growing exponentially in a rich medium, we observed that loss of Gtr1 or Pib2 strongly decreased the TORC1 activity levels (Figures 4B and 4C). However, in the same conditions, the loss of Rps26a did not significantly alter the TORC1 activity levels in exponentially growing cells (Figures 4B-C and 5A-B). Therefore, the loss of Rps26a in exponentially growing cells triggers the intracellular accumulation of asparagine and glutamine in a TORC1-independent manner. Importantly, loss of Rps26a impaired the proper 35S-pre-rRNA processing (Table 5: GO:0042274; GO:0030490; GO:0000462, GO:0000460, GO:0000466, GO:0000463), which, as a consequence, diminished the formation of mature 80S ribosomes (Table 5: GO:0042254, GO:0000028, GO:0042255). Accumulation of intracellular asparagine and glutamine upon Rps26a depletion may therefore result from the activation of defensive and pro-survival

mechanisms such as proteasome system and autophagy to cope for the accumulation of both misassembled ribosomal proteins and immature pre-ribosomal particles.

Also, it has been reported that ribosomal mutant cells tend to upregulate the degradative pathways in response to an increased generation of Reactive Oxygen Species (ROS) (Azad et al., 2009). In line with this, *rps26a*Δ cells displayed high levels of proteins involved in the mitochondrial cristae formation (MICOS complex) (Table 5: GO:0042407), which, when overexpressed, have been described to alter the mitochondrial morphology and to promote ROS formation (Koob et al., 2015). Furthermore, loss of Rps26a reduced the levels of proteins involved in glutathione biosynthesis, which may lead to a dampening in the concentration of intracellular glutathione hence to compromised protection against ROS (Gostimskaya & Grant, 2016). We therefore hypothesize that *rps26a*Δ cells would accumulate intracellular asparagine and glutamine due to (a) a reduced consumption of amino acids as a direct consequence of general protein translation inhibition (Table 5: GO:0002181, GO:0006412), (b) a continuous degradation, by the proteasome system and autophagy, of misassembled ribosomal proteins, immature pre-ribosomal particles, and oxidized organelles (Figure 14). Even though all these results suggest that *rps26a*Δ cells may be under oxidative stress, it would be essential to confirm this in the lab. Furthermore, proteasome and autophagy activities should be measured in *rps26a*Δ cells and compared to those of wild-type cells.

Finally, there was no perfect match between the observed changes in our *rps26a*Δ cells proteome and the mRNA affinities reported for Rps26a-containing and depleted ribosomes (Ferretti et al., 2017) (data not shown). These lead us to conclude that the specific translation of specific mRNAs by Rps26a-containing ribosomes (Ferretti et al., 2017) cannot fully explain the changes in the proteome of the *rps26a*Δ cells. Possibly, the proteome of the *rps26a*Δ cells may be determined simultaneously by; 1) the specific loss of the Rps26a-containing ribosomes (Ferretti et al., 2017); 2) the translation of "strong" mRNAs caused by the non-specific reduction in the number of PICs (Pre-Initiation Complexes) (Gaikwad et al., 2021); and 3) a compensatory mechanism that tries to re-gain the cellular homeostasis lost because of 1 and 2.

Our current hypothesis could fit for most slow-growth ribosomal mutants. However, according to the measurements carried out by Mülleder and colleagues, *rpl23b*Δ and *rps17a*Δ slow-growth mutants did not accumulate intracellular asparagine or glutamine. Nonetheless, there are two significant differences between our conditions and those

employed by Mülleder and colleagues: First, Mülleder and colleagues employed mutants from the viable yeast knockout haploid collection - which sometimes are not properly characterized and harbor secondary mutations - while we use *de novo* ribosomal mutants. Second, they grew cells exponentially in minimal media (lacking amino acids), while we grew cells in rich media hence containing amino acids. Therefore, it is possible that since we cultured cells in a rich medium, slow-growth *rpl23b* $\Delta$  and *rps17a* $\Delta$  mutants may still accumulate intracellular asparagine and glutamine. To prove that, we recently started collaborating with Dr. S. Laxman and his group in Bangalore to measure the intracellular concentration of amino acids in our strains under our growth conditions.

All the slow-growth ribosomal mutants we tested protected TORC1 from inactivation upon nitrogen starvation. We suspect that this protection may be explained by an intracellular accumulation of amino acids, particularly asparagine and glutamine. We have shown that loss of Rps26a protects TORC1 upon nitrogen starvation in an Arf1-dependent manner, and in parallel to the EGO and Pib2. Notably, the Arf1-GTPase plays a crucial role in autophagy induction (van der Vaart et al., 2010; Yang & Rosenwald, 2016). At this point, the exact mechanism by which loss of Rps26a affects TORC1 via Arf1 remains unclear. Nevertheless, we can hypothesize the following: (i) in exponentially growing and replete cells, loss of Rps26a may alter the status of Arf1-GTPase activity (by affecting the protein levels of certain Arf1-GTPase regulators) (Table 4). Despite high levels of TORC1 activity, Arf1 may then promote autophagy, thus the accumulation of intracellular amino acids. (ii) The latter (in particular asparagine and glutamine), in an Arf1-dependent manner, may then stimulate TORC1 activity even upon nitrogen depletion from the medium (Figure 14). According to this model, the observed reduced TORC1 activity in the *arf1* $\Delta$  *rps26a* $\Delta$  mutant cells would result from the prevention of autophagy and subsequent intracellular amino acid accumulation and the failure to positively signal to the TORC1 kinase in an amino acid-dependent manner. The Arf1-GTPase is involved in autophagy induction but also in the AP-3 pathway, and in mitochondrial morphology (Ackema et al., 2014; Schoppe et al., 2020; van der Vaart et al., 2010). Therefore, loss of Arf1 may impact directly or indirectly the TORC1 pathway by different means. At this stage, a better characterization of the *arf1* null mutant is needed.

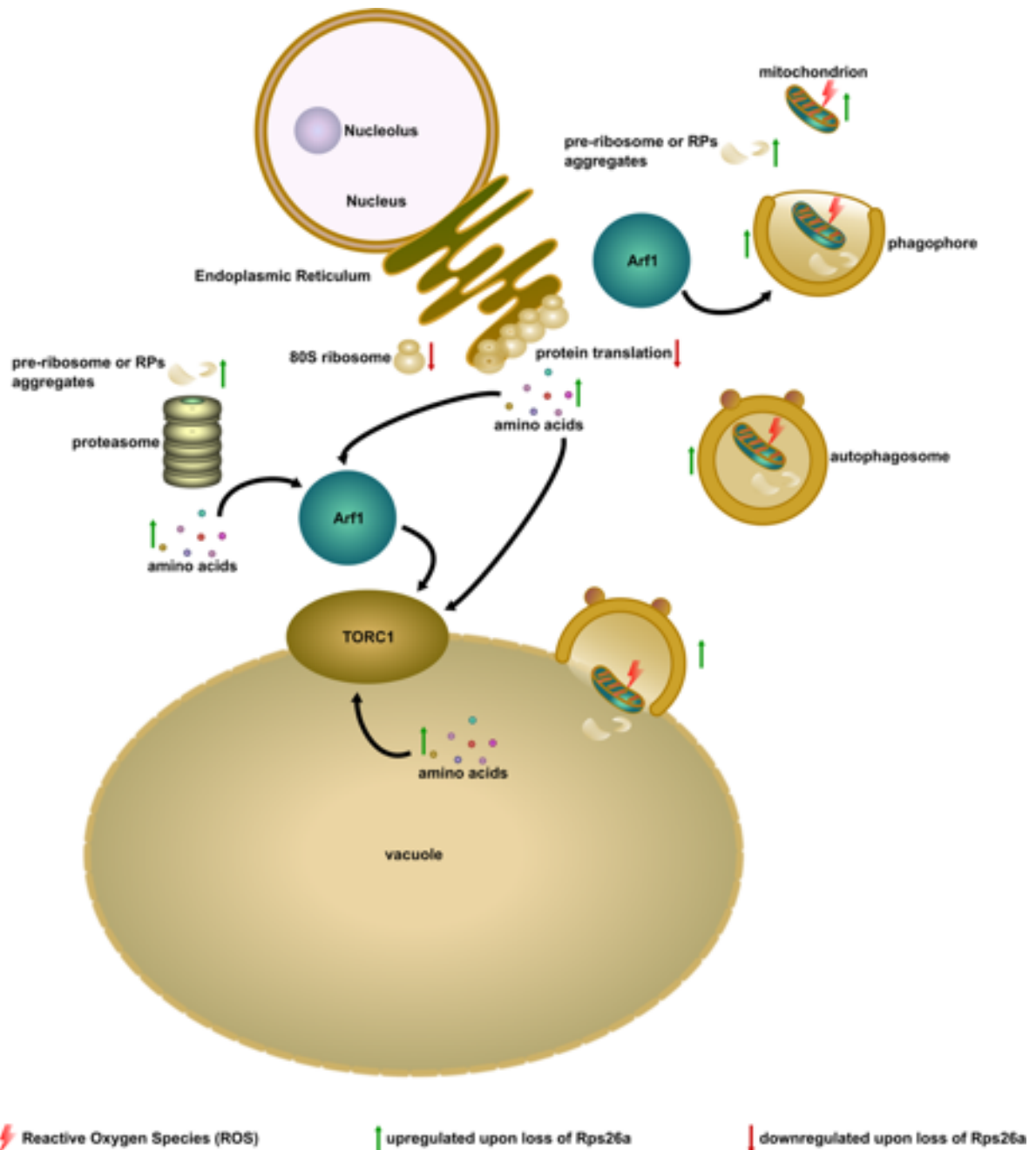


**Figure 14: Loss of Rps26a may protect TORC1 from inactivation upon nitrogen starvation through the intracellular accumulation of amino acids.** Two main processes would promote the intracellular accumulation of amino acids: 1) the general translation inhibition, 2) the upregulation of degradative pathways (ubiquitin-Proteasome system and autophagy). In this model, Arf1 is proposed to have a dual role: on one side, Arf1 is crucial for the phagophore formation; on the other side, Arf1 seems to activate TORC1 in response to intracellular amino acids accumulation. Some of the icons used here were taken and adapted from reactome (Sidiropoulos et al., 2017).

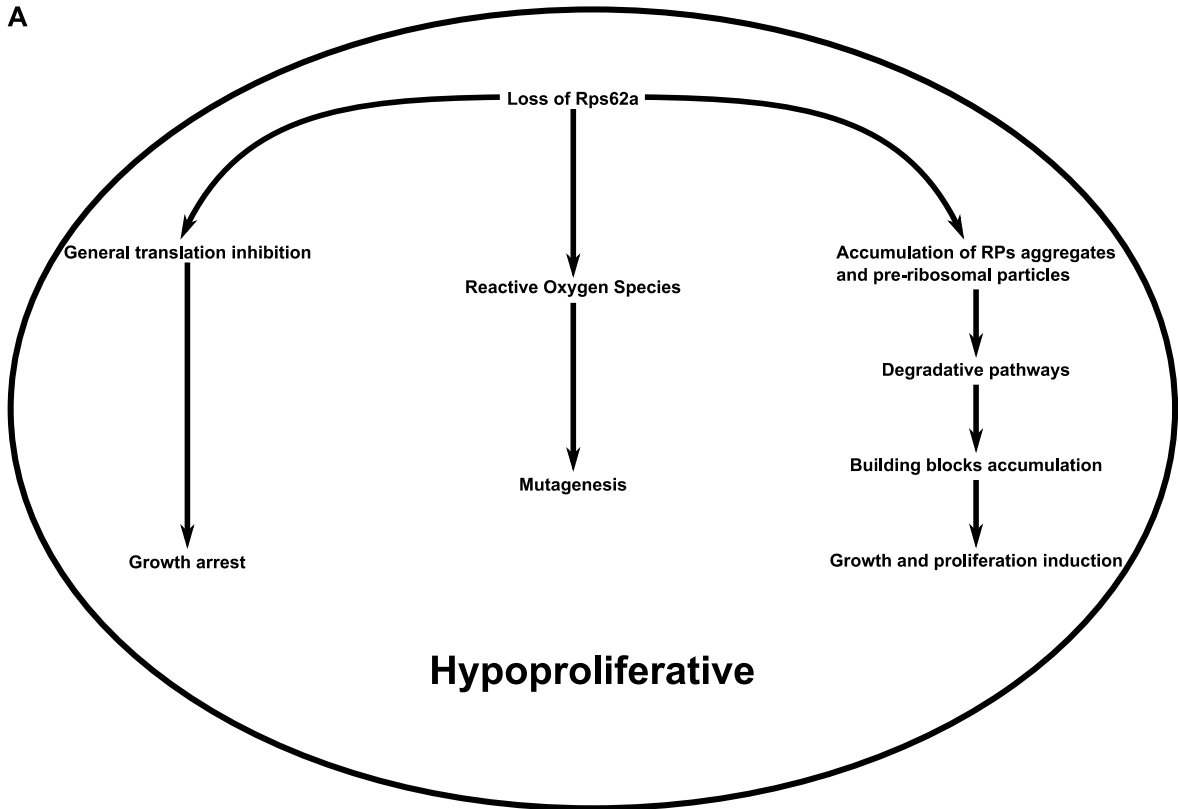
It is quite puzzling how ribosomopathies and cancer development are exactly linked, or in other words, how hypoproliferative cells can become hyperproliferative. Some authors have speculated that the appearance and selection of specific secondary mutations might, on one side, alleviate the stress response and, on the other side, restore the average number of ribosomes per cell. In this scenario, and if a secondary

mutation do not restore the expression or functionality of the originally mutant protein, cells would recover their translational capacity but not their ability to homeostatically control ribosome biogenesis and protein translation, thereby altering the translome (Armistead & Triggs-Raine, 2014; Ruggero, 2013; Sulima et al., 2017; Sulima et al., 2019). Interestingly, there are also examples of cancer cells that either underexpress or overexpress ribosomal protein genes (Ajore et al., 2017; Vlachos, 2017), demonstrating, once more, the close relationship between ribosomopathies and cancer development.

Figure 15A tries to summarize the balance of forces that would inhibit and promote cell growth following the loss of the ribosomal protein Rps26a. For reasons not fully understood, ribosomal mutants that lead to the development of ribosomopathies have been proposed to produce more Reactive Oxygen Species (Azad et al., 2009). Let us consider, on one side, the high selective pressure that applies to such slow-growth cells and, on the other side, their increased ability to accumulate mutations as a consequence of higher ROS generation. It is, therefore, not surprising that mutations restoring the normal protein translational capacity or mutations disrupting the stress signal derived from translational inhibition get selected through the evolution. (Figure 15B). The additional mutation may not restore the expression or functionality of the originally mutant protein. The production of ribosomal protein aggregates and pre-ribosomal particles will then still occur, thereby triggering the hyperactivation of cellular degradation pathways, the accumulation of cellular building blocks as well as the activation of cellular growth and proliferation programs. (Figure 15B).

To limit the possibility that a ribosomopathy progresses to cancer, it would be worth studying the exact mechanisms by which a ribosomal mutant can increase ROS formation and induce degradation pathways (e.g., autophagy and the proteasome system). For ribosomopathy patients not to develop cancer, we may try to reduce oxidative stress and increase autophagy. On the other hand, once the patient has developed cancer, efforts could be directed towards inhibiting autophagy, which in this context would act in a cytoprotective manner towards the cancer cell.

A



B

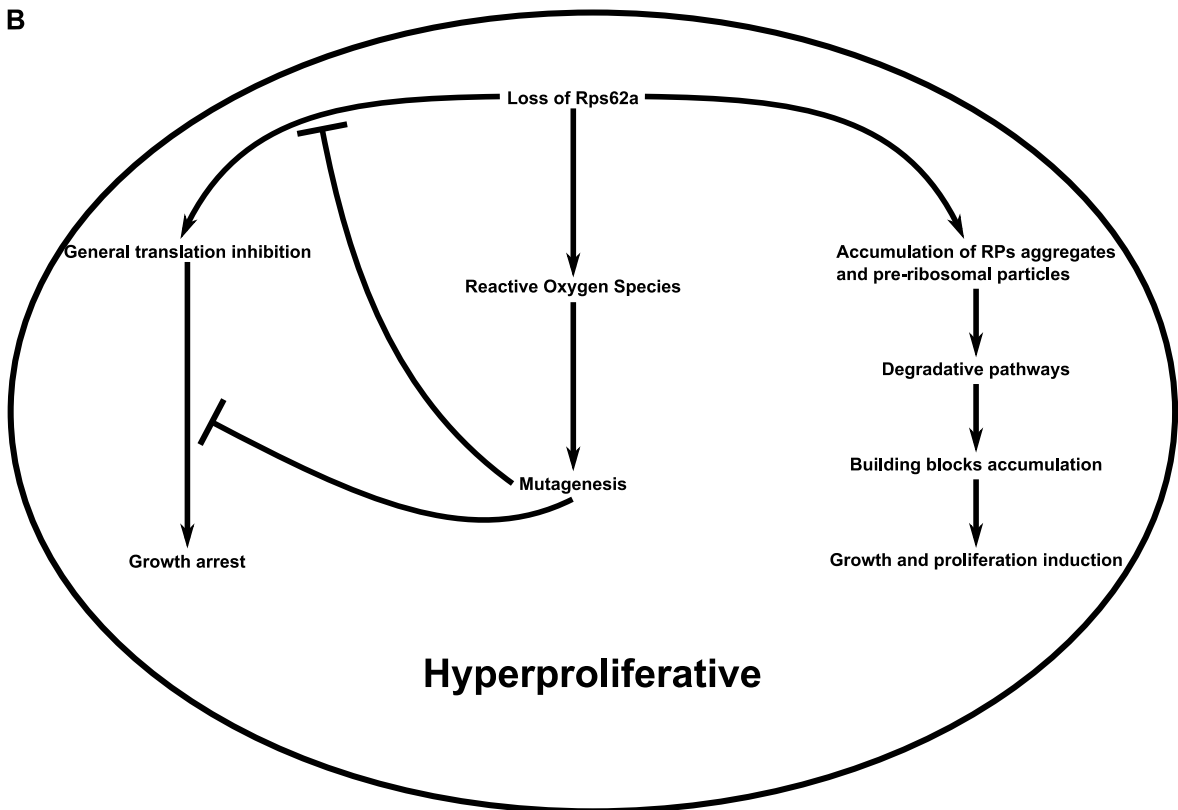


**Figure 15: Balance of forces that may inhibit and promote cell growth following the loss of the ribosomal protein Rps26a.** Hypoproliferative cells may become hyperproliferative by accumulating mutations restoring the normal protein translational capacity or disrupting the stress signal derived from translational inhibition.



### 3.5: BIBLIOGRAPHY

- Ackema, K. B., Hench, J., Böckler, S., Wang, S. C., Sauder, U., Mergentaler, H., Westermann, B., Bard, F., Frank, S., & Spang, A. (2014). The small GTP ase Arf1 modulates mitochondrial morphology and function. *The EMBO Journal*, 33(22), 2659–2675. <https://doi.org/10.15252/emboj.201489039>
- Aghaei, M., Karami-Tehrani, F., Salami, S., & Atri, M. (2005). Adenosine deaminase activity in the serum and malignant tumors of breast cancer: The assessment of isoenzyme ADA1 and ADA2 activities. *Clinical Biochemistry*, 38(10), 887–891. <https://doi.org/10.1016/j.clinbiochem.2005.05.015>
- Ajore, R., Raiser, D., McConkey, M., Jöud, M., Boidol, B., Mar, B., Saksena, G., Weinstock, D. M., Armstrong, S., Ellis, S. R., Ebert, B. L., & Nilsson, B. (2017). Deletion of ribosomal protein genes is a common vulnerability in human cancer, especially in concert with *TP 53* mutations. *EMBO Molecular Medicine*, 9(4), 498–507. <https://doi.org/10.15252/emmm.201606660>
- Albert, B., Knight, B., Merwin, J., Martin, V., Ottoz, D., Gloor, Y., Bruzzone, M. J., Rudner, A., & Shore, D. (2016). A Molecular Titration System Coordinates Ribosomal Protein Gene Transcription with Ribosomal RNA Synthesis. *Molecular Cell*, 64(4), 720–733. <https://doi.org/10.1016/j.molcel.2016.10.003>
- Alter, B. P., Giri, N., Savage, S. A., & Rosenberg, P. S. (2018). Cancer in the National Cancer Institute inherited bone marrow failure syndrome cohort after fifteen years of follow-up. *Haematologica*, 103(1), 30–39. <https://doi.org/10.3324/haematol.2017.178111>
- An, H., & Harper, J. W. (2020). Ribosome Abundance Control Via the Ubiquitin–Proteasome System and Autophagy. *Journal of Molecular Biology*, 432(1), 170–184. <https://doi.org/10.1016/j.jmb.2019.06.001>
- Anderson, J. S. J. (1998). The 3' to 5' degradation of yeast mRNAs is a general mechanism for mRNA turnover that requires the SKI2 DEVH box protein and 3' to 5' exonucleases of the exosome complex. *The EMBO Journal*, 17(5), 1497–1506. <https://doi.org/10.1093/emboj/17.5.1497>
- Armistead, J., & Triggs-Raine, B. (2014). Diverse diseases from a ubiquitous process: The ribosomopathy paradox. *FEBS Letters*, 588(9), 1491–1500. <https://doi.org/10.1016/j.febslet.2014.03.024>
- Axt, K., French, S. L., Beyer, A. L., & Tollervey, D. (2014). Kinetic Analysis Demonstrates a Requirement for the Rat1 Exonuclease in Cotranscriptional Pre-rRNA Cleavage. *PLoS ONE*, 9(2), e85703. <https://doi.org/10.1371/journal.pone.0085703>
- Azad, M. B., Chen, Y., & Gibson, S. B. (2009). Regulation of Autophagy by Reactive Oxygen Species (ROS): Implications for Cancer Progression and Treatment. *Antioxidants & Redox Signaling*, 11(4), 777–790. <https://doi.org/10.1089/ars.2008.2270>
- Badis, G., Chan, E. T., van Bakel, H., Pena-Castillo, L., Tillo, D., Tsui, K., Carlson, C. D., Gossett, A. J., Hasinoff, M. J., Warren, C. L., Gebbia, M., Talukder, S., Yang, A., Mnaimneh, S., Terterov, D., Coburn, D., Li Yeo, A., Yeo, Z. X., Clarke, N. D., ... Hughes, T. R. (2008). A Library of Yeast Transcription Factor Motifs Reveals a Widespread Function for Rsc3 in Targeting Nucleosome Exclusion at Promoters. *Molecular Cell*, 32(6), 878–887. <https://doi.org/10.1016/j.molcel.2008.11.020>
- Ball, S. E., McGuckin, C. P., Jenkins, G., & Gordon-Smith, E. C. (1996). Diamond-Blackfan anaemia in the U.K.: Analysis of 80 cases from a 20-year birth cohort. *British Journal of Haematology*, 94(4), 645–653. <https://doi.org/10.1046/j.1365-2141.1996.d01-1839.x>
- Beau, I., Esclatine, A., & Codogno, P. (2008). Lost to translation: When autophagy targets mature ribosomes. *Trends in Cell Biology*, 18(7), 311–314. <https://doi.org/10.1016/j.tcb.2008.05.001>
- Belyy, A., Levanova, N., Tabakova, I., Rospert, S., & Belyi, Y. (2016). Ribosomal Protein Rps26 Influences 80S Ribosome Assembly in *Saccharomyces cerevisiae*. *MSphere*, 1(1). <https://doi.org/10.1128/mSphere.00109-15>
- Ben-Shem, A., Garreau de Loubresse, N., Melnikov, S., Jenner, L., Yusupova, G., & Yusupov, M. (2011). The Structure of the Eukaryotic Ribosome at 3.0 Å Resolution. *Science*, 334(6062), 1524–1529. <https://doi.org/10.1126/science.1212642>



- Berger, A. B., Decourty, L., Badis, G., Nehrbass, U., Jacquier, A., & Gadal, O. (2007). Hmo1 Is Required for TOR-Dependent Regulation of Ribosomal Protein Gene Transcription. *Molecular and Cellular Biology*, 27(22), 8015–8026. <https://doi.org/10.1128/MCB.01102-07>
- Binda, M., Péli-Gulli, M.-P., Bonfils, G., Panchaud, N., Urban, J., Sturgill, T. W., Loewith, R., & De Virgilio, C. (2009). The Vam6 GEF Controls TORC1 by Activating the EGO Complex. *Molecular Cell*, 35(5), 563–573. <https://doi.org/10.1016/j.molcel.2009.06.033>
- Bosio, M. C., Fermi, B., Spagnoli, G., Levati, E., Rubbi, L., Ferrari, R., Pellegrini, M., & Dieci, G. (2017). Abf1 and other general regulatory factors control ribosome biogenesis gene expression in budding yeast. *Nucleic Acids Research*, 45(8), 4493–4506. <https://doi.org/10.1093/nar/gkx058>
- Camici, M., Tozzi, M. G., Allegrini, S., Del Corso, A., Sanfilippo, O., Daidone, M. G., De Marco, C., & Ipata, P. L. (1990). Purine salvage enzyme activities in normal and neoplastic human tissues. *Cancer Biochemistry Biophysics*, 11(3), 201–209.
- Choesmel, V., Fribourg, S., Aguisa-Toure, A.-H., Pinaud, N., Legrand, P., Gazda, H. T., & Gleizes, P.-E. (2008). Mutation of ribosomal protein RPS24 in Diamond-Blackfan anemia results in a ribosome biogenesis disorder. *Human Molecular Genetics*, 17(9), 1253–1263. <https://doi.org/10.1093/hmg/ddn015>
- Cole, S. E., LaRiviere, F. J., Merrikh, C. N., & Moore, M. J. (2009). A Convergence of rRNA and mRNA Quality Control Pathways Revealed by Mechanistic Analysis of Nonfunctional rRNA Decay. *Molecular Cell*, 34(4), 440–450. <https://doi.org/10.1016/j.molcel.2009.04.017>
- Coleman, R. A., & Trader, D. J. (2019). Methods to Discover and Evaluate Proteasome Small Molecule Stimulators. *Molecules*, 24(12), 2341. <https://doi.org/10.3390/molecules24122341>
- Dammann, R., Lucchini, R., Koller, T., & Sogo, J. M. (1993). Chromatin structures and transcription of rDNA in yeast *Saccharomyces cerevisiae*. *Nucleic Acids Research*, 21(10), 2331–2338. <https://doi.org/10.1093/nar/21.10.2331>
- Danilova, N., Sakamoto, K. M., & Lin, S. (2008). Ribosomal protein S19 deficiency in zebrafish leads to developmental abnormalities and defective erythropoiesis through activation of p53 protein family. *Blood*, 112(13), 5228–5237. <https://doi.org/10.1182/blood-2008-01-132290>
- de la Cruz, J., Karbstein, K., & Woolford, J. L. (2015). Functions of Ribosomal Proteins in Assembly of Eukaryotic Ribosomes In Vivo. *Annual Review of Biochemistry*, 84(1), 93–129. <https://doi.org/10.1146/annurev-biochem-060614-033917>
- Dokládál, L., Stumpe, M., Pillet, B., Hu, Z., Garcia Osuna, G. M., Kressler, D., Dengjel, J., & De Virgilio, C. (2021). Global phosphoproteomics pinpoints uncharted Gcn2-mediated mechanisms of translational control. *Molecular Cell*, 81(9), 1879–1889.e6. <https://doi.org/10.1016/j.molcel.2021.02.037>
- Durak, I., Bedük, Y., Kavutcu, M., Süzer, O., Yaman, Ö., Oztürk, H. S., Canbolat, O., & Ulutepe, S. (1997). Activity of the Enzymes Participating in Purine Metabolism of Cancerous and Noncancerous Human Kidney Tissues. *Cancer Investigation*, 15(3), 212–216. <https://doi.org/10.3109/07357909709039717>
- Fargo, J. H., Kratz, C. P., Giri, N., Savage, S. A., Wong, C., Backer, K., Alter, B. P., & Glader, B. (2013). Erythrocyte adenosine deaminase: Diagnostic value for Diamond-Blackfan anaemia. *British Journal of Haematology*, 160(4), 547–554. <https://doi.org/10.1111/bjh.12167>
- Farrar, J. E., Nater, M., Caywood, E., McDevitt, M. A., Kowalski, J., Takemoto, C. M., Talbot, C. C., Meltzer, P., Esposito, D., Beggs, A. H., Schneider, H. E., Grabowska, A., Ball, S. E., Niewiadomska, E., Sieff, C. A., Vlachos, A., Atsidaftos, E., Ellis, S. R., Lipton, J. M., ... Arceci, R. J. (2008). Abnormalities of the large ribosomal subunit protein, Rpl35a, in Diamond-Blackfan anemia. *Blood*, 112(5), 1582–1592. <https://doi.org/10.1182/blood-2008-02-140012>
- Fernández-Pevida, A., Kressler, D., & de la Cruz, J. (2015). Processing of preribosomal RNA in *Saccharomyces cerevisiae*: Yeast pre-rRNA processing. *Wiley Interdisciplinary Reviews: RNA*, 6(2), 191–209. <https://doi.org/10.1002/wrna.1267>
- Ferreira-Cerca, S., Pöll, G., Kühn, H., Neueder, A., Jakob, S., Tschochner, H., & Milkereit, P. (2007). Analysis of the In Vivo Assembly Pathway of Eukaryotic 40S Ribosomal Proteins. *Molecular Cell*, 28(3), 446–457. <https://doi.org/10.1016/j.molcel.2007.09.029>
- Ferretti, M. B., Ghalei, H., Ward, E. A., Potts, E. L., & Karbstein, K. (2017). Rps26 directs mRNA-specific translation by recognition of Kozak sequence elements. *Nature Structural & Molecular Biology*, 24(9), 700–707. <https://doi.org/10.1038/nsmb.3442>

- Fingerman, I., Nagaraj, V., Norris, D., & Vershon, A. K. (2003). Sfp1 Plays a Key Role in Yeast Ribosome Biogenesis. *Eukaryotic Cell*, 2(5), 1061–1068. <https://doi.org/10.1128/EC.2.5.1061-1068.2003>
- Freckleton, G., Lippman, S. I., Broach, J. R., & Tavazoie, S. (2009). Microarray Profiling of Phage-Display Selections for Rapid Mapping of Transcription Factor–DNA Interactions. *PLoS Genetics*, 5(4), e1000449. <https://doi.org/10.1371/journal.pgen.1000449>
- French, S. L., Osheim, Y. N., Cioci, F., Nomura, M., & Beyer, A. L. (2003). In Exponentially Growing *Saccharomyces cerevisiae* Cells, rRNA Synthesis Is Determined by the Summed RNA Polymerase I Loading Rate Rather than by the Number of Active Genes. *Molecular and Cellular Biology*, 23(5), 1558–1568. <https://doi.org/10.1128/MCB.23.5.1558-1568.2003>
- Fujii, K., Kitabatake, M., Sakata, T., Miyata, A., & Ohno, M. (2009). A role for ubiquitin in the clearance of nonfunctional rRNAs. *Genes & Development*, 23(8), 963–974. <https://doi.org/10.1101/gad.1775609>
- Gaikwad, S., Ghobakhlou, F., Young, D. J., Visweswarajah, J., Zhang, H., & Hinnebusch, A. G. (2021). Reprogramming of translation in yeast cells impaired for ribosome recycling favors short, efficiently translated mRNAs. *ELife*, 10, e64283. <https://doi.org/10.7554/eLife.64283>
- Gallagher, J. E. G. (2004). RNA polymerase I transcription and pre-rRNA processing are linked by specific SSU processome components. *Genes & Development*, 18(20), 2506–2517. <https://doi.org/10.1101/gad.1226604>
- Gao, M., & Kaiser, C. A. (2006). A conserved GTPase-containing complex is required for intracellular sorting of the general amino-acid permease in yeast. *Nature Cell Biology*, 8(7), 657–667. <https://doi.org/10.1038/ncb1419>
- Gazda, H. T., Grabowska, A., Merida-Long, L. B., Latawiec, E., Schneider, H. E., Lipton, J. M., Vlachos, A., Atsidaftos, E., Ball, S. E., Orfali, K. A., Niewiadomska, E., Da Costa, L., Tchernia, G., Niemeyer, C., Meerpohl, J. J., Stahl, J., Schrott, G., Glader, B., Backer, K., ... Sieff, C. A. (2006). Ribosomal Protein S24 Gene Is Mutated in Diamond-Blackfan Anemia. *The American Journal of Human Genetics*, 79(6), 1110–1118. <https://doi.org/10.1086/510020>
- Gazda, H. T., Preti, M., Sheen, M. R., O'Donohue, M.-F., Vlachos, A., Davies, S. M., Kattamis, A., Doherty, L., Landowski, M., Buros, C., Ghazvinian, R., Sieff, C. A., Newburger, P. E., Niewiadomska, E., Matysiak, M., Glader, B., Atsidaftos, E., Lipton, J. M., Gleizes, P.-E., & Beggs, A. H. (2012). Frameshift mutation in p53 regulator *RPL26* is associated with multiple physical abnormalities and a specific pre-ribosomal RNA processing defect in diamond-blackfan anemia. *Human Mutation*, 33(7), 1037–1044. <https://doi.org/10.1002/humu.22081>
- Gazda, H. T., Sheen, M. R., Vlachos, A., Choesmel, V., O'Donohue, M.-F., Schneider, H., Darras, N., Hasman, C., Sieff, C. A., Newburger, P. E., Ball, S. E., Niewiadomska, E., Matysiak, M., Zaucha, J. M., Glader, B., Niemeyer, C., Meerpohl, J. J., Atsidaftos, E., Lipton, J. M., ... Beggs, A. H. (2008). Ribosomal Protein L5 and L11 Mutations Are Associated with Cleft Palate and Abnormal Thumbs in Diamond-Blackfan Anemia Patients. *The American Journal of Human Genetics*, 83(6), 769–780. <https://doi.org/10.1016/j.ajhg.2008.11.004>
- Gostimskaya, I., & Grant, C. M. (2016). Yeast mitochondrial glutathione is an essential antioxidant with mitochondrial thioredoxin providing a back-up system. *Free Radical Biology & Medicine*, 94, 55–65. <https://doi.org/10.1016/j.freeradbiomed.2016.02.015>
- Guetsova, M. L., Lecoq, K., & Daignan-Fornier, B. (1997). The isolation and characterization of *Saccharomyces cerevisiae* mutants that constitutively express purine biosynthetic genes. *Genetics*, 147(2), 383–397.
- Graifer, D. (2004). Variable and conserved elements of human ribosomes surrounding the mRNA at the decoding and upstream sites. *Nucleic Acids Research*, 32(11), 3282–3293. <https://doi.org/10.1093/nar/gkh657>
- Hall, D. B., Wade, J. T., & Struhl, K. (2006). An HMG Protein, Hmo1, Associates with Promoters of Many Ribosomal Protein Genes and throughout the rRNA Gene Locus in *Saccharomyces cerevisiae*. *Molecular and Cellular Biology*, 26(9), 3672–3679. <https://doi.org/10.1128/MCB.26.9.3672-3679.2006>
- Hirschhorn, R., & Ratech, H. (1980). Isozymes of adenosine deaminase. *Isozymes*, 4, 131–157.
- Ho, Y.-H., & Gasch, A. P. (2015). Exploiting the yeast stress-activated signaling network to inform on stress biology and disease signaling. *Current Genetics*, 61(4), 503–511. <https://doi.org/10.1007/s00294-015-0491-0>

- Honma, Y., Kitamura, A., Shioda, R., Maruyama, H., Ozaki, K., Oda, Y., Mini, T., Jenö, P., Maki, Y., Yonezawa, K., Hurt, E., Ueno, M., Uritani, M., Hall, M. N., & Ushimaru, T. (2006). TOR regulates late steps of ribosome maturation in the nucleoplasm via Nog1 in response to nutrients. *The EMBO Journal*, 25(16), 3832–3842. <https://doi.org/10.1038/sj.emboj.7601262>
- Houseley, J., LaCava, J., & Tollervey, D. (2006). RNA-quality control by the exosome. *Nature Reviews Molecular Cell Biology*, 7(7), 529–539. <https://doi.org/10.1038/nrm1964>
- Huber, A., French, S. L., Tekotte, H., Yerlikaya, S., Stahl, M., Perepelkina, M. P., Tyers, M., Rougemont, J., Beyer, A. L., & Loewith, R. (2011). Sch9 regulates ribosome biogenesis via Stb3, Dot6 and Tod6 and the histone deacetylase complex RPD3L. *The EMBO Journal*, 30(15), 3052–3064. <https://doi.org/10.1038/emboj.2011.221>
- Janov, A. J., Leong, T., Nathan, D. G., & Guinan, E. C. (1996). Diamond-Blackfan Anemia Natural History and Sequelae of Treatment: *Medicine*, 75(2), 77–87. <https://doi.org/10.1097/00005792-199603000-00004>
- Jorgensen, P. (2002). Systematic Identification of Pathways That Couple Cell Growth and Division in Yeast. *Science*, 297(5580), 395–400. <https://doi.org/10.1126/science.1070850>
- Jorgensen, P. (2004). A dynamic transcriptional network communicates growth potential to ribosome synthesis and critical cell size. *Genes & Development*, 18(20), 2491–2505. <https://doi.org/10.1101/gad.1228804>
- Kampen, K. R., Sulima, S. O., Vereecke, S., & De Keersmaecker, K. (2020). Hallmarks of ribosomopathies. *Nucleic Acids Research*, 48(3), 1013–1028. <https://doi.org/10.1093/nar/gkz637>
- Kief, D. R., & Warner, J. R. (1981). Hierarchy of elements regulating synthesis of ribosomal proteins in *Saccharomyces cerevisiae*. *Molecular and Cellular Biology*, 1(11), 1016–1023. <https://doi.org/10.1128/mcb.1.11.1016-1023.1981>
- Koob, S., Barrera, M., Anand, R., & Reichert, A. S. (2015). The non-glycosylated isoform of MIC26 is a constituent of the mammalian MICOS complex and promotes formation of crista junctions. *Biochimica et Biophysica Acta (BBA) - Molecular Cell Research*, 1853(7), 1551–1563. <https://doi.org/10.1016/j.bbamcr.2015.03.004>
- Koš, M., & Tollervey, D. (2010). Yeast Pre-rRNA Processing and Modification Occur Cotranscriptionally. *Molecular Cell*, 37(6), 809–820. <https://doi.org/10.1016/j.molcel.2010.02.024>
- Kos-Braun, I. C., Jung, I., & Koš, M. (2017). Tor1 and CK2 kinases control a switch between alternative ribosome biogenesis pathways in a growth-dependent manner. *PLOS Biology*, 15(3), e2000245. <https://doi.org/10.1371/journal.pbio.2000245>
- Kraft, C., Deplazes, A., Sohrmann, M., & Peter, M. (2008). Mature ribosomes are selectively degraded upon starvation by an autophagy pathway requiring the Ubp3p/Bre5p ubiquitin protease. *Nature Cell Biology*, 10(5), 602–610. <https://doi.org/10.1038/ncb1723>
- Kunkel, J., Luo, X., & Capaldi, A. P. (2019). Integrated TORC1 and PKA signaling control the temporal activation of glucose-induced gene expression in yeast. *Nature Communications*, 10(1), 3558. <https://doi.org/10.1038/s41467-019-11540-y>
- LaCava, J., Houseley, J., Saveanu, C., Petfalski, E., Thompson, E., Jacquier, A., & Tollervey, D. (2005). RNA Degradation by the Exosome Is Promoted by a Nuclear Polyadenylation Complex. *Cell*, 121(5), 713–724. <https://doi.org/10.1016/j.cell.2005.04.029>
- Laferte, A. (2006). The transcriptional activity of RNA polymerase I is a key determinant for the level of all ribosome components. *Genes & Development*, 20(15), 2030–2040. <https://doi.org/10.1101/gad.386106>
- LaRiviere, F. J., Cole, S. E., Ferullo, D. J., & Moore, M. J. (2006). A Late-Acting Quality Control Process for Mature Eukaryotic rRNAs. *Molecular Cell*, 24(4), 619–626. <https://doi.org/10.1016/j.molcel.2006.10.008>
- Lebaron, S., Segerstolpe, Å., French, S. L., Dudnakova, T., de Lima Alves, F., Granneman, S., Rappsilber, J., Beyer, A. L., Wieslander, L., & Tollervey, D. (2013). Rrp5 Binding at Multiple Sites Coordinates Pre-rRNA Processing and Assembly. *Molecular Cell*, 52(5), 707–719. <https://doi.org/10.1016/j.molcel.2013.10.017>
- Lempiäinen, H., & Shore, D. (2009). Growth control and ribosome biogenesis. *Current Opinion in Cell Biology*, 21(6), 855–863. <https://doi.org/10.1016/j.ceb.2009.09.002>
- Liko, D., Slattery, M. G., & Heideman, W. (2007). Stb3 Binds to Ribosomal RNA Processing Element Motifs That Control Transcriptional Responses to Growth in *Saccharomyces cerevisiae*. *Journal of Biological Chemistry*, 282(36), 26623–26628. <https://doi.org/10.1074/jbc.M704762200>



- Lippman, S. I., & Broach, J. R. (2009). Protein kinase A and TORC1 activate genes for ribosomal biogenesis by inactivating repressors encoded by Dot6 and its homolog Tod6. *Proceedings of the National Academy of Sciences*, 106(47), 19928–19933. <https://doi.org/10.1073/pnas.0907027106>
- Lipton, J. M., Atsidaftos, E., Zyskind, I., & Vlachos, A. (2006). Improving clinical care and elucidating the pathophysiology of Diamond Blackfan anemia: An update from the Diamond Blackfan Anemia Registry. *Pediatric Blood & Cancer*, 46(5), 558–564. <https://doi.org/10.1002/pbc.20642>
- Loewith, R., & Hall, M. N. (2011). Target of Rapamycin (TOR) in Nutrient Signaling and Growth Control. *Genetics*, 189(4), 1177–1201. <https://doi.org/10.1534/genetics.111.133363>
- Mahajan, M., Tiwari, N., Sharma, R., Kaur, S., & Singh, N. (2013). Oxidative Stress and Its Relationship With Adenosine Deaminase Activity in Various Stages of Breast Cancer. *Indian Journal of Clinical Biochemistry*, 28(1), 51–54. <https://doi.org/10.1007/s12291-012-0244-5>
- Marion, R. M., Regev, A., Segal, E., Barash, Y., Koller, D., Friedman, N., & O’Shea, E. K. (2004). Sfp1 is a stress- and nutrient-sensitive regulator of ribosomal protein gene expression. *Proceedings of the National Academy of Sciences*, 101(40), 14315–14322. <https://doi.org/10.1073/pnas.0405353101>
- Martin, D. E., Soulard, A., & Hall, M. N. (2004). TOR Regulates Ribosomal Protein Gene Expression via PKA and the Forkhead Transcription Factor FHL1. *Cell*, 119(7), 969–979. <https://doi.org/10.1016/j.cell.2004.11.047>
- McKnight, J. N., Boerma, J. W., Breeden, L. L., & Tsukiyama, T. (2015). Global Promoter Targeting of a Conserved Lysine Deacetylase for Transcriptional Shutoff during Quiescence Entry. *Molecular Cell*, 59(5), 732–743. <https://doi.org/10.1016/j.molcel.2015.07.014>
- Meng, D., Yang, Q., Wang, H., Melick, C. H., Navlani, R., Frank, A. R., & Jewell, J. L. (2020). Glutamine and asparagine activate mTORC1 independently of Rag GTPases. *Journal of Biological Chemistry*, 295(10), 2890–2899. <https://doi.org/10.1074/jbc.AC119.011578>
- Meng, X., Tackmann, N. R., Liu, S., Yang, J., Dong, J., Wu, C., Cox, A. D., & Zhang, Y. (2016). RPL23 Links Oncogenic RAS Signaling to p53-Mediated Tumor Suppression. *Cancer Research*, 76(17), 5030–5039. <https://doi.org/10.1158/0008-5472.CAN-15-3420>
- Michel, A. H., Hatakeyama, R., Kimmig, P., Arter, M., Peter, M., Matos, J., De Virgilio, C., & Kornmann, B. (2017). Functional mapping of yeast genomes by saturated transposition. *ELife*, 6, e23570. <https://doi.org/10.7554/eLife.23570>
- Mougey, E. B., O’Reilly, M., Osheim, Y., Miller, O. L., Beyer, A., & Sollner-Webb, B. (1993). The terminal balls characteristic of eukaryotic rRNA transcription units in chromatin spreads are rRNA processing complexes. *Genes & Development*, 7(8), 1609–1619. <https://doi.org/10.1101/gad.7.8.1609>
- Mülleider, M., Calvani, E., Alam, M. T., Wang, R. K., Eckerstorfer, F., Zelezniak, A., & Ralser, M. (2016). Functional Metabolomics Describes the Yeast Biosynthetic Regulome. *Cell*, 167(2), 553–565.e12. <https://doi.org/10.1016/j.cell.2016.09.007>
- Nagalakshmi, U., Wang, Z., Waern, K., Shou, C., Raha, D., Gerstein, M., & Snyder, M. (2008). The Transcriptional Landscape of the Yeast Genome Defined by RNA Sequencing. *Science*, 320(5881), 1344–1349. <https://doi.org/10.1126/science.1158441>
- Nakashima, N., Noguchi, E., & Nishimoto, T. (1999). *Saccharomyces cerevisiae* Putative G Protein, Gtr1p, Which Forms Complexes With Itself and a Novel Protein Designated as Gtr2p, Negatively Regulates the Ran/Gsp1p G Protein Cycle Through Gtr2p. *Genetics*, 152(3), 853–867. <https://doi.org/10.1093/genetics/152.3.853>
- Osheim, Y. N., French, S. L., Keck, K. M., Champion, E. A., Spasov, K., Dragon, F., Baserga, S. J., & Beyer, A. L. (2004). Pre-18S Ribosomal RNA Is Structurally Compacted into the SSU Processome Prior to Being Cleaved from Nascent Transcripts in *Saccharomyces cerevisiae*. *Molecular Cell*, 16(6), 943–954. <https://doi.org/10.1016/j.molcel.2004.11.031>
- Ossareh-Nazari, B., Niño, C. A., Bengtson, M. H., Lee, J.-W., Joazeiro, C. A. P., & Dargemont, C. (2014). Ubiquitylation by the Ltn1 E3 ligase protects 60S ribosomes from starvation-induced selective autophagy. *Journal of Cell Biology*, 204(6), 909–917. <https://doi.org/10.1083/jcb.201308139>
- Péli-Gulli, M.-P., Sardu, A., Panchaud, N., Raucchi, S., & De Virgilio, C. (2015). Amino Acids Stimulate TORC1 through Lst4-Lst7, a GTPase-Activating Protein Complex for the Rag Family GTPase Gtr2. *Cell Reports*, 13(1), 1–7. <https://doi.org/10.1016/j.celrep.2015.08.059>

- Peña, C., Schütz, S., Fischer, U., Chang, Y., & Panse, V. G. (2016). Prefabrication of a ribosomal protein subcomplex essential for eukaryotic ribosome formation. *ELife*, 5, e21755. <https://doi.org/10.7554/eLife.21755>
- Pestov, D. G., & Shcherbik, N. (2012). Rapid Cytoplasmic Turnover of Yeast Ribosomes in Response to Rapamycin Inhibition of TOR. *Molecular and Cellular Biology*, 32(11), 2135–2144. <https://doi.org/10.1128/MCB.06763-11>
- Philippi, A., Steinbauer, R., Reiter, A., Fath, S., Leger-Silvestre, I., Milkereit, P., Griesenbeck, J., & Tschochner, H. (2010). TOR-dependent reduction in the expression level of Rrn3p lowers the activity of the yeast RNA Pol I machinery, but does not account for the strong inhibition of rRNA production. *Nucleic Acids Research*, 38(16), 5315–5326. <https://doi.org/10.1093/nar/gkq264>
- Pisarev, A. V., Kolupaeva, V. G., Yusupov, M. M., Hellen, C. U., & Pestova, T. V. (2008). Ribosomal position and contacts of mRNA in eukaryotic translation initiation complexes. *The EMBO Journal*, 27(11), 1609–1621. <https://doi.org/10.1038/emboj.2008.90>
- Plassart, L., Shayan, R., Montellese, C., Rinaldi, D., Larburu, N., Pichereaux, C., Froment, C., Lebaron, S., O'Donohue, M.-F., Kutay, U., Marcoux, J., Gleizes, P.-E., & Plisson-Chastang, C. (2021). The final step of 40S ribosomal subunit maturation is controlled by a dual key lock. *ELife*, 10, e61254. <https://doi.org/10.7554/eLife.61254>
- Powers, T., & Walter, P. (1999). Regulation of Ribosome Biogenesis by the Rapamycin-sensitive TOR-signaling Pathway in *Saccharomyces cerevisiae*. *Molecular Biology of the Cell*, 10(4), 987–1000. <https://doi.org/10.1091/mbc.10.4.987>
- Puddu, F., Herzog, M., Selivanova, A., Wang, S., Zhu, J., Klein-Lavi, S., Gordon, M., Meirman, R., Millan-Zambrano, G., Ayestaran, I., Salguero, I., Sharan, R., Li, R., Kupiec, M., & Jackson, S. P. (2019). Genome architecture and stability in the *Saccharomyces cerevisiae* knockout collection. *Nature*, 573(7774), 416–420. <https://doi.org/10.1038/s41586-019-1549-9>
- Qiu, H. (2002). Mutations that bypass tRNA binding activate the intrinsically defective kinase domain in GCN2. *Genes & Development*, 16(10), 1271–1280. <https://doi.org/10.1101/gad.979402>
- Ramenghi, U., Campagnoli, M. F., Garelli, E., Carando, A., Brusco, A., Bagnara, G. P., Strippoli, P., IZZI, G. C., Brandalise, S., Riccardi, R., & Dianzani, I. (2000). Diamond-Blackfan Anemia: Report of Seven Further Mutations in the RPS19 Gene and Evidence of Mutation Heterogeneity in the Italian Population. *Blood Cells, Molecules, and Diseases*, 26(5), 417–422. <https://doi.org/10.1006/bcmd.2000.0324>
- Reimand, J., Isserlin, R., Voisin, V., Kucera, M., Tannus-Lopes, C., Rostamianfar, A., Wadi, L., Meyer, M., Wong, J., Xu, C., Merico, D., & Bader, G. D. (2019). Pathway enrichment analysis and visualization of omics data using g:Profiler, GSEA, Cytoscape and EnrichmentMap. *Nature Protocols*, 14(2), 482–517. <https://doi.org/10.1038/s41596-018-0103-9>
- Rudra, D., Mallick, J., Zhao, Y., & Warner, J. R. (2007). Potential Interface between Ribosomal Protein Production and Pre-rRNA Processing. *Molecular and Cellular Biology*, 27(13), 4815–4824. <https://doi.org/10.1128/MCB.02062-06>
- Ruggero, D. (2013). Translational Control in Cancer Etiology. *Cold Spring Harbor Perspectives in Biology*, 5(2), a012336–a012336. <https://doi.org/10.1101/cshperspect.a012336>
- Schawaldner, S. B., Kabani, M., Howald, I., Choudhury, U., Werner, M., & Shore, D. (2004). Growth-regulated recruitment of the essential yeast ribosomal protein gene activator Iff1. *Nature*, 432(7020), 1058–1061. <https://doi.org/10.1038/nature03200>
- Schmid, M., & Jensen, T. H. (2008). The exosome: A multipurpose RNA-decay machine. *Trends in Biochemical Sciences*, 33(10), 501–510. <https://doi.org/10.1016/j.tibs.2008.07.003>
- Schoppe, J., Mari, M., Yavavli, E., Auffarth, K., Cabrera, M., Walter, S., Fröhlich, F., & Ungermann, C. (2020). AP-3 vesicle uncoating occurs after HOPS-dependent vacuole tethering. *The EMBO Journal*, 39(20). <https://doi.org/10.15252/emboj.2020105117>
- Schütz, S., Fischer, U., Altvater, M., Nerurkar, P., Peña, C., Gerber, M., Chang, Y., Caesar, S., Schubert, O. T., Schlenstedt, G., & Panse, V. G. (2014). A RanGTP-independent mechanism allows ribosomal protein nuclear import for ribosome assembly. *ELife*, 3, e03473. <https://doi.org/10.7554/eLife.03473>
- Sharifulin, D., Khairulina, Y., Ivanov, A., Meschaninova, M., Ven'yaminova, A., Graifer, D., & Karpova, G. (2012). A central fragment of ribosomal protein S26 containing the eukaryote-specific motif YxxPKxYxK is a key component of the ribosomal binding site of mRNA region 5' of the E site codon. *Nucleic Acids Research*, 40(7), 3056–3065. <https://doi.org/10.1093/nar/gkr1212>

- Sidiropoulos, K., Viteri, G., Sevilla, C., Jupe, S., Webber, M., Orlic-Milacic, M., Jassal, B., May, B., Shamovsky, V., Duenas, C., Rothfels, K., Matthews, L., Song, H., Stein, L., Haw, R., D'Eustachio, P., Ping, P., Hermjakob, H., & Fabregat, A. (2017). Reactome enhanced pathway visualization. *Bioinformatics* (Oxford, England), 33(21), 3461–3467. <https://doi.org/10.1093/bioinformatics/btx441>
- Stenson, P. D., Mort, M., Ball, E. V., Evans, K., Hayden, M., Heywood, S., Hussain, M., Phillips, A. D., & Cooper, D. N. (2017). The Human Gene Mutation Database: Towards a comprehensive repository of inherited mutation data for medical research, genetic diagnosis and next-generation sequencing studies. *Human Genetics*, 136(6), 665–677. <https://doi.org/10.1007/s00439-017-1779-6>
- Sturm, M., Cheng, J., Baßler, J., Beckmann, R., & Hurt, E. (2017). Interdependent action of KH domain proteins Krr1 and Dim2 drive the 40S platform assembly. *Nature Communications*, 8(1), 2213. <https://doi.org/10.1038/s41467-017-02199-4>
- Sulima, S., Kampen, K., & De Keersmaecker, K. (2019). Cancer Biogenesis in Ribosomopathies. *Cells*, 8(3), 229. <https://doi.org/10.3390/cells8030229>
- Sulima, S. O., Hofman, I. J. F., De Keersmaecker, K., & Dinman, J. D. (2017). How Ribosomes Translate Cancer. *Cancer Discovery*, 7(10), 1069–1087. <https://doi.org/10.1158/2159-8290.CD-17-0550>
- Sung, M.-K., Reitsma, J. M., Sweredoski, M. J., Hess, S., & Deshaies, R. J. (2016). Ribosomal proteins produced in excess are degraded by the ubiquitin–proteasome system. *Molecular Biology of the Cell*, 27(17), 2642–2652. <https://doi.org/10.1091/mbc.e16-05-0290>
- Talkish, J., Biedka, S., Jakovljevic, J., Zhang, J., Tang, L., Strahler, J. R., Andrews, P. C., Maddock, J. R., & Woolford, J. L. (2016). Disruption of ribosome assembly in yeast blocks cotranscriptional pre-rRNA processing and affects the global hierarchy of ribosome biogenesis. *RNA*, 22(6), 852–866. <https://doi.org/10.1261/rna.055780.115>
- Tatehashi, Y., Watanabe, D., & Takagi, H. (2016).  $\gamma$ -Glutamyl kinase is involved in selective autophagy of ribosomes in *Saccharomyces cerevisiae*. *FEBS Letters*, 590(17), 2906–2914. <https://doi.org/10.1002/1873-3468.12318>
- Ukai, H., Araki, Y., Kira, S., Oikawa, Y., May, A. I., & Noda, T. (2018). Gtr/Ego-independent TORC1 activation is achieved through a glutamine-sensitive interaction with Pib2 on the vacuolar membrane. *PLoS Genetics*, 14(4), e1007334. <https://doi.org/10.1371/journal.pgen.1007334>
- Urban, J., Soulard, A., Huber, A., Lippman, S., Mukhopadhyay, D., Deloche, O., Wanke, V., Anrather, D., Ammerer, G., Riezman, H., Broach, J. R., De Virgilio, C., Hall, M. N., & Loewith, R. (2007). Sch9 Is a Major Target of TORC1 in *Saccharomyces cerevisiae*. *Molecular Cell*, 26(5), 663–674. <https://doi.org/10.1016/j.molcel.2007.04.020>
- van der Vaart, A., Griffith, J., & Reggiori, F. (2010). Exit from the Golgi Is Required for the Expansion of the Autophagosomal Phagophore in Yeast *Saccharomyces cerevisiae*. *Molecular Biology of the Cell*, 21(13), 2270–2284. <https://doi.org/10.1091/mbc.e09-04-0345>
- Vaňáčová, Š., Wolf, J., Martin, G., Blank, D., Dettwiler, S., Friedlein, A., Langen, H., Keith, G., & Keller, W. (2005). A New Yeast Poly(A) Polymerase Complex Involved in RNA Quality Control. *PLoS Biology*, 3(6), e189. <https://doi.org/10.1371/journal.pbio.0030189>
- Vanrobays, E., Leplus, A., Osheim, Y. N., Beyer, A. L., Wacheul, L., & Lafontaine, D. L. J. (2008). TOR regulates the subcellular distribution of DIM2, a KH domain protein required for cotranscriptional ribosome assembly and pre-40S ribosome export. *RNA*, 14(10), 2061–2073. <https://doi.org/10.1261/rna.1176708>
- Varlakhanova, N. V., Mihalevic, M., Bernstein, K. A., & Ford, M. G. J. (2017). Pib2 and EGO Complex are both required for activation of TORC1. *Journal of Cell Science*, jcs.207910. <https://doi.org/10.1242/jcs.207910>
- Vlachos, A. (2017). Acquired ribosomopathies in leukemia and solid tumors. *Hematology*, 2017(1), 716–719. <https://doi.org/10.1182/asheducation-2017.1.716>
- Vlachos, A., Klein, G. W., & Lipton, J. M. (2001). The Diamond Blackfan Anemia Registry: Tool for Investigating the Epidemiology and Biology of Diamond—Blackfan Anemia: *Journal of Pediatric Hematology/Oncology*, 23(6), 377–382. <https://doi.org/10.1097/00043426-200108000-00015>
- Vlachos, A., Rosenberg, P. S., Atsidaftos, E., Kang, J., Onel, K., Sharaf, R. N., Alter, B. P., & Lipton, J. M. (2018). Increased risk of colon cancer and osteogenic sarcoma in Diamond-Blackfan anemia. *Blood*, 132(20), 2205–2208. <https://doi.org/10.1182/blood-2018-05-848937>

- von der Haar, T. (2008). A quantitative estimation of the global translational activity in logarithmically growing yeast cells. *BMC Systems Biology*, 2(1), 87. <https://doi.org/10.1186/1752-0509-2-87>
- Wade, C. H., Umbarger, M. A., & McAlear, M. A. (2006). The budding yeast rRNA and ribosome biosynthesis (RRB) regulon contains over 200 genes. *Yeast*, 23(4), 293–306. <https://doi.org/10.1002/yea.1353>
- Waliullah, T. M., Yeasmin, A. M., Kaneko, A., Koike, N., Terasawa, M., Totsuka, T., & Ushimaru, T. (2017). Rim15 and Sch9 kinases are involved in induction of autophagic degradation of ribosomes in budding yeast. *Bioscience, Biotechnology, and Biochemistry*, 81(2), 307–310. <https://doi.org/10.1080/09168451.2016.1234928>
- Warner, J. R. (1999). The economics of ribosome biosynthesis in yeast. *Trends in Biochemical Sciences*, 24(11), 437–440. [https://doi.org/10.1016/S0968-0004\(99\)01460-7](https://doi.org/10.1016/S0968-0004(99)01460-7)
- Wei, Y., & Zheng, X. F. S. (2010). Maf1 regulation: A model of signal transduction inside the nucleus. *Nucleus*, 1(2), 162–165. <https://doi.org/10.4161/nucl.1.2.11179>
- Whitehouse, D. B., Hopkinson, D. A., Pilz, A. J., & Arredondo, F. X. (1986). Adenosine Deaminase Activity in a Series of 19 Patients with the Diamond-Blackfan Syndrome. In W. L. Nyhan, L. F. Thompson, & R. W. E. Watts (Eds.), *Purine and Pyrimidine Metabolism in Man V* (Vol. 195A, pp. 85–92). Springer US. [https://doi.org/10.1007/978-1-4684-5104-7\\_14](https://doi.org/10.1007/978-1-4684-5104-7_14)
- Woods, R. A., Roberts, D. G., Stein, D. S., & Filpula, D. (1984). Adenine Phosphoribosyltransferase Mutants in *Saccharomyces cerevisiae*. *Microbiology*, 130(10), 2629–2637. <https://doi.org/10.1099/00221287-130-10-2629>
- Woolford, J. L., & Baserga, S. J. (2013). Ribosome Biogenesis in the Yeast *Saccharomyces cerevisiae*. *Genetics*, 195(3), 643–681. <https://doi.org/10.1534/genetics.113.153197>
- Wyers, F., Rougemaille, M., Badis, G., Rousselle, J.-C., Dufour, M.-E., Boulay, J., Régnault, B., Devaux, F., Namane, A., Séraphin, B., Libri, D., & Jacquier, A. (2005). Cryptic Pol II Transcripts Are Degraded by a Nuclear Quality Control Pathway Involving a New Poly(A) Polymerase. *Cell*, 121(5), 725–737. <https://doi.org/10.1016/j.cell.2005.04.030>
- Yang, S., & Rosenwald, A. G. (2016). Autophagy in *Saccharomyces cerevisiae* requires the monomeric GTP-binding proteins, Arl1 and Ypt6. *Autophagy*, 12(10), 1721–1737. <https://doi.org/10.1080/15548627.2016.1196316>
- Yuan, W., Guo, S., Gao, J., Zhong, M., Yan, G., Wu, W., Chao, Y., & Jiang, Y. (2017). General Control Nonderepressible 2 (GCN2) Kinase Inhibits Target of Rapamycin Complex 1 in Response to Amino Acid Starvation in *Saccharomyces cerevisiae*. *Journal of Biological Chemistry*, 292(7), 2660–2669. <https://doi.org/10.1074/jbc.M116.772194>
- Zhang, J., Andersen, J., Sun, H., Liu, X., Sonenberg, N., Nie, J., & Shi, Y. (2020). Aster-C coordinates with COP I vesicles to regulate lysosomal trafficking and activation of mTORC1. *EMBO Reports*, 21(9). <https://doi.org/10.15252/embr.201949898>
- Zhang, Y., Smith, A. D., Renfrow, M. B., & Schneider, D. A. (2010). The RNA Polymerase-associated Factor 1 Complex (Paf1C) Directly Increases the Elongation Rate of RNA Polymerase I and Is Required for Efficient Regulation of rRNA Synthesis. *Journal of Biological Chemistry*, 285(19), 14152–14159. <https://doi.org/10.1074/jbc.M110.115220>
- Zhao, Y., McIntosh, K. B., Rudra, D., Schawalter, S., Shore, D., & Warner, J. R. (2006). Fine-Structure Analysis of Ribosomal Protein Gene Transcription. *Molecular and Cellular Biology*, 26(13), 4853–4862. <https://doi.org/10.1128/MCB.02367-05>
- Zhu, C., Byers, K. J. R. P., McCord, R. P., Shi, Z., Berger, M. F., Newburger, D. E., Saulrieta, K., Smith, Z., Shah, M. V., Radhakrishnan, M., Philippakis, A. A., Hu, Y., De Masi, F., Pacek, M., Rolfs, A., Murthy, T., LaBaer, J., & Bulyk, M. L. (2009). High-resolution DNA-binding specificity analysis of yeast transcription factors. *Genome Research*, 19(4), 556–566. <https://doi.org/10.1101/gr.090233.108>

**OUTLOOK**



In Chapter I, both genetic screens yielded several leads that would be worth exploring in the future. As next steps, we could study the sensitivity of the isolated Tor1 variants to sublethal concentrations of rapamycin and monitor their activity *in vivo*; test whether the loss of Cyc8, Cts1, or GID complex components (e.g., Vid30, Rmd5, Vid24, Vid28, Gid7, Gid8, and Fyv10) suppresses the Gtr1<sup>S20L</sup>-mediated growth inhibition; test whether the expression of the kex2<sup>D105A</sup>, kex2<sup>S708\*</sup>, or Opy1<sup>N250K</sup> variant suppresses the Gtr1<sup>S20L</sup>-mediated growth inhibition, analyze the epistasis between Opy1 and Gtr1 or Pib2; and analyze how Opy1 overexpression affects the subcellular localization of Gtr1, Ego1, Tor1, and Pib2.

The studies summarized in Chapter II revealed a Gcn4-dependent branch of TORC1 regulation in *S. cerevisiae*. Since this branch of TORC1 regulation may involve the expression of a functional homolog of Sestrin2 or REDD1 (*i.e.*, ATF-regulated negative regulators of TORC1), we could compare the proteome of leucine-starved *gcn4*Δ cells with those of leucine-starved wild-type cells and leucine-starved *sui2*<sup>S52A</sup> cells. In addition, we identified Hos4 and Snd1 as putative Gcn2 targets that may be involved in regulating TORC1 activity. It would therefore be interesting to perform Gcn2 *in vitro* kinase assays using Hos4 and Snd1 as candidate substrates. If phosphorylation of these proteins on the sites identified *in vivo* is confirmed, the next step would be to create the phosphomimetic and non-phosphorylatable variants of Hos4<sup>T688</sup>, Snd1<sup>S516</sup>, Snd1<sup>S603</sup>, and Snd1<sup>T605</sup> residues and to study their effects on the TORC1 activity of leucine-starved cells.

Finally, the studies reported in Chapter III revealed an Arf1-dependent branch of TORC1 regulation in *S. cerevisiae*. The exact mechanism by which Arf1 affects TORC1 activity remains unclear to date. To verify that *rps26a*Δ cells (and other slow-growth ribosomal mutants) accumulate high intracellular asparagine and glutamine levels, we plan, in collaboration with Dr. Sunil Laxman's group, to measure the intracellular concentration of amino acids in a heterogeneous subset of slow-growth and normal-growth ribosomal mutants growing exponentially in synthetic complete (SC) medium. Also, we intend to measure the intracellular concentration of amino acids in wild-type, *gtr1*Δ, *rps26a*Δ, *arf1*Δ, *rps26a*Δ *gtr1*Δ, and *rps26a*Δ *arf1*Δ cells growing exponentially in SC and then starved of nitrogen for 2.5 minutes. To verify that *rps26a*Δ cells (and other slow-growth ribosomal mutants) are under oxidative stress, we could quantify the amount of ROS generated in these mutants. To study the impact that the loss of Rps26a or Arf1 has on the cellular degradation pathways, we could measure and compare the

proteasome and autophagy activities of wild-type, *rps26a* $\Delta$ , *arf1* $\Delta$ , and *rps26a* $\Delta$  *arf1* $\Delta$  cells by using any of the methods described by Coleman and Trader in 2019 (Coleman & Trader, 2019). Moreover, to assess if Arf1 plays a role in the subcellular localization of TORC1 components, using confocal microscopy, we could study the effects of the loss of Arf1 on fluorescently-tagged Tor1 and Sch9 subcellular distribution. We could also perform Co-Immunoprecipitation (Co-IP) analysis to examine whether Arf1 physically interacts, *in vivo*, with the TORC1 complex kinase, and whether this interaction is affected by the presence or absence of amino acids in the culture medium.

## **MATERIAL AND METHODS**

## Yeast strains, plasmids, and growth conditions

The *Saccharomyces cerevisiae* strains and plasmids used in Chapters I, II, and III are listed in Tables 1 and 2, respectively. The pFA6a system-based PCR toolbox (Janke et al., 2004) was used for gene deletion or tagging. Unless stated otherwise, the strains were transformed with the required empty centromeric plasmids listed in Table 2 to be rendered prototrophic. Unless stated otherwise, cells were pre-cultured in Synthetic Dropout (SD; 0.17% yeast nitrogen base, 0.5% ammonium sulfate [AS], 0.2% dropout mix [USBiological, D9540], and 2% glucose) medium up to the middle-log phase. Then, the cultures were diluted in Synthetic Complete medium (SC; SD with all amino acids). For *in vivo* SILAC experiments, wild-type and *gcn2Δ* strains were grown in SD medium lacking histidine and uracil containing either non-labeled or labeled lysine and arginine variants: “Heavy” L-arginine-<sup>13</sup>C<sub>6</sub>-<sup>15</sup>N<sub>4</sub> (Arg10) and L-lysine-<sup>13</sup>C<sub>6</sub>-<sup>15</sup>N<sub>2</sub> (Lys8), or “medium” L-arginine-<sup>13</sup>C<sub>6</sub> (Arg6) and L-lysine-<sup>2</sup>H<sub>4</sub> (Lys4) amino acids (Sigma-Aldrich) were used as labels.

For *in vitro* DML (Dimethyl Labeling) experiments, wild-type and *gcn2Δ* strains were grown in SD medium lacking histidine and uracil. Cells were starved for leucine for 1 h. For rapamycin treatment, wild-type and *rps26aΔ* cells were grown exponentially in SC medium and then treated for the indicated times with 200 ng/ml of rapamycin. For label-free proteome analysis, wild-type and *rps26aΔ* cells were grown exponentially in SC medium. Note that for leucine starvation experiments, cells were auxotrophic for leucine; for histidine starvation experiments, cells were auxotrophic for histidine; and for uracil starvation experiments, cells were auxotrophic for uracil.

## Saturated transposon analysis in yeast (SATAY)

The pipeline for this experiment is depicted in Chapter I, Figure 6. W303 *gtr1Δ* cells, in which the *ADE2* locus is interrupted by a miniDs transposon, were transformed with a 2μ plasmid coding for a galactose-inducible Ac transposase and a 600 bp repair template for homology-directed repair (HDR) of the *ADE2* locus, a plasmid coding for Gtr1<sup>S20L</sup> under the control of a doxycycline-inducible promoter, and empty vectors to complement the rest of the auxotrophies (except adenine). A preculture (1<sup>st</sup> preculture) was done with 4 ml of SD medium at OD<sub>600</sub> of 0.1. The 1<sup>st</sup> preculture was grown overnight at 30°C and shaken at 160 rpm in a Multitron Standard Infors incubator, the

same instrument used for all further incubations. The following day, cells were diluted in 25 ml of a modified SD medium (0.2% Glucose and 2% Raffinose) at OD600 of 0.1 (2<sup>nd</sup> Preculture) and grown as previously described during 15-20 hours. Then, a sample of cells was plated on SD (non-selective) medium and on SD-Adenine (selective) medium to estimate the proportion of transposon clones, resulting in 0.005% of the total number of cells. Another sample of cells was used to inoculate 100 ml of SGal medium (like SD but substituting Glucose with Galactose) at OD600 of 0.2 (galactose induction). Cells were grown as previously described, and after 20 hours and 55 hours of incubation, a sample of cells was plated on SD (non-selective) medium and on SD-Adenine (selective) medium to estimate the proportion of transposon clones, resulting, respectively, in 0.05% and 0.5% of the total number of cells.

After 55 hours of incubation, another sample of cells was used to inoculate 2 L of SD - Adenine medium at OD600 of 0.35 (45 millions of transposon mutants in total); this served for the expansion of the transposon mutant library through the selection of adenine prototrophs. Cells were grown as previously during 70 hours, and a sample of cells was plated on SD (non-selective) medium and on SD-Adenine (selective) medium to estimate the proportion of transposon clones, resulting in 100% of the total number of cells. Another sample of cells was used to inoculate 2 L of SD - Adenine + 10 µg/ml of doxycycline at OD600 of 0.1; this was meant for the selection of suppressors able to overcome the inhibitory effect caused by overexpression of Gtr1<sup>S20L</sup>. Cells were grown as previously described during 5 cell cycles. A sample of cells was used to inoculate 2 L of SD - Adenine + 10 µg/ml of doxycycline at OD600 of 0.1, and the rest of the cells was filtered and frozen in liquid nitrogen. Cells were grown as previously described during 5 cell cycles, filtered, and frozen in liquid nitrogen. Genomic DNA was prepared following the protocol below (see Preparation of genomic DNA from yeast) and treated by Dr. Kornmann and colleagues as previously described (Michel et al., 2019). The results obtained from the W303 *gtr1*Δ Gtr1<sup>S20L</sup> overexpressing cells were compared with those of the wild-type W303 strain previously described (Michel et al., 2019). Data are accessible at [http://genome-euro.ucsc.edu/s/AgnesHM/Guillermo\\_Gtr1S20L\\_Wig\\_25Feb2020](http://genome-euro.ucsc.edu/s/AgnesHM/Guillermo_Gtr1S20L_Wig_25Feb2020), where DoxA and DoxB correspond to the Gtr1<sup>S20L</sup> overexpressing population while 20181122.A-NC\_R1.fastq\_trimmed corresponds to the wild-type population.

## Preparation of genomic DNA from yeast

Adapted from the protocol in Current Protocols in Molecular Biology (Ausubel, F.M., Brent, R., Kingston, R.E., Moore, D.D., Seidman, J.G., Smith, J.A. and Struhl, K. (1994) Current Protocols in Molecular Biology, Vol. 2, John Wiley & Sons, Inc., New York, NY, pp. 13.11.1–13.11.4).

1. Grow a 10 ml (2 x 5 ml) culture of yeast in YPD (Yeast extract Peptone Dextrose) overnight to stationary phase in glass culture tubes.
2. Dilute the cells until 0.2 in 55 ml fresh YPD. Grow the culture in 1L (ideally) or 200 ml Erlenmeyer flask during 6 hours (or until OD = 1) at 120-140 rpm shaking at 30°C.
3. Split the culture in two 50 ml falcon tubes. Spin down for 5 min at 3000 x g and discard the supernatant.
4. Add 30 ml of water in the tubes and vortex to resuspend the cells.
5. Spin down for 5 min at 3000 x g and discard the supernatant. Leave a bit of water to resuspend the pellet.
6. Transfer the cells to a 2 x 2 ml safe-lock Eppendorf tube and spin down for 30 sec at 3000 x g. Aspirate the supernatant. (one tube will be kept as a backup in the -80°C freezer and the other will be processed as below).
7. Resuspend by pipetting the cell pellet in 200 µl of breaking buffer. Add 0.3 g glass beads (~200 µl volume) and 200 µl phenol/chloroform/isoamyl alcohol (Wear gloves and do it under the hood).
8. Cover the lid of the tubes with parafilm. Break the cells using Precellys 24 setting the following program:  
  
2500 rpm x 3 times x 30 sec of shaking x 30 sec of resting
9. Add 200 µl TE buffer and vortex briefly.
10. Microcentrifuge 5 min at high speed, at room temperature, and transfer aqueous layer to a clean microcentrifuge tube (Around 420 µl). Add 1 ml of 100% ethanol and mix by inversion.
11. Microcentrifuge 3 min at high speed, at room temperature. Discard the supernatant and add 1 ml of 70% ethanol and mix by inversion.
12. Microcentrifuge 3 min at high speed, at room temperature. Remove the supernatant and resuspend the pellet in 0.4 ml of TE buffer (to facilitate the resuspension set the tubes at 600 rpm shaking, 37°C, pipet up and down for total resuspension).

13. Add 5  $\mu$ l of 20 mg/ml DNase-free RNase A, mix by brief vortexing, and incubate 5 min, shaking at 600 rpm and 37°C.
14. Add 10  $\mu$ l of 4 M ammonium acetate and 1 ml of 100% ethanol. Mix by inversion.
15. Microcentrifuge 3 min at high speed, at room temperature. Add 1 ml of 70% ethanol. Mix by inversion.
16. Microcentrifuge 3 min at high speed, at room temperature. Discard the supernatant and spin down again for 10 seconds. Remove the rest of the volume with the pipet and dry the pellet under the hood.
17. Resuspend DNA pellet in 100  $\mu$ l of TE buffer incubating the samples for 10 min, shaking at 600 rpm and 37°C.
18. Take 5  $\mu$ l of DNA and dilute 10 times using 45  $\mu$ l of TE. Follow the instructions to measure the concentration of DNA using Qubit Invitrogen kit.

**Breaking buffer**

2% (v/v) Triton X-100	For 200 ml:	4 ml Triton X-100
1% (v/v) sodium dodecyl sulfate (SDS)		20 ml 10% SDS
100 mM NaCl		4 ml 5 M NaCl
10 mM Tris·Cl, pH 8.0		2 ml 1 M Tris-HCl, pH 8.0
1 mM EDTA, pH 8.0		0.4 mL 0.5 M EDTA, pH 8.0
Store $\leq$ 1 year at room temperature		

**TE buffer:**

10 mM Tris·Cl, pH 7.5 or pH 8.0	For 200 ml:	2 ml 1 M Tris-HCl, pH 7.5/8.0
1 mM EDTA, pH 8.0		0.4 ml 0.5 M EDTA, pH 8.0

**GO enrichment analyses**

GO enrichment analysis was performed in two steps using g:profiler and the EnrichmentMap application (app) of Cytoscape as previously described (Reimand et al., 2019). A list of gene or protein IDs showing a significant difference (p-value < 0.05) between the wild-type and the mutant strains were introduced in the g:profiler software. Unless stated otherwise, the selected significance threshold was 0.05, and electronic GO annotations were filtered out. A GEM file was created and fed into the EnrichmentMap app of Cytoscape (select Generic/gProfiler/Enrichment analysis). An FDR q-value cutoff of 0.1 and sparse connectivity was selected. Finally, a publication-ready picture was exported and edited with Inkscape.

## In vivo TORC1 kinase assay

*In vivo* TORC1 activity was assayed as previously described (Péli-Gulli et al., 2015) using phosphospecific anti-Sch9-pThr<sup>737</sup> and anti-Sch9 to probe endogenous Sch9.

### Tables

Name	Genotype	Source	Chapter (Figure)
KT1960	MAT $\alpha$ ; <i>ura3-52, leu2, his3, trp1</i>	Pedruzzi et al., 2003	1 (4); 2 (1, 2, 3); 3 (3, 4, 5, 8A-B, 9A, 10, 12A, 13)
KT1961	MAT $\alpha$ ; <i>ura3-52, leu2, his3, trp1</i>	Pedruzzi et al., 2003	
GMGO003	[KT1960] <i>gtr1<math>\Delta</math>::natMX4, HIS3::mCherry-ALP</i>	Hatakeyama et al., 2019	1 (4); 3(4A-C, 6, 8A, 9A, 11A, 12A)
GMGO004	[KT1961] <i>gtr1<math>\Delta</math>::natMX4, HIS3::mCherry-ALP</i>	Hatakeyama et al., 2019	
GMGO023	[GMGO004] <i>ego1<sup>N175fs</sup></i>	Hatakeyama et al., 2019	1 (2A)
GMGO024	[GMGO004] <i>ego3<sup>A49P</sup></i>	Hatakeyama et al., 2019	1 (2A)
GMGO025	[GMGO004] <i>gtr2<sup>E42*</sup></i>	Hatakeyama et al., 2019	1 (2A)
GMGO026	[GMGO003] <i>gtr2<sup>E185*</sup></i>	Hatakeyama et al., 2019	1 (2A)
GMGO027	[GMGO004] <i>gtr2<sup>283fs</sup></i>	Hatakeyama et al., 2019	1 (2A)
GMGO029	[GMGO004] <i>TOR1<sup>A1928D</sup></i>	Hatakeyama et al., 2019	1 (2A)
GMGO030	[GMGO004] <i>tco89<sup>Q140fs</sup></i>	Hatakeyama et al., 2019	1 (2A)
GMGO031	[GMGO003] <i>vps41<sup>N465fs</sup></i>	Hatakeyama et al., 2019	1 (2A)
GMGO032	[GMGO003] <i>apm3<sup>W31*</sup></i>	Hatakeyama et al., 2019	1 (2A)
GMGO033	[GMGO003] <i>akr1<sup>W725*</sup></i>	Hatakeyama et al., 2019	1 (2A)
MB36-4B	[BY4741/2] MAT $\alpha$ ; <i>gtr1<math>\Delta</math>::kanMX, his3, leu2, ura3</i>	Hatakeyama et al., 2019	1 (2A)
YAS063	[MB36-4B] <i>vps33<sup>L18P</sup></i>	Hatakeyama et al., 2019	1 (2A)
YAS064	[MB36-4B] <i>ego1<sup>R9*</sup></i>	Hatakeyama et al., 2019	1 (2A)
YAS066	[MB36-4B] <i>vps11<sup>Q76*</sup></i>	Hatakeyama et al., 2019	1 (2A)
YAS067	[MB36-4B] <i>vam6<sup>Q391*</sup></i>	Hatakeyama et al., 2019	1 (2A)
YAS068	[MB36-4B] <i>apl6M<sup>613R</sup></i>	Hatakeyama et al., 2019	1 (2A)
YAS069	[MB36-4B] <i>apl6<sup>M1V</sup></i>	Hatakeyama et al., 2019	1 (2A)
YAS070	[MB36-4B] <i>gtr2<sup>C231W</sup></i>	Hatakeyama et al., 2019	1 (2A)
YL515	[BY4741/2] MAT $\alpha$ ; <i>his3<math>\Delta</math>1, leu2<math>\Delta</math>0, ura3<math>\Delta</math>0</i>	Binda et al., 2009	1 (2B)
MB27	[YL515] <i>gtr1<math>\Delta</math>::HIS3</i>	Binda et al., 2009	1 (2B)
NP51-3C	[MB27] <i>ego2<math>\Delta</math>::KanMX</i>	Powis et al., 2015	1 (2B)
GMGO010	[MB27] <i>tor1<math>\Delta</math>::KanMX</i>	Hatakeyama et al., 2019	1 (2B)



GMGO011	[MB27] <i>akr1Δ::KanMX</i>	Hatakeyama et al., 2019	1 (2B)
GMGO012	[MB27] <i>vps11Δ::KanMX</i>	Hatakeyama et al., 2019	1 (2B)
GMGO013	[MB27] <i>vps16Δ::KanMX</i>	Hatakeyama et al., 2019	1 (2B)
GMGO014	[MB27] <i>vps18Δ::KanMX</i>	Hatakeyama et al., 2019	1 (2B)
GMGO015	[MB27] <i>vps33Δ::KanMX</i>	Hatakeyama et al., 2019	1 (2B)
GMGO016	[MB27] <i>vps41Δ::KanMX</i>	Hatakeyama et al., 2019	1 (2B)
GMGO017	[MB27] <i>apl5Δ::KanMX</i>	Hatakeyama et al., 2019	1 (2B)
GMGO018	[MB27] <i>apl6Δ::KanMX6</i>	Hatakeyama et al., 2019	1 (2B)
GMGO019	[MB27] <i>apm3Δ::KanMX</i>	Hatakeyama et al., 2019	1 (2B)
GMGO020	[MB27] <i>aps3Δ::KanMX</i>	Hatakeyama et al., 2019	1 (2B)
MP02-1B	[YL516] <i>gtr1Δ::KanMX, tco89Δ::HIS3</i>	Hatakeyama et al., 2019	1 (2B)
MP06-8B	[YL515] <i>gtr1Δ::KanMX, gtr2Δ::KanMX</i>	Binda et al., 2009	1 (2B)
MP11-4C	[YL516] <i>gtr1Δ::KanMX, vam6Δ::KanMX</i>	Hatakeyama et al., 2019	1 (2B)
MP261-1D	[YL515] <i>gtr1Δ::HIS3, ego1Δ::HIS3</i>	Hatakeyama et al., 2019	1 (2B)
MP263-24C	[YL516] <i>gtr1Δ::HIS3, ego3Δ::KanMX</i>	Hatakeyama et al., 2019	1 (2B)
YL516	[BY4741/2] MATa; <i>his3Δ1, leu2Δ0, ura3Δ0</i>	Binda et al., 2009	1 (3A)
RKH329	[YL516] <i>EGO1-GFP::HIS3</i>	Hatakeyama et al., 2019	1 (3A)
RKH352	[RKH329] <i>apl5Δ::KanMX</i>	Hatakeyama et al., 2019	1 (3A)
RKH346	[RKH329] <i>apl6Δ::KanMX</i>	Hatakeyama et al., 2019	1 (3A)
RKH348	[RKH329] <i>vps41Δ::KanMX</i>	Hatakeyama et al., 2019	1 (3A)
RKH338	[RKH329] <i>vam6Δ::KanMX</i>	Hatakeyama et al., 2019	1 (3A)
RKH94	[YL516] <i>GFP-GTR1</i>	Hatakeyama et al., 2019	1 (3B)
RKH356	[RKH94] <i>apl5Δ::KanMX</i>	Hatakeyama et al., 2019	1 (3B)
RKH330	[RKH94] <i>apl6Δ::KanMX</i>	Hatakeyama et al., 2019	1 (3B)
RKH332	[RKH94] <i>vps41Δ::KanMX</i>	Hatakeyama et al., 2019	1 (3B)
RKH334	[RKH94] <i>vam6Δ::KanMX</i>	Hatakeyama et al., 2019	1 (3B)
SKY222	[BY4741] MATa; <i>his3Δ1, leu2Δ0, ura3Δ0, met15Δ0, LEU2::GFP-TOR1</i>	Kira et al., 2014	1 (3C)
RKH358	[SKY222] <i>apl5Δ::KanMX</i>	Hatakeyama et al., 2019	1 (3C)
RKH319	[SKY222] <i>apl6Δ::KanMX</i>	Hatakeyama et al., 2019	1 (3C)
RKH324	[SKY222] <i>vps41Δ::KanMX</i>	Hatakeyama et al., 2019	1 (3C)
RKH336	[SKY222] <i>vam6Δ::KanMX</i>	Hatakeyama et al., 2019	1 (3C)
MP5361	[W303] MATND; <i>ura3-1 leu2-3, 112 his3-11, 15 trp1-1 ade2-1</i>	This study	1 (5)
GMGO120	[MP5361] <i>gtr1Δ::hphNT1</i>	This study	1 (5)
MP5050	[KT1960] <i>gcn2Δ::hphNT1</i>	Dokládál et al., 2021	2 (2, 3); 3 (8B-C)
HQY346	MATa; <i>ura3-52 leu2-3 leu2-112 trp1-Δ63 gcn2Δ gcd2Δ::hisG (GCD2<sup>K627T</sup>, TRP1) GAL2<sup>+</sup></i>	Qiu, 2002	2 (1)

GMGO021	[KT1960] <i>gcn4Δ::kanMX4</i>	Dokládál et al., 2021	2 (2); 3 (8B)
GMGO022	[KT1960] <i>gcn2Δ::hphNT1 gcn4Δ::kanMX4</i>	Dokládál et al., 2021	2 (2); 3 (8B)
GMGO037	[KT1960] <i>ygl188c-aΔ::hphNT1</i>	This study	3 (3)
GMGO037G	[KT1960] <i>YGL188C-A-GDGAGLIN-EnvyGFP::SpHis5</i>	This study	3 (3A, 3C)
GMGO053	[KT1960] <i>rps26aΔ::hphNT1</i>	This study	3 (3C, 4, 5, 8A, 9, 11, 12B, 13)
GMGO054	[KT1960] <i>rps26aΔ::hphNT1</i>	This study	3 (4A)
GMGO055	[KT1960] <i>rps26aΔ::hphNT1</i>	This study	3 (4A)
5166	[KT1960] <i>pib2Δ::HIS3</i>	This study	3 (4A-C, 7)
( <i>pib2D::HIS3</i> )			
GMGO056	[KT1960] <i>gtr1Δ::natMX4, rps26aΔ::hphNT1</i>	This study	3 (6, 8A, 9A, 11A, 12B)
GMGO122	[KT1961] <i>rps26aΔ::hphNT1, pib2Δ::HIS3</i>	This study	3 (7)
MP6612	[KT1960] <i>rps26aΔ::hphNT1, gcn2Δ::KanMX</i>	This study	3 (8C)
MP6617	[KT1960] <i>rps26aΔ::hphNT1, aah1Δ::KanMX</i>	This study	3 (9B)
GMGO171	[KT1960] <i>arf1Δ::KanMX6</i>	This study	3 (10)
GMGO180	[KT1960] <i>arf1Δ::KanMX6, rps26aΔ::hphNT1</i>	This study	3 (11A-C)
MP6608	[KT1960] <i>rps26aΔ::hphNT1, arf2Δ::HIS3</i>	This study	3 (11A)
GMGO183	[KT1960] <i>gcs1Δ::KanMX6, rps26aΔ::hphNT1</i>	This study	3 (11A-B, 11D)
GMGO-MPG164-3B	[KT1961] <i>gtr1Δ::natMX4, arf1Δ::kanMX6</i>	This study	3 (11A)
GMGO-MPG168-1B	[KT1960] <i>arf1Δ::KanMX6, rps26aΔ::hphNT1, gtr1Δ::natMX4</i>	This study	3 (11A)
GMGO201	[KT1961] <i>rpl16aΔ::KanMX</i>	This study	3 (12A)
GMGO202	[KT1960] <i>gtr1Δ::natMX4, rpl16aΔ::KanMX</i>	This study	3 (12A)
GMGO203	[KT1960] <i>rpl17bΔ::KanMX</i>	This study	3 (12A)
GMGO204	[KT1961] <i>gtr1Δ::natMX4, rpl17bΔ::KanMX</i>	This study	3 (12A)
GMGO205	[KT1961] <i>rps25aΔ::KanMX</i>	This study	3 (12A)
GMGO206	[KT1961] <i>gtr1Δ::natMX4 rps25aΔ::KanMX</i>	This study	3 (12A)
GMGO207	[KT1960] <i>rps25bΔ::KanMX</i>	This study	3 (12A)
GMGO208	[KT1961] <i>gtr1Δ::natMX4, rps25bΔ::KanMX</i>	This study	3 (12A)
GMGO209	[KT1961] <i>rps26bΔ::KanMX</i>	This study	3 (12A)
GMGO210	[KT1961] <i>gtr1Δ::natMX4 rps26bΔ::KanMX</i>	This study	3 (12A)
GMGO211	[KT1961] <i>rpl20bΔ::KanMX</i>	This study	3 (12B)
GMGO212	[KT1960] <i>gtr1Δ::natMX4, rpl20bΔ::KanMX</i>	This study	3 (12B)
GMGO213	[KT1961] <i>rpl23bΔ::KanMX</i>	This study	3 (12B)
GMGO214	[KT1961] <i>gtr1Δ::natMX4, rpl23bΔ::KanMX</i>	This study	3 (12B)
GMGO215	[KT1960] <i>rps17aΔ::KanMX</i>	This study	3 (12B)
GMGO216	[KT1961] <i>gtr1Δ::natMX4, rps17aΔ::KanMX</i>	This study	3 (12B)
GMGO217	[KT1961] <i>rps24aΔ::KanMX</i>	This study	3 (12B)
GMGO218	[KT1960] <i>gtr1Δ::natMX4, rps24aΔ::KanMX</i>	This study	3 (12B)

**Table 1: List of strains used in Chapters I, II, and III.**

Name	Description	Source	Chapter (Figure)
pRS413	CEN/ARS, <i>HIS3</i>	Sikorski & Hieter, 1989	1 (2, 3B-C, 4, 5); 2(1, 2, 3); 3 (3, 4, 5, 6, 8A-B, 9, 10, 11, 12, 13)
pRS414	CEN/ARS, <i>TRP1</i>	Sikorski & Hieter, 1989	1 (2A, 4); 3 (3, 4, 5, 6, 7, 8A, 9, 10, 11, 12, 13)
pRS415	CEN/ARS, <i>LEU2</i>	Sikorski & Hieter, 1989	1 (2A, 3A-B, 4, 5); 2(1, 2, 3); 3 (3, 4, 5, 6, 7, 8A-B, 9, 10, 11, 12, 13)

pRS416	CEN/ARS, <i>URA3</i>	Sikorski & Hieter, 1989	1 (2, 3A-B, 4); 2(1, 2, 3); 3 (3, 4, 5, 6A-C, 7A-C, 8, 9, 10, 11, 12, 13)
pMB1580	CEN/ARS, <i>LEU2</i> , <i>GAL1p-GST-GTR1<sup>S20L</sup></i>	Binda et al., 2009	1 (2, 4A)
YCplac33-EGO1-GST	CEN/ARS, <i>URA3</i> , <i>EGO1-GST</i>	Powis et al., 2015	1 (2A)
pSIVu-EGO3-GFP	Integrative, <i>URA3</i> , <i>EGO3-EGFP</i>	Hatakeyama et al., 2019	1 (2A)
pRS416-GTR2-V5-HIS <sub>6</sub>	CEN/ARS, <i>URA3</i> , <i>GTR2-V5-HIS<sub>6</sub></i>	Hatakeyama et al., 2019	1 (2A)
pRS316-TOR1-HA	CEN/ARS, <i>URA3</i> , <i>TOR1-HA</i>	Hatakeyama et al., 2019	1 (2A)
YCplac33-TCO89	CEN/ARS, <i>URA3</i> , <i>TCO89</i>	Hatakeyama et al., 2019	1 (2A)
YEplac195-GAL1-VAM6	2 $\mu$ , <i>URA3</i> , <i>GAL1p-VAM6</i>	Hatakeyama et al., 2019	1 (2A)
BG1805-GAL1-VPS41-TAP	2 $\mu$ , <i>URA3</i> , <i>GAL1p-VPS41-TAP</i>	Open Biosystems	1 (2A)
BG1805-GAL1-VPS33-TAP	2 $\mu$ , <i>URA3</i> , <i>GAL1p-VPS33-TAP</i>	Open Biosystems	1 (2A)
BG1805-GAL1-VPS11-TAP	2 $\mu$ , <i>URA3</i> , <i>GAL1p-VPS11-TAP</i>	Open Biosystems	1 (2A)
BG1805-GAL1-APL6-TAP	2 $\mu$ , <i>URA3</i> , <i>GAL1p-APL6-TAP</i>	Open Biosystems	1 (2A)
YEplac195-GAL1-APM3	2 $\mu$ , <i>URA3</i> , <i>GAL1p-APM3</i>	Hatakeyama et al., 2019	1 (2A)
BG1805-GAL1-AKR1-TAP	2 $\mu$ , <i>URA3</i> , <i>GAL1p-AKR1-TAP</i>	Open Biosystems	1 (2A)
p1379	CEN/ARS, <i>URA3</i> , <i>MET15</i>	Hatakeyama et al., 2019	1 (3C)
psivh_OPY1p_OP Y1_OPY1t	Integrative, <i>HIS3</i> , <i>OPY1p-OPY1-OPY1t</i>	This study	1 (4)
pBK549	CEN/ARS, <i>URA3</i> , <i>ADE2-MiniDs-ADE2</i> , <i>GALp-AcTransposase</i>	Michel et al., 2017	1 (5)
pSIVh-YGL188C-A WT-RPS26A	Integrative, <i>HIS3</i> , <i>RPS26Ap-RPS26A-RPS26At</i>	This study	3 (4F)
pRS416-Gtr1	CEN/ARS, <i>URA3</i> , <i>GTR1p-GTR1</i>	Péli-Gulli et al., 2015	3 (6A-B, 6D)
pRS416-Gtr1-S20L	CEN/ARS, <i>URA3</i> , <i>GTR1-GTR1<sup>S20L</sup></i>	Péli-Gulli et al., 2015	3 (6A-B, 6E)
pRS416-Gtr1-Q65L	CEN/ARS, <i>URA3</i> , <i>GTR1-GTR1<sup>Q65L</sup></i>	Péli-Gulli et al., 2015	3 (6A-B, 6F)
p416-PIB2	CEN/ARS, <i>URA3</i> , <i>PIB2p-PIB2</i>	Michel et al., 2017	3 (7A-B, 7D)
p416-PIB2( $\Delta$ 533-620aa)	CEN/ARS, <i>URA3</i> , <i>PIB2p-PIB2<sup>\Delta</sup>533-620</i>	Michel et al., 2017	3 (7A-B, 7E)
p416-PIB2 $\Delta$ N164aa	CEN/ARS, <i>URA3</i> , <i>PIB2p-PIB2<sup>\Delta</sup>N164</i>	Michel et al., 2017	3 (7A-B, 7F)
FRP880_PACT1(-1-520)-LexA-ER-haB112-TCYC1	CEN/ARS, <i>HIS3</i> , <i>ACT1-LexA-ER-haB112</i>	Ottoz et al., 2014	3 (8C)
psivl-LexA(4)-CYC1p-Gcn2 <sup>F842L</sup>	CEN/ARS, <i>LEU2</i> , <i>LexA(4)-CYC1p-Gcn2<sup>F842L</sup></i>	This study	3 (8C)

**Table 2: List of plasmids used in Chapters I, II, and III.**

REAGENT OR RESOURCE	SOURCE	IDENTIFIER
<b>Antibodies</b>		
Rabbit anti-Sch9-pThr737(1:10000)	De Virgilio lab	N/A
Goat anti-Sch9 (1:1000)	De Virgilio lab	N/A
Rabbit phospho-EIF2S1 (Ser 52) (1:2000)	Invitrogen	44-728G
Rabbit anti-Sui2 (1:2000)	Perzmaier et al., 2013	N/A
Rabbit anti-Ygl188c-a (1:1000)	GenScript	U5313EA160

### Bacterial strains

E. coli DH5 $\alpha$	CGSC	12384
Ammonium sulfate	MP Biomedicals	4808211
Arg10	Sigma-Aldrich	608033
Arg6	Sigma-Aldrich	643440
Drop-out Mix Complete, all amino acids	US Biological	D9515
Drop-out Mix Synthetic, minus Ade, Arg, His, Leu, Lys, Trp, Ura	US Biological	D9545
Drop-out Mix Synthetic, minus Ade, His, Leu, Trp, Ura	US Biological	D9540-05
Drop-out Mix Synthetic, minus His, Leu, Trp, Ura	US Biological	D9540
DTT	Applichem	A1101-0025
Lys4	Sigma-Aldrich	616192
Lys8	Sigma-Aldrich	608041
Pefabloc	Sigma-Aldrich	76307
PhosSTOP	Roche	04-906-837-001
Rapamycin	LC Laboratories	R-5000
TCA	Sigma-Aldrich	27242
Trypsin	Promega	V5113
Yeast nitrogen base	CONDA	1553-00
YPD broth	US Biological	Y2075

### Critical commercial assays

ECL Western Blotting Detection	GE Healthcare	RPN2106
Radiance Plus Sensitive ECL	Azure Biosystems	AC2103

### Software and algorithms

Cytoscape	Shannon, 2003	<a href="https://cytoscape.org">https://cytoscape.org</a>
g:Profiler	Raudvere et al., 2019	<a href="https://biit.cs.ut.ee/gprofiler/gost">https://biit.cs.ut.ee/gprofiler/gost</a>
ImageJ	NIH	<a href="https://imagej.nih.gov/ij/index.html">https://imagej.nih.gov/ij/index.html</a>
MaxQuant	Cox and Mann, 2008	<a href="https://maxquant.net/maxquant/">https://maxquant.net/maxquant/</a>
Perseus	Tyanova et al., 2016	<a href="https://maxquant.net/perseus/">https://maxquant.net/perseus/</a>
RapidMiner	RapidMiner, Inc.	<a href="https://rapidminer.com">https://rapidminer.com</a>
Inkscape	The Inkscape Project	<a href="https://inkscape.org">https://inkscape.org</a>

**Table 3: Highlighted reagents and resources used in Chapters I, II, and III.**

## Bibliography

- Binda, M., Péli-Gulli, M.-P., Bonfils, G., Panchaud, N., Urban, J., Sturgill, T. W., Loewith, R., & De Virgilio, C. (2009). The Vam6 GEF controls TORC1 by activating the EGO complex. *Molecular Cell*, 35(5), 563–573. <https://doi.org/10.1016/j.molcel.2009.06.033>
- Cox, J., & Mann, M. (2008). MaxQuant enables high peptide identification rates, individualized p.p.b.-range mass accuracies and proteome-wide protein quantification. *Nature Biotechnology*, 26(12), 1367–1372. <https://doi.org/10.1038/nbt.1511>
- Dokládal, L., Stumpe, M., Pillet, B., Hu, Z., Garcia Osuna, G. M., Kressler, D., Dengjel, J., & De Virgilio, C. (2021). Global phosphoproteomics pinpoints uncharted Gcn2-mediated mechanisms of translational control. *Molecular Cell*, 81(9), 1879–1889.e6. <https://doi.org/10.1016/j.molcel.2021.02.037>
- Hatakeyama, R., Péli-Gulli, M.-P., Hu, Z., Jaquenoud, M., Garcia Osuna, G. M., Sardu, A., Dengjel, J., & De Virgilio, C. (2019). Spatially Distinct Pools of TORC1 Balance Protein Homeostasis. *Molecular Cell*, 73(2), 325–338.e8. <https://doi.org/10.1016/j.molcel.2018.10.040>
- Hu, Z., Raucci, S., Jaquenoud, M., Hatakeyama, R., Stumpe, M., Rohr, R., Reggiori, F., De Virgilio, C., & Dengjel, J. (2019). Multilayered Control of Protein Turnover by TORC1 and Atg1. *Cell Reports*, 28(13), 3486–3496.e6. <https://doi.org/10.1016/j.celrep.2019.08.069>
- Janke, C., Magiera, M. M., Rathfelder, N., Taxis, C., Reber, S., Maekawa, H., Moreno-Borchart, A., Doenges, G., Schwob, E., Schiebel, E., & Knop, M. (2004). A versatile toolbox for PCR-based

- tagging of yeast genes: New fluorescent proteins, more markers and promoter substitution cassettes. *Yeast*, 21(11), 947–962. <https://doi.org/10.1002/yea.1142>
- Michel, A. H., Hatakeyama, R., Kimmig, P., Arter, M., Peter, M., Matos, J., De Virgilio, C., & Kornmann, B. (2017). Functional mapping of yeast genomes by saturated transposition. *ELife*, 6, e23570. <https://doi.org/10.7554/eLife.23570>
- Michel, A. H., van Schie, S., Mosbach, A., Scalliet, G., & Kornmann, B. (2019). *Exploiting homologous recombination increases SATAY efficiency for loss- and gain-of-function screening* [Preprint]. *Cell Biology*. <https://doi.org/10.1101/866483>
- Ottoz, D. S. M., Rudolf, F., & Stelling, J. (2014). Inducible, tightly regulated and growth condition-independent transcription factor in *Saccharomyces cerevisiae*. *Nucleic Acids Research*, 42(17), e130–e130. <https://doi.org/10.1093/nar/gku616>
- Pedruzzi, I., Dubouloz, F., Cameroni, E., Wanke, V., Roosen, J., Winderickx, J., & De Virgilio, C. (2003). TOR and PKA signaling pathways converge on the protein kinase Rim15 to control entry into G0. *Molecular Cell*, 12(6), 1607–1613. [https://doi.org/10.1016/s1097-2765\(03\)00485-4](https://doi.org/10.1016/s1097-2765(03)00485-4)
- Péli-Gulli, M.-P., Sardu, A., Panchaud, N., Raucchi, S., & De Virgilio, C. (2015). Amino Acids Stimulate TORC1 through Lst4-Lst7, a GTPase-Activating Protein Complex for the Rag Family GTPase Gtr2. *Cell Reports*, 13(1), 1–7. <https://doi.org/10.1016/j.celrep.2015.08.059>
- Perzmaier, A. F., Richter, F., & Seufert, W. (2013). Translation initiation requires cell division cycle 123 (Cdc123) to facilitate biogenesis of the eukaryotic initiation factor 2 (eIF2). *The Journal of Biological Chemistry*, 288(30), 21537–21546. <https://doi.org/10.1074/jbc.M113.472290>
- Powis, K., Zhang, T., Panchaud, N., Wang, R., De Virgilio, C., & Ding, J. (2015). Crystal structure of the Ego1-Ego2-Ego3 complex and its role in promoting Rag GTPase-dependent TORC1 signaling. *Cell Research*, 25(9), 1043–1059. <https://doi.org/10.1038/cr.2015.86>
- Qiu, H. (2002). Mutations that bypass tRNA binding activate the intrinsically defective kinase domain in GCN2. *Genes & Development*, 16(10), 1271–1280. <https://doi.org/10.1101/gad.979402>
- Raudvere, U., Kolberg, L., Kuzmin, I., Arak, T., Adler, P., Peterson, H., & Vilo, J. (2019). g:Profiler: A web server for functional enrichment analysis and conversions of gene lists (2019 update). *Nucleic Acids Research*, 47(W1), W191–W198. <https://doi.org/10.1093/nar/gkz369>
- Shannon, P. (2003). Cytoscape: A Software Environment for Integrated Models of Biomolecular Interaction Networks. *Genome Research*, 13(11), 2498–2504. <https://doi.org/10.1101/gr.1239303>
- Sikorski, R. S., & Hieter, P. (1989). A system of shuttle vectors and yeast host strains designed for efficient manipulation of DNA in *Saccharomyces cerevisiae*. *Genetics*, 122(1), 19–27.
- Tolonen, A. C., & Haas, W. (2014). Quantitative Proteomics Using Reductive Dimethylation for Stable Isotope Labeling. *Journal of Visualized Experiments*, 89, 51416. <https://doi.org/10.3791/51416>
- Tyanova, S., Temu, T., Sinitcyn, P., Carlson, A., Hein, M. Y., Geiger, T., Mann, M., & Cox, J. (2016). The Perseus computational platform for comprehensive analysis of (prote)omics data. *Nature Methods*, 13(9), 731–740. <https://doi.org/10.1038/nmeth.3901>

# ACKNOWLEDGEMENTS

This long journey would not have been possible without the support of many people. Therefore, I would like to thank:

Professors Claudio De Virgilio, Jörn Dengjel, and Sophie Martin for reading, correcting, and improving this thesis;

Claudio for having allowed me to work in his lab and having renewed his trust in me during these years;

Professors Benoit Kornmann, Laurent Falquet, and Doctors Agnès Michel, Michael Stumpe, and Zehan Hu for having collaborated with us;

Floriane, Malika, and Susi for their help. Especially to Malika not only for her ability to solve problems but also for her kindness;

The UniFR staff and especially Evelyn, Jean-Daniel, and Olga for making things easier to manage;

My Bachelor students Alain, Bastien, and Fabienne for being curious and willful;

Dieter and Alfonso for teaching me so many things about ribosomes;

My group colleagues. Especially to Aurélien, Marco, Raffa, and Serena. Thanks for your help and for making the daily life lively and joyful;

Marie-Pierre for her invaluable support, help, and trust. She was my mentor and she is now a friend;

TORC1 because no one is grateful enough to this fantastic kinase;

Tim for sharing your time, energy, and passion with me. Thank you for introducing me to your fantastic family and teaching me Jiu-Jitsu;

Alfonso, Esther, Gina y José, por los buenos momentos compartidos juntos y los que aún quedan por compartir;

Carolina y su forma de enseñar la ciencia, sin haberla conocido dudo mucho que hubiese estudiado Biología;

Los Pupilos de Popa, por todas nuestras discusiones, sin vosotros mi día a día sería aburrido;

Capi, Darío, Jorge, Lola y Migue, por su amistad;

Mis familiares cercanos, en particular mi padre y mi madre;

Finalmente, querría hacer una mención especial a Cristina, por haberme acompañado y apoyado durante todo este proceso. Eres la mejor persona que conozco y a la que más admiro.



# GUILLERMO M. GARCÍA OSUNA

PhD Candidate in Biochemistry

## Personal information

**Residence permit:** C

**Date of birth:** 02/12/1991

**Phone:** 077 966 4720

**Email:** gmiguelgosuna@gmail.com

**Address:** Promenade de Castellane 14, 1110 Morges (VD)

**LinkedIn:** [www.linkedin.com/in/gmgo](http://www.linkedin.com/in/gmgo)

## Skills

- **Bibliographic management**

PubMed, Scopus, ProQuest, MedlinePlus, Global Health, Mendeley

- **Data processing and analysis**

Excel, GraphPad, Cytoscape, RapidMiner, Perseus, ImageJ

- **Communication and Illustration**

Microsoft Teams, Zoom, Word, Google Docs, PowerPoint, Prezi, Inkscape, Canva

## Education

### PhD Candidate in Biochemistry

*University of Fribourg* | Feb. 2017 to present

- Co-organized one scientific retreat centered on orienting professionally PhD students
- Co-hosted 3 professional speakers coming from biotech companies

### MSc in Biochemistry plus BS in Biology

*University of Granada* | Sep. 2009 to Sep. 2014

- Led the Biochemistry studentship body:
- Scheduled several exams and organized the graduation ceremony

## Experience

### Research Assistant in Molecular Biology

*University of Fribourg* | Feb. 2017 to present

- Managed three scientific projects shedding light on eukaryotic cell growth control
- Co-authored 3 scientific publications in 4 years
- Settled a high-throughput transposon-based genetic screen technology
- Communicated scientific findings to the scientific community via more than 20 presentations, several manuscripts, and one poster
- Coordinated the collaboration between our group and two international groups
- Mentored 3 bachelor students and corrected 3 bachelor thesis
- Supervised more than 100 bachelor students during practical laboratory work

### Research Assistant in Microbiology

*University of Lausanne* | Jan. 2016 to Jan. 2017

- Designed a culture medium supporting the growth of a microbial community able to degrade pollutants

### Research Internship in Neuroscience

*EPFL* | Jul. 2015 to Dec. 2015

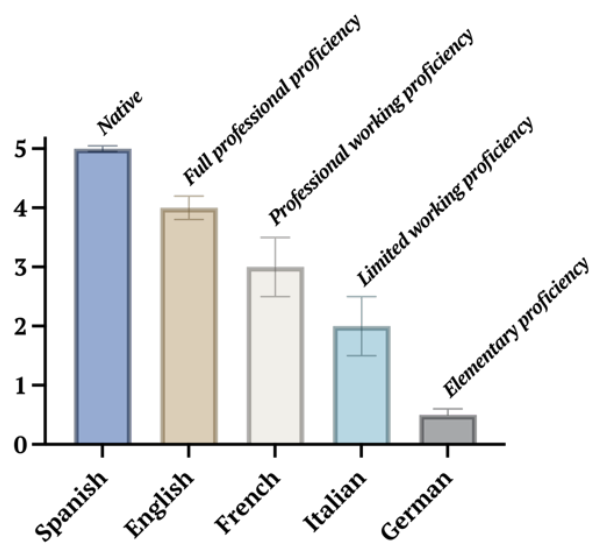
- Managed a scientific project focused on studying the molecular mechanism behind Alzheimer's disease
- Co-authored two scientific publications in 6 months

## Publications

- <sup>1</sup> Nicastro, R., Raucci, S., Michel, A. H., Stumpe, M., **Garcia Osuna, G. M.**, Jaquenoud, M., Kornmann, B., & De Virgilio, C. (2021). Indole-3-acetic acid is a physiological inhibitor of TORC1 in yeast. *PLOS Genetics*, 17(3), e1009414. <https://doi.org/10.1371/journal.pgen.1009414>
- <sup>1</sup> Dokládál, L., Stumpe, M., Pillet, B., Hu, Z., **Garcia Osuna, G. M.**, Kressler, D., Dengjel, J., & De Virgilio, C. (2021). Global phosphoproteomics pinpoints uncharted Gcn2-mediated mechanisms of translational control. *Molecular Cell*, 81(9), 1879-1889.e6. <https://doi.org/10.1016/j.molcel.2021.02.037>
- <sup>1</sup> Hatakeyama, R., Péli-Gulli, M.-P., Hu, Z., Jaquenoud, M., **Garcia Osuna, G. M.**, Sardu, A., Dengjel, J., & De Virgilio, C. (2019). Spatially Distinct Pools of TORC1 Balance Protein Homeostasis. *Molecular Cell*, 73(2), 325-338.e8. <https://doi.org/10.1016/j.molcel.2018.10.040>
- <sup>2</sup> Gerber, H., Wu, F., Dimitrov, M., **Garcia Osuna, G. M.**, & Fraering, P. C. (2017). Zinc and Copper Differentially Modulate Amyloid Precursor Protein Processing by  $\gamma$ -Secretase and Amyloid- $\beta$  Peptide Production. *Journal of Biological Chemistry*, 292(9), 3751-3767. <https://doi.org/10.1074/jbc.M116.754101>
- <sup>2</sup> Ayciriex, S., Gerber, H., **Osuna, G. M.**, Chami, M., Stahlberg, H., Shevchenko, A., & Fraering, P. C. (2016). The lipidome associated with the  $\gamma$ -secretase complex is required for its integrity and activity. *Biochemical Journal*, 473(3), 321-334. <https://doi.org/10.1042/BJ20150448>

<sup>1</sup> University of Fribourg <sup>2</sup> École Polytechnique Fédérale de Lausanne

## Languages



## References

- Prof. Dr. Claudio De Virgilio (UniFR)  
Phone: +41 26 300 8656  
Mail: claudio.devirgilio@unifr.ch
- Dra. Sara Mitri (UniL)  
Phone: +41 21 692 56 12  
Mail: sara.mitri@unil.ch
- Dr. Patrick C. Fraering  
Mail: fraeringpatrick@hotmail.com